CHALMERS
UNIVERSITY OF TECHNOLOGY

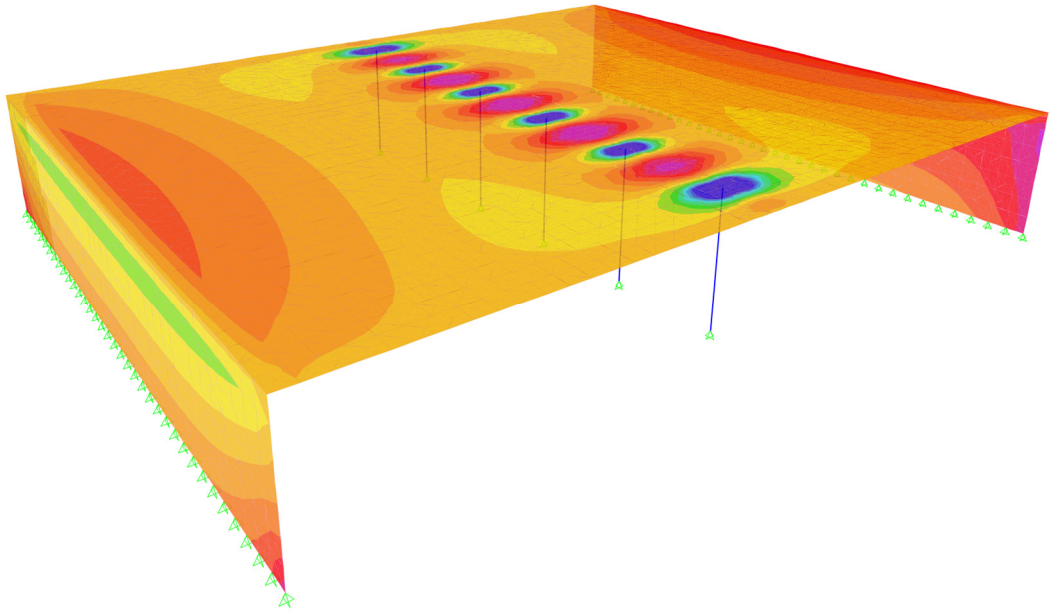

Modelling Techniques for Post-tensioned Concrete Slab Bridges

Master's Thesis in the Master's Programme Structural Engineering and Building Technology

JOEL ERIKSSON
ADAM JONSSON

Department of Civil and Environmental Engineering
Division of Structural Engineering
Concrete Structures
CHALMERS UNIVERSITY OF TECHNOLOGY
Master's Thesis BOMX02-17-31
Gothenburg, Sweden 2017

MASTER'S THESIS BOMX02-17-31

Modelling Techniques for Post-tensioned Concrete Slab Bridges

Master's Thesis in the Master's Programme Structural Engineering and Building Technology

JOEL ERIKSSON

ADAM JONSSON

Department of Civil and Environmental Engineering
Division of Structural Engineering
Concrete Structures
CHALMERS UNIVERSITY OF TECHNOLOGY
Göteborg, Sweden 2017

Modelling Techniques for Post-tensioned Concrete Slab Bridges

Master's Thesis in the Master's Programme Structural Engineering and Building Technology

JOEL ERIKSSON

ADAM JONSSON

Examensarbete BOMX02-17-31/ Institutionen för bygg- och miljöteknik,
Chalmers tekniska högskola 2017

Department of Civil and Environmental Engineering
Division of Structural Engineering
Concrete Structures
Chalmers University of Technology
SE-412 96 Göteborg
Sweden
Telephone: + 46 (0)31-772 1000

Cover:
Stress distribution in a shell element model.
Department of Civil and Environmental Engineering
Göteborg, Sweden, 2017

Modelling Techniques for Post-tensioned Concrete Slab Bridges

Master's thesis in the Master's Programme Structural Engineering and Building Technology

JOEL ERIKSSON
ADAM JONSSON
Department of Civil and Environmental Engineering
Division of Structural Engineering
Concrete Structures
Chalmers University of Technology

ABSTRACT

Post-tensioned concrete slab bridges are a common bridge type for short spans. In such a bridge, there are three-dimensional effects in the bridge slab, partly because of a slabs ability to distribute load in both the longitudinal and the transverse direction and partly because the prestressing induces stresses in both directions of the slab. When such bridge is to be designed, these effects need to be described correctly using numerical models. The aim of this study was to investigate the influence of the prestressing on the structural behavior in the bridge slab, and how different modelling techniques describe the behavior. Further, since the post-tensioning tendons are placed in the longitudinal direction only and therefore cannot prevent cracking in the transverse direction, the behavior of the bridge slab due to cracking has been investigated.

In this project, the FE software SAP2000 has been used, where mainly two types of FE models have been analyzed: a beam grillage model and a shell model. Moment distributions in the slab in these models have been compared to investigate how they describe the behavior of the slab caused by the prestressing load. Further, the response due to cracking has been investigated in the shell model by modifying the Poisson's ratio and the transverse stiffness of the slab.

The produced results have shown that the Poisson's ratio had great influence on the transverse moment distribution in the shell model. Since the beam grillage model, for natural reasons, cannot describe transverse contraction, the results from the shell model and beam grillage model were different when the Poisson's ratio in the shell model was set to 0.2, which correspond to uncracked concrete. However, when the Poisson's ratio was set to zero, the results from the models were similar. Reducing the transverse stiffness, due to cracking, had little influence on the moment distribution in the bridge slab.

A requirement in Eurocode turned out to be problematic for this type of post-tensioned bridge. The requirement concerns stresses in the concrete around the prestressing tendons and a clarification of how the requirement should be interpreted is needed.

Key words: FEM, slab bridge, prestressing, post-tensioning, beam elements, shell elements, cracking, Poisson's ratio, transverse stiffness

Modelleringstekniker för efterspända betongplattbroar

Examensarbete inom masterprogrammet Structural Engineering and Building Technology

JOEL ERIKSSON
ADAM JONSSON
Institutionen för bygg- och miljöteknik
Avdelningen för konstruktionsteknik
Betongbyggnad
Chalmers tekniska högskola

SAMMANFATTNING

Efterspända betongplattbroar är en vanlig brotyp för korta spännvidder. I en sådan brotyp finns tredimensionella effekter i broplattan, dels på grund av att lasten kan spridas i både längd- och tvärriktningen och dels på grund av att förspänningen framkallar spänningar i plattans båda riktningar. Vid dimensionering av en sådan bro behöver dessa effekter beskrivas korrekt med hjälp av numeriska modeller. Detta arbete syftar till att undersöka hur förspänningen påverkar verkningssättet i broplattan, samt hur olika modelleringstekniker beskriver detta. Ytterligare har verkningssättet i broplattan till följd av uppsprickning undersökts. Detta eftersom att förspänningen endast är placerad i längdriktningen och därför inte kan förhindra sprickbildning i plattans tvärriktning.

I detta arbete har FE-programmet SAP2000 använts där i huvudsak två typer av FE-modeller har analyserats, vilka är balkrost- och skalmodell. Momentfördelningar i plattan i dessa modeller har jämförts för att undersöka hur de beskriver verkningssättet i broplattan orsakad av förspänningslasten. Vidare har responsen till följd av sprickbildning undersökts för skalmodellen genom att modifiera tvärkontraktionstalet och styvheten i tvärled för plattan.

Framtagna resultat har visat att tvärkontraktionstalet hade stor betydelse för momentfördelningen i tvärled i skalmodellen. Eftersom att balkrostmodellen, av naturliga skäl, inte kan ta hänsyn till tvärkontraktion medförde detta att skal- och balkrostmodellen gav olika resultat när tvärkontraktionstalet i skalmodellen var satt till 0,2, vilket motsvarar osprucken betong. Däremot när tvärkontraktionstalet var satt till noll, vilket motsvarar sprucken betong, var resultaten för modellerna enhetliga. Att reducera styvheten i tvärriktningen, till följd av uppsprickning, visade sig ha liten inverkan på momentfördelningen i broplattan.

Ett krav i Eurokod visade sig vara problematiskt för den här typen av efterspänd bro. Kravet gäller spänningar i betongen kring spännarmeringen och ett förtydligande av hur detta krav ska tolkas behövs.

Nyckelord: FEM, plattrambro, efterspänning, förspänning, balkelement, skalelement, böjmoment, sprickning, tvärkontraktion, Poissons tal, styvhet i tvärled

Contents

Preface

In this master's thesis project, the finite element method has been used to investigate how different modelling techniques describe the structural behavior in a post-tensioned concrete slab bridge. This project was carried out at Norconsult's office in Gothenburg between January 2017 and June 2017.

We would like to thank our supervisor Ginko Georgiev at Norconsult for valuable guidance and sharing of knowledge throughout the project. We would also like to thank our examiner Morgan Johansson at Norconsult/Chalmers for his engagement in the project and helpful input.

Göteborg, June 2017

Joel Eriksson & Adam Jonsson

Notations

Roman upper case letters

A_p	Cross section area of prestressing tendons
E	Young's modulus
G	Shear modulus
G_k	Self-weight and permanent load
I	Moment of inertia
K	Torsional stiffness
M	Bending moment
Mi	Bending moment in a beam element about the local i-axis
Mii	Bending and twisting moment in a shell element in the local ii-direction
P	Prestressing force
Q_k	Live load
Ri	Rotational degree of freedom about the local i-axis
T	Torsional moment
Ui	Translational degree of freedom in the local i-axis
Vi	Shear force in a beam element in the local 1-i plane

Roman lower case letters

e	Eccentricity
f_{ck}	Characteristic concrete strength
$f_{p0,1k}$	Nominal yield strength of prestressing tendons
f_{pk}	Nominal tensile strength of prestressing tendons
k	Wobble coefficient
m_i	Bending moment per unit length in i-direction
m_{it}	Design moment for reinforcement in i-direction
q	Distributed load
t_x	Torsional moment used to calculate the design moment for reinforcement
w	Crack width
x	x-coordinate
y	y-coordinate
z	z-coordinate

Greek letters

α	Change of slope of the tendon profile
γ_i	Partial factor for load i
Δs	Anchorage set slip
ε	Strain
μ	Coefficient of friction
μ_1, μ_2	Factors used to calculate the design moment for reinforcement
ν	Poisson's ratio
ξ	Reduction factor for unfavourable permanent loads

σ	Stress
$\sigma_{allowed}$	Maximum allowed tension stress in prestressing tendons
σ_i	Normal stress in i direction
σ_p	Tendon stress

1 Introduction

1.1 Background

Concrete bridges are a common solution for short and mid-range span bridges in Sweden. A big advantage with concrete is that it is moldable, i.e. it can be shaped in many ways for different applications. Common concrete bridge types are portal frame and slab bridges (short spans), beam-and-slab bridges (small-mid range span) and box girder bridges (midrange/larger spans).

In concrete bridges, it is common to use prestressed reinforcement. An advantage with prestressed reinforcement is that it allows for better usage of the material per meter length, thus making possible bridging larger spans. The prestressed concrete is also designed to be uncracked during its serviceable lifetime, which significantly increases the durability of the concrete structure.

The prestressed reinforcement is naturally placed along the main bearing direction of the bridge structure, i.e. the longitudinal direction. For a typical beam-type structure this becomes also the main reinforcement and using the beam theory for section force distribution gives a rather straight forward methodology for analysis and design. The structural response of a slab bridge, on the other hand, is more complex since e.g. loads, stresses and stiffness not only distributes in the longitudinal direction, but also in the transverse direction. For such cases, it is not always possible to describe the behavior using a 2D beam model. To be able to correctly represent the complex response of a slab structure, a common solution is to use the finite element method (FEM).

Mainly three types of elements are commonly used in FE-analysis. Those are beam, shell and solid elements. These elements are better suited for different applications and should be chosen depending on the objective of the analysis. A FE model is an approximation and is not able to capture every effect that exist in reality. Furthermore, a very detailed model (e.g. solid elements), can be extremely impractical to use for design purposes. It is therefore not obvious in what way a concrete slab bridge should be modelled – how to represent the concrete structure itself or how to apply the prestressing. It is equally important to choose modelling technique that would be practical so that the current requirements and wanted output by the design codes are satisfied.

There are naturally regulations regarding concrete structures that must be fulfilled. The Eurocode does for example specify limits for stresses such as maximum allowable tensile stress in certain regions. This makes the choice of modelling technique important, since it should be able to describe the stresses in those regions. However, at the same time the regulations can in some applications be rather vague and hard to interpret.

1.2 Problem description

In order to illustrate the problem at hand, a typical post-tensioned concrete slab bridge is chosen, see Figure 1.1. The chosen bridge has three-dimensional behavior due to the nature of a slab, which distributes load in both the longitudinal and the transverse direction. The columns will also give rise to load distribution in the transverse direction. The prestressing adds further complexity to the structure as it induces stresses to the whole structure, not only parallel to the tendons but also perpendicular to the tendons. It is not obvious what effects the prestressing have perpendicular to the tendons for this type of bridge.

The process of bridge design is tightly connected to regulations that must be followed and requirements in the code that must be fulfilled. The accurate representation of the structural behavior under the relevant loads is essential to that process. Thus, the three-dimensional behavior in the slab and the effects caused by the prestressing have to be described in a correct way. To achieve this, numerical models that can produce sectional forces and stresses, for which the code sets requirements, are needed.

There are several alternatives for the implementation of numerical models with the finite element method by the means of element type. Two of them stand out as viable practical choices: a model based on shell elements and a model using beam elements. However, it is not obvious if both of these models are able to describe the three-dimensional effects from the prestressing in a correct way.

The prestressing tendons are placed in the longitudinal direction of the bridge to control or prevent cracking. However, the prestressing cannot prevent cracking in the transverse direction. Thus, it may be reasonable to assume that the slab will crack in the transverse direction. Cracking affects the stiffness distribution and therefore also the response of the slab. The numerical model must be able to correctly reflect this behavior.

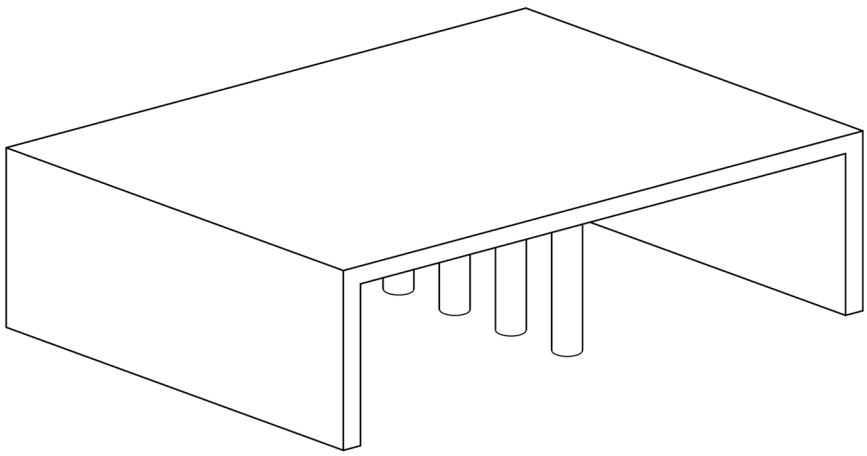

Figure 1.1 Schematic illustration of a post-tensioned concrete slab bridge.

1.3 Aim and objective

The aim of this master thesis was to look into and evaluate modelling techniques for post-tensioned concrete slab bridges, and the following questions were identified for the evaluation:

- How should a post-tensioned concrete slab bridge be modelled in 3D FEM concerning:
  - Choice of element types?
  - Application of the prestressing?
- If the slab cracks in the transverse direction, how will it affect the overall behavior of the structure?
- How should the requirements in the Eurocode be interpreted for this type of structure?

1.4 Limitations

One specific bridge geometry was considered for the analyses. The geometry was chosen so that a clear two-way behavior was obtained and to describe the effect of the post-tensioning. It was also made as simple as possible, e.g. no curved slab or changed dimensions of sections, to eliminate effects that a complicated geometry might cause. Further, support conditions, number of spans and dimensions were not changed as this study mainly focused on the influence of post-tensioning and modelling techniques.

The analysis in this project was limited to numerical models with linear elastic response. Only moment distributions in both the longitudinal and the transverse direction have been investigated.

Besides the prestressing load, the bridge has only been subjected to a uniformly distributed external load. Since the influence of the post-tensioning was the focus in this study, the effects from e.g. variable positions of the traffic load were not of interest.

1.5 Method

A literature study was performed to gain knowledge in the following subjects:

- Concrete slab bridges, in particular their three-dimensional structural behavior
- Post-tensioning in general and how to implement it in the FE software
- FE modelling, including element types, implementation of post-tensioning and modelling of slabs
- Regulations concerning slab bridges and post-tensioning

The FE modelling in the study has been carried out using the FE software SAP2000 (CSI, 2016). Mainly two techniques have been used to create the FE models. The first is a shell model which mostly consist of shell elements and the second is a beam grillage model which only consist of beam elements. In SAP2000, there are two different methods to define the prestressing load and both have been used in order to investigate its influence on the response in the slab.

To be able to investigate the influence of cracking in the slab, the Poisson's ratio and the Young's modulus have been modified to represent a cracked concrete slab. In reality, it is the moment of inertia that change when a section cracks and not the Young's modulus. However, in FE modelling it is easy to change Young's modulus and by doing so, the stiffness is reduced.

The results for the bridge slab is presented as moment distributions in predetermined sections for chosen loads. The output from SAP2000 has been exported to Excel for post-processing and plotting of moment diagrams. The results of the analysis are checked against the regulations to see whether the requirements can be met and equally important – where the regulations are straightforward and where certain interpretations are needed in the design of this particular type of structure.

1.6 Outline of the report

Chapter 2: This chapter contain theories concerning post-tensioned concrete slab bridges and FEM. Further, applications used in SAP2000 are presented and described.

Chapter 3: Description of the FEM modelling. In this chapter, geometries, materials, static system, boundary conditions and loads are presented and how these are implemented in the models in SAP2000.

Chapter 4: Presentation of the results from the different evaluations.

Chapter 5: Discussion of the results from the FE-analysis. The chapter also includes a discussion of the modelling.

Chapter 6: This chapter present the conclusions drawn in this thesis and also suggestions for further studies.

Chapter 7: References

2 Theoretical background

2.1 Bridges

Many types of concrete bridges exist with a variety of design and span lengths. Bridges can be shaped in many different ways and the design depends on e.g. the environmental conditions at the location. Examples of bridge types are girder, cantilever, suspension, arch, cable-stayed, box-girder, slab and slab-girder bridge. The different bridge types are suitable for different span lengths.

Concrete bridges may be prestressed to increase the durability. The bridges mentioned above can all be prestressed. However, the prestressing tendons can be arranged in various ways for different types of bridges. In e.g. a girder bridge the tendons are placed in the girder, in a slab bridge the tendons are placed in the slab, but in a box-girder bridge the tendons can be placed either in the webs of the box or placed externally; i.e. not embedded in the concrete.

A common bridge type for short spans is the slab bridge, which can have one or multiple spans. The slab may be simply supported at the ends or connected to the supports, allowing moment to be transferred, and intermediate supports may consist of either columns or walls. When the slab is fully connected to supporting walls at the ends it is called a portal frame bridge.

Slab bridges can be used for many different purposes, for example as railway, road, pedestrian and bicycle bridges and wildlife crossings. This bridge type can be very wide, which may be advantageous, e.g. if the bridge shall have several traffic lanes. Such a bridge type is also advantageous if the bridge should serve as a wildlife crossing, which need to be wide in relation to its length (Jakobi & Adelsköld, 2012).

2.2 Load distribution in concrete slabs

A slab is a structural member that allows load to be distributed in more than one direction. How the load is distributed in a slab is governed by its boundary conditions and stiffness distribution.

Boundary conditions for a slab could for example be simply supported or fixed along the edges. Since a fixed edge provides more stiffness, more load will be attracted to that edge. Figure 2.1 shows how the load distribution may differ in a slab, subjected to a uniformly distributed load, with different boundary conditions. In the figure, it can be seen how the degree of fixation affect the load distribution and that a stiffer support attracts more load.

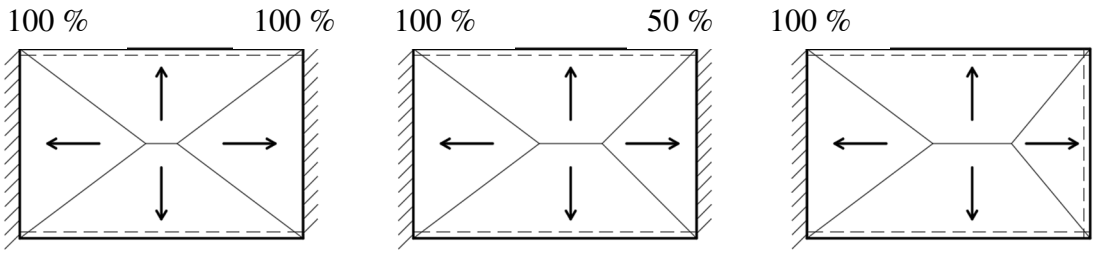

Figure 2.1 Load distribution in a slab, subjected to uniformly distributed load, with different degree of fixation on the right boundary (Engström, 2014).

To further describe the structural response in a slab, the moment distributions for different cases of support conditions are illustrated in Figure 2.2 to Figure 2.4. The illustrations are made by Hallbjörn (2015).

In Figure 2.2, the moment distribution for a slab simply supported along two edges loaded with a point load is shown. It is clear that mostly positive moment, i.e. tensile stresses on the bottom face, develop in the longitudinal direction. However, close to the supports, the moments change direction and small negative moments, i.e. tensile stresses on the top face, develop. This suggests that the load is distributed not only in the longitudinal direction, but also in the transverse direction.

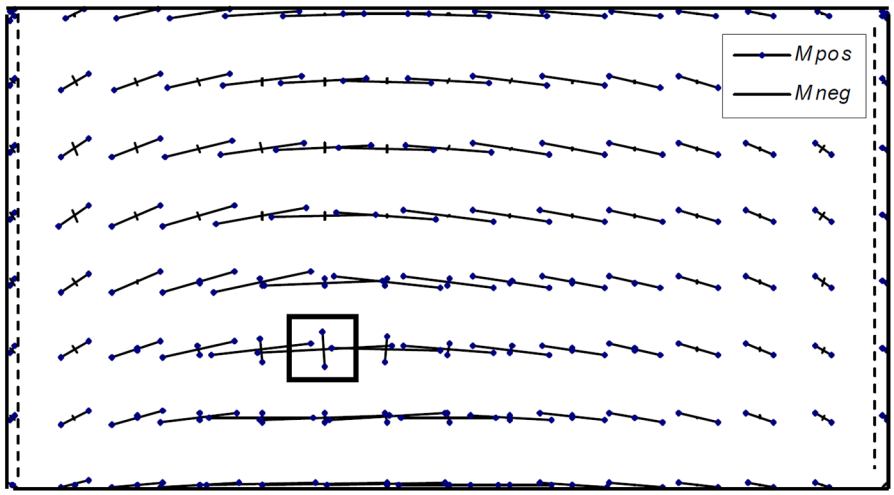

Figure 2.2 Moment distribution for a slab, simply supported along the two short edges, loaded by a point load (the square), according to Hallbjörn (2015).

In Figure 2.3, the slab is instead simply supported along all its edges. Most of the load will be distributed in the transverse direction since load will mainly be carried the shortest distance (Engström, 2014). This can clearly be seen in the figure where the largest moments develop in the transverse direction.

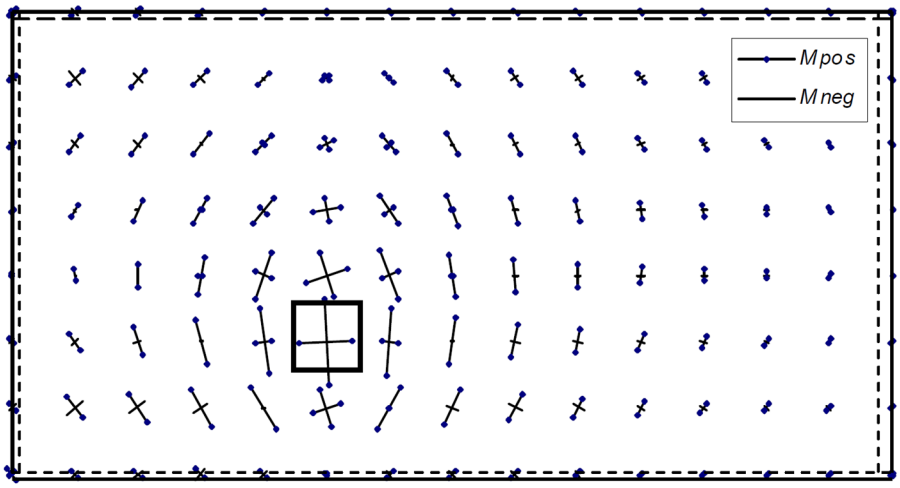

Figure 2.3 Moment distribution for a slab, simply supported along all edges, loaded by a point load (the square), according to Hallbjörn (2015).

In Figure 2.4, the slab is fixed along one edge while the other edges are free. In similarity to a beam, large negative moments develop along the fixed support. However, at the point load, positive moments develop, mostly in the longitudinal direction, which is different from a beam.

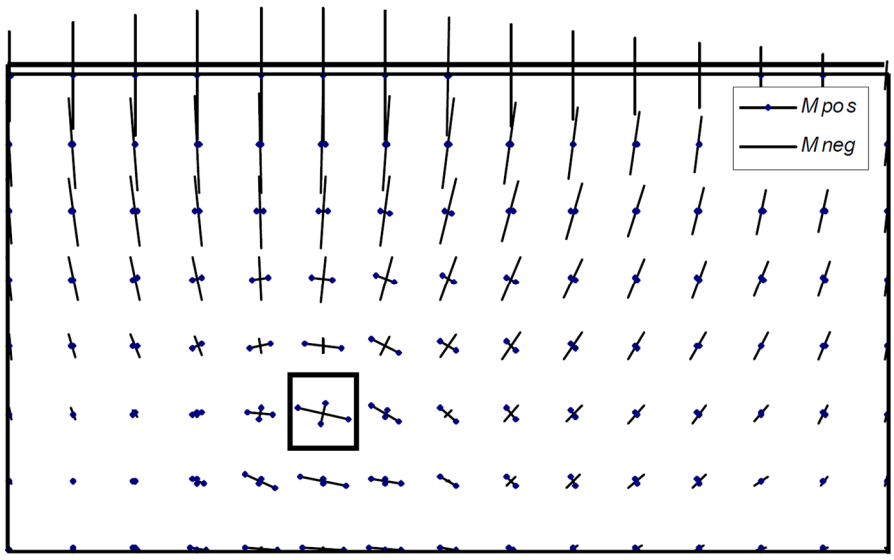

Figure 2.4 Moment distribution for a slab, fixed along one edge, loaded by a point load (the square), according to Hallbjörn (2015).

Based on these figures, it is clear that the boundary conditions affect the moment distribution of a slab and that the moment distributes in more than one direction. It is important that a model is able to capture these effects correctly and that the boundary conditions are carefully considered.

The load distribution does not only depend on loading and boundary conditions, but also on the stiffness distribution. In a cracked concrete slab the stiffness depends on the reinforcement. Since a slab is statically indeterminate, it can have any load distribution, as long as equilibrium is fulfilled, and hence the designer can influence the load distribution in a slab by choosing reinforcement distribution.

2.3 Concrete

Concrete is strong in compression but weak in tension i.e. the part of a concrete member that is in tension will crack and cause failure in the section at an early stage, see M_{cr} in Figure 2.5a. To increase the capacity of a member the concrete need to be reinforced in the zones where tensile stresses appear.

There are different methods for reinforcing concrete. The most common is to use regular steel reinforcement placed in the tensile zone. This kind of reinforcement will however not prevent cracking, but keep the equilibrium in a section when the concrete cracks. This will allow a concrete member to take more load, since the reinforcement will now transfer the tensile stresses when the concrete cracks. A consequence of cracking is decreased flexural stiffness of the member, and is visualized as a decreased slope in Figure 2.5b.

In order to maintain an uncracked concrete section and utilize the full stiffness, cracking in all sections should be avoided. By prestressing the element with a compressive force before the external load is applied, a higher load is required before cracks develop. Thus, the moment required for cracks to develop, M_{cr}, will increase and the response will maintain the steeper slope (state I) for higher loads. This implies that a higher stiffness can be utilized in the service state. When the prestressed concrete member cracks, the response become more complex than for a reinforced concrete member. However, the ultimate strength is not significantly affected by the prestressing.

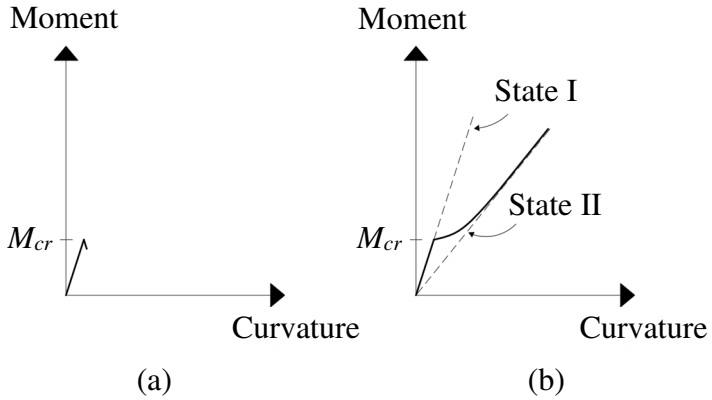

Figure 2.5 Schematic response of a concrete section a) plain concrete b) reinforced concrete

In a structural analysis of a concrete member, cracking needs to be considered since the stiffness of the member is affected by cracking. If the tensile stresses in a section does not exceed the tensile strength of the concrete, the section can be assumed uncracked. In an analysis of an uncracked section the whole concrete section can be utilized including the reinforcement, see Figure 2.6a. This is called state I.

If the stresses instead do exceed the tensile strength of concrete, the section can be assumed cracked. In such sections, the part of the concrete that is in tension cannot be utilized and only the reinforcement can transfer tensile stresses, see Figure 2.6b. Since parts of the cross section cannot be utilized, the moment of inertia will decrease, leading to a loss in stiffness. This is called state II.

In both state I and II the response of the section is linear elastic. However, if the response in either the concrete or the reinforcement begins to behave in a non-linear way, the section is in state III (Al-Emrani, et al., 2011), see Figure 2.6c.

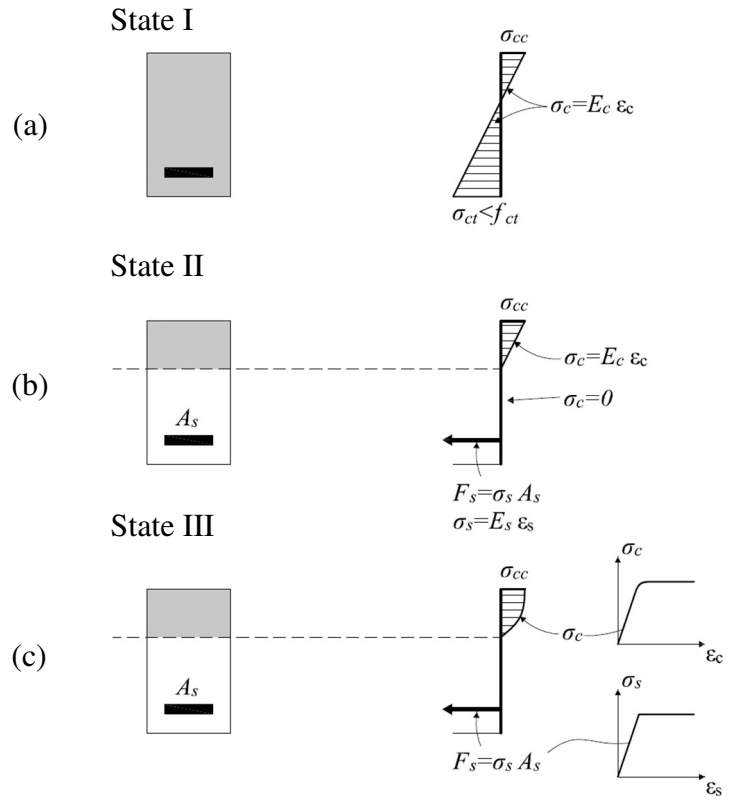

Figure 2.6 Different states for reinforced concrete. a) Uncracked state. b) Cracked state, linear response. c) Cracked state, non-linear response.

2.4 The Poisson effect

The Poisson effect describes the phenomena that occurs in a material when it is compressed or stretched. When the material is loaded it will expand or contract in the direction perpendicular to the load, see Figure 2.7. This effect is measured by the Poisson's ratio, which is the ratio between the strains perpendicular and parallel to the loading. In design, the value of the Poisson's ratio is chosen. For a concrete slab, the Poisson's ratio should be set to 0.2 when the slab is assumed uncracked and zero when the slab is assumed cracked, according to Eurocode.

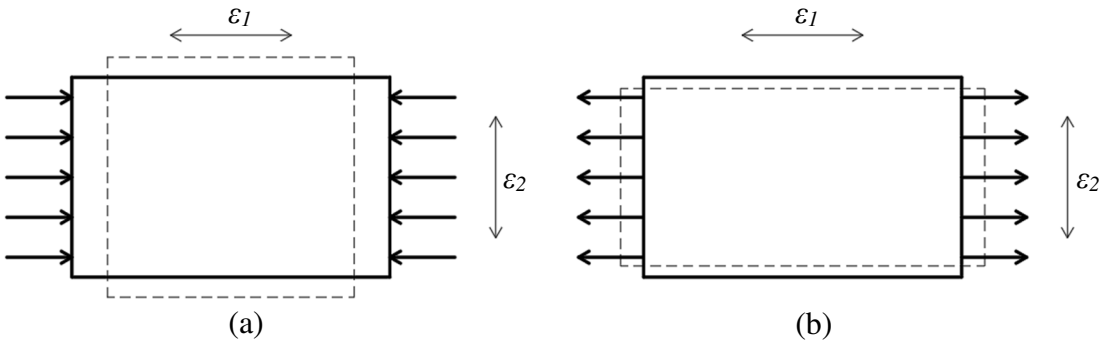

Figure 2.7 Illustration of the Poisson effect. a) transverse expansion due to longitudinal compression. b) transverse contraction due to longitudinal elongation.

2.5 Orthotropic material

Unlike an isotropic material where the material properties are the same in all directions, the properties in an orthotropic material vary in each direction. When it comes to a reinforced concrete slab, it can be assumed isotropic as long as it is uncracked. However, when the concrete slab cracks in one direction, the stiffness is reduced in the cracked direction; i.e. the slab becomes orthotropic. This lead to a redistribution of loads, where more load is taken in the stiffer direction.

2.6 Prestressing

2.6.1 Prestressing techniques

The prestressing of a concrete member is in most cases done by pre- or post-tensioning. The distinctive difference between the methods is whether the concrete is cast before or after the tension force is applied to the steel tendons. The prestressing steel, referred here as tendons, can be individual strands, multiple strands, wires or bars – almost always certified for a specific type of prestressing method.

The pre-tensioning method is more or less restricted to prefabricated elements and is not relevant for the current project.

Prestressing by post-tensioning is done by tensioning the tendons after the concrete is cast and has gained strength. The tendons are placed in ducts either before or after casting. The ducts are always placed in the mold before casting. When the concrete has hardened, the tendons are tensioned by a hydraulic jack, from one or both ends, introducing compressive stresses to the concrete. After the tendons have been tensioned, the ducts are grouted protecting the tendons from corrosion, see Figure 2.8. The grout also creates a bond between the concrete and the tendons and is usually cement based (Hewson, 2003).

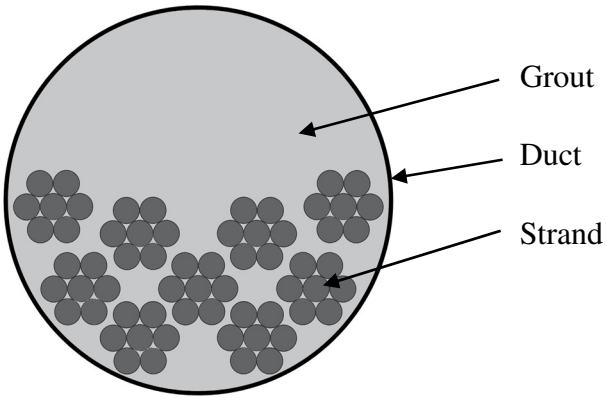

Figure 2.8 Cross section of grouted duct with multiple strands.

An advantage with post-tensioning is that the ducts can be placed in a shape corresponding to the moment curve. This allows the prestressing to more effectively counteract the moment caused by external loading and by that, eliminate or decrease the tensile stresses.

A two-span beam, subjected to an evenly distributed load, will naturally get positive moment in the fields and negative moment at the mid support. Hence the tendons in Figure 2.9 are placed so that the prestressing will counteract these moments and therefore be favorable in both spans and at the interior support.

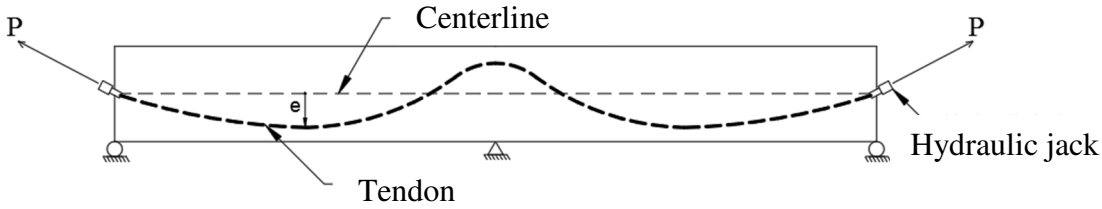

Figure 2.9 Schematic tendon profile for a two-span beam.

2.6.2 Primary and restraining effects

The prestressing force, P, and its eccentricity, e, from the center of gravity of the cross section, give rise to a moment $P \cdot e$. This moment is called "Primary moment" and since it depends on the eccentricity it will vary as the tendon profile varies. For the case with the beam in Figure 2.9, the resulting primary moment would be positive over the mid support and negative in the spans, see Figure 2.10.

The prestressing in the span in the beam in Figure 2.9 wants to deform the beam upwards and the prestressing over the mid-support want to deform the beam downwards. This deformation is caused by the primary moment. However, the mid-support will prevent the beam from vertical displacement, causing a restraining force. This restraining force give rise to a restraint moment, see Figure 2.10. In a statically determinate structure, there is nothing that can cause this kind of restraining force, hence restraint moments will only occur in statically indeterminate structures.

The resultant moment caused by the prestressing will consist of the combined effect from the primary moment and the restraint moment, see Figure 2.10. For a statically

determinate structure, the resultant moment will be equal to the primary moment since no restraint moments appear in such structures.

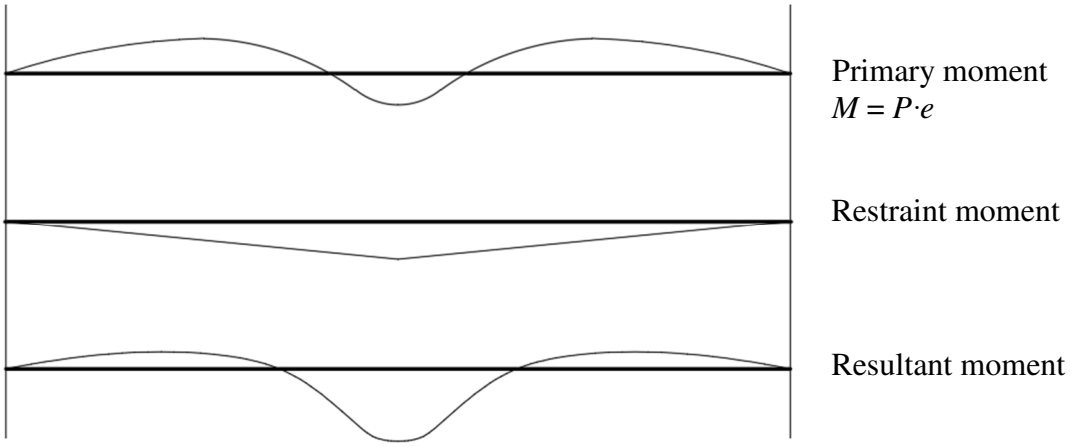

Figure 2.10 Schematic moment distributions for primary moment, restraint moment and resultant moment caused by the prestressing

2.6.3 Immediate prestress losses

There are mainly three immediate losses that occurs in a post-tensioned concrete member: frictional loss, anchor slip and elastic shortening.

Friction occurs between the prestressing steel and the ducts because of intended or unintended curvature of the tendon profile. Due to frictional losses, the prestressing force, P, will decrease along the length of the tendon. The frictional loss due to unintended curvature is referred to as “wobble friction” and is always present, even in straight profiles.

For curved profiles, the rate of frictional loss depends on the curvature i.e. greater curvature result in larger friction and thus larger loss. Since the frictional loss increases along the length, the loss can be quite substantial at the far end of the tendon. However, if the tendon is instead tensioned from both ends, the losses are more evenly distributed along the member (Collins & Mitchell, 1991), see Figure 2.11.

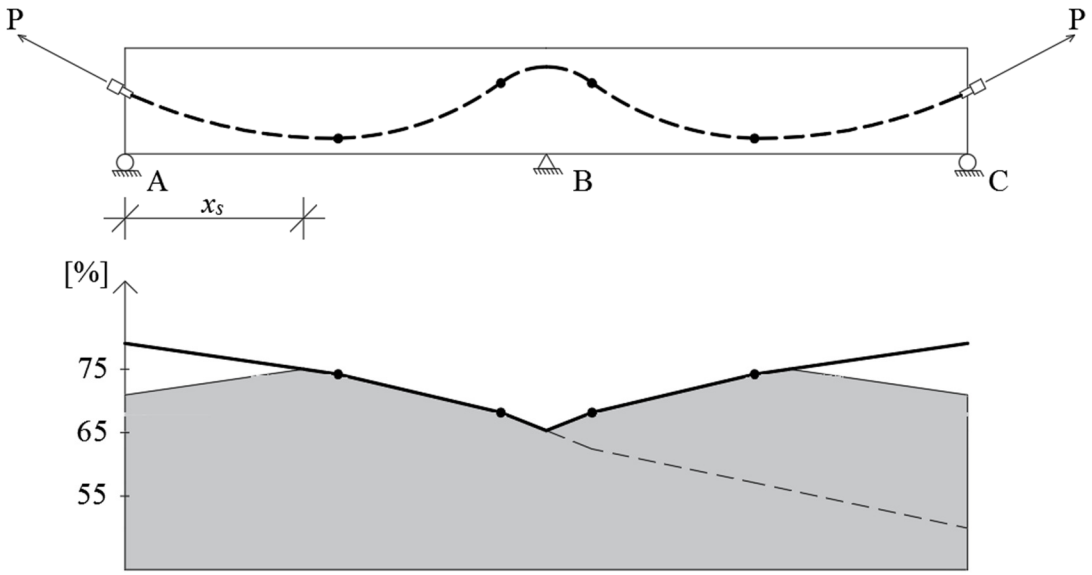

Figure 2.11 Schematic illustration of how the prestressing force varies along the length of a post-tensioned beam, tensioned from both ends, due to frictional loss and anchor slip. The vertical axis shows percentage of the ultimate capacity of the tendon. The thick line shows the tendon force before anchorage. The dashed line shows how the prestressing force would vary if only tensioned from end A.

In most anchoring systems, the tendons will slip into the ducts, causing a decrease of strain and therefore decreased prestressing force at the ends. However, the anchor slip is counteracted by friction in the ducts and at a certain distance, x_s, from the anchor, the prestressing is assumed to be unaffected by the anchor slip, see Figure 2.11.

When a member has multiple tendons, elastic shortening will occur during tensioning. As one tendon is tensioned the concrete will shorten leading to decreased strain in all previously tensioned tendons. This decrease of strain lead to a decreased prestressing force.

2.6.4 Long-term prestress losses

In addition to the immediate losses, there are other phenomena decreasing the effect of the prestressing during long time. The most dominant are shrinkage, creep and relaxation.

Concrete will naturally shrink due to drying and the chemical reaction during hardening. This is a slow process and will continue during the entire lifetime of the concrete. Since the shrinkage give rise to shortening of the concrete the strain will also decrease in the tendons leading to a decreased prestressing force.

When concrete is loaded, the deformation can be divided into instant and time dependent. The instant deformation is elastic and the time dependent is called creep and will increase over time. The creep deformation is stress dependent and proportional to the concrete stress. The creep caused by the compression from the prestressing will cause shortening of the concrete. Also, this lead to decreased strain of the tendons and decreased prestressing force.

The force needed to keep a steel tendon at a constant elongated strain will decrease over time. This phenomenon is called relaxation. This effect has substantial influence when the steel is subjected to large strains, which is the case for prestressed steel. This will lead to decreased prestressing force over time.

2.7 FEM-theory

2.7.1 Orientation

The finite element method is a numerical method and an approximation which can be used to describe the behavior of a structure. In a FE model the structure is discretized into a finite number of elements. These elements can be of different types such as beam, shell and solid elements. The choice of elements will affect the result of the analysis and it is important to choose elements that effectively can describe what should be investigated. This section will introduce important concepts in FEM. Also, the beam and shell elements will be described and how they are implemented in the software SAP2000 (CSI, 2016).

2.7.2 Discretization

A structural element, e.g. a beam, can be analytically described using differential equations. These equations describe the behavior in every section of the structural element. However, these equations can be rather complex and difficult to solve. In FEM, the structural element is discretized into a finite number of smaller elements, see Figure 2.12. These elements are simpler and easier to describe than the complex structural element. The finite elements are connected in nodes where translations and rotations are described. From these, the stresses and sectional forces can be calculated and approximated over the element.

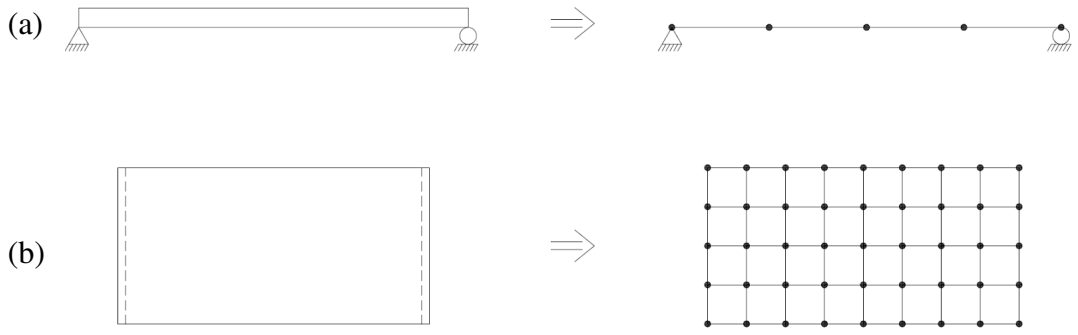

Figure 2.12 Examples of discretization of continuous systems a) A beam divided into four beam elements. b) A slab divided into 32 shell elements.

2.7.3 Beam

2.7.3.1 Beam theory

A beam is characterized by its extension in the longitudinal direction relative to its height and width is large. The member is loaded in its transversal direction and distributes the load in its longitudinal direction.

There are mainly two theories describing the behavior of a beam which are the Euler-Bernoulli and the Timoshenko beam theories. Essential for both theories are the assumption that plane sections remain plane during deformation. A significant difference for the theories are that the Euler-Bernoulli theory also assumes that plane sections remain normal to the beam axis, but Timoshenko allows for the sections to rotate. The Timoshenko beam theory is more suited for beams with great height relative to its width (Ottosen & Petersson, 1992).

2.7.3.2 Beam element

A beam is in reality a three-dimensional object, but its axial extension dominates the structural response. This allows the beam to be simplified, through some assumptions in FEM, into a linear element. A beam element is confined by two nodes. Every node has a number of degrees of freedom that describes translation and rotation. From the degrees of freedom, quantities such as moments and stresses can be calculated.

2.7.3.3 Beam element in SAP2000

In SAP2000, a beam or column can be described by a so called “frame object”. This object is drawn in the interface of SAP2000 and is defined between two points. To this object, different cross-sectional properties and loads are assigned, which can vary over the length. When an analysis is run in SAP2000, the frame objects is automatically converted into frame elements (CSI, 2016).

A frame element is confined by two nodes, in similarity to the beam element, and each node has six degrees of freedom. These describe translation along the local 1, 2 and 3 axis, and rotation around the local 1, 2 and 3 axis, see Figure 2.13a. This allows the frame element to describe biaxial bending, torsion, axial deformation and biaxial shear deformation. The internal forces shown in Figure 2.13b can be found at any section along the element, and are calculated by integrating the stresses over the cross section (CSI, 2016).

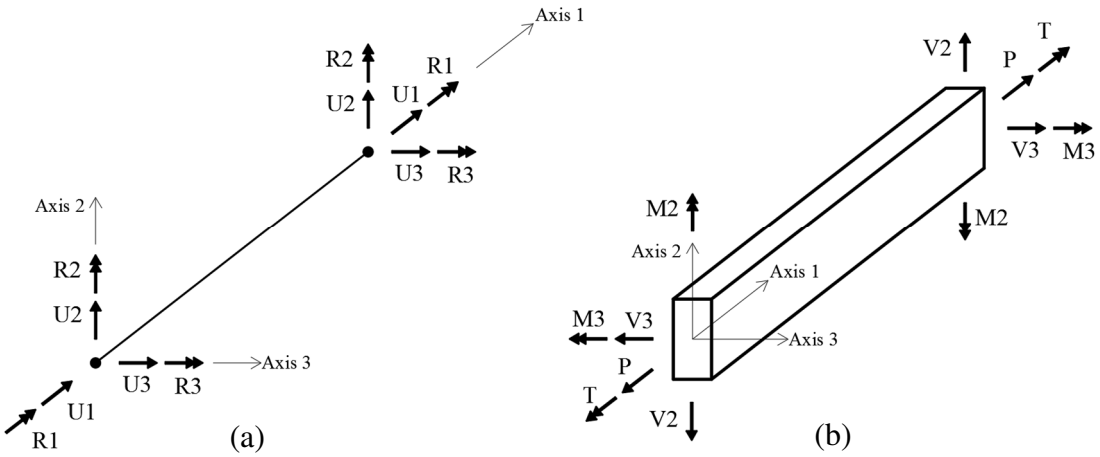

Figure 2.13 a) Degrees of freedom for a frame element in SAP2000. b) Internal forces and the local coordinate system for a frame element in SAP2000.

If the Self-Weight Load is activated in SAP2000, the self-weight of the frame object is automatically calculated. The load will be a distributed load along the length of the frame and is calculated by multiplying the density of the applied material with the area of the cross section. The self-weight load always acts in the global negative z-direction. Distributed loads can be applied in a specified direction as "Distributed Span Loads" with the unit N/m. Hereafter, the "frame object" will be referred to as "beam element".

2.7.4 Plate

2.7.4.1 Plate theory

A plate can generally be described as a structure with a relatively small thickness compared to its dimensions in the plane and is loaded in the normal direction to the plane. In similarity to the beam theories, the plate theory is based on a number of assumptions linked to the characteristics of the plate.

The two most common theories when it comes to plates are the Kirchhoff and the Mindlin-Reissner plate theories. Similar to the Euler-Bernoulli beam theory, Kirchhoff assumes that plane sections normal to the mid-plane remain plane and normal to the mid-plane during loading. Also, the assumption that shear stresses are present in absence of shear strain is included in Kirchhoff's theory. This means that Kirchhoff's theory is most suitable for thin plates where the shear strains are small. For thick plates, shear strains may be of greater magnitude and then it is not clear if Kirchhoff's assumptions hold. To consider shear strains in plates the Mindlin-Reissner plate theory is more suitable (Ottosen & Petersson, 1992).

2.7.4.2 Plate elements

In FE modelling the most simple type of plate has three or four nodes where each node has three degrees of freedom that describes translation normal to the plane and rotation about the axes of the plane, see Figure 2.14a. This element can therefore only manage out of plane loading i.e. membrane action cannot be described since no in plane translational degrees of freedom are present.

To describe membrane action, a different type of plate element is used. Each node in this element has two degrees of freedom that only describes in plane translation, see Figure 2.14b. This only allows in plane loading of the element.

Plate and membrane elements can be combined to be able to describe both plate and membrane behavior. This type of element is called shell element and has accordingly translational degrees of freedom in all directions and rotational degrees of freedom about the axes of the plane in every node, see Figure 2.14c. This enables the shell element to manage both in and out of plane loading.

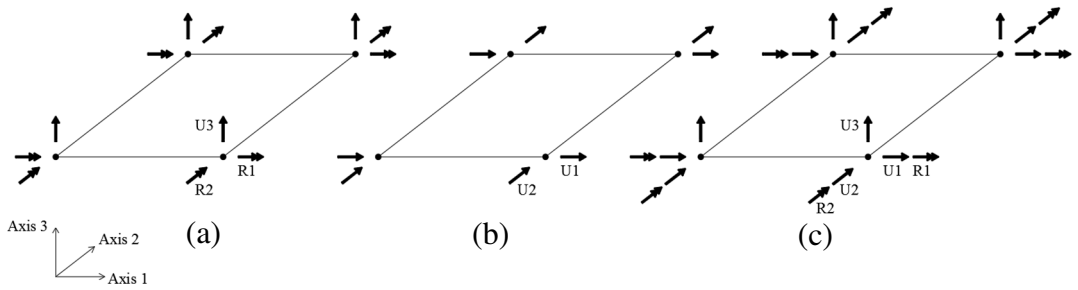

Figure 2.14 Degrees of freedom and the local coordinate system for a) a plate element, b) a membrane element, c) a shell element.

2.7.4.3 Shell element in SAP2000

In SAP200, a shell element is divided into four different types: Membrane, Plate, Shell and Layered. The type Membrane correspond to the membrane element described above with the additional ability to describe "drilling moment", see Figure 2.15b. This moment is caused by rotation about the out of plane axis. The type Plate correspond to the plate element described above, see Figure 2.15a. The type Shell is a combination of the Membrane and the Plate and can describe translation in all directions and rotation about all axes, see Figure 2.15c. The local axes 1 and 2 are always in the plane of the element, and axis 3 is always normal to the plane (CSI, 2016).

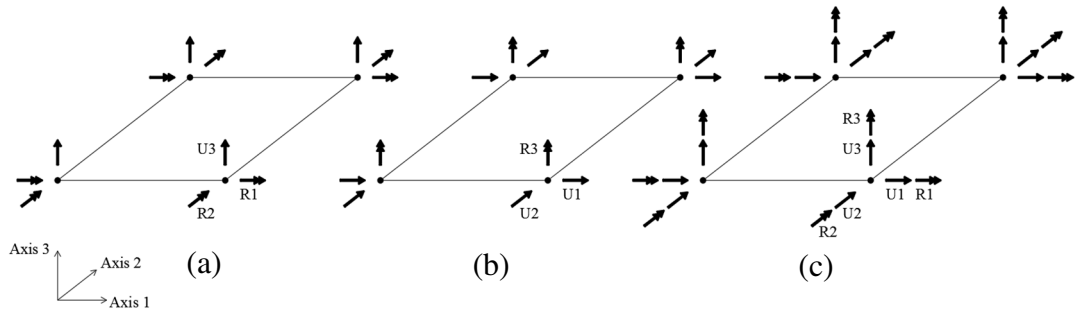

Figure 2.15 Degrees of freedom and the local coordinate system for a) the Plate, b) the Membrane, c) the Shell element, in SAP2000.

Internal forces and moments are calculated automatically in SAP2000 by integrating the corresponding stresses over the thickness of the element. Moments and their notation in a shell element in SAP2000 are defined in Figure 2.16. The moments are given per unit length.

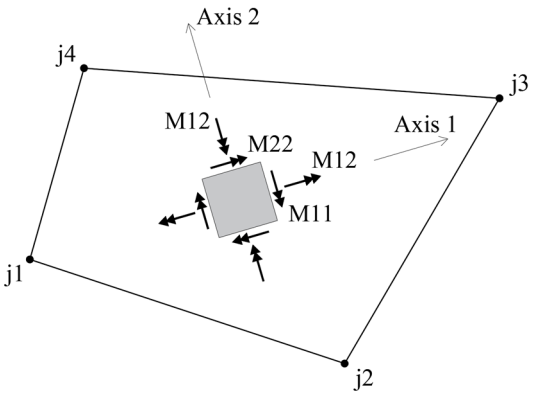

Figure 2.16 Definition of internal moments relative to its local axes for an arbitrary shell element enclosed by the nodes j1-j4 in SAP2000.

The Shell element can be defined as thick or thin where a thick element is described by the Mindlin-Reissner theory and the thin by the Kirchhoff theory. The three types of elements, Membrane, Plate and Shell, only allows linear elastic response and homogenous material.

The fourth type of shell element is called Layered. This type of element has multiple layers where each layer can have different material properties and thicknesses etc. It also allows for non-linear response of the materials.

If the Self-Weight Load is activated in SAP2000, the self-weight is automatically applied in the negative z-direction to all elements in the model. In the shell elements, the self-weight is evenly distributed over the element and are equal to the density of the applied material times the thickness of the element.

Uniform load can be applied in a specified direction, which applies the distributed load with the unit N/m^2 to the mid-surface of the element. The distributed load is multiplied by the mid-surface area and is apportioned to the nodes of the element.

2.7.5 The tendon object

The tendon object in SAP2000 is a special type of object used to model prestressing and post-tensioning and is not an ordinary finite element. The object is drawn as a line and the program automatically connects the tendon object to the nodes in the elements which it passes through. The tendon object can be embedded in beams, shells, planes, asolids and solids.

When a line has been drawn, the tendon profile can be defined. The profile can be e.g. straight or parabolic between the defined points. Also materials and section need to be assigned to the tendon object. The program will automatically discretize the object into smaller objects, and the length of the objects can be chosen. Each joint has six degrees of freedom. However, no additional degrees of freedom are introduced to the model since the tendon object is constrained by the element it passes through, i.e. the load in the tendon is transferred to the nodes of the element.

The prestressing load can be defined either as a force [N] or as a stress [Pa], which requires the correct cross-sectional area of the tendon to be specified, and corresponds to the tension in the tendon before losses. Also where the load is applied need to be

specified i.e. if the tendon is tensioned from one or both ends. The losses due to friction and anchor slip is automatically calculated by SAP2000. This requires the change of slope of the tendon profile between x and the jacking end, α, coefficient of friction, μ, the wobble coefficient, k, and the anchorage set slip, Δs, to be specified. SAP2000 use Equation 2.1 to calculate the frictional loss for the prestressing load along the tendon (Kalny, 2013).

$$P(x) = P_0 \cdot e^{-(\mu\alpha + k^* x)} \tag{2.1}$$

where

$$k^* = \mu \cdot k \tag{2.2}$$

Note that Equation 2.1 is slightly different than Equation 2.3 which is given in Eurocode 2.

$$P(x) = P_0 \cdot e^{-\mu(\alpha + kx)} \tag{2.3}$$

These equations are basically the same. The difference is how the wobble coefficient, k, is defined. In addition to these losses elastic shortening, creep, shrinkage and relaxation need to be specified. These additional losses are given as a loss in stress [Pa] and have to be calculated by hand.

There are two ways to define the prestressing load in SAP2000. The first is to define it as a load and the other is to define it as an element.

2.7.5.1 Tendon as load

When the prestressing load is defined as load, it is only considered as a load that act upon the element in which it is placed, and not as an actual object in the model. Losses, such as shrinkage, creep and elastic shortening, must be specified manually as stress losses and cannot be calculated by the program. Note that the self-weight and contribution to stiffness of the tendon is not considered, since the tendon is only considered as a load.

2.7.5.2 Tendon as element

When the prestressing load is defined as elements, the tendon is represented by independent elements. For linear elastic analysis, the losses due to shrinkage, creep and relaxation need to be specified manually as stress losses. However, the losses due to elastic shortening is automatically calculated by SAP2000. If a non-linear analysis is carried out, the prestressing load must be defined as elements. SAP2000 can in this case, i.e. in a non-linear analysis, calculate the losses due to long term effects automatically. Since the tendon is represented by elements, their self-weight and stiffness will automatically be considered.

2.8 Modelling of a slab in FEM

2.8.1 Modelling using shell elements

A slab can be modelled using shell elements. A shell element extends in the plane in a similar way as a slab does. This allow a shell model to describe the geometry of a slab very well. A shell element can describe load distribution in all directions, which is necessary to describe its behavior. Also, an advantage with shell elements is that the applied load can be defined as an area load on the element.

2.8.1.1 Problem with singularities

When modelling a slab supported by a column, the connection is usually modelled in a single point. This will cause a singularity in the FE solution. That means that the results in that point will be incorrect and should not be used in design. According to Pacoste (2012) there are two methods to handle such singularities. The first is to model the column in a way so that the singularity does not appear.

The other method is to disregard the results in the point where the singularities appear; instead the results are evaluated in adjacent nodes. The nodes of interest depend on the support condition. If the slab and column are monolithically connected, the interesting section will be at the edge of the column. If instead the slab is simply supported, the interesting section depend on the contact surface, see Figure 2.17. If the surface consists of a very stiff bearing plate, the interesting section will appear at the edge of the plate, as indicated in Figure 2.17a. If instead the bearing plate is flexible, the interesting section will appear between the edge of the plate and the center of the support, see Figure 2.17b.

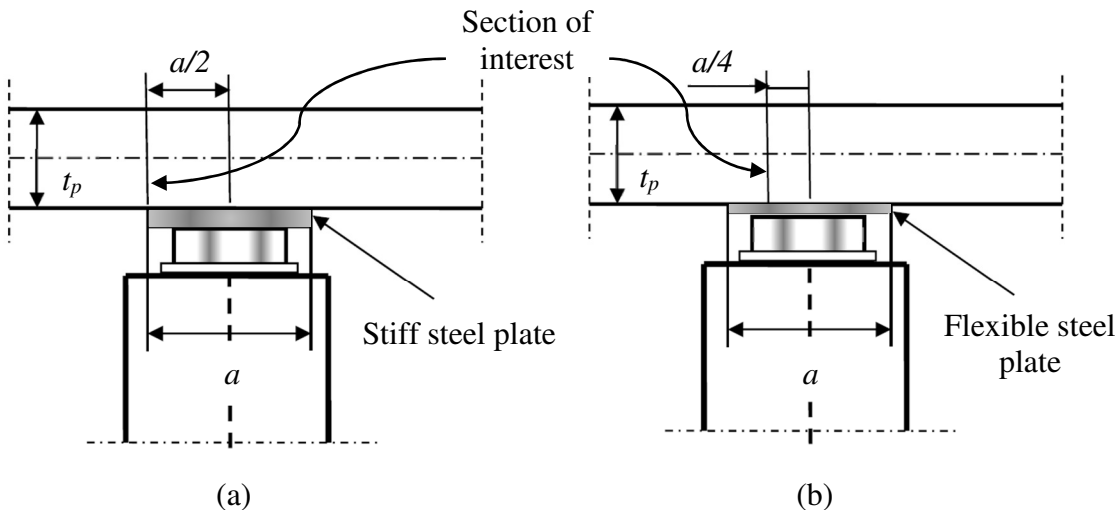

Figure 2.17 Location of the section of interest in a slab, at a column support, depending on the stiffness of the contact surface. a) stiff bearing plate, b) flexible bearing plate, according to Pacoste (2012).

To be able to get results in the interesting sections, there need to be nodes in those sections and hence may require the mesh around the column to be refined.

2.8.1.2 Mesh refinements

If the mesh is refined in a limited area, there will be sections at which the mesh size change, see Figure 2.18. The smaller elements create nodes along the edges of the larger elements. But these nodes are not automatically connected to the larger elements.

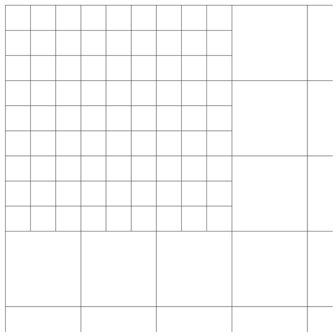

Figure 2.18 Area where elements of different mesh size meet.

To get the transition between mesh sizes to work, some measures need to be taken. One measure is to use distorted elements, whose shape is adjusted to connect the elements of different size. Examples of this can be seen in Figure 2.19.

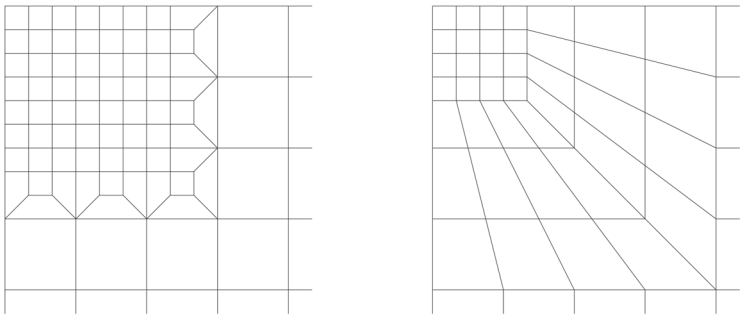

Figure 2.19 Two examples of transition between different mesh sizes using distorted elements.

Another measure to solve the transition between the mesh sizes in SAP2000 is to use "edge constraints". This means that the nodes that are on the edges of a larger element will be connected to the corner nodes of the larger element. This allows the mesh to remain the same. The deformation of the nodes on the edges is determined by interpolating the deformation of the corner nodes.

According to CSI (2016), using "edge constraints" instead of distorted elements could give more accurate results. Regardless of which technique is used, the accuracy of the results at the transition is governed by the larger element. For this reason, the transition sections should be avoided in sections where accurate results are wanted.

2.8.1.3 Combined effect of bending and torsional moment

According to Hallbjörn (2015), the reinforcement in a concrete slab should be designed with regard to the combined effect of bending and torsional moment. The reinforcement that should take positive moments should be designed for the moments according to Equation 2.4 and 2.5.

$$m_{xt} = m_x + \mu_1 |t_x| \tag{2.4}$$

$$m_{yt} = m_y + \frac{1}{\mu_1} |t_x| \tag{2.5}$$

The reinforcement that should take negative moments should be designed for the moments according to Equation 2.6 and 2.7.

$$m_{xt} = m_x - \mu_2 |t_x| \tag{2.6}$$

$$m_{yt} = m_y - \frac{1}{\mu_2} |t_x| \tag{2.7}$$

where

m_x and m_y	are the bending moments in x- and y- direction and corresponds to the moments M11 and M22 in Figure 2.16
μ_1 and μ_2	are factors chosen with respect to practical aspects, often close to 1
t_x	is the corresponding torsional moment and corresponds to the moment M12 in Figure 2.16

As shown in Figure 2.16, SAP2000 outputs the bending and torsional moments separately. These moments need to be combined manually in the post-processing of the results.

2.8.1.4 Property modifiers

In SAP2000 it is possible to modify sectional properties by scale factors. This means that e.g. the bending stiffness corresponding to M11, M22 and M12 may be changed by assigning scale factors in SAP2000 named property modifier. This can be used to describe orthotropic behavior in a structural member which arise e.g. when cracking occurs. The property modifiers are given as input for the analysis. However, it is not clear in the software manual how the property modifier factors affect the analysis.

2.8.2 Modelling using a grillage

2.8.2.1 Geometry

A slab can also be modelled using a grillage, consisting of beam elements which are evenly placed in both the longitudinal and transversal direction. Hewson (2003) suggests that the ratio between the spacing of the longitudinal and the transversal beam elements should be between 1:1 and 1:2 to accurately capture the structural response of the slab.

A beam element extends in one dimension between two nodes. The element cross section is assigned by defining the height and width. The height corresponds to the height of the slab and the width correspond to the spacing between the elements.

How the beam elements should be placed is not obvious, especially concerning the beams along the edge of the slab. Since the assigned width of the cross section extend on both sides of the element, the placement of the element need to be considered. If the

outermost beam element is placed on the edge of the slab, the width of that element need to be half the spacing to match the total area of the slab. A consequence of this placement is that half of the cross section will be outside of the real slab area, see Figure 2.20a. There will also be a gap between the cross sections of the two outermost beam elements. This means that the real geometry of the slab is not perfectly reflected in the model.

If instead the outermost beam is placed away from the edge of the slab according to Figure 2.20b, all beam elements can have the same width, and the total area will correspond to the real area of the slab. However, a disadvantage for not placing the outermost beam element on the edge is that the placement of the transversal beams is not obvious. If the transversal beams are modeled to the centerline of the outermost longitudinal beam, the stiffness of the slab will not be correctly reflected. That is because the transverse beams will not reach the edge of the real slab i.e. parts of the slab in the transverse direction is missing.

If instead the transverse beams are modeled to the edge of the real slab, the parts extending beyond the outermost longitudinal beam will be short consoles. This will cause a negative moment in the transverse direction over the outermost longitudinal beam. Neither is a correct reflection of reality.

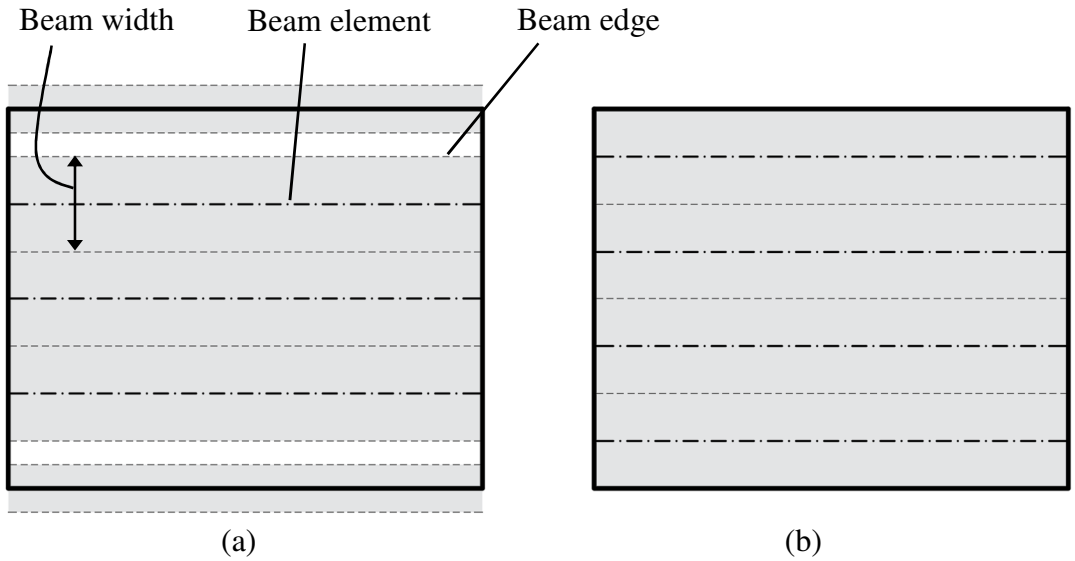

Figure 2.20 Placement of longitudinal beams in a grillage model. The thick line shows the real geometry of the slab. a) The outermost beam element is placed on the edge of the slab area. b) The outermost beam element is placed a bit away from the edge of the slab area.

2.8.2.2 Loads

The loads need to be adjusted in a grillage model to be able to reflect the real slab. The beam element can only describe a distributed load as a line load, which implies that the area load need to be converted into a line load. This is done by multiplying the area load with the cross-sectional width of the beam.

Line loads can be applied in different ways. One way is to apply all the load to the longitudinal beams, i.e. no load on the transversal beams. This may be reasonable if the load is mainly carried in the longitudinal direction. However, if the structural response in the transverse direction is of interest, all load may be applied on the transverse beams instead. For example, if the moment distribution in the transverse direction is of interest, the load could advantageously be placed only on the transverse beams to get a smooth moment curve. If the load, in this case, would be applied only on the longitudinal beams, they would act as point loads on the transverse beams causing a jagged moment curve. A third option is to apply half the load on the longitudinal beams and half the load on the transverse beams.

Since the cross sections of the longitudinal and transversal beams are overlapping, the self-weight will be doubled if no measures are taken. The self-weight can, in similarity to the distributed load, be applied either only in the longitudinal direction, only in the transversal direction or half in each direction. This can be done by modifying the density assigned to the beams.

2.8.2.3 Additional considerations concerning modelling of a grillage

To reflect the behavior of an isotropic elastic slab, the torsional stiffness of the beams in the grillage need to be adjusted. According to Hewson (2003), the torsional stiffness for both the longitudinal and transversal beams should be set equal to twice the moment of inertia of the longitudinal beams i.e.

$$K = 2I \tag{2.8}$$

where

K is the torsional stiffness in a beam
I is the moment of inertia of a longitudinal beam

Another important aspect that need to be considered when using a grillage model is that the effect of the Poisson's ratio cannot be included in such a model. This is important to keep in mind, especially for prestressed structures, where this effect may have considerable influence.

2.9 Decompression limit in Eurocode

Eurocode sets requirements for concrete structures. There are specific requirements for post-tensioned structural members that need to be fulfilled. Such a requirement concerning crack widths is presented in Table 2.1. A post-tensioned concrete bridge need to fulfill the requirement of decompression under the frequent load combination. This means that the concrete, up to 100 mm from the tendon, should be in compression. However, the code does not distinguish stress orientation. The Swedish road administration states that this requirement should be fulfilled.

Table 2.1 Recommended values of crack widths w_{max} and relevant combination rules according to EN 1992-2:2005. Note that the requirements for the crack widths are different in Sweden, but the decompression requirement still applies.

Exposure Class	Reinforced members and prestressed members without bonded tendons	Prestressed members with bonded tendons
	Quasi-permanent load combination	Frequent load combination
X0, XC1	0,3[a]	0,2
XC2, XC3, XC4	0,3	0,2[b]
XD1, XD2, XD3 XS1, XS2, XS3		Decompression

[a] For X0, XC1 exposure classes, crack width has no influence on durability and this limit is set to guarantee acceptable appearance. In the absence of appearance conditions this limit may be relaxed.

[b] For these exposure classes, in addition, decompression should be checked under the quasi-permanent combination of loads.

In Norway, on the other hand, the requirement of decompression is more detailed. According to a calculation guide issued by the Norwegian public roads administration, the decompression requirement only applies in the longitudinal direction of a bridge (Johansen, 2017). This implies that tensile stresses are allowed to occur perpendicular to the tendons.

3 Description of FE-analysis

3.1 Geometry

3.1.1 Bridge geometry

The geometry of the bridge has been inspired by a real bridge, specifically a wildlife crossing, but with simplified dimensions. This is justified since the aim is to evaluate the effect of the prestressing on such a bridge, and a more complex geometry would not affect the outcome of interest. This allows the real dimensions to be somewhat adjusted for sake of simplicity.

The bridge is a two-span concrete frame bridge supported by walls at the ends and concrete columns in the middle. The walls are one meter thick and the columns are circular with a diameter of one meter, and the total height of the bridge is 7.5 meters. The slab is one meter thick and is post-tensioned in the longitudinal direction. A section of the bridge with relevant dimensions can be seen in Figure 3.1 and a plan view in Figure 3.2.

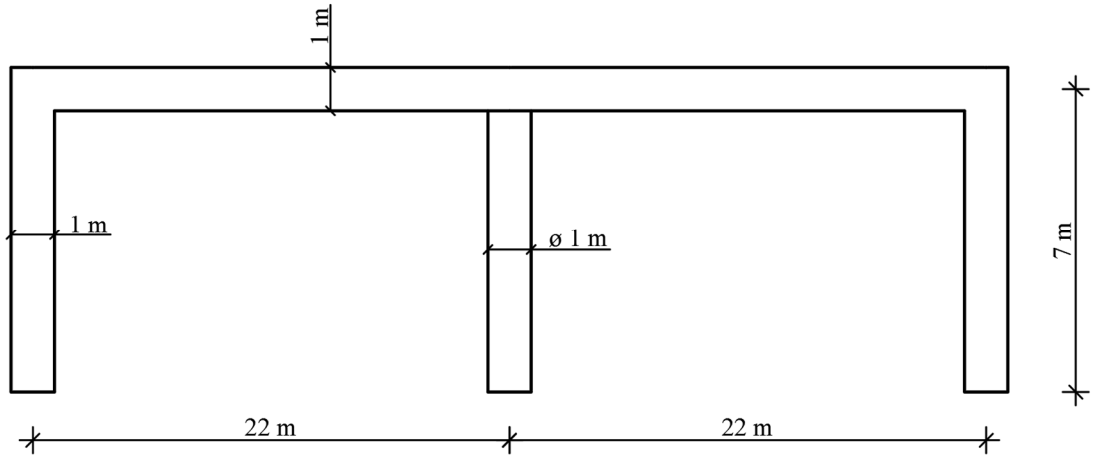

Figure 3.1 Section in the longitudinal direction of the bridge.

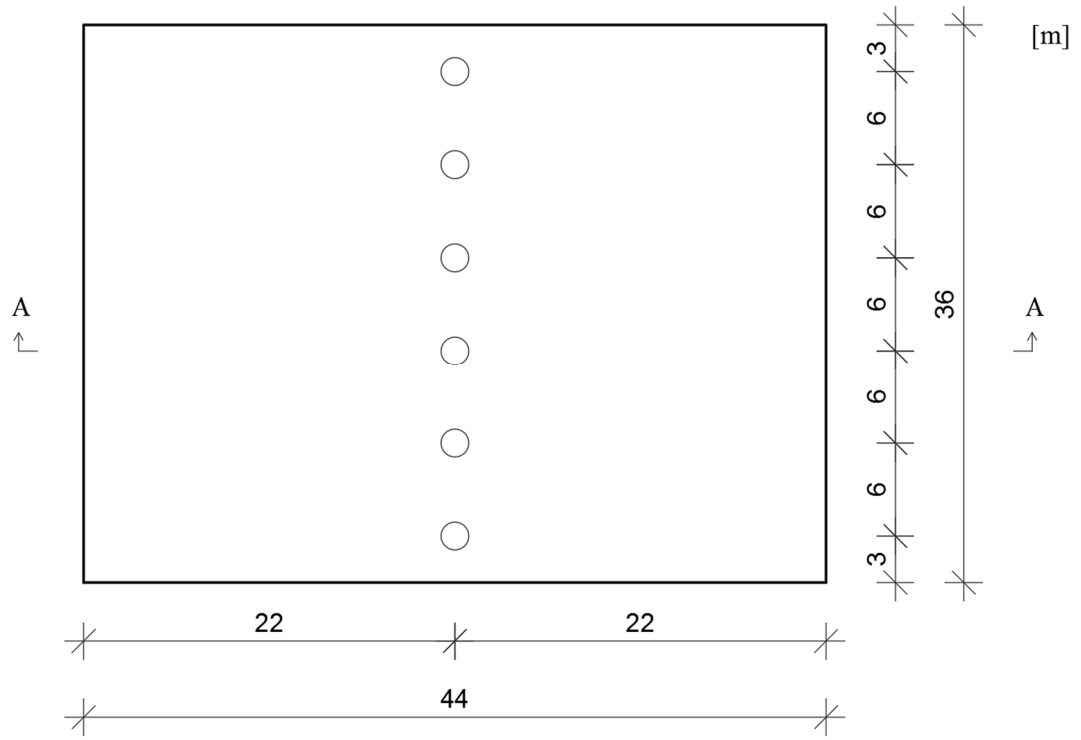

Figure 3.2 Plan view of the portal frame bridge.

3.1.2 Tendon geometry

The prestressing tendons consist of 19 strands, each with an area of 140 mm^2, which correspond to a tendon area of 2660 mm^2. The tendons are assumed to have parabolic shape and are placed every 500 mm along the bridges transverse direction. The maximum eccentricities of the tendon, from the sectional centroid, e_f and e_s are 340 mm, see Figure 3.3. The tendon is placed so that the eccentricity is zero where the centroids of the slab and outer walls meet. A schematic illustration of the tendon profile can be seen in Figure 3.3, and the profile is specified in Appendix A.

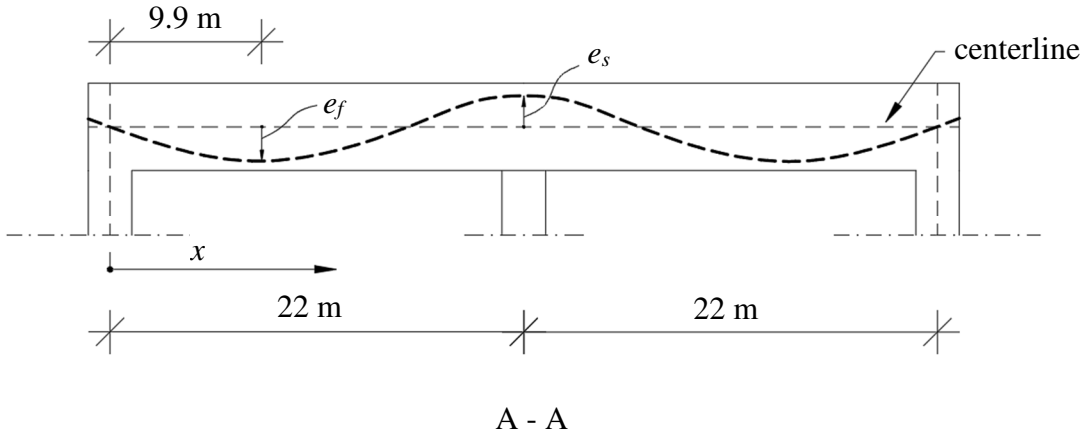

Figure 3.3 Section A-A, showing a cross section in the longitudinal direction with a schematic tendon profile. Scale in height and width is not the same.

3.2 Materials

3.2.1 Concrete

The materials have been chosen the same or similar to the real bridge. The slab, the walls and the columns consist of concrete C45/55. Some of the material data for the concrete is presented in Table 3.1. More material data is found in Appendix B.

Table 3.1 Material data for concrete C45/55.

Concrete			C45/55
Characteristic strength	f_{ck}	[MPa]	45
Young´s modulus	E_{cm}	[GPa]	36

3.2.2 Steel

The tendons consist of steel strands that are placed in corrugated steel ducts. The steel is of grade Y1860S7 and are of type VSL 6-19. Some of the material data for the steel is presented in Table 3.2. More material properties for the materials and coefficients concerning frictional losses of tendon force in the steel ducts are specified in Appendix B.

Table 3.2 Material data for steel Y1860S7.

Steel			Y1860S7
Nominal yield strength	$f_{p0,1k}$	[MPa]	1636
Nominal tensile strength	f_{pk}	[MPa]	1860
Young´s modulus	E_p	[GPa]	195

3.3 Loads and load combinations

3.3.1 Introduction

In addition to the prestressing load, the bridge is only subjected to uniformly distributed loads, including self-weight, permanent load and live load. This is a simplification which is justified since the aim is to evaluate the effects of the prestressing.

3.3.2 Permanent loads

3.3.2.1 Self-weight

The self-weight of the structure is automatically calculated in SAP2000 and depends on the densities and volumes of the materials.

3.3.2.2 Other permanent loads

Since the real bridge is a “wildlife crossing”, a substantial part of the permanent load consists of earth fill. Underneath the earth fill there is a layer of cellular plastic, and closest to the concrete there is a waterproofing layer consisting of asphalt. The total load of the earth fill is approximated to

q_{perm} = 20 kN/m^2

3.3.2.3 Prestressing load

The bridge slab is also subjected to a prestressing load. This load will vary along the tendon, as explained in Section 2.6.3. The tendons are tensioned from both ends. In reality, every other post-tensioning tendon is tensioned from each side; i.e. the first tendon is tensioned from the left side and the second from the right side etc. However, in SAP2000, it is possible to tension each tendon from both sides simultaneously. For practical reasons, the prestressing load has been applied at both ends of the tendon in the models. This is further described for each model respectively later in this chapter.

It is desired to achieve as high stress as possible in the tendon after anchorage. However, due to anchor slip, the maximum tendon stress will not appear at the end of the tendon, see Section 2.6.3. Hence, a higher stress is required during pretensioning, to make sure that the tendons are fully utilized.

Eurocode 2 states limits to the highest allowable stress in a tendon. In this case, the highest allowable stress after anchorage is calculated in Appendix C to

$\sigma_{allowed}$ = 1391 MPa

To be able to reach $\sigma_{allowed}$, the required tensioning stress before anchorage is calculated in Appendix C to

σ_p = 1436 MPa

Due to elastic shortening and long term effects, as explained in Section 2.6.4, the tendon stress will decrease. In SAP2000, in linear analyses, the losses are specified manually by the user as reductions in stress. The losses due to elastic shortening and long term-effects are calculated in Appendix C and are presented in Table 3.3.

Table 3.3 Stress losses due to elastic shortening and long-term effects.

Effects	Stress loss [MPa]
Immediate	
Elastic shortening	39.2
Long-term	
Creep	45.1
Shrinkage	41.3
Relaxation	67.0
Total	193

3.3.3 Live load

The live load is applied in both spans and is approximated to

q_{live} = 10 kN/m^2

3.3.4 Load combinations

Five load combinations according to Eurocode will be evaluated. Two of the load combinations are for ultimate limit state and three are for serviceability limit state. The load combinations are presented in Table 3.4. The bridge will be subjected to the following loads.

- G_k – self-weight and permanent load
- P – Prestressing load
- Q_k – Live load

The partial coefficients and reduction factors have been chosen in accordance with a bike and pedestrian bridge, since no information is provided for a "wildlife crossing" in Eurocode. However, these factors are not of great importance in this study, since the aim is to evaluate the effects of the prestressing.

Table 3.4 Load combinations

Load combination	Design value of load effect
ULS	
6.10a	$\gamma_G G_k "+" \gamma_P P "+" \gamma_Q \psi_Q Q_k$
6.10b	$\xi \gamma_G G_k "+" \gamma_P P "+" \gamma_Q Q_k$
SLS	
Characteristic	$G_k "+" P "+" Q_k$
Frequent	$G_k "+" P "+" \psi_1 Q_k$
Quasi-permanent	$G_k "+" P "+" \psi_2 Q_k$

Where

γ_G = 1.35
γ_P = 1.0
γ_Q = 1.5
ψ_Q = 0.4
ξ = 0.85
ψ_1 = 0.4
ψ_2 = 0

In addition to these load combinations, the bridge will be analyzed for each load separately.

SAP2000 will generate resultant moments caused by the post-tensioning. The restraint moments have been generated separately by analyzing a hyperstatic load case of the prestressing load. The primary moment is not automatically generated in SAP2000 and need to be produced manually in post-processing of the results. This is done by subtracting the restraint moment from the resultant moment in Excel.

3.4 Static systems

In Figure 3.4, the static model can be seen. Every column is pinned at the bottom and has a pinned connection to the slab in the top. The frame walls are pinned along the

bottom edge, but moment can be transferred between the slab and the walls. Post-tensioning tendons are placed in the longitudinal direction every half meter. The load q is an evenly distributed area load consisting of both a live load and a permanent load.

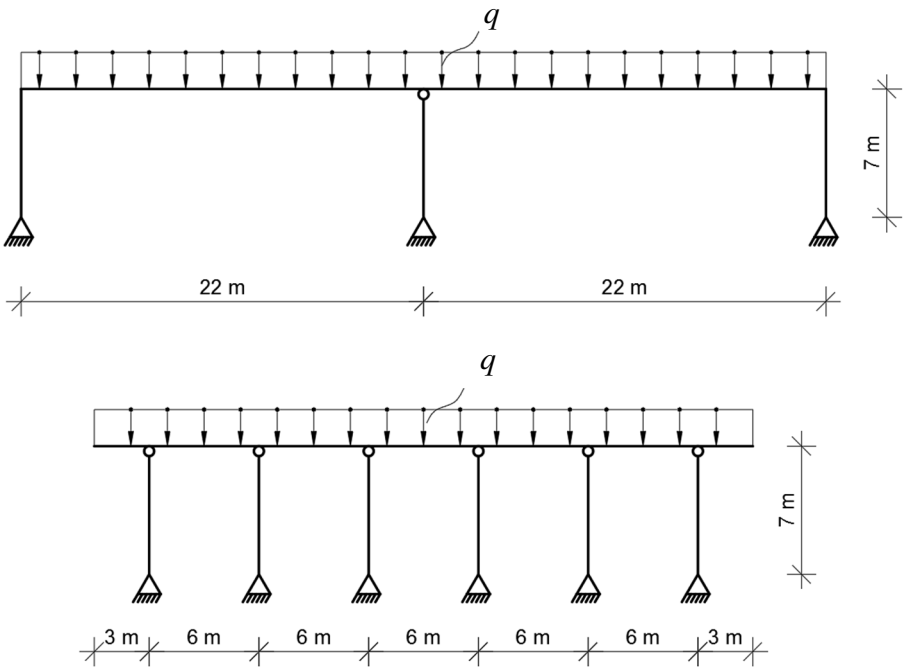

Figure 3.4 Static model of the bridge. The section at the top shows the cross section in the longitudinal direction. The section at the bottom shows the cross section in the transversal direction at the columns.

3.5 FE models

3.5.1 Shell model

3.5.1.1 Geometry

In the shell model the slab has been modeled with shell elements of the type ”thin” (Kirchhoff formulation). This is justified since the thick formulation is only necessary if the thickness is larger than one tenth to one fifth of the span (CSI, 2016). The dimension of each element is one by one meter and the thickness is one meter. The walls are also modeled with shell elements and has the same dimensions as the slab elements. The columns are modeled as beam elements. The walls are pinned in all nodes along its bottom edge and connected to the slab in the top. The columns are pinned at the bottom and the moment between the column and the slab is released in SAP2000. Figure 3.5 shows the shell model with its elements and boundary conditions.

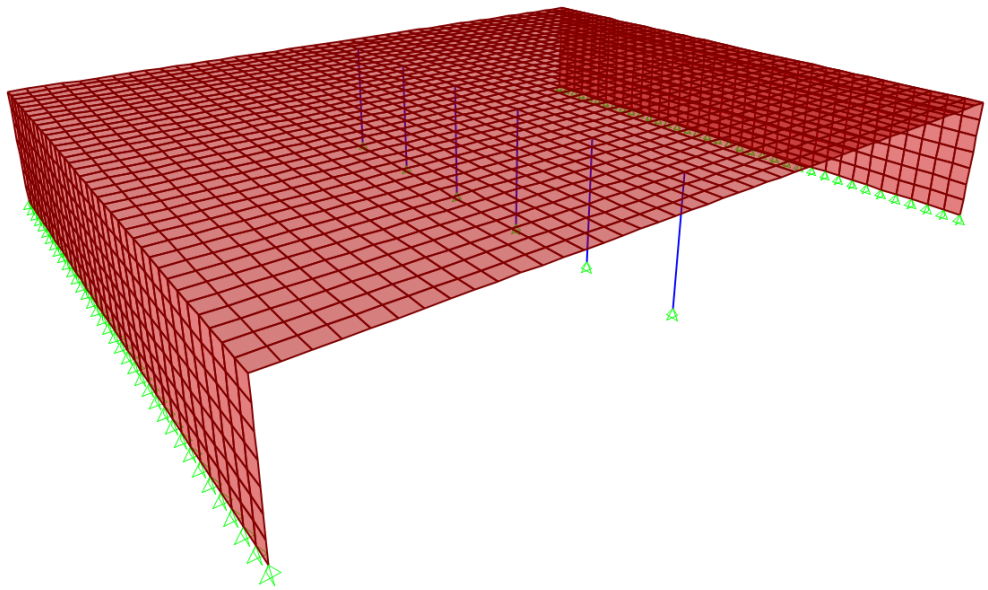

Figure 3.5 The shell model in SAP2000.

The same tendon profile has been used in both models. The tendons in the shell model are placed one meter apart. Since the tendons in the real bridge are placed every half meter, the area of the tendons in the model need to be modified. The area of the tendon in the model is calculated using Equation 3.1. The area of the outermost tendons, which are placed on the edges, is half the area of the other tendons.

$$A_{p,model} = A_{p,real} \cdot \frac{element\ width}{real\ tendon\ spacing} \tag{3.1}$$

where

$A_{p,model}$ is the area of a tendon in the model
$A_{p,real}$ is the area of a real tendon

In this case, the tendon area of one tendon in the model, except the outermost tendons, is two times the area of the real tendon i.e.

A_p = 5320 mm^2

The outermost tendons have an area of

$A_{p,outer}$ = 2660 mm^2

The tendons are modelled in two different ways. In the first case as an element and in the second as a load. These two ways of modeling the tendons are described in Section 2.7.5.

3.5.1.2 Mesh

As described in Section 2.8.1.1, the results in the slab at connection with the column will not be relevant due to singularities in the FEM solution. Since the connection between the slab and column is hinged, the result will be reliable halfway between the edge and the center of the column. This applies for quadratic cross sections, which

means that circular cross sections should be transformed into equivalent quadratic cross sections. To find the section of interest, the columns are assumed, for simplicity, to be 1 x 1 m, which means that the section of interest is 0.25 m from the center of the column. To get results in these sections, the elements around the columns have been meshed to an element size of 0.25 x 0.25 m to make sure that there are nodes in the section of interest, see Figure 3.6. Since the structural behavior of the slab in the transverse direction over the columns is of interest, the remaining elements between the columns have been meshed to an element size of 0.5 x 0.5 m to get more accurate results.

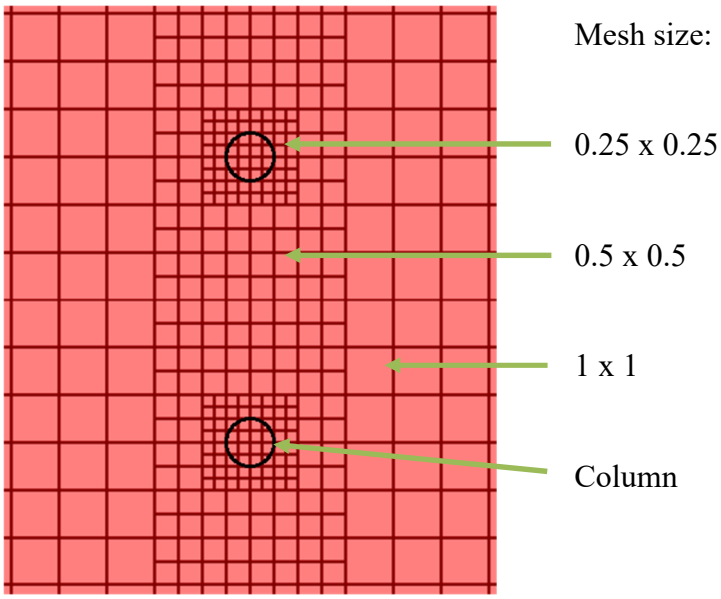

Figure 3.6 Mesh refinement around the columns. The circles represent the real columns.

In post-processing of the results in Excel, the moments in the nodes, where the columns connect to the slab, has been removed. This means that the moments in the nodes 0.25 m from the center of the columns will be the peak moments over the columns, see Figure 3.7.

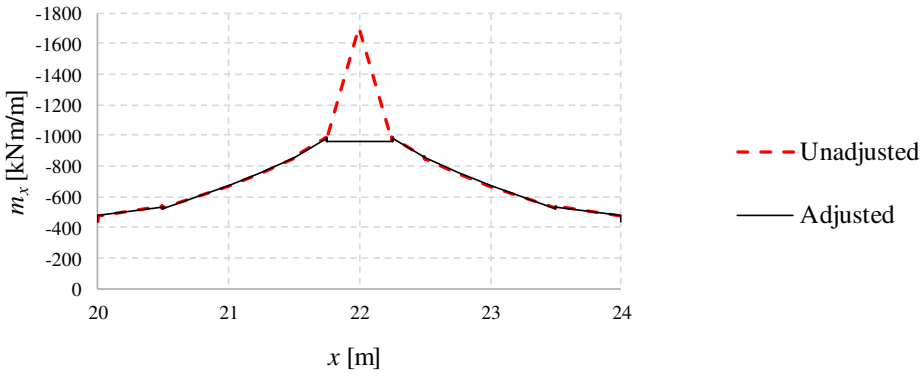

Figure 3.7 Illustration of adjusted moment curve in the slab over a column in order to avoid the effect of singularity.

Since the mesh is refined within limited areas, there will be sections at which the mesh change size. To get the transition between the different mesh sizes to function, "edge constraints" have been assigned to the elements at the transition sections. "Edge

constraints" were used since, as mentioned in Section 2.8.1.2, it could give more accurate results than by using distorted elements.

3.5.1.3 Loads

Permanent load and live load are applied in the negative z-direction as uniform load on the shell elements. The self-weight is automatically applied in the negative z-direction to all elements in the model.

The prestressing load is assigned by defining the stress which is applied at both ends. This is a simplification, but it is justified since one tendon in the model represents two tendons in the real bridge. The assigned stress is

$\sigma_p = 1436$ MPa

as described in Section 3.3.2.3. It is convenient to define the prestressing load as a stress since it is independent of the tendon area. The losses presented in Table 3.3 have been used as input for the prestressing load in SAP2000.

3.5.1.4 Cracked slab

To evaluate the influence of cracking in the transverse direction, an orthotropic material has been used in some of the shell models. When the transverse section is assumed to be cracked, the transverse stiffness, E_2, is reduced by a factor of 0.5 or 0.1; i.e.

$E_2 = 0.5\ E_1$

and

$E_2 = 0.1\ E_1$

The factor 0.5 is assumed to correspond to a cracked slab section and the factor 0.1 has been used to highlight what influence a reduced transverse stiffness have on the overall structural behavior of the bridge. Also the Poisson's ratio, v_{12}, has been set to zero, in accordance with Eurocode, when the transverse section is assumed to be cracked; i.e.

$v_{12} = 0$

The shear modules are affected when either Young's modulus or the Poisson's ratio is modified. The shear modules are not calculated automatically in SAP2000 and need to be given as input, and can be found in Appendix D.

Also the method of using property modifiers, see Section 2.8.1.4, has been used to take cracking into account. In this model, an isotropic material has been used with unmodified Young's modules and only the Poisson's ratio, v, has been modified to

$v = 0$

Instead of modifying the Young's modulus in the transverse direction, the bending stiffness corresponding to M22 and M12 has been modified with a factor of 0.1. This has been done to evaluate how well this method is consistent with the above-mentioned

method for defining an orthotropic material and if an isotropic material can describe the behavior of a cracked slab.

3.5.2 Grillage model

3.5.2.1 Geometry

The slab consists of several beam elements in both the longitudinal and the transversal direction, see Figure 3.8. The beam elements in the longitudinal direction are placed one meter apart. The spacing of the transverse beam elements is chosen to one meter which will give an even spacing. According to Hewson (2003), the ratio between the spacing of the longitudinal and transversal beam elements should be between 1:1 and 1:2 to get reasonable structural behaviour in the grillage model. The chosen spacing is within these ratios.

Both the longitudinal and transversal beam elements are assigned cross sections with a thickness of one meter and widths equal to their spacing, i.e. one meter. However, the width of the outermost beam elements has been halved to match the real area of 44 x 36 m in accordance with Figure 2.20a.

The walls also consist of beam elements in both vertical and transversal direction. The vertical beam elements of the wall are identical to the longitudinal beam elements of the slab concerning spacing and assigned cross sections. The vertical beam elements are pinned at the bottom and connected to the longitudinal beam elements of the slab at the top.

The transversal beam elements of the walls are placed with an even spacing of one meter. The ratio between the spacing of the vertical and transversal beam elements of the walls also fulfill Hewson´s suggestion.

As mentioned in Section 2.8.2.3, the torsional stiffness of the beams need to be modified, according to Hewson (2003). In SAP2000, the torsional stiffness is modified by assigning a so called “property modifier”, see Section 2.8.1.4, which is a factor that scales the stiffness. This factor has been calculated in Appendix E.

The columns are modeled with beam elements and are pinned at the bottom. The connection between the column and the slab does not transfer any moment i.e. the moments M2 and M3, defined in Figure 2.13, are released.

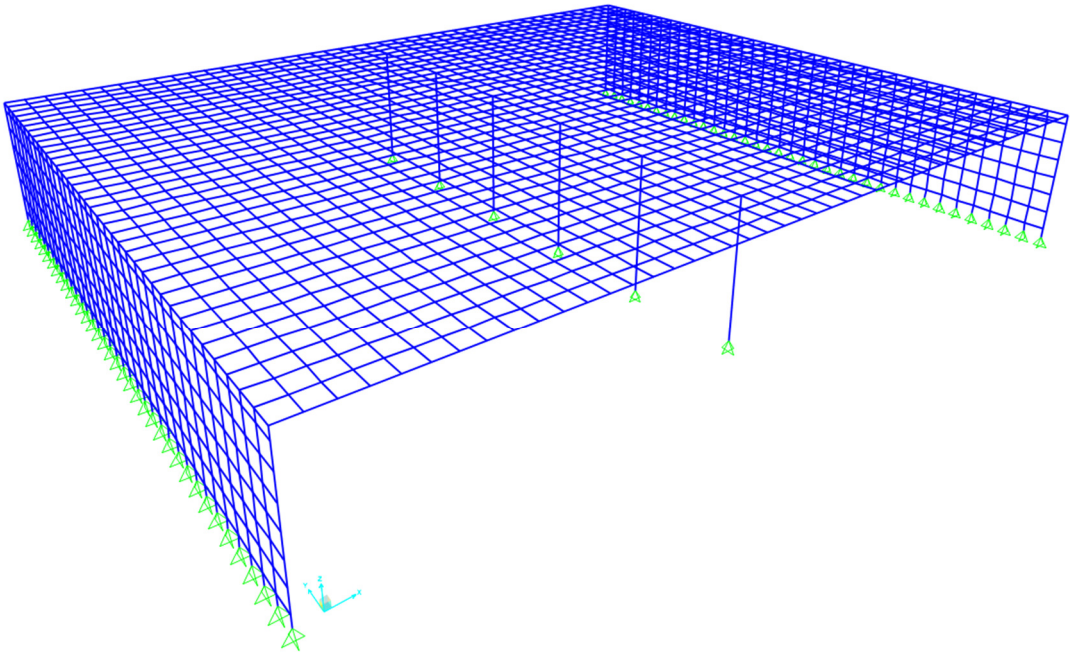

Figure 3.8 The grillage model in SAP2000.

One tendon has been placed in each longitudinal beam element i.e. every meter. Equation 3.1 gives the area of the tendon in the model and is two times the area of the real tendon i.e.

$A_p = 5320$ mm^2

The tendons in the outermost beams have an area of

$A_{p,outer} = 2660$ mm^2

The tendons are modelled in two different ways. In the first case as an element and in the second as a load. These two ways of modeling the tendons are described in Section 2.7.5.

3.5.2.2 Load

Permanent and live loads are applied in the negative z-direction as "Distributed Span Loads" with the unit N/m. The applied load on a beam element is calculated by multiplying the width of its cross section with the area load to get a line load. The self-weight is automatically applied in the negative z-direction to all elements in the model.

As mentioned in Section 2.8.2.2, the load can be applied in different ways; i.e. only on the longitudinal beams, only on the transversal beams or half of the load in each direction. Since it is not obvious which approach is most reasonable, all three approaches have been evaluated.

When the load is applied only in the longitudinal or the transversal direction, the applied loads on the respective beam elements are

q_{perm} = 20 kN/m

and

q_{live} = 10 kN/m

When half the load is applied in each direction, the applied loads on the beam elements are

q_{perm} = 10 kN/m

and

q_{live} = 5 kN/m

Since the cross sections of the longitudinal/vertical and transversal beam elements overlap, the densities of the materials assigned to the beam elements need to be adjusted, otherwise the self-weight of the structure would be doubled. When all load is applied on the longitudinal beams, the density for the material assigned to the transversal beams are set to zero. In a similar way, the density of the material assigned to the longitudinal beams are set to zero when the load is applied only to the transversal beams. When the load is applied in both directions, the density of the material assigned to both the longitudinal and transversal beams are halved.

The prestressing load is assigned by defining the stress which is applied at both ends of the tendons. This is a simplification, but it is justified since one tendon in the model represents two tendons in the real bridge. The assigned stress is

σ_p = 1436 MPa

as described in Section 3.3.2.3. It is convenient to define the prestressing load as a stress since it is independent of the tendon area. The losses presented in Table 3.3 have been used as input for the prestressing load in SAP2000.

3.5.3 2D model

3.5.3.1 Geometry

A 2D model has been created for comparison with a 3D model. The 2D model represents a one meter strip of the bridge in the longitudinal direction over a column.

The model consists of beam elements, see Figure 3.9. The beam that represent the slab and the columns at the ends, that represent the walls, have a cross section of 1x1 m. The column in the middle is modelled in the same way as the previous models.

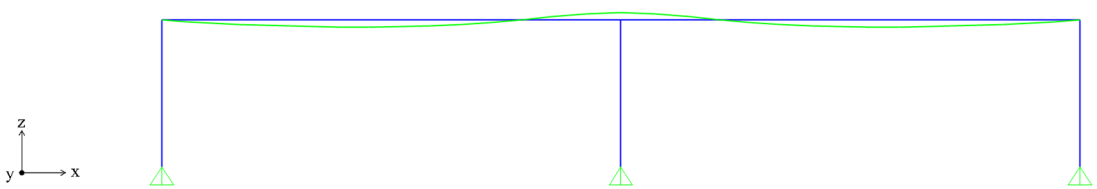

Figure 3.9 The 2D model in SAP2000. The tendon is visible.

One tendon has been placed in the longitudinal beam element and is modeled as element. Equation 3.1 gives the area of the tendon in the model and is two times the area of the real tendon i.e.

$A_p = 5320 \text{ mm}^2$

3.5.3.2 Load

Permanent and live loads are applied in the negative z-direction as "Distributed Span Loads" with the unit N/m. The applied load on a beam element is calculated by multiplying the width of its cross section with the area load to get a line load. The self-weight is automatically applied in the negative z-direction to all elements in the model. The applied loads on the longitudinal beam elements are

$q_{perm} = 20 \text{ kN/m}$

and

$q_{live} = 10 \text{ kN/m}$

The tendons load is assigned by defining the stress which is applied at the ends. This is a simplification, but it is justified since one tendon in the model represents two tendons in the real bridge. The assigned stress is

$\sigma_p = 1436 \text{ MPa}$

as described in Section 3.3.2.3. The losses presented in Table 3.3 have been used as input for the prestressing load in SAP2000.

3.6 Verification of models

The shell and grillage models with tendons modelled as load or element has been verified by comparing the reaction forces provided by SAP2000 to the hand calculated self-weight of the bridge and the external loads. All other models are variants of the verified models with modifications that does not affect the load on the structure.

As mentioned in Section 2.7.5, the self-weight of the tendons is only considered if the tendons are modelled as element. Therefore, the models where the tendons are modelled as element or load has been compared to hand calculations with or without the self-weight of the tendons.

The largest deviation between the hand calculated total load and the reactions from SAP2000 is 0.01 %, see Appendix F.

3.7 Sensitivity analysis

As discussed in Section 2.8.1.2, results extracted from transition sections may not be accurate. In the analysis, results have been extracted in two sections which coincide with transition sections, see Figure 3.10a. To ensure that the results in these sections are reliable, a sensitivity analysis has been performed.

The sensitivity analysis consists of a comparison of the moment distributions in the sections shown in Figure 3.10, for two shell models with different meshes. Figure 3.10a show the original mesh used in all shell models in the analyses. Figure 3.10b shows the mesh modified to avoid transition sections where results are extracted.

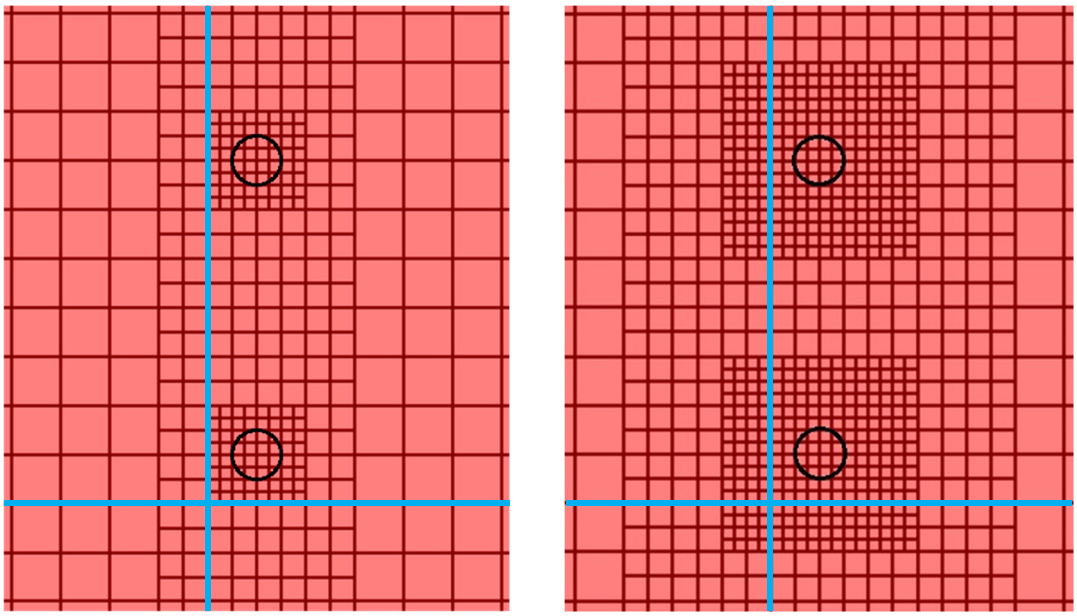

(a) (b)

Figure 3.10 Meshes used in the sensitivity analysis and the sections from which results are extracted. a) Original mesh used in all shell models. b) Modified mesh to avoid transition sections in sections where results are extracted.

This analysis show that the results seem reliable since the moment distributions are similar and in the same order of magnitude. An example of the results can be seen in Figure 3.11. All other results from the sensitivity analysis can be found in Appendix G.

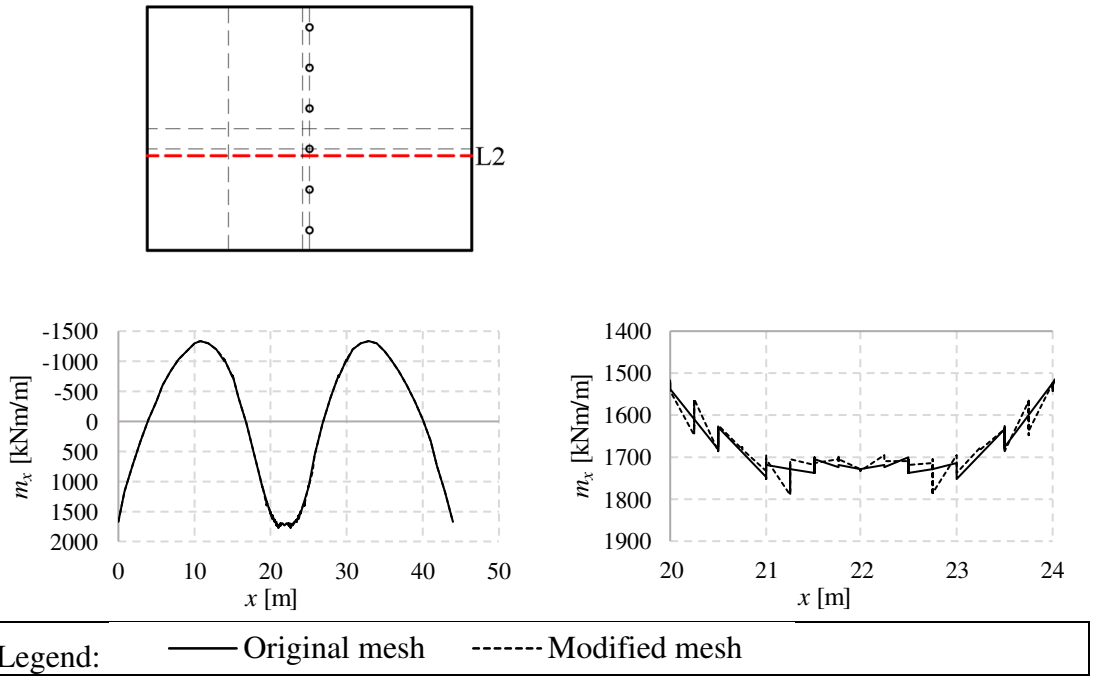

Figure 3.11 Resultant moment distribution m_x caused by prestressing load for a shell model with different mesh. The left diagram shows the moment distribution along the section L2 and the right diagram shows a zoomed part of the moment distribution.

4 Results of the FE-analysis

4.1 Definition of sections and points

In this thesis, moment distributions for the load combinations presented in Section 3.3.4 have been chosen to be presented in the sections shown in Figure 4.1.

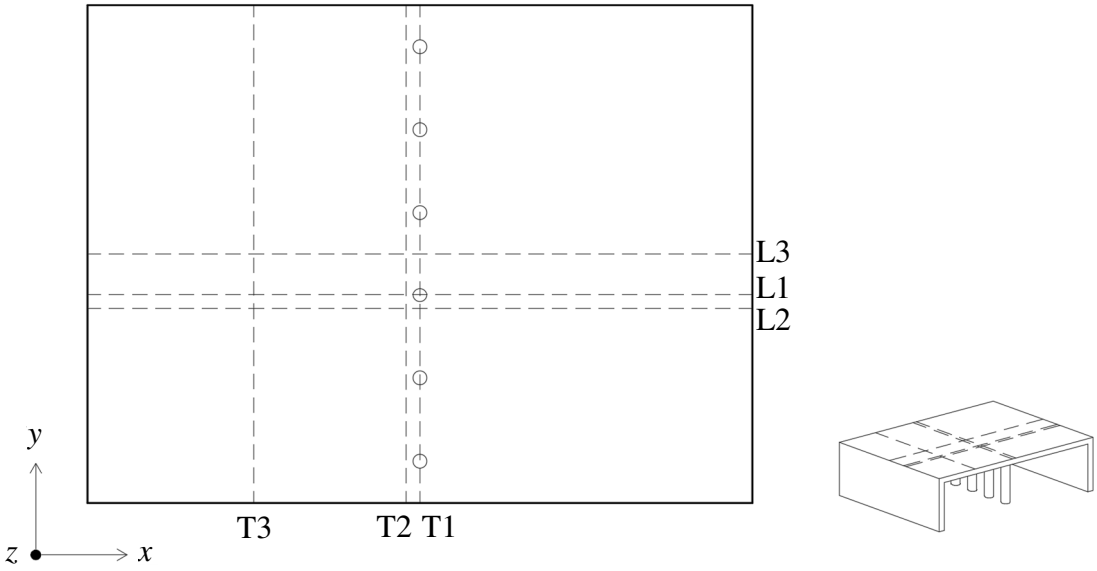

Figure 4.1 Output sections.

The sections L1, L2 and L3 extends in the longitudinal direction. L1 is located over a mid-column, L2 is offset by one meter from L1 and L3 is located between the two mid-columns. The sections T1, T2 and T3 extends in the transversal direction. T1 is located over the columns, T2 is offset by one meter from T1 and T3 is located in the middle of the left span. In Table 4.1, the coordinates for the sections are specified.

Table 4.1 Coordinates for the output sections.

Section	x [m]	y [m]
L1	0 - 44	15
L2	0 - 44	14
L3	0 - 44	18
T1	22	0 - 36
T2	21	0 - 36
T3	11	0 - 36

To be able to compare the results from different models more precise, certain points have been chosen in which the magnitudes of the moments are specified. The moments in these points and the deviation for each evaluation are compiled in tables which can be found in Appendix H. For the sections L1, L2 and L3, the points are located at $x = 22$, where the row of columns is located, and in the span between the columns and the end wall. The point in the span is located where the maximum moment appear which can either be in the span or at the end support. For the sections T1 and T2 the points are located at $y = 15$, over a column, and at $y = 18$ which is between two columns. For the section T3, the point is located at $y = 18$; i.e. in the middle of the section. The points in which results have been specified are presented in Table 4.2.

Table 4.2 Points in the sections at which moments have been specified.

Sections	Point 1	Point 2
L1	$x = 22$ (over a column)	Span / outer support
L2	$x = 22$	Span / outer support
L3	$x = 22$	Span / outer support
T1	$y = 15$ (over a column)	$y = 18$
T2	$y = 15$	$y = 18$
T3	$y = 18$	

4.2 Bending moment convention

To be able to compare the results from the models, a common notation for moments is needed. In this study, the moments are defined with respect to the global coordinate system according to Figure 4.2. The moment m_x is the moment that the reinforcement in the x-direction should be designed for. In the same way, the moment m_y is the moment that the reinforcement in the y-direction should be designed for.

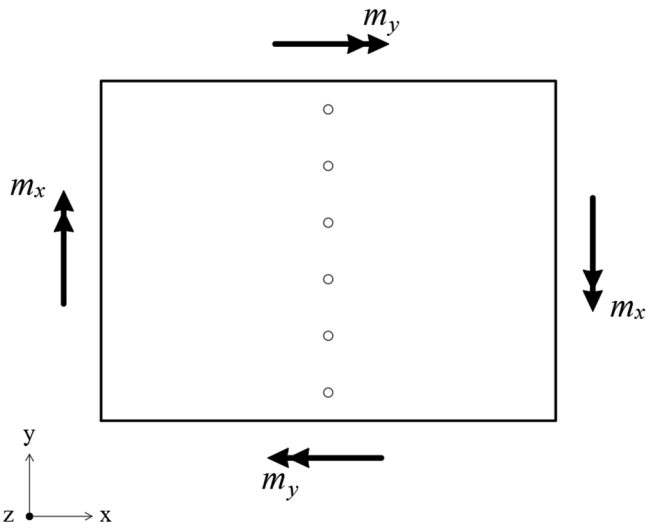

Figure 4.2 Definition of global bending and torsional moments relative to the global coordinate system of the bridge.

All shell elements in the shell models used in this thesis are oriented so that the local axis 1 coincide with the global x-axis, the local axis 2 coincide with the global y-axis and the local axis 3 coincide with the global z-axis. As mentioned in Section 2.8.1.3, the bending and torsional moments need to be combined. This implies that M11 combined with M12, defined in Section 2.7.4.3, correspond to m_x and M22 combined with M12 correspond to m_y.

As shown in Figure 2.13, the local coordinate system for a beam element depend on the orientation of the element. The beam elements in the slab, in the grillage models used in this thesis, are oriented so that the local axis 2 always coincide with the global z-axis. This implies that the moment M3, also defined in Figure 2.13, will correspond to m_x and m_y depending on the global orientation of the beam element. M3 corresponds to m_x if the beam element is oriented in the global x-direction and m_y if the beam element is oriented in the global y-direction. Note that the spacing between the beam elements is one meter which means that M3 will correspond to a moment per unit width.

4.3 Application of loads on a grillage model

As discussed in Section 3.5.2.2, three different ways to apply the load on the beam grillage have been compared to investigate if it influences the results. Moment distributions in two sections are presented in Figure 4.3. All results from this comparison are presented in Appendix H.1.

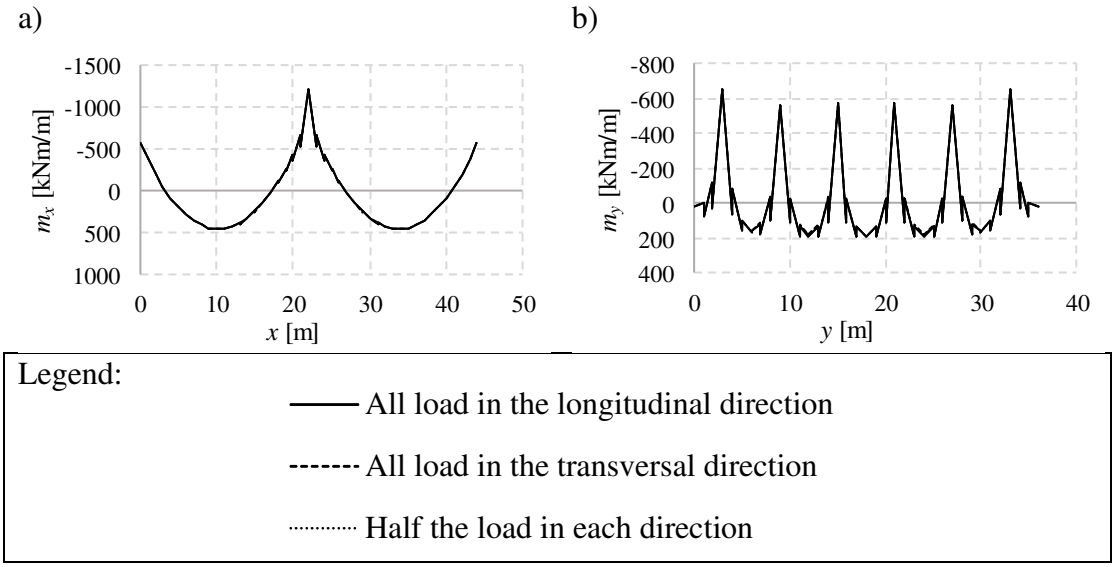

Figure 4.3 Moment distributions caused by permanent load. a) Section L1. b) Section T1.

From this, it is clear that the direction in which the load is applied has little influence on the moment distributions in the grillage models. Since the direction in which the load is applied have little influence, only models with the load applied in the longitudinal direction has been used in further comparisons.

4.4 Defining the prestressing load either as load or element

As mentioned in Section 2.7.5, the prestressing load can be defined either as load or element in SAP2000. The difference between defining the prestressing either as load or element have been evaluated for both a beam grillage model and a shell model. Moment distributions along section L1 in the two models are presented in Figure 4.4. All results are presented in Appendix H.2.

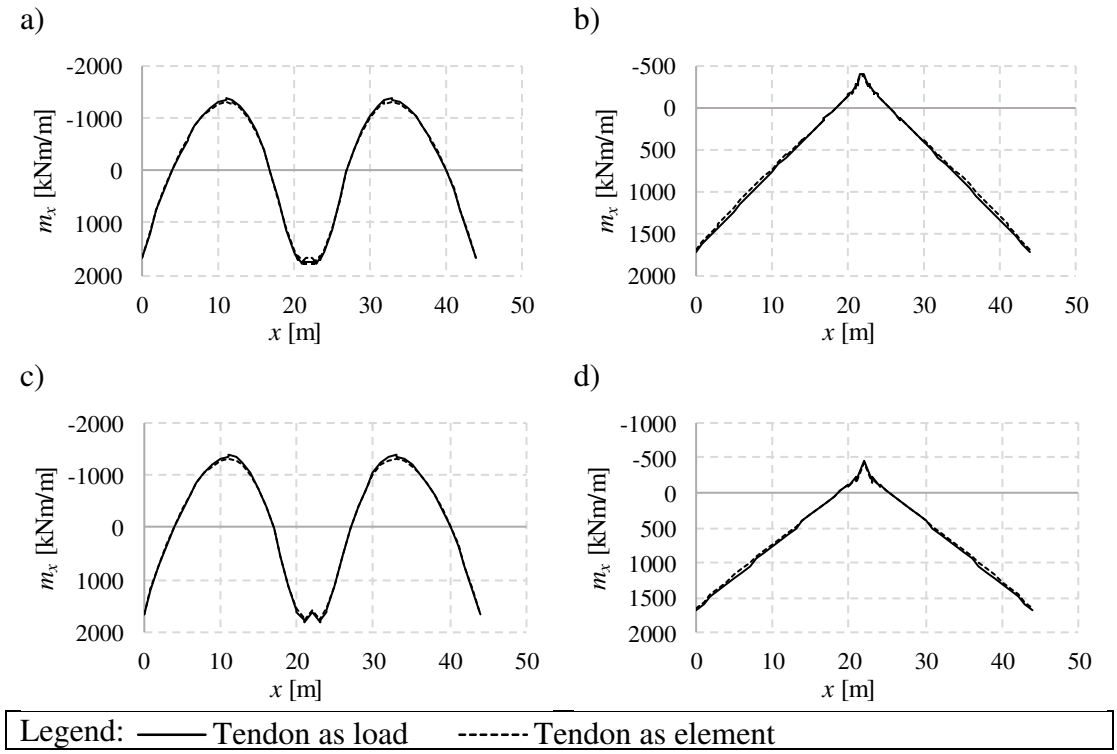

Figure 4.4 Moment distribution m_x along section L1. a) Resultant moment in the shell model. b) Restraint moment in the shell model. c) Resultant moment in the beam grillage model. d) Restraint moment in the beam grillage model.

From this, it is clear that the way of defining the prestressing load has little influence on the moment distributions in both the grillage and shell models. The difference is, in a majority of the cases, less than 5 %. In a few cases, the deviation is greater in the shell model. However, this occur at the connection between a column and the slab where there is problem with singularity. Even though singularities have been accounted for, the effect is not completely excluded. Of natural reasons, greater percentage deviations also appear where the magnitudes of the moments are relatively small.

However, since the difference between the ways of defining the prestressing load is small, it has only been defined as elements in further comparisons.

4.5 Comparison of 2D and 3D models

The 2D model was created for comparison with a 3D model to see how well their results coincide. The moment distribution for the 2D model has been compared with the moment distributions along L1 and L3 for a shell model. Moment distributions in two sections are presented in Figure 4.5. All result from this comparison is presented in Appendix H.3.

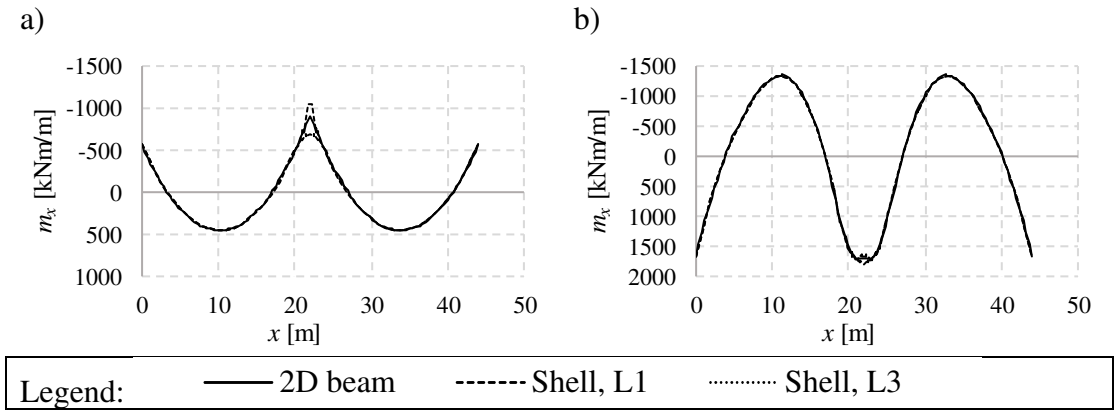

Figure 4.5 Moment distributions in the longitudinal direction for the 2D model and a shell model in section L1 and L3. a) Moment distribution caused by the permanent load, b) resultant moment caused by the prestressing load.

The moment distribution for the 2D model is similar to the distributions for the shell model. However, there is a difference at the middle support where the moment in the 2D model is in between the moments for the sections in the shell model, which is expected.

4.6 Comparison between shell and grillage models

One of the main objectives with this thesis is to investigate how the choice of elements in FEM affect the results in the bridge slab. In this comparison, a shell model has been compared with a beam grillage model. In both models, the prestressing load has been defined as elements and the distributed load has been applied in the longitudinal direction only on the beam grillage model. All load combinations have been analyzed for this comparison and the results are presented in Appendix H.4.

Figure 4.6 and Figure 4.7 shows results along the sections L1 and T1, respectively. The moments caused only by permanent or prestressing load are presented for both the longitudinal direction, $m_{x,}$ and the transverse direction, m_y. Figure 4.8 and Figure 4.9 shows the deformation in x and y direction, respectively, caused by the prestressing load only, as contour plots generated in SAP2000.

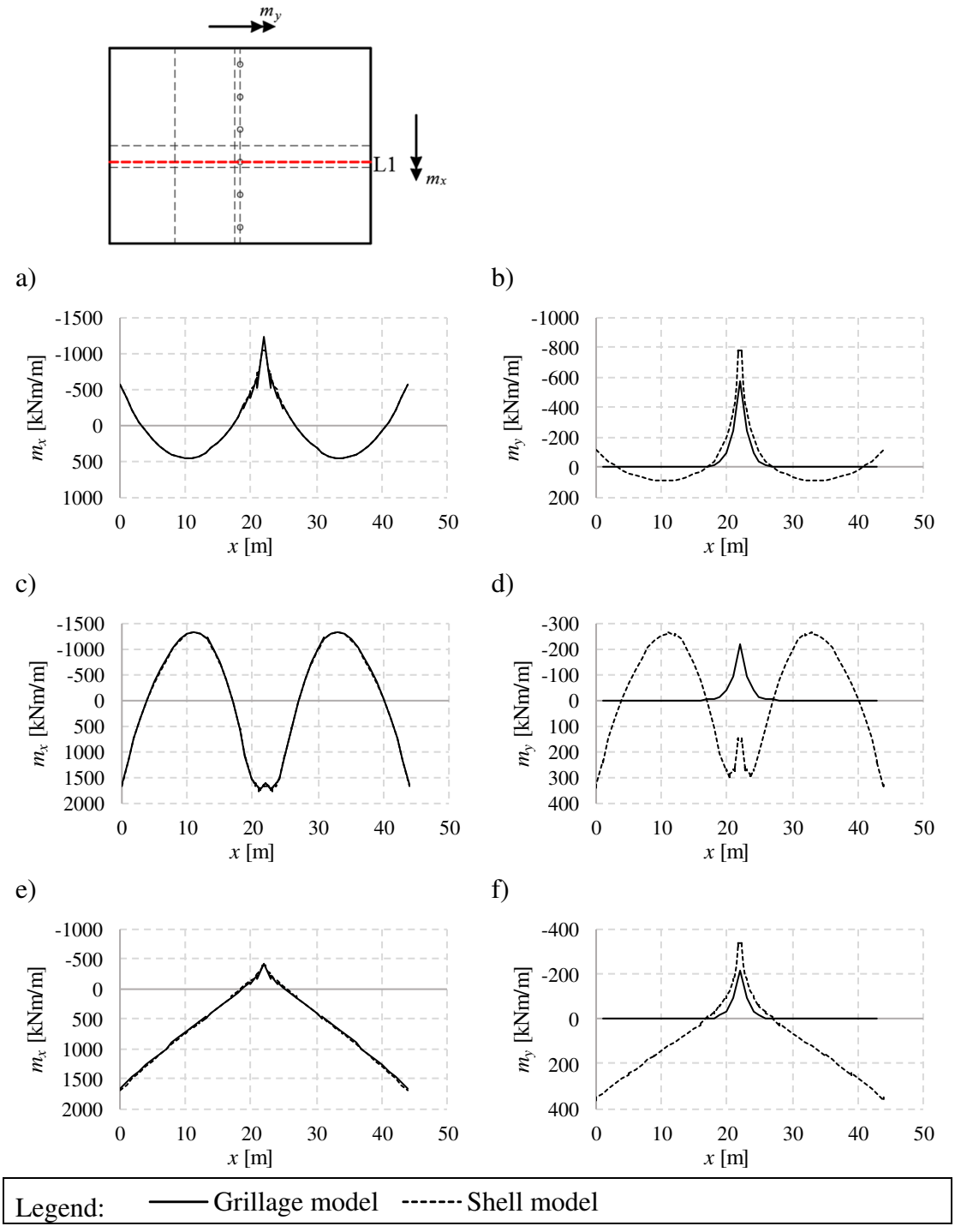

Figure 4.6 Moment distributions along the section L1 for a grillage and a shell model. The left column shows the moment m_x and the right column shows the moment m_y. a) and b) shows the moment caused by the permanent load. c) and d) is the resultant moment caused by the prestressing load. e) and f) is the restraint moment caused by the prestressing load.

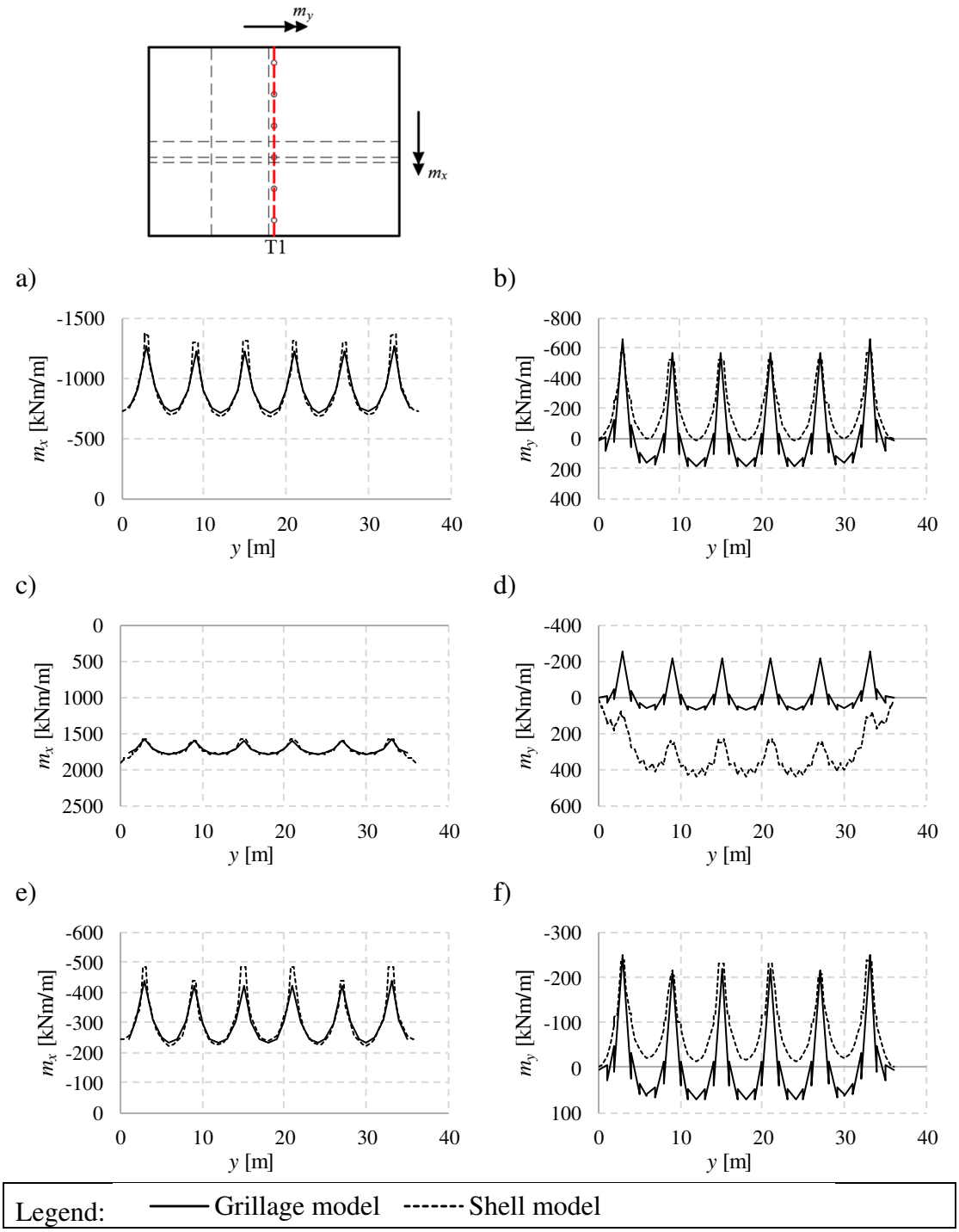

Figure 4.7 Moment distributions along the section T1 for a grillage and a shell model. The left column shows the moment m_x and the right column shows the moment m_y. a) and b) shows the moment caused by the permanent load. c) and d) is the resultant moment caused by the prestressing load. e) and f) is the restraint moment caused by the prestressing load.

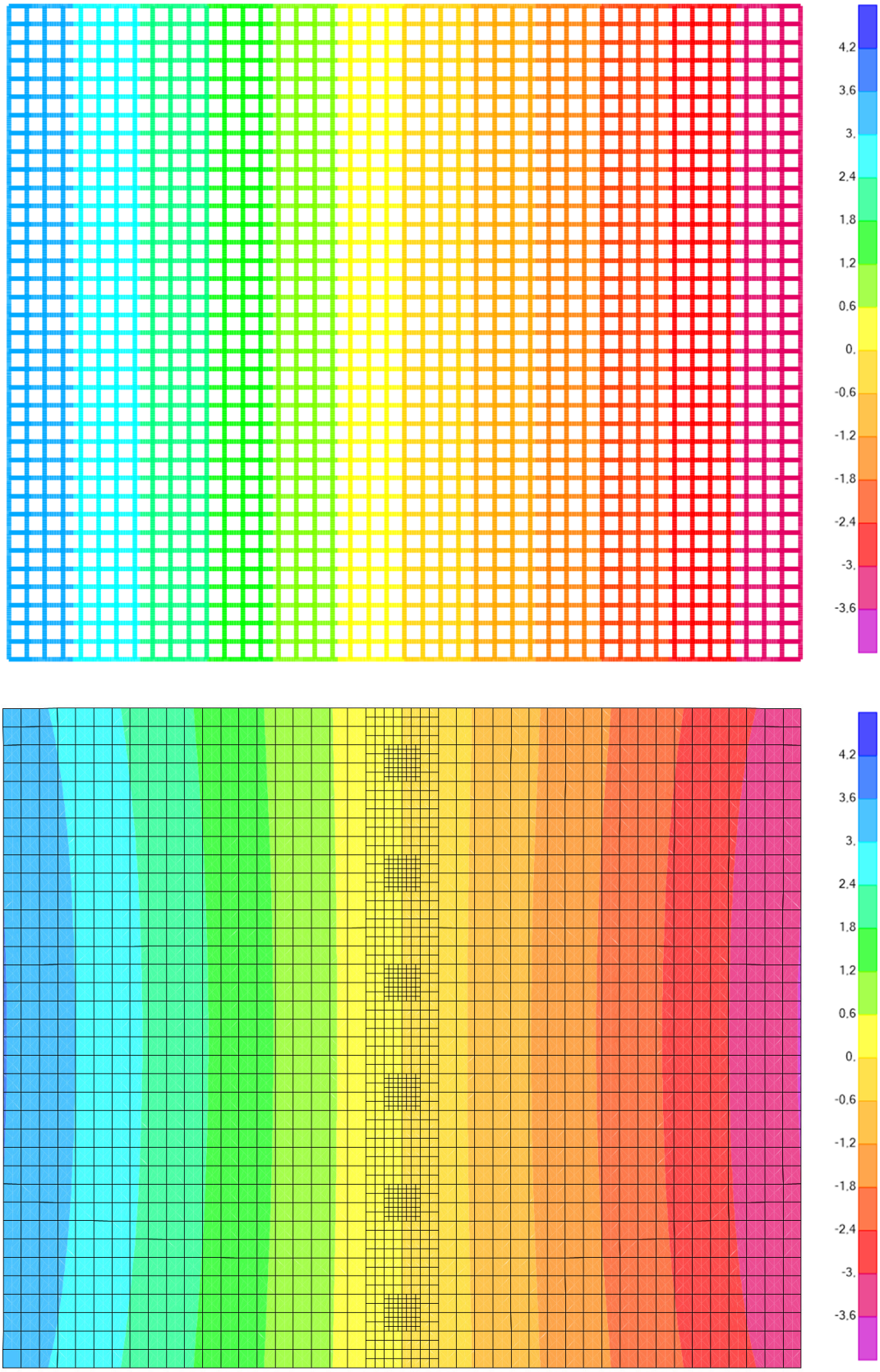

Figure 4.8 *Contour plot of the deformation in mm in the x direction. The top plot represents the grillage model and the bottom plot represents the shell model.*

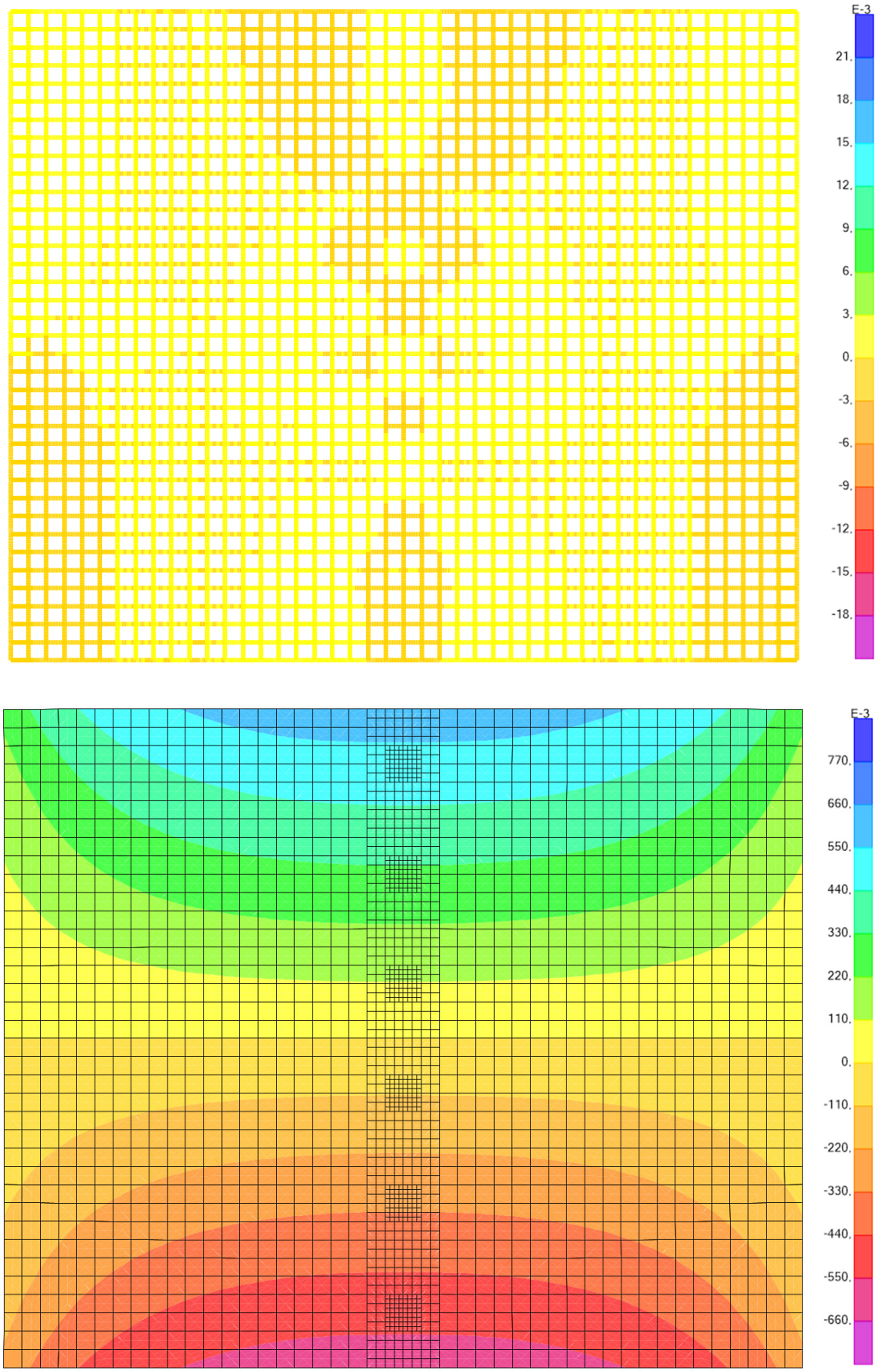

Figure 4.9 *Contour plot of the deformation in mm in the y direction. The top plot represents the grillage model and the bottom plot represents the shell model*

In Figure 4.6 and Figure 4.7, it is clear that the moment distributions in the longitudinal direction, m_x, for the grillage and shell models are similar. However, the moment distributions in the transverse direction differ between the models. The same tendency occurs in all evaluated sections.

Note that the moments in the longitudinal direction at the supports in Figure 4.6 differ between the models. It is at the column supports that the singularity appears in the shell model. The moment distributions in the other regions are similar.

In Figure 4.8, it is clear that the deformation in the *x*-direction caused by the prestressing load is similar for the grillage and the shell models. Figure 4.9 show that the deformation in the *y*-direction of the models is different and that the deformation in the grillage model is small. This implies that the grillage model cannot describe the transverse expansion, as mentioned in Section 2.8.2.3.

4.7 Influence of transverse contraction

When a concrete slab is assumed cracked, the Eurocode allows the Poisson's ratio to be set to zero, as mentioned in Section 2.4. For this reason, a grillage model has been compared to a shell model with orthotropic material where the Poisson's ratio was set to zero; i.e.

$$\nu_{12} = 0$$

As mentioned in Section 2.8.2.3, a grillage model cannot describe transverse contraction/expansion that are caused by an axial load and therefore no adjustments were needed. All results from this comparison are presented in Appendix H.5.

Figure 4.10 and Figure 4.11 shows results along the sections L1 and T1, respectively. The moments caused only by permanent or prestressing load are presented for both the longitudinal direction, m_x, and the transverse direction, m_y. Figure 4.12 shows the deformation in *y*-direction, caused by the prestressing load only, as a contour plot generated in SAP2000.

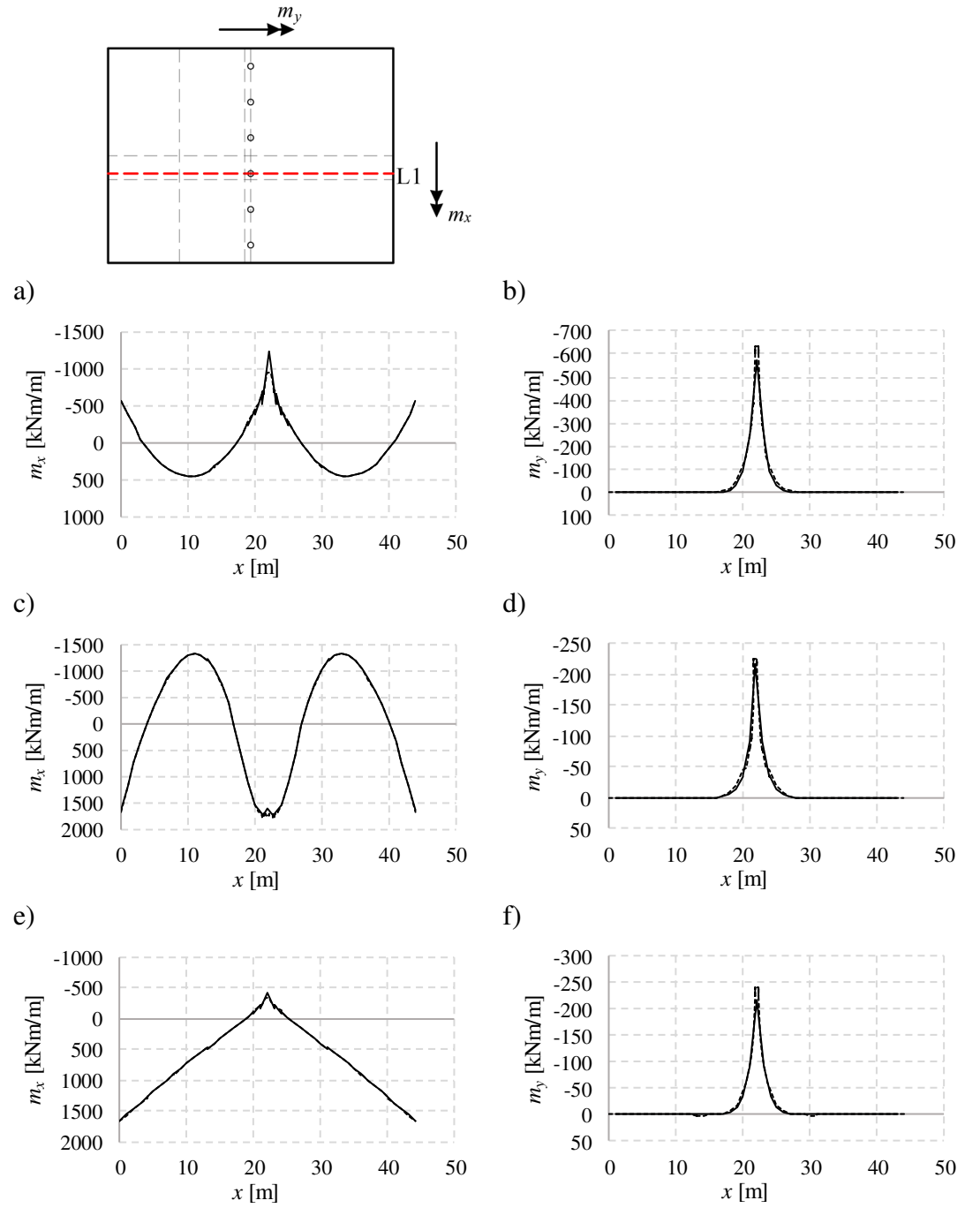

Figure 4.10 Moment distributions along the section L1 for a grillage and a shell model where the Poisson's ratio is set to 0. The left column shows the moment m_x and the right column shows the moment m_y. a) and b) shows the moment caused by the permanent load. c) and d) is the resultant moment caused by the prestressing load. e) and f) is the restraint moment caused by the prestressing load.

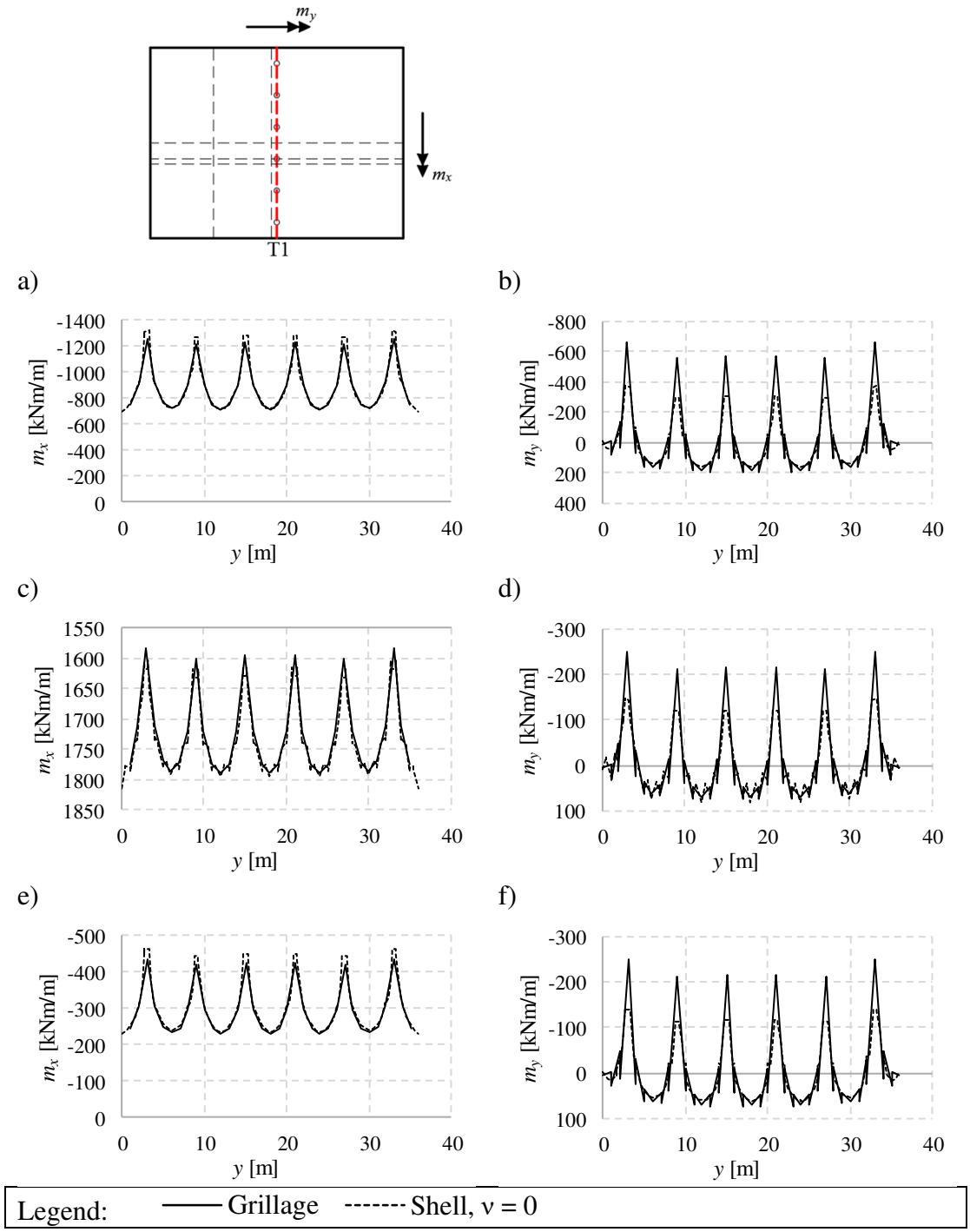

Figure 4.11 Moment distributions along the section T1 for a grillage and a shell model where the Poisson's ratio is set to 0. The left column shows the moment m_x and the right column shows the moment m_y. a) and b) shows the moment caused by the permanent load. c) and d) is the resultant moment caused by the prestressing load. e) and f) is the restraint moment caused by the prestressing load.

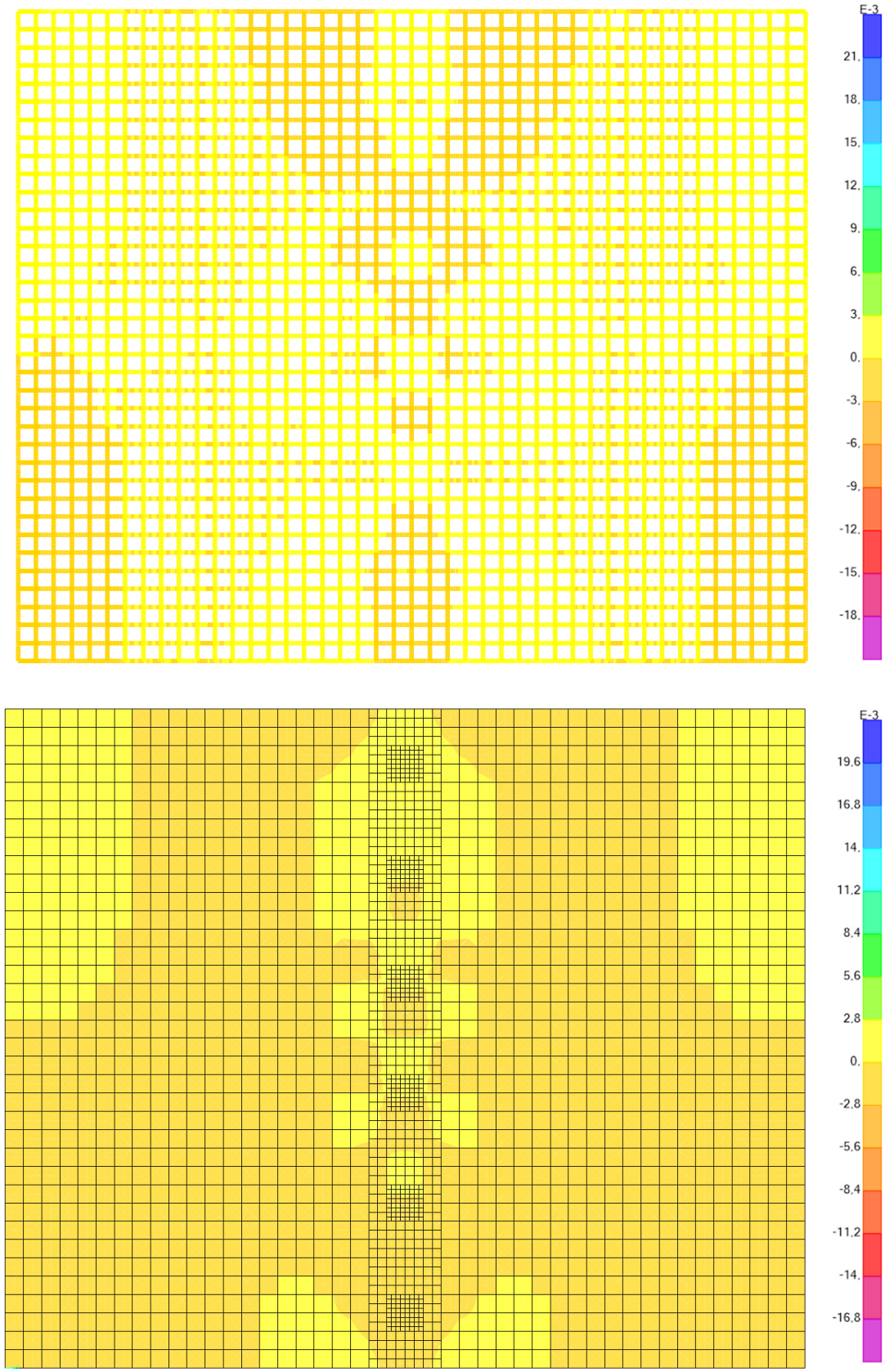

Figure 4.12 Contour plot of the deformation in mm in the y direction. The top plot represents the grillage model and the bottom plot represents the shell model where the Poisson's ratio is set to zero

From Figure 4.10 and Figure 4.11, it is clear that the moment distributions in both the longitudinal and transverse direction for the grillage and shell models are similar. The same tendency occurs in all evaluated sections.

In a majority of the cases, the deviation of the results between the models is less than 1 %. The moments at the columns and the transverse moment distribution in section T1 deviates substantially between the models. However, the tendency of the moment distribution is similar.

Figure 4.12 shows that the shell model with Poisson's ratio set to zero has negligible deformation in the y-direction caused by the prestressing; i.e. in similarity to the grillage model.

4.8 Influence of reduced stiffness in the transverse direction

4.8.1 Introduction

In this section, models with different transverse stiffness have been compared. This has been done to investigate how changed stiffness, due to cracking, affects the overall behavior of the bridge. The changed stiffness has been defined using different methods.

4.8.2 Reduction with a factor of 0.5

In this comparison, two shell models with orthotropic material is treated. In both models, the Poisson's ratio is set to zero, but the transverse stiffness, E_2, is reduced by a factor of 0.5 in one of the models; i.e.

$$E_2 = 0.5E_1$$

Figure 4.13 shows some results along the section T1. The moments caused by only permanent or prestressing load are presented for both the longitudinal direction, $m_{x,}$ and the transverse direction, m_y. All results from this comparison are presented in Appendix H.6.1.

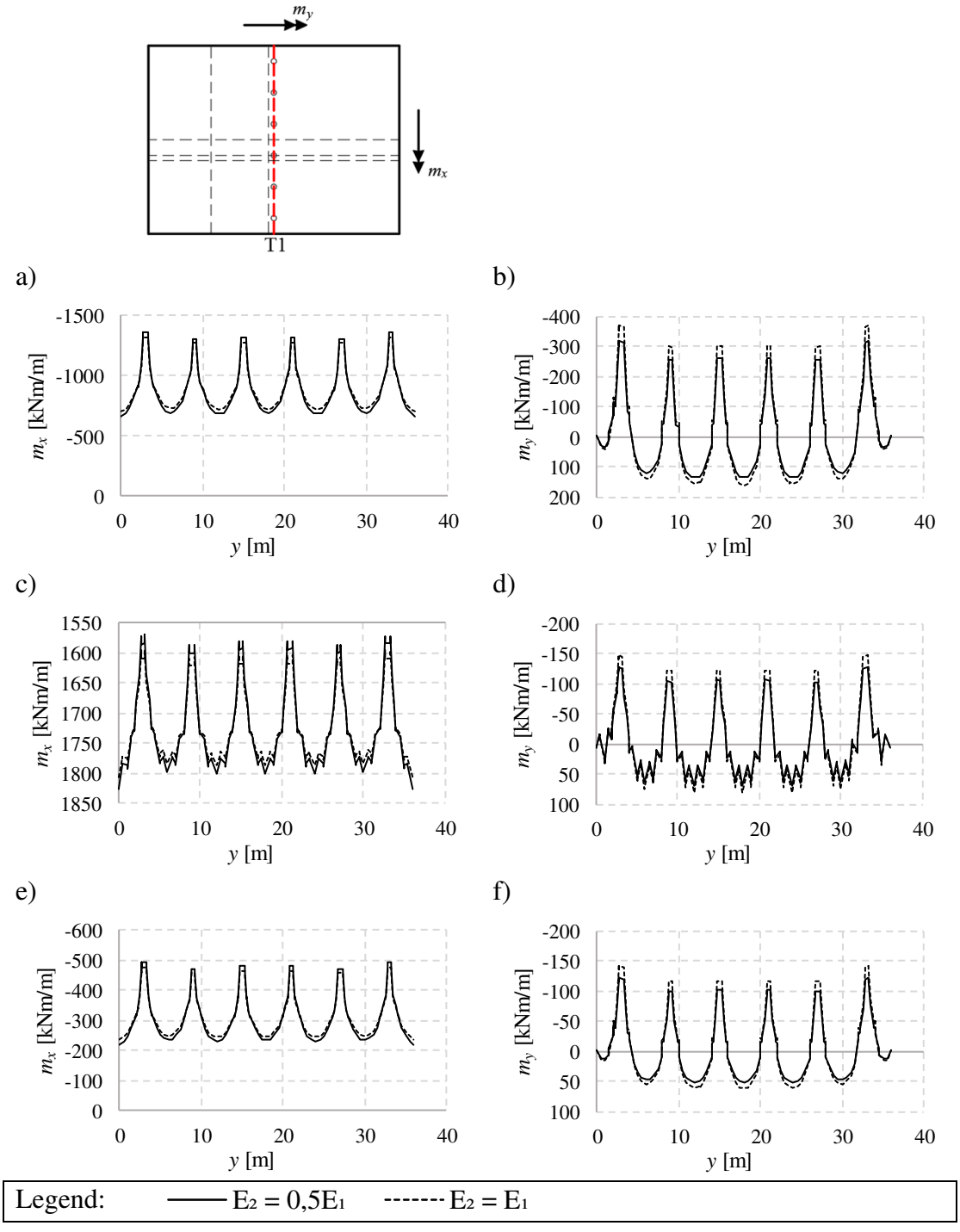

Figure 4.13 Moment distributions along the section T1 for two shell models with different transverse stiffness, E_2. The left column shows the moment m_x and the right column shows the moment m_y. a) and b) shows the moment caused by the permanent load. c) and d) is the resultant moment caused by the prestressing load. e) and f) is the restraint moment caused by the prestressing load.

The influence of reduced transverse stiffness is clearly visible in the section T1 over the columns. In the model where the stiffness is reduced, the moment curve for m_x has been stretched vertically so that the difference between the maximum and minimum

moment has increased. In a similar way, the moment curve for m_y has been compressed vertically so that the difference between the maximum and minimum moment has decreased.

In Table 4.3, the moments at a support and a span for the graphs in Figure 4.13 are presented. In the model with reduced stiffness, the moment in the transverse direction, m_y, has decreased approximately 10-15% in the evaluated points. The moment in the longitudinal direction, m_x, has changed up to 5% in the evaluated points. In the span between the columns and the wall, the influence of reduced stiffness has little effect and the deviation is less than 0.5%.

Table 4.3 Moments in kNm/m at certain points in the graphs shown in Figure 4.13 and the deviation between the models.

Moment m_x [kNm/m]			
Figure 4.13	a)	c)	e)
Stiffness	Support y = 15	Support y = 15	Support y = 15
Reduced	-1323	1594	-480
Regular	-1281	1617	-463
Deviation [%]	3.3	-1.4	3.6
	Span y = 18	Span y = 18	Span y = 18
Reduced	-686	1800	-233
Regular	-719	1785	-246
Deviation [%]	-4.6	0.8	-5.2
Moment m_y [kNm/m]			
Figure 4.13	b)	d)	f)
Stiffness	Support y = 15	Support y = 15	Support y = 15
Reduced	-262	-106	-102
Regular	-303	-123	-117
Deviation [%]	-13.3	-13.6	-13.3
	Span y = 18	Span y = 18	Span y = 18
Reduced	135	70	52
Regular	159	81	62
Deviation [%]	-14.9	-13.5	-14.9

4.8.3 Reduction with a factor of 0.1

To highlight the influence of reduced stiffness in the transverse direction, an additional comparison has been made. In this comparison, two shell models with orthotropic material is treated. In both models, the Poisson's ratio is set to zero, but the transverse stiffness, E_2, is reduced by a factor of 0.1 in one of the models i.e.

$E_2 = 0.1E_1$

Moment distributions along section T1 in the two models are presented in Figure 4.14. All results from this comparison are presented in Appendix H.6.2.

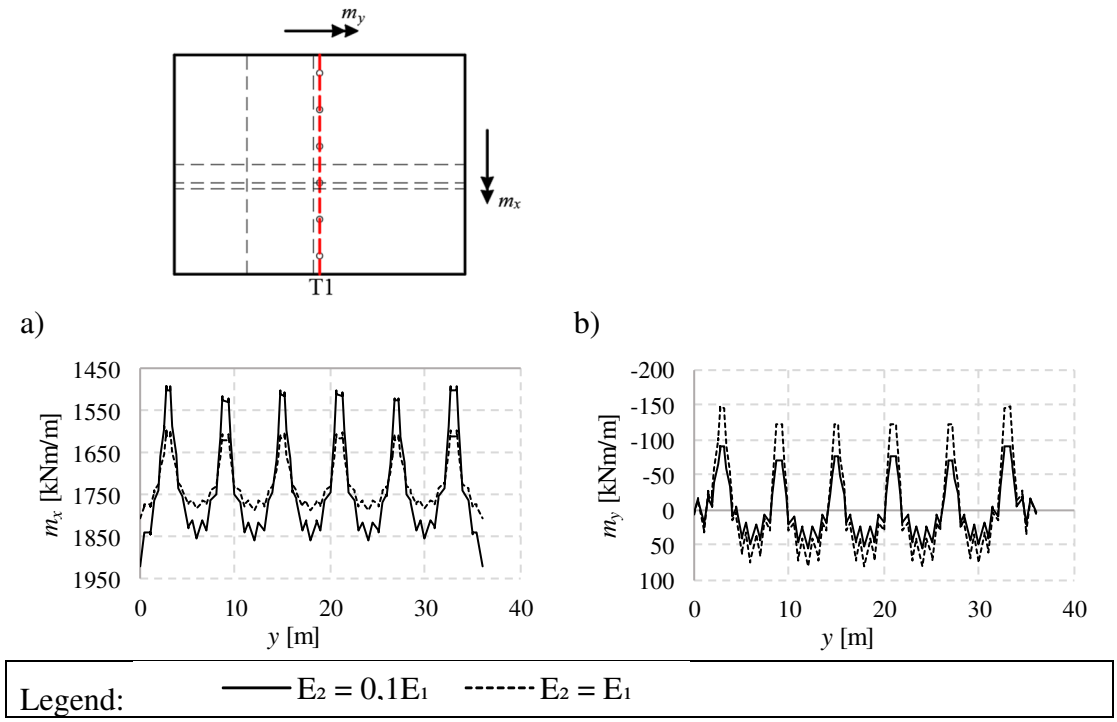

Figure 4.14 Resultant moment distributions along the section T1 for two shell models with different transverse stiffness, E_2. a) m_x. b) m_y.

Similar to the comparison in Section 4.8.2, the effect of reduced stiffness is most prominent in section T1. In the model with reduced stiffness, the moment in the transverse direction, m_y, has decreased approximately 34-40% in the evaluated points. The moment in the longitudinal direction, m_x, has changed up to 25% in the evaluated points. In the span between the columns and the wall, the influence of reduced stiffness has little effect and the deviation is less than 0.5%.

4.8.4 Reduction using property modifiers

As mentioned in Section 2.8.1.4, the stiffness can be modified by "property modifiers" in SAP2000. It can, for practical reasons, be convenient to use isotropic material in FE modelling. For that reason, this method of modifying stiffness has been compared with the method of using an orthotropic material.

In this comparison, shell models with orthotropic and isotropic material have been compared. In the models, the Poisson's ratio is set to zero but the stiffness has been modified in different ways. In the model with orthotropic material, the transverse stiffness, E2, is reduced by a factor of 0.1; i.e.

$E_2 = 0.1E_1$

In the models with isotropic material, property modifiers have been used to reduce the bending stiffness, corresponding to moment M22 and M12, by a factor of 0.1. Moment distributions along section T1 in the two models are presented in Figure 4.15. All results from this comparison are presented in Appendix H.6.3.

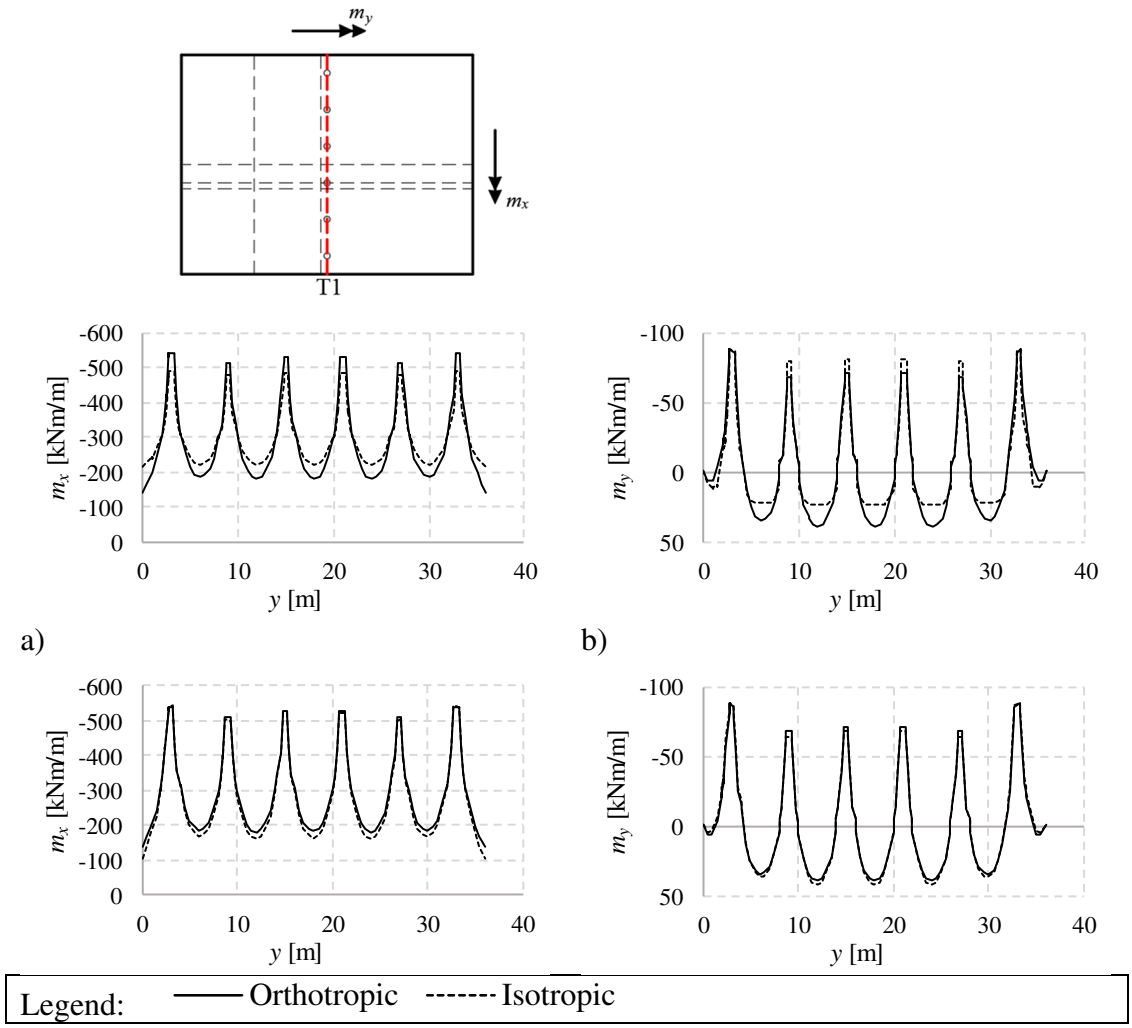

Figure 4.15 Restraint moment distributions along the section T1 for the two shell models. a) and b) Only bending stiffness corresponding to M22 is reduced. c) and d) Bending stiffness corresponding to both M22 and M12 is reduced.

When both the bending stiffness, corresponding to M22 and M12, was reduced, the model gave similar results as the model with orthotropic material. However, when only the bending stiffness corresponding to M22 was reduced, the results did not match well. This indicates that it is not enough to only reduce the bending stiffness corresponding to M22.

4.9 Tensile stresses

As mentioned in Section 2.9, Eurocode requires the concrete close to the tendons to be compressed under the frequent load combination. For that reason, the stress distribution in the slab has been studied for that load combination to examine the stresses close to the tendons. A shell model, that was assumed uncracked, i.e. $\nu = 0.2$, was used in this study.

In Figure 4.16 and Figure 4.17, the stress distributions in the longitudinal direction, σ_x, are shown for the top and bottom face of the slab. Figure 4.18 and Figure 4.19 shows the stress distribution in the transverse direction, σ_y, for the top and bottom face of the slab.

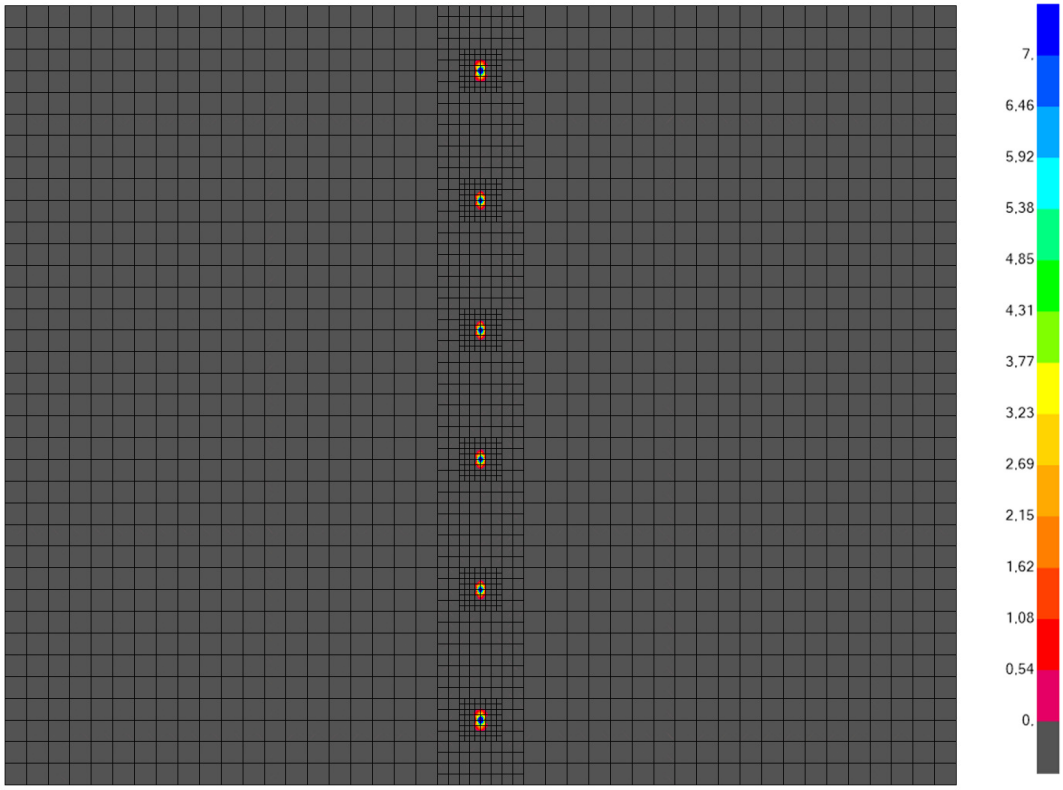

Figure 4.16 Tensile stresses in the longitudinal direction σ_x [MPa] on the top face of the slab under frequent load combination. Note that the scale is adjusted so that all compressive stresses are shown in gray.

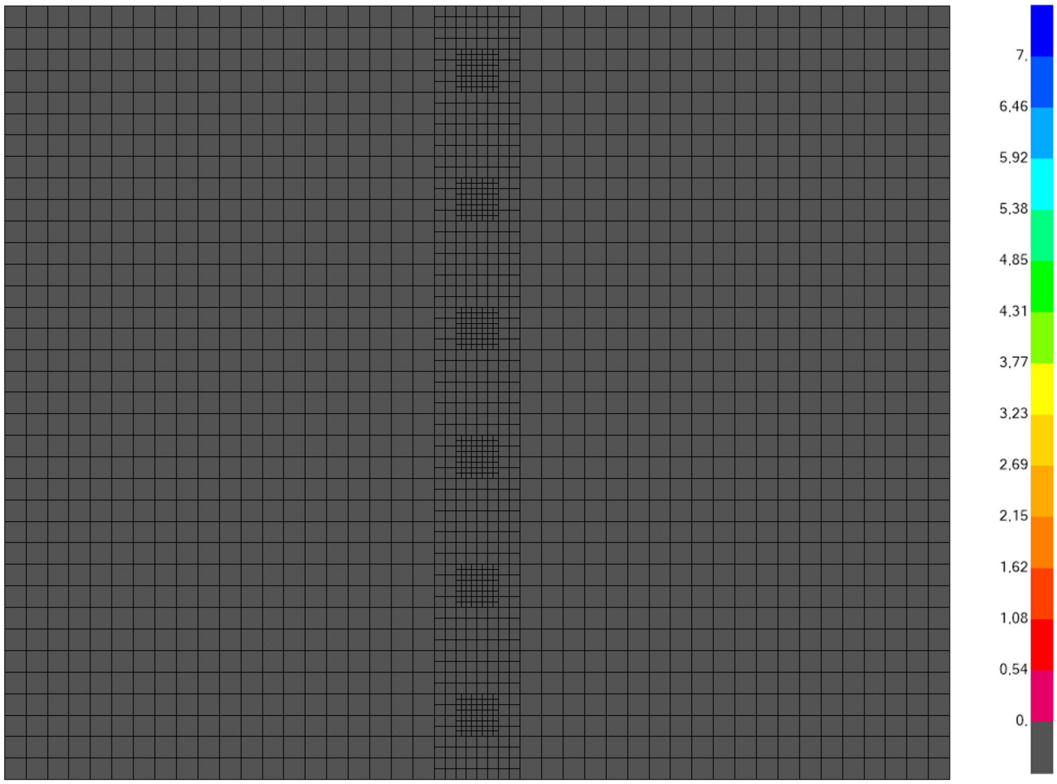

Figure 4.17 Tensile stresses in the longitudinal direction σ_x [MPa] on the bottom face of the slab under frequent load combination. Note that the scale is adjusted so that all compressive stresses are shown in gray.

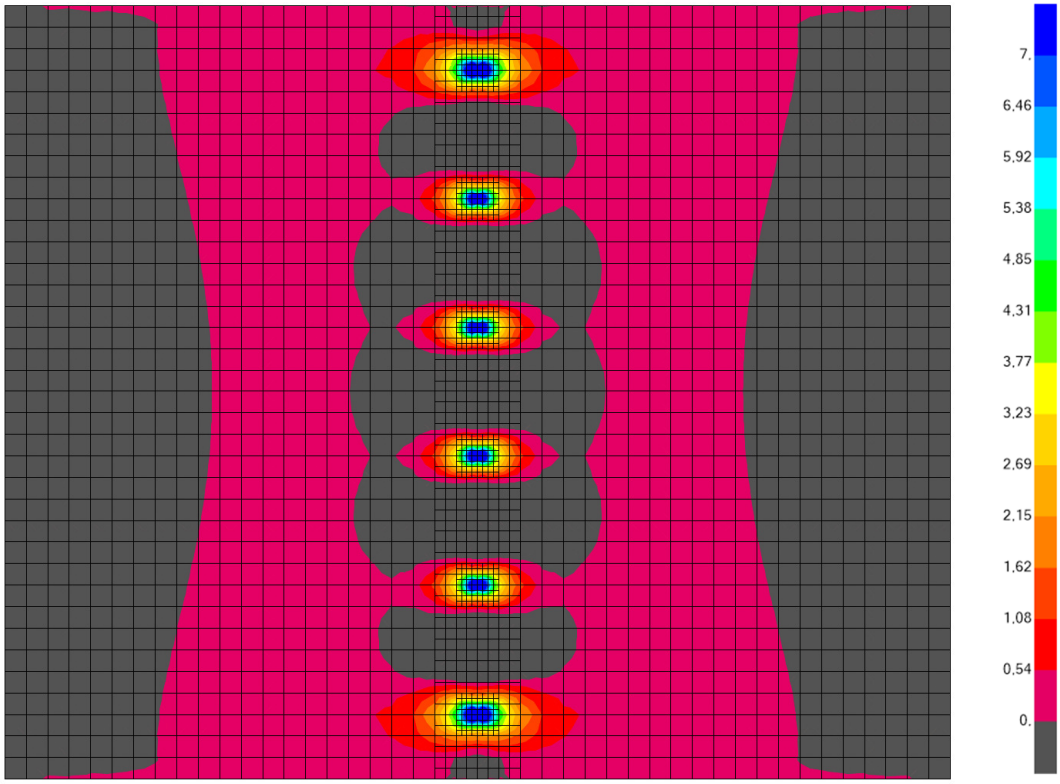

Figure 4.18 Tensile stresses in the transverse direction σ_y [MPa] on the top face of the slab under frequent load combination. Note that the scale is adjusted so that all compressive stresses are shown in gray.

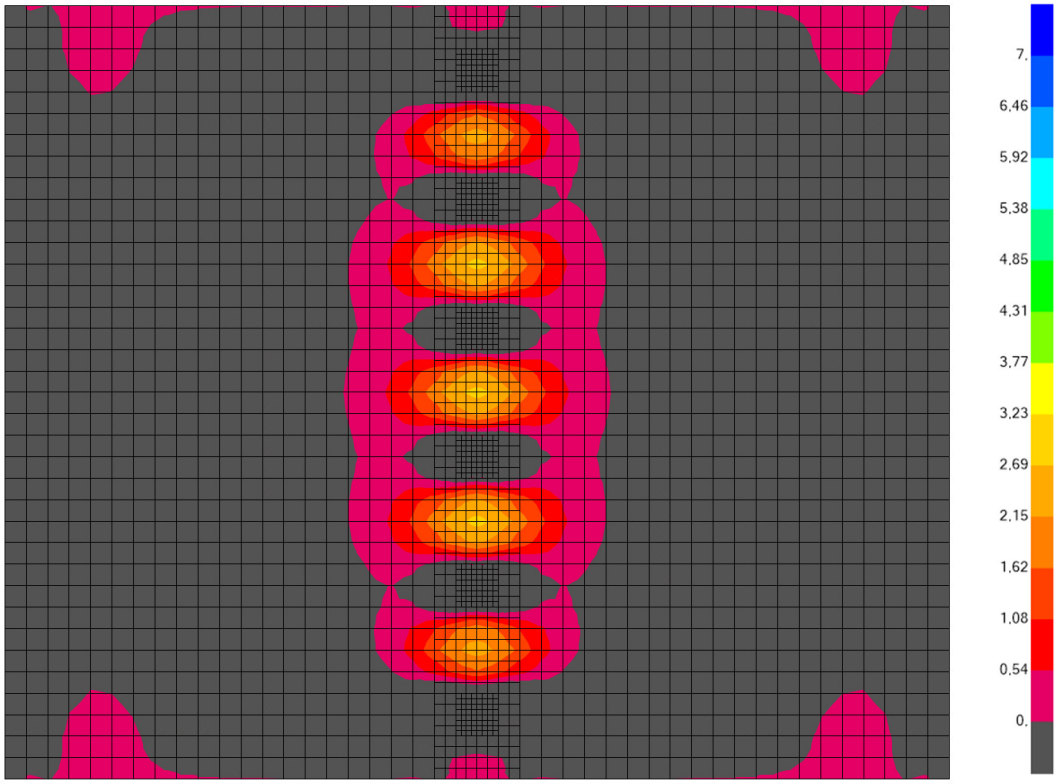

Figure 4.19 Tensile stresses in the transverse direction σ_y [MPa] on the bottom face of the slab under frequent load combination. Note that the scale is adjusted so that all compressive stresses are shown in gray.

Figure 4.16 and Figure 4.17 clearly show that the whole slab is in compression in the longitudinal direction for this load combination. Note that the tensile stresses that can be seen in Figure 4.16 appear in at the location where the columns connect to the slab.

Figure 4.18 and Figure 4.19 clearly show that tensile stresses appear on both the top and bottom face. Figure 4.20 shows a zoomed region of a column from Figure 4.18 and Figure 4.19. The values shown are in MPa and are taken 0.25 m from the center of the column.

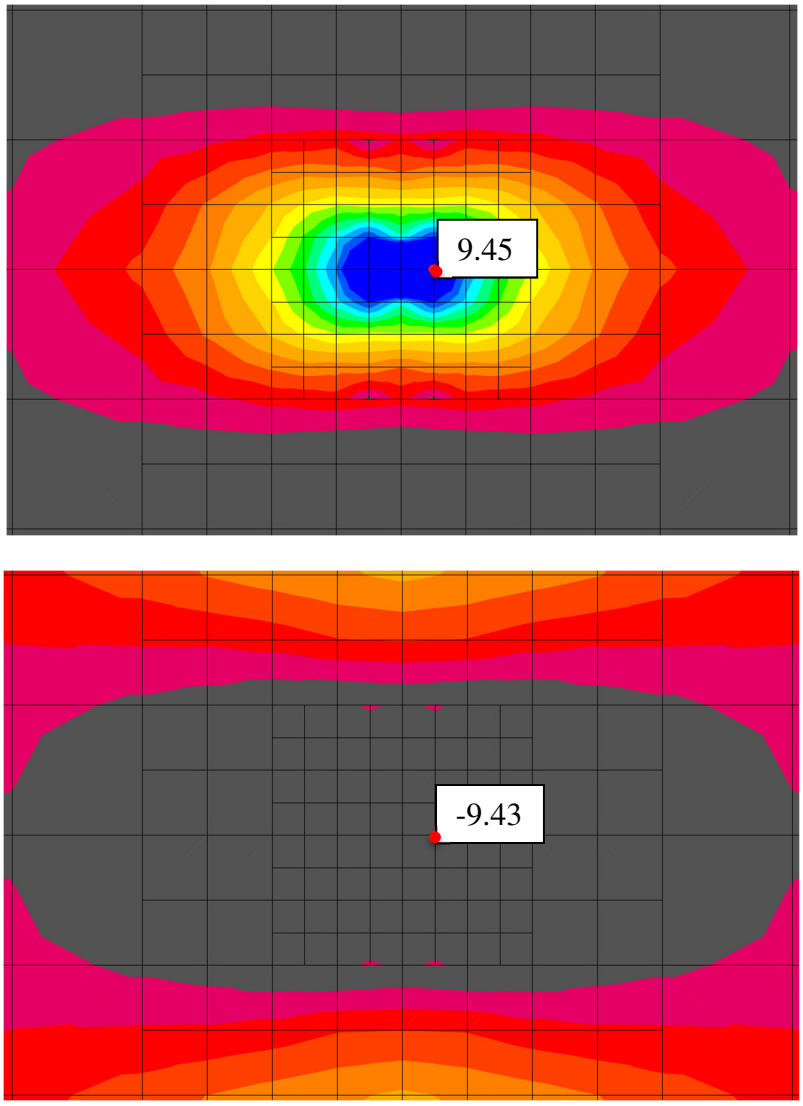

Figure 4.20 The stress in a point close to a column. The upper plot show the stresses on the top face and the lower plot show the stresses on the bottom face of the slab.

The stresses in the slab at the column is 9.45 MPa on the top-face and -9.43 MPa on the bottom face. This implies, by means of linear distribution, that the top half of the cross section is in tension. Note that the tendons are located close to the top face at the columns.

5 Discussion about the FE-analysis

5.1 Practical experience of the FE modelling

A large part of this thesis was the modelling in SAP2000 and the following post-processing in Excel. There have been significant differences in how the models have been built. In this Section, the practical experiences related to the modeling is discussed.

The shell models were relatively simple to create in SAP2000. Both the walls and the slab were created as separate shell elements which could easily be divided into the desired element size. It is intuitive to represent a slab with shell elements due to their shape and the possibility to apply area loads directly on the elements. A complication with shell models is the singularity that appear at point supports, as mentioned in Section 2.8.1.1. This required the mesh to be adjusted around the columns and it also led to extra work in the post-processing.

The beam grillage models required more attention to detail in SAP2000. The spacing between the beam elements had great influence on how the model should be built. It determined the cross section of each beam element, and also the magnitude of the loads to be applied. During the course of work, different spacings of the beam elements have been tried, but in the end a spacing of one meter was chosen to match the element size of the shell models. A change of the spacing in the grillage model led to extra work, since basically the whole model had to be remade. This means that the element mesh is not easily adjusted. Another complication when using a beam grillage is to decide how to represent the geometry of the slab in a good way, as discussed in Section 2.8.2.1. An advantage with the beam grillage model is that no singularities appear at point supports. This made the post-processing easier compared to the shell model.

Since a beam element cannot be subjected to an area load, the load had to be transformed into several line loads. These loads depend on the element spacing and had to be recalculated and reapplied when the element mesh was changed. As discussed in Section 2.8.2.2, also the self-weight had to be modified since the cross sections of the longitudinal and transversal beams overlapped.

The easiest model to create was the 2D model. It only consists of a few elements in two dimensions and no special considerations had to be taken. The beam grillage model required more work than the shell model, especially when the mesh had to be adjusted. This extra work could be avoided if the desired element mesh is known from the beginning; i.e. no extensive adjustments of the model are needed.

The post-tensioning tendons were easy to model in SAP2000. The tendons could be modelled in the same way in all models using the ”tendon object”. In this study, it was convenient to be able to define the prestressing load as a stress since the tendon area was changed during the course of the work. However, the long-term effects had to be calculated manually and was input as stresses in SAP2000.

The most time-consuming part of this project was to post process the results from SAP2000 in Excel. Data management is a big part of the FE modeling in SAP2000 for this type of analysis and a well-structured data handling system is therefore important.

5.2 Evaluation of results

This study has shown that the choice of Poisson's ratio may have significant influence on the structural response in a slab. According to Eurocode 2, the Poisson's ratio should be set to 0.2 for an uncracked concrete slab and zero when cracked. When a beam grillage model was compared to shell models, with Poisson's ratio set to 0.2 and 0, respectively, the results in the longitudinal direction matched for both cases. However, when the Poisson's ratio was 0.2 in the shell model, the results in the transverse direction were significantly different. In many cases, the grillage model completely missed moments that developed in the transverse direction. However, when the Poisson's ratio was set to zero in the shell model, the results from the two models were very similar in the transverse direction as well. This was expected since the grillage model is unable to describe transverse contraction/expansion in a slab. It can be concluded that the influence of the Poisson effect was greater than expected.

How the prestressing load is defined in SAP2000 has no significant influence on the results in this thesis. As mentioned in Section 2.7.5, the prestressing load can be defined either as load or element. However, when the prestressing load is defined as element, the self-weight and stiffness is considered. This may be important to consider for other geometries.

It has been shown that reduced stiffness in the transverse direction has little influence on the moment distribution in the slab. The moments in the mid-span are mostly unaffected by the reduced stiffness, but a noticeable tendency could be observed at the columns. In this region, the moment in the transverse direction, m_y, decreased and the moment in the longitudinal direction, m_x, increased. This implies that some of the moment is redistributed from the transverse to the longitudinal direction, which was expected. The results in Section 4.8.4 implies that it is possible to describe orthotropic behavior in an isotropic material by using "property modifiers" in SAP2000. However, only moment distributions have been compared and it is possible that using "property modifiers" may have consequences not detected in this analysis.

Tensile stresses were detected in the concrete close to the tendons under the frequent load combination. This is problematic since the Eurocode 2, as mentioned in Section 2.9, states a decompression requirement. This will be discussed further in Section 5.3. The tensile stresses appeared in the transverse direction over the columns and were large enough to cause cracking. In the longitudinal direction, the concrete was solely compressed.

In all shell models, the problem with singularity has been accounted for as explained in Section 3.5.1.2. In many cases where the moment distributions showed good conformity in general, a difference could still be observed at the columns. The difference probably depends on that the singularity, despite the taken measures, still somewhat influence the results in the region around the columns.

5.3 Evaluation of decompression requirement

The decompression requirement, presented in Section 2.9, states that the concrete 100 mm from the tendon should be in compression under frequent load combination. However, the code does not distinguish the stress orientation for the decompression

requirement. This is problematic for the studied bridge type, since this analysis has shown that tensile stresses develop perpendicular to the tendons. These tensile stresses are difficult to avoid since more prestressing in the longitudinal direction will not help.

This problem has been treated in a Norwegian calculation guide (Johansen, 2017). According to this, the decompression requirement only applies in the longitudinal direction. This implies that tensile stresses perpendicular to the tendons are allowed. However, no such recommendations are given by the Swedish road administration.

The interpretation by Johansen give rise to questions concerning the purpose of the requirement. If the requirement concerns durability; i.e. the concrete should protect the tendons from the environment, it could be argued that no cracks should be allowed since it does not matter in which direction a crack appears.

From a modeling perspective, it is also necessary to know if the decompression requirement applies in all directions or only parallel to the tendon. Depending on whether the concrete is cracked or not decide what the value for the Poisson's ratio should be. In this study, the Poisson's ratio has had great influence on the results.

6 Conclusion and suggestions for further studies

6.1 Conclusions

- For a frame portal bridge, with intermediate columns and post-tensioning tendons in the longitudinal direction, tensile stresses in the transverse direction cannot be controlled by the post-tensioning. In the studied bridge, tensile stresses in the transverse direction appeared in the concrete close to the tendons. This means that the decompression requirement is not fulfilled. There is a clarification from the Norwegian road administration concerning this requirement that states that the decompression requirement only applies in the longitudinal direction. No such recommendation exists in Sweden and a similar clarification of how to interpret this requirement is therefore needed.

- The shell and beam grillage models resulted in significantly different moment distributions in the transverse direction when the Poisson's ratio, in shell model, was set to 0.2, which correspond to an uncracked concrete section. However, when the Poisson's ratio was set to zero, which correspond to a cracked concrete section, the difference between the moment distributions in the two models were small.

- In this project, the simulation of reduced transverse stiffness had little influence on the moment distributions in most parts of the slab. Moment redistributions could be observed in the region around the columns. In this region, the moment in the longitudinal direction increased slightly while the transverse moment decreased slightly.

- There was no difference in the results depending on how the prestressing load was defined in SAP2000. In this project, both methods available in SAP2000 of defining the prestressing load, either as load or element, have been evaluated for both beam grillage and shell models.

- In this thesis, it did not matter in what direction the load was applied on the beam grillage model. Three different ways of applying an evenly distributed load on the modelled slab has been evaluated. Either all load on the longitudinal beam elements, all load on the transverse beam elements or half the load in each direction.

6.2 Suggestions for further studies

- In this project, only one set of boundary conditions for the bridge have been used. Other boundary conditions could be investigated, especially for the connection between the slab and columns. For example, if this connection could also transfer moments, it would be interesting to evaluate if this would give rise to higher restraining forces due to the prestressing.

- Since only one type of bridge has been evaluated in this study, it would be of interest to evaluate other post-tensioned bridge types. Is the decompression requirement problematic for other bridge types as well?

- How is the decompression requirement in Eurocode interpreted in other European countries, except for Sweden and Norway? Are there similar requirements in other regulations, for example the American code?

- It may be favorable to use isotropic materials in FE modelling. In this project, it has been shown that in SAP2000 orthotropic behavior can be described using an isotropic material modified by "property modifiers" for moment distributions. However, further studies are needed to investigate if this also is possible when other sectional forces or stresses are of interest, for example shear force and normal force.

- In practice, it is favorable to use beam grillage models, since these often are less complicated than for example shell models. It has been shown that the Poisson effect has had great influence on the response in a shell model in this project. A beam grillage model cannot describe this effect. Is it possible to modify a beam grillage model so that it can account for the Poisson effect?

7 References

Al-Emrani, M., Engström, B., Johansson, M. & Johansson, P. (2011) *Bärande konstruktioner - Del 1* (Load bearing structures - Part 1. In Swedish). Göteborg: Chalmers University of Technology.

Collins, M. P. & Mitchell, D. (1991) *Prestressed Concrete Structures.* Englewood Cliffs: Prentice-Hall, Inc.

CSI. (2016) *CSI Analysis Reference Manual.* Berkely: Computers & Structures, Inc.

Engström, B. (2011) *Design and analysis of prestressed concrete structures,* Göteborg: Chalmers University of Technology.

Engström, B. (2014) *Design and analysis of slabs and flat slabs.* Göteborg: Chalmers University of Technology.

Hallbjörn, L. (2015) *Betongplattor, beräkning och dimensionering* (Concrete slabs, calculation and design. In Swedish). Stockholm: Royal Institute of Technology.

Hewson, N. R. (2003) *Prestressed Concrete Bridges.* Bodmin: Thomas Telford Publishing.

Jakobi, M. & Adelsköld, T. (2012) *Effektiv utformning av ekodukter och faunabroar* (Effective design of ecoducts and wildlife crossings. In Swedish). Borlänge: Trafikverket.

Johansen, H. (2017) *Beregningsveiledning for etteroppspente betongbruer* (Calculation guidelines for PT concrete bridges. In Norwegian). Oslo: Statens vegvesen.

Kalny, O. (2013) Prestress losses. In *CSI Knowledge Base.* https://wiki.csiamerica.com (2017-03-21).

Liu, G. R. & Quek, S. S. (2003) *Finite Element Method: A Practical Course.* Oxford: Elsevier Science Ltd.

Ottosen, N. & Petersson, H. (1992) *Introduction to the Finite Element Method.* Edingburgh : Pearson Education Limited.

Pacoste, C., Plos, M. & Johansson, M. (2012) *Recommendations for finite element analysis for the design of reinforced concrete slabs,* Stockholm: Royal Institute of Technology.

Appendix A Tendon geometry

The eccentricity of the tendon is measured from the centroid of the slab. The points along the slab, where eccentricities are specified, are measured from the centroid of the wall, see *x* in Figure 3.3. The highlighted eccentricities in Table A.1 were chosen as input in SAP2000, the other was automatically calculated by the program.

Table A.1 Tendon profile

Distance from end support [m]	Eccentricity [m]
0	**0**
5.0	-0.255
9.9	**-0.340**
14.3	-0.216
18.7	0.155
20.4	0.294
22.0	**0.340**
23.7	0.294
25.3	0.155
29.7	-0.216
34.1	**-0.340**
39.1	-0.255
44.0	**0**

Appendix B Material properties

Material properties for concrete class C45/55 is presented in Table B.1 according to Eurocode 2.

Table B.1 Material properties for concrete class C45/55.

Concrete			C45/55
Characteristic strength	f_{ck}	[MPa]	45
Mean strength	f_{cm}	[MPa]	53
Mean tensile strength	f_{ctm}	[MPa]	3,8
Young´s modulus	E_{cm}	[GPa]	36
Poisson´s ratio	ν		0.2 / 0
Density	ρ	[kg/m^3]	2500

The material properties for the tendons is presented in Table B.2, and are taken from the manufacturer of VSL post-tension systems.

Table B.2 Material properties for the strands.

Strand			prEN 10138 - 3 (2009) Y1860S7
Nominal diameter	d	[mm]	15.3
Nominal cross section	A_p	[mm^2]	140
Nominal mass	M	[kg/m]	1.093
Nominal yield strength	$f_{p0,1k}$	[MPa]	1636
Nominal tensile strength	f_{pk}	[MPa]	1860
Specif./min. breaking load	F_{pk}	[kN]	260.4
Young´s modulus	E_p	[GPa]	approx. 195
Relaxation after 1000 h at 20 °C and 0.7 x F_{pk}		[%]	max. 2.5

Coefficients concerning frictional losses of tendon force in the steel ducts are specified in Table B.3.

Table B.3 Coefficient concerning frictional losses.

Internal bonded tendon with corrugated steel duct (bare strand)			Recommended value
Coefficient of friction between the prestressing steel and the duct	μ	[rad^{-1}]	0.18
Wobble factor per unit length	k	[rad / m]	0.005
	k*	[1 / m]	9 x 10^{-4}
Anchor set	Δs	[m]	0.006

Appendix C Prestressing load

Concrete class: C45/55

$f_{ck} := 45\,MPa$

$f_{cm} := f_{ck} + 8MPa = 53\,MPa$

$E_c := 36\,GPa$

$A_c := 0.5m \cdot 1m = 0.5\,m^2$

Steel A 416 G270

Young's modulus: $E_p := 195\,GPa$

Tendon area: $A_p := 19 \cdot 140\,mm^2 = 2.66 \times 10^{-3}\,m^2$

Relaxation factor: $\chi_{1000} := 2.5\%$

Yield strength: $f_{p0.1k} := 1636\ MPa$

Tensile strength: $f_{pk} := 1860\,MPa$

Friction coefficient: $\mu_{curve} := 0.18$

Wobble factor: $k := 0.005\frac{1}{m}$

Anchor slip: $\Delta s := 6mm$

Relaxation class: 2

Cross sectional constants

$$\alpha := \frac{E_p}{E_c} = 5.417$$

$A_I := A_c + (\alpha - 1) \cdot A_p = 0.512\,m^2$

Assumptions

Assume outdoor conditions for the RH => RH=80%

$RH := 80\%$

Assumed age of concrete when load is applied

$t_0 := 28$

Prestressing force/stress

Maximum allowed tendon stress after anchorage

$\sigma_{i.allowed} := \min\left(0.85 \cdot f_{p0.1k}, 0.75 \cdot f_{pk}\right) = 1391 \cdot MPa$

$P_{i.allowed} := \sigma_{i.allowed} \cdot A_p = 3699 \cdot kN$

Maximum allowed tendon stress after anchorage

$\sigma_{i.allowed.before} := \min\left(0.9 \cdot f_{p0.1k}, 0.8 \cdot f_{pk}\right) = 1472 \cdot MPa$

We want to know the tendon force at the active end which result in the allowed tendon force, $P_{i.allowed}$, at x_S. We guess P_i to be able to calculate x_S. When x_S is found the tendon force in that point can be calculated and should not exceed $P_{i.allowed}$.

Guess:

$P_i := 3820 \cdot kN \quad => \quad \sigma_i := \frac{P_i}{A_p} = 1436 \cdot MPa \quad \sigma_i < \sigma_{i.allowed.before} = 1 \quad ok!$

d is the equation of the tendon profile, measured from the top of the cross section. This equation is found by using trendline of the tendon profile for 0<x<18,7m

$d := -0.0048 x^2 + 0.0833 x + 0.4766$

$d'(x) := -0.0096 \cdot x + 0.0833$

$d'' := -0.0096$

Assume linear decrease of tendon force in the first segment, see figure.

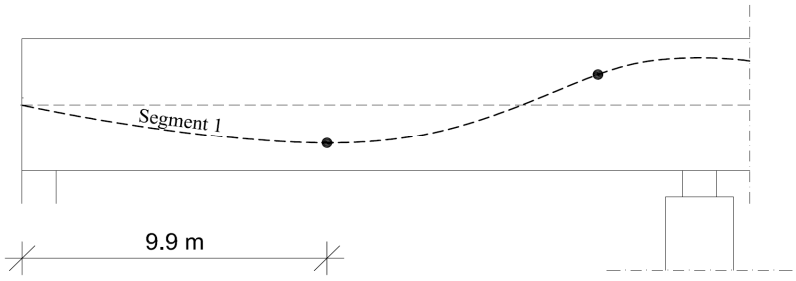

Length of segment 1:

$x_{segment1} := 9.9\,m$

Change of slope within the first segment:

$\alpha_{slope} := d'(0) - d'\left(x_{segment1} \cdot \frac{1}{m}\right) = 0.095$

This formula is used in SAP2000 to calculate the tendon force at a distance x from the active end. NOTE: Eurocode 2 suggests a slightly different formula.

$$P_{i.segment1} := P_i \cdot \exp\left[-\mu_{curve} \cdot \left(\alpha_{slope} + k \cdot x_{segment1}\right)\right] = 3722 \cdot kN$$

p is the change in force per unit length, calculated from a tendon force diagram, assuming linear variation of the tendon force within the segment.

$$\Delta p := \frac{P_i - P_{i.segment1}}{x_{segment1}} = 9.909 \cdot \frac{kN}{m}$$

The anchor set can then be calculated

$$l_{set} := \sqrt{\frac{\Delta s \cdot A_p \cdot E_p}{\Delta p}} = 17.722\ m$$

The tendon force at that point is:

$$P_{i.max} := P_i \cdot \exp\left[-\mu_{curve} \cdot \left(\alpha_{slope} + k \cdot l_{set}\right)\right] = 3696 \cdot kN$$

$P_{i.max} \sim P_{i.allowed}$ ok!

The tendon force which should be applied at the active end is:

$$P_i = 3820 \cdot kN$$

Shrinkage

$\varepsilon_{cs} := \varepsilon_{cd} + \varepsilon_{ca}$

Drying shrinkage

$\varepsilon_{cd.\infty} := k_h \cdot \beta_{RH} \cdot \varepsilon_{cdi}$

$\varepsilon_{cdi} := 0.235 \cdot 10^{-3}$ Assume cement class S

$\beta_{RH} := 0.756$

Perimeter of cross section exposed to drying: $u := 0.5\,m$ Assume no drying upwards

$h_0 := \frac{2 \cdot A_c}{u} = 2\,m$

Since $h_0 > 500mm$ => $k_h := 0.7$

$\varepsilon_{cd.\infty} := k_h \cdot \beta_{RH} \cdot \varepsilon_{cdi} = 1.244 \times 10^{-4}$

Autogenous shrinkage

$\varepsilon_{ca.\infty} := 0.0875 \cdot 10^{-3}$

Total shrinkage strain:

$\varepsilon_{cs} := \varepsilon_{cd.\infty} + \varepsilon_{ca.\infty} = 2.119 \times 10^{-4}$

Stress loss due to shrinkage:

$\sigma_{shrinkage.loss} := E_p \cdot \varepsilon_{cs} = 41.313\,MPa$

Creep

$\varphi := \varphi_{RH} \cdot \beta_{fcm} \cdot \beta_{t0}$

$f_{cm} > 35\ MPa \Rightarrow$

$h_0 := h_0 \cdot 1000 \frac{1}{m} = 2 \times 10^3$ "Removes" the unit

$$\varphi_{RH} := \left[1 + \frac{1 - RH}{0.1 \cdot \sqrt[3]{h_0}} \cdot \left(\frac{35MPa}{f_{cm}} \right)^{0.7} \right] \cdot \left(\frac{35MPa}{f_{cm}} \right)^{0.2} = 1.14$$

$\beta_{fcm} := 2.31$

$$\beta_{t0} := \frac{1}{0.1 + t_0^{0.2}} = 0.437$$

$\varphi := \varphi_{RH} \cdot \beta_{fcm} \cdot \beta_{t0} = 1.152$

Loss due to creep

$$\sigma_c := \frac{P_{i.allowed}}{A_I} = 7.228\,MPa$$

$$\varepsilon_{creep} := \varphi \cdot \frac{\sigma_c}{E_c} = 2.312 \times 10^{-4}$$

$\sigma_{creep.loss} := E_p \cdot \varepsilon_{creep} = 45.086\,MPa$

Relaxation

Relaxation class 2 = >

$$\mu := \frac{\sigma_{i.allowed}}{f_{pk}} = 0.748$$

We are looking for the final value of the relaxation = > $t := 500000$ [hours]

$$\chi_t := 0.66 \cdot \chi_{1000} \cdot \exp(9.1 \cdot \mu) \cdot \left(\frac{t}{1000}\right)^{0.75 \cdot (1-\mu)} \cdot 10^{-3} = 0.048$$

$$\sigma_{relaxation.loss} := \chi_t \cdot \sigma_{i.allowed} = 67.026 \cdot MPa$$

Elastic shortening

$$\varepsilon_{c.shortening} := \frac{\sigma_c}{E_c} = 2.008 \times 10^{-4}$$

$$\sigma_{elastic.sh.loss} := \varepsilon_{c.shortening} \cdot E_p = 39.153 \cdot MPa$$

Total stress loss

$$\sigma_{loss} := \sigma_{shrinkage.loss} + \sigma_{creep.loss} + \sigma_{relaxation.loss} + \sigma_{elastic.sh.loss} = 192.577 \cdot MPa$$

$$\frac{\sigma_{loss}}{\sigma_{i.allowed}} = 13.849 \cdot \%$$

Appendix D Shear modulus

Orthotropic material with $E_2=0.5E_1$ and $\nu_{12}=0$

$E_1 := 36GPa \quad E_2 := 18GPa \quad E_3 := 36GPa$ Young's modulus

$\nu_{12} := 0 \quad \nu_{13} := 0.2 \quad \nu_{23} := 0.2$ Poisson's ratio

$$G_{12} := \frac{E_1 \cdot E_2}{\left(E_1 + E_2 + 2\nu_{12} \cdot E_1\right)} = 12 \cdot GPa$$ Shear modulus

$$G_{13} := \frac{E_1 \cdot E_3}{\left(E_1 + E_3 + 2\nu_{13} \cdot E_1\right)} = 15 \cdot GPa$$

$$G_{23} := \frac{E_2 \cdot E_3}{\left(E_2 + E_3 + 2\nu_{23} \cdot E_2\right)} = 10.588 \cdot GPa$$

Orthotropic material with $E_2=0.1E_1$ and $\nu_{12}=0$

$E_1 := 36GPa \quad E_2 := 3.6GPa \quad E_3 := 36GPa$ Young's modulus

$\nu_{12} := 0 \quad \nu_{13} := 0.2 \quad \nu_{23} := 0.2$ Poisson's ratio

$$G_{12} := \frac{E_1 \cdot E_2}{\left(E_1 + E_2 + 2\nu_{12} \cdot E_1\right)} = 3.273 \cdot GPa$$ Shear modulus

$$G_{13} := \frac{E_1 \cdot E_3}{\left(E_1 + E_3 + 2\nu_{13} \cdot E_1\right)} = 15 \cdot GPa$$

$$G_{23} := \frac{E_2 \cdot E_3}{\left(E_2 + E_3 + 2\nu_{23} \cdot E_2\right)} = 3.158 \cdot GPa$$

Appendix E Stiffness modifier for torsional stiffness

Longitudinal beam:

$h := 1\,m$
$b := 1\,m$

The torsional stiffness should be equal to 2·I for the longitudinal beam elements. In SAP2000, the torsional stiffness can be modified by assigning a property modifier. To find the property modifier factor, k, the following equation can be used:

$$k := \frac{2 \cdot I}{K}$$

where I is the moment of inertia of the longitudinal beam and K is the torsional stiffness of the beam to be modified.
Moment of inertia of the longitudinal beam:

$$I_{long} := \frac{b \cdot h^3}{12} = 0.083\ m^4$$

The torsional constant given by SAP2000 for the longitudinal beam elements:

$$K_{long} := 0.1408\,m^4$$

The torsional constant given by SAP2000 for the transversal beam elements:

$$K_{trans} := 0.1408\ m^4$$

The torsional constants are the same for the longitudinal and transversal beams
The stiffness modifier, k, can then be calculated.

$$k := \frac{2 \cdot I_{long}}{K_{long}} = 1.184$$

Appendix F Verification of models

Table F.1 Hand calculation of the total load of the bridge and external loads

Self-weight of concrete	24.99	kN/m^3
Self-weight of steel	76.97	kN/m^3
Slab		
Area	1584	m^2
Thickness	1	m
Volume	1584	m^3
Total dead load	39584	kN
Column		
Diameter	1	m
Height	7	m
Number of columns	6	
Total volume of columns	33	m^3
Total dead load	824	kN
Wall		
Area of both walls	504	m
Thickness	1	m
Total volume walls	504	m^3
Total dead load	12595	kN
Tendons		
Length of one tendon	44	m
Area of one tendon	5320	mm^2
Number of tendons	36	
Total volume of tendons	8	m^3
Total dead load	650	kN
Total dead load	**53653**	kN
Permanent load	20	kN/m^2
Live load	10	kN/m^2
Area of slab	1584	m^2
Total external load	**47520**	kN
Total load including self-weight of tendons	**101173**	kN
Total load excluding self-weight of tendons	**100523**	kN

Table F.2 Total reaction forces from the SAP-models. The reactions from the models with tendons modelled as element are compared with the total load including self-weight of tendons. The models with tendons modelled as load are compared with the total load excluding self-weight of tendons.

Model	Total reactions in SAP2000 [kN]	Deviation from total load
Shell model		
Tendon as element	101175	0.00%
Tendon as load	100529	-0.01%
Grillage model		
Tendon as element		
All load in longitudinal direction	101175	-0.002%
All load in transverse direction	101175	-0.002%
Half the load in each direction	101175	-0.002%
Tendon as load		
All load in longitudinal direction	100529	-0.01%
All load in transverse direction	100529	-0.01%
Half the load in each direction	100529	-0.01%

Appendix G Sensitivity analysis

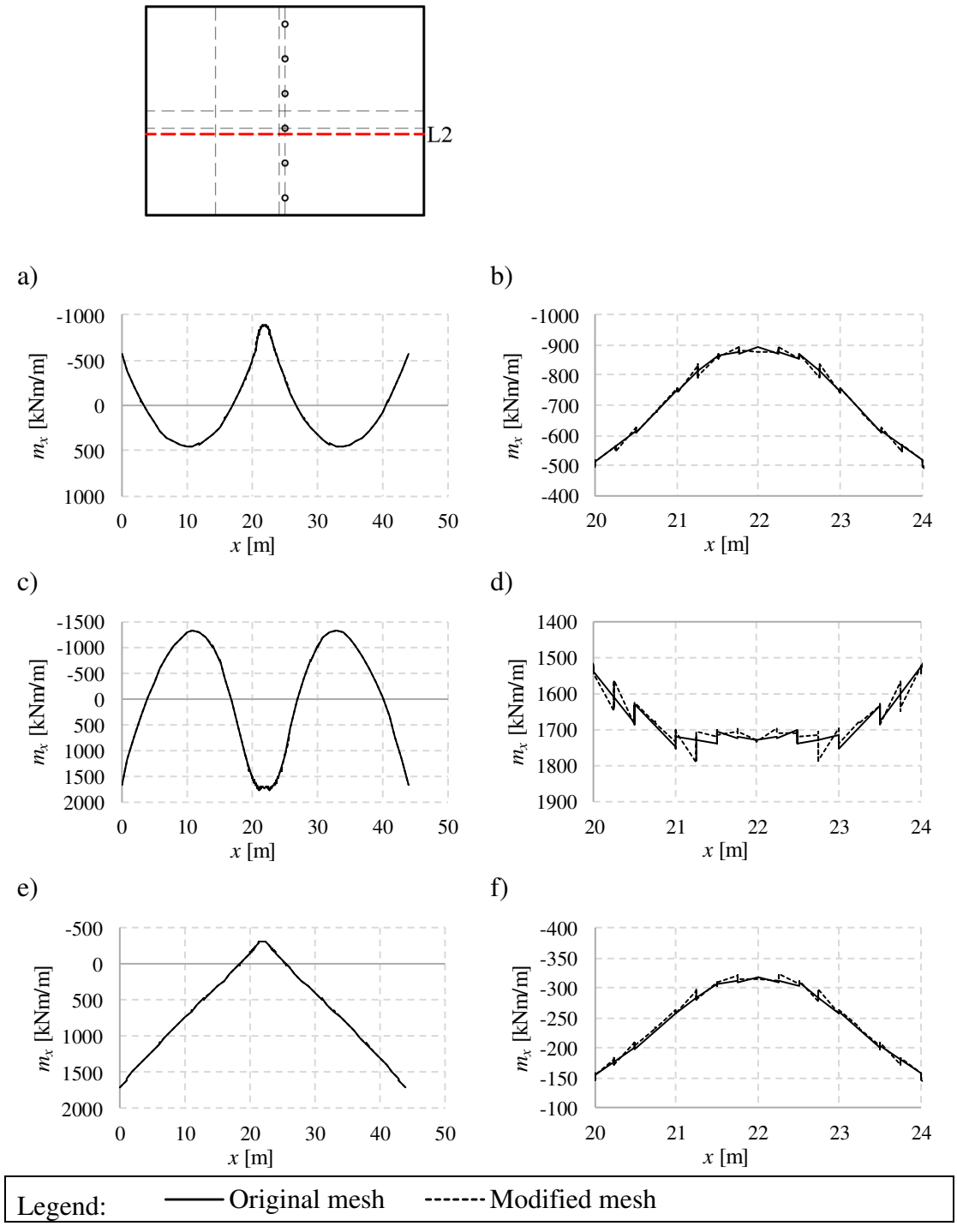

Figure G.1 Moment distributions along the section L2 for a shell model with different mesh. The left column shows the moment m_x and the right column shows a zoomed part of the moment distribution. a) and b) shows the moment caused by the permanent load. c) and d) is the resultant moment caused by the prestressing load. e) and f) is the restraint moment caused by the prestressing load

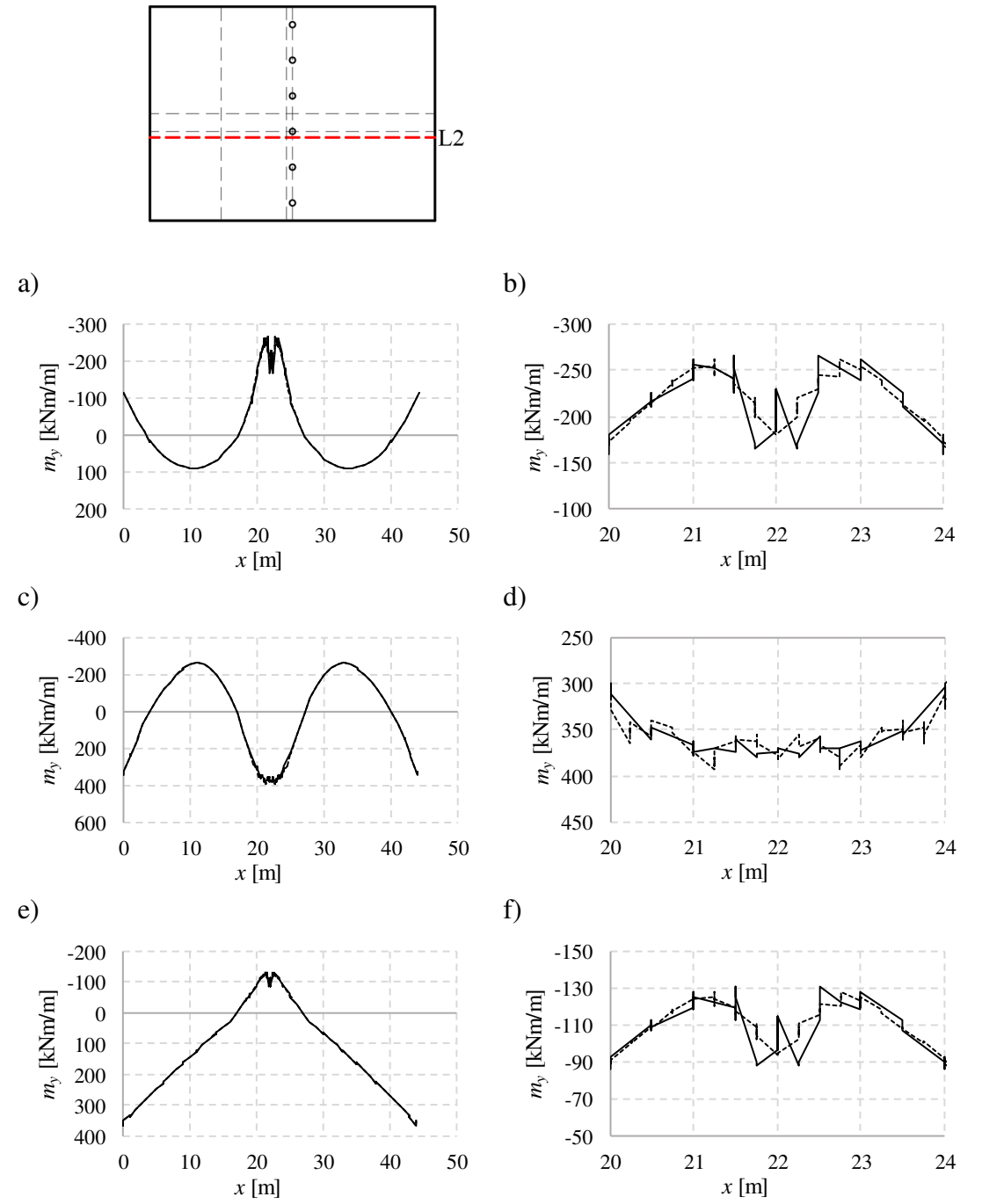

Figure G.2 Moment distributions along the section L2 for a shell model with different mesh. The left column shows the moment m_y and the right column shows a zoomed part of the moment distribution. a) and b) shows the moment caused by the permanent load. c) and d) is the resultant moment caused by the prestressing load. e) and f) is the restraint moment caused by the prestressing load

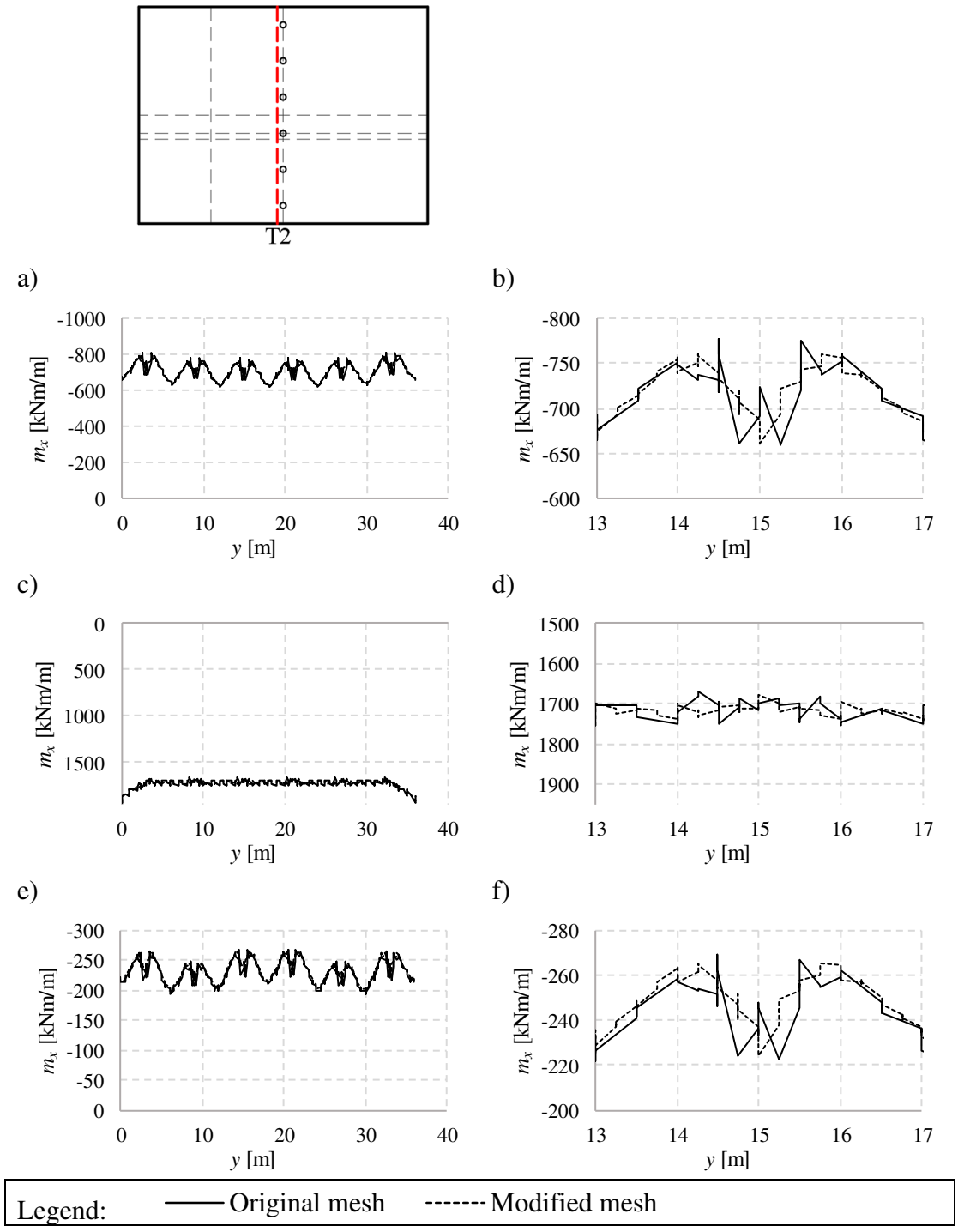

Figure G.3 Moment distributions along the section T2 for a shell model with different mesh. The left column shows the moment m_x and the right column shows a zoomed part of the moment distribution. a) and b) shows the moment caused by the permanent load. c) and d) is the resultant moment caused by the prestressing load. e) and f) is the restraint moment caused by the prestressing load

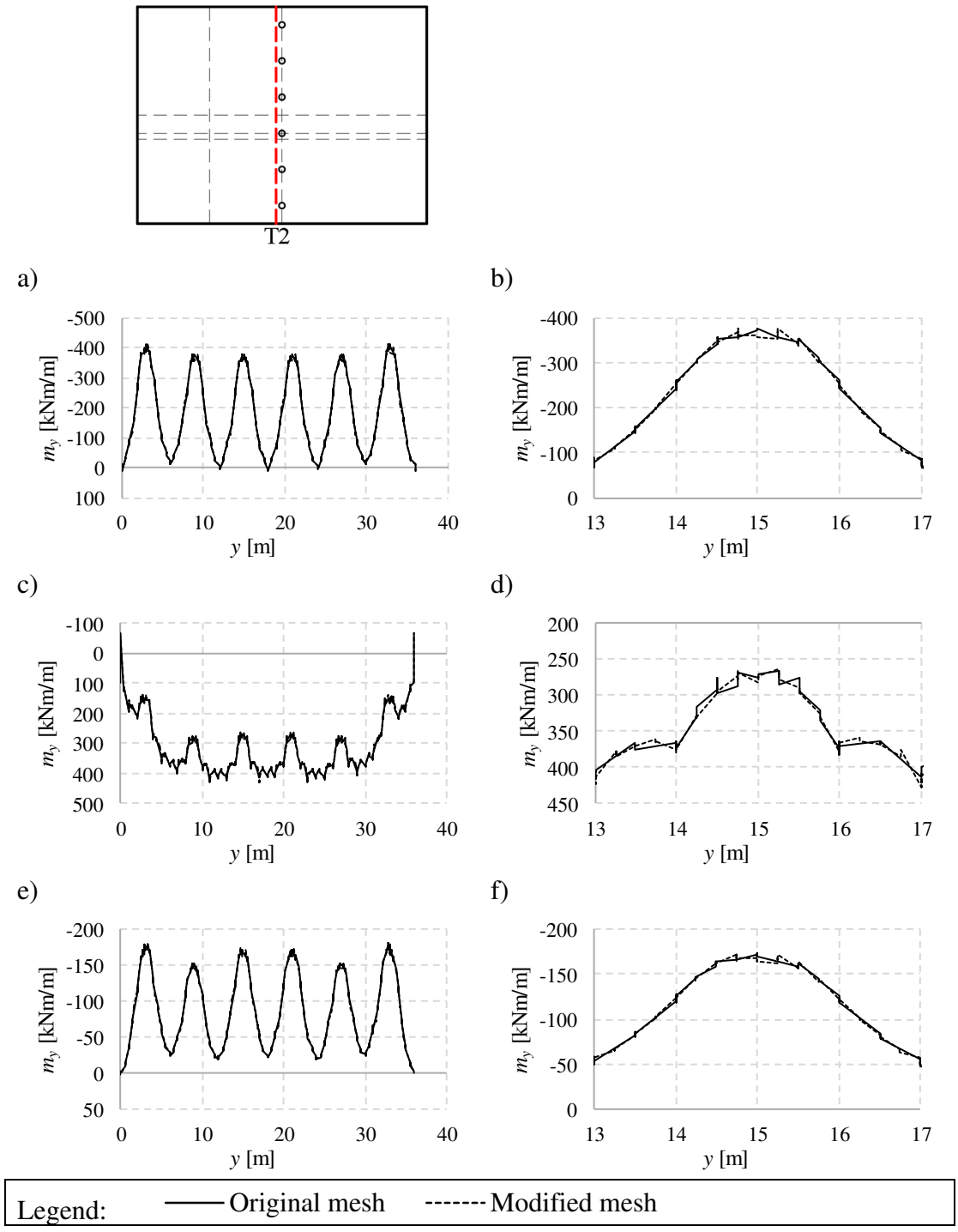

Figure G.4 Moment distributions along the section T2 for a shell model with different mesh. The left column shows the moment m_y and the right column shows a zoomed part of the moment distribution. a) and b) shows the moment caused by the permanent load. c) and d) is the resultant moment caused by the prestressing load. e) and f) is the restraint moment caused by the prestressing load

Appendix H Results

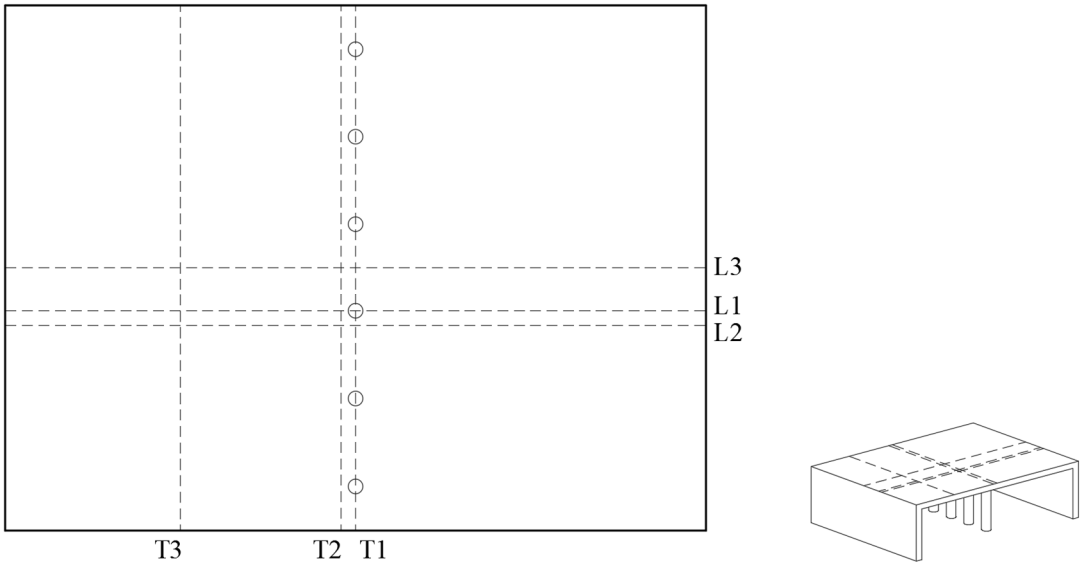

Figure H.1 Output sections.

H.1 Application of loads on a grillage model

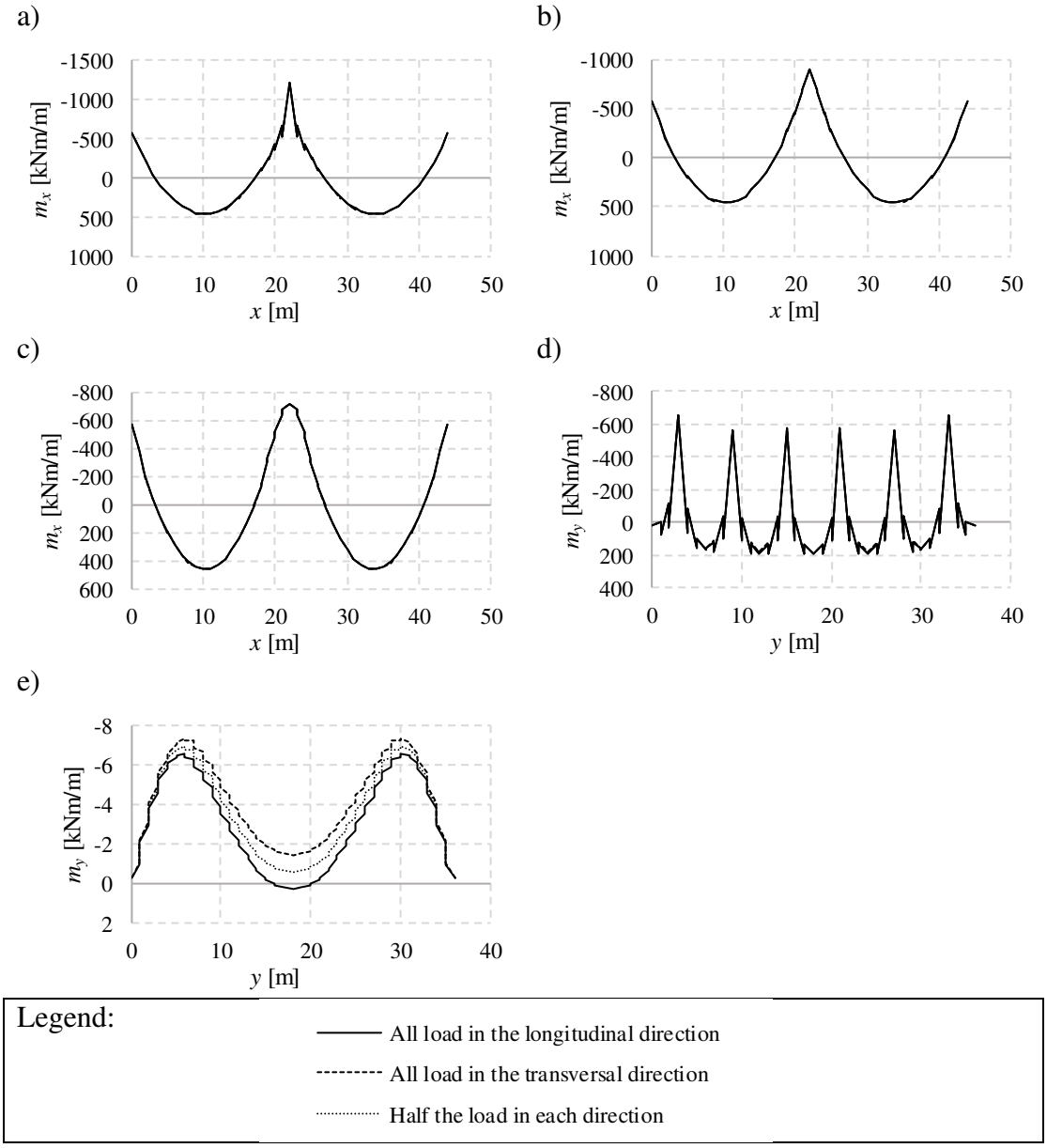

Figure H.2 Moment caused by the permanent load in section a) L1, b) L2, c) L3, d) T1, e) T3.

Table H.1 Comparison of the moments [kNm/m] in Figure H.2 at certain points. If no coordinate is specified, the given value is the peak value in that region. Deviation is the difference between the moments when the load has been applied in different ways. All load applied in the longitudinal direction is used as reference.

Section	**Loaded direction**		**Moment [kNm/m]**	**Deviation [%]**		**Moment [kNm/m]**	**Deviation [%]**
L1	Longitudinal	Support x=22	-1226	-	Span	457	
	Transversal		-1225	0.1		458	-0.4
	Half in each direction		-1226	0.1		457	-0.2
L2	Longitudinal	Support x=22	-897	-	Span	457	-
	Transversal		-896	0.2		458	-0.4
	Half in each direction		-897	0.1		458	-0.2
T1	Longitudinal	Support y = 15	-572	-	Span y = 18	185	-
	Transversal		-574	-0.3		184	0.9
	Half in each direction		-573	-0.2		184	0.5
T3	Longitudinal	Support y = 15	-716	-	Span y = 18	456	-
	Transversal		-714	0.2		458	-0.4
	Half in each direction		-715	0.1		457	-0.2
L3	Longitudinal	Mid y = 18	0.3	-		-	-
	Transversal		-1.4	-		-	-
	Half in each direction		-1.2	-		-	-

H.2 Defining the prestressing load either as load or element

H.2.1 Grillage

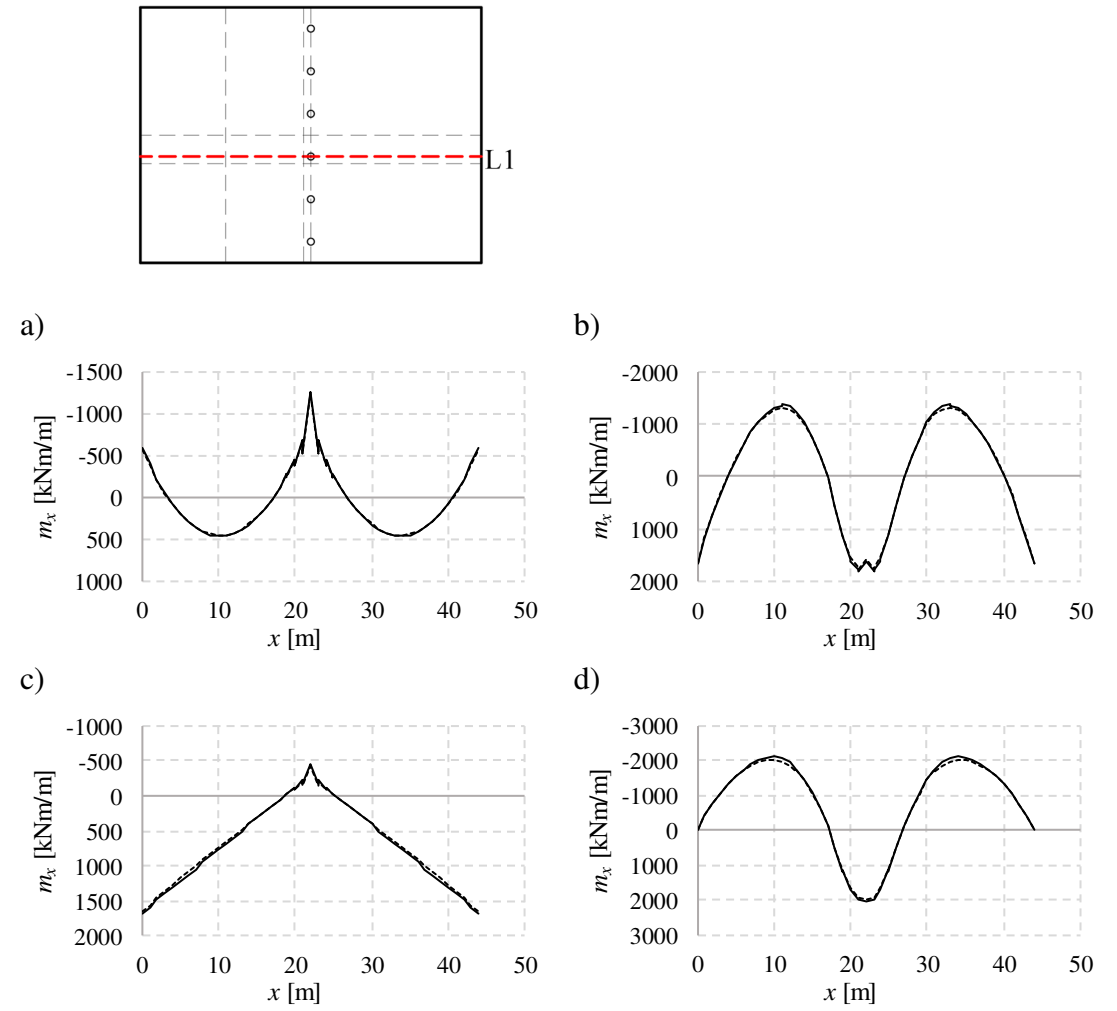

Figure H.3 Results along the section L1. a) Moment caused by the permanent load, b) resultant moment, c) restraint moment, d) primary moment

Table H.2 Comparison of the moments [kNm/m] in Figure H.3 at certain points. If no coordinate is specified, the given value is the peak value in that region. Deviation is the difference between the moments when the prestressing load is defined as either load or element.

	a	b	c	d
Tendon modeled as:	Support x=22	Support x=22	Support x=22	Support x=22
Load	-1253	1636	-443	2079
Element	-1226	1596	-424	2019
Deviation [%]	2.16	2.56	4.53	2.97
	Span	Span	Left support	Span
Load	470	-1371	1675	-2089
Element	457	-1321	1655	-2022
Deviation [%]	3.01	3.81	1.20	3.30

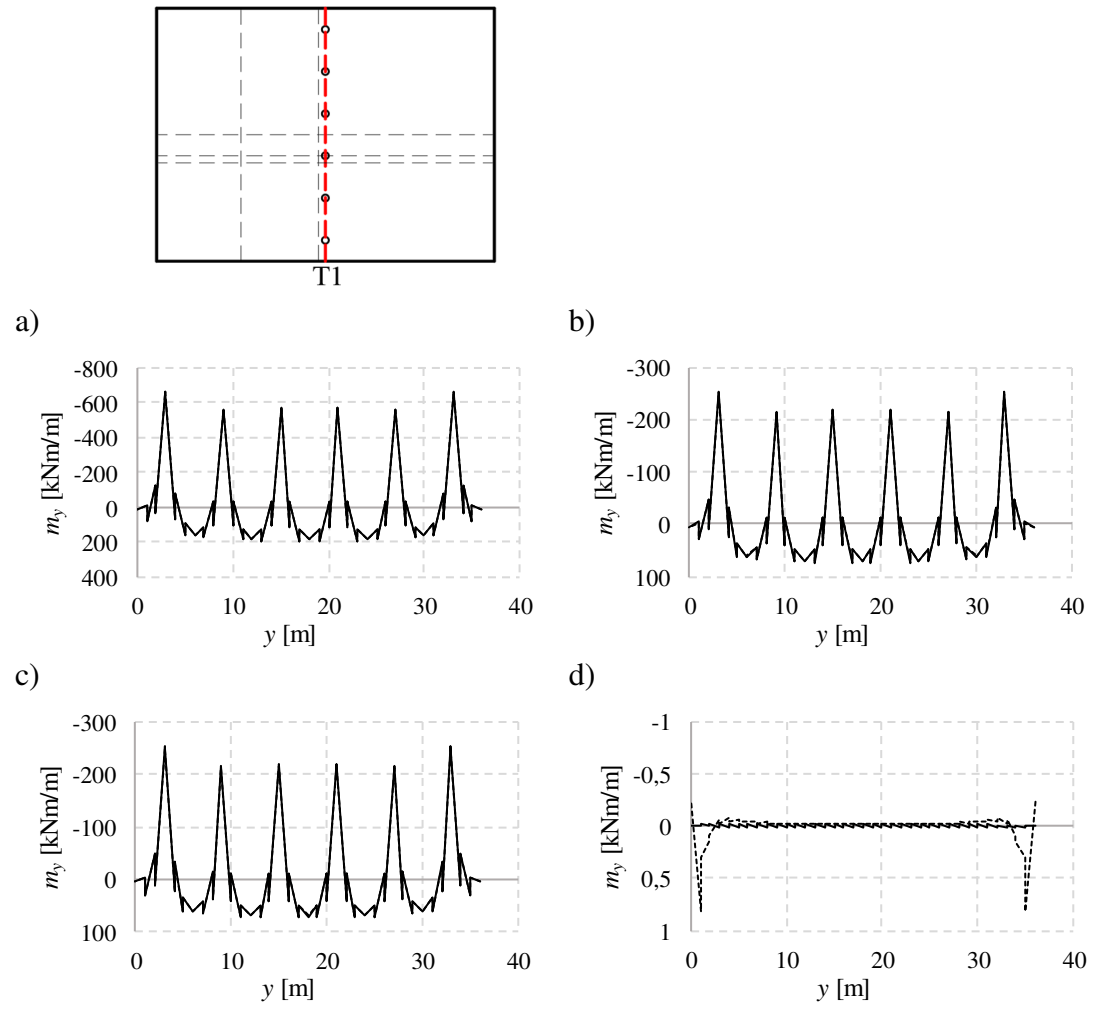

Figure H.4 Results along the section T1. a) Moment caused by the permanent load, b) resultant moment, c) restraint moment, d) primary moment

Table H.3 Comparison of the moments [kNm/m] in Figure H.4 at certain points. If no coordinate is specified, the given value is the peak value in that region. Deviation is the difference between the moments when the prestressing load is defined as either load or element.

	a	b	c	d
Tendon modeled as:	Support y=15	Support y=15	Support y=15	-
Load	-572	-220	-220	-
Element	-572	-217	-217	-
Deviation [%]	-0.06	1.43	1.43	-
	Span y=18	Span y=18	Span y=18	-
Load	185	71	71	-
Element	185	70	70	-
Deviation [%]	0.07	1.56	1.54	-

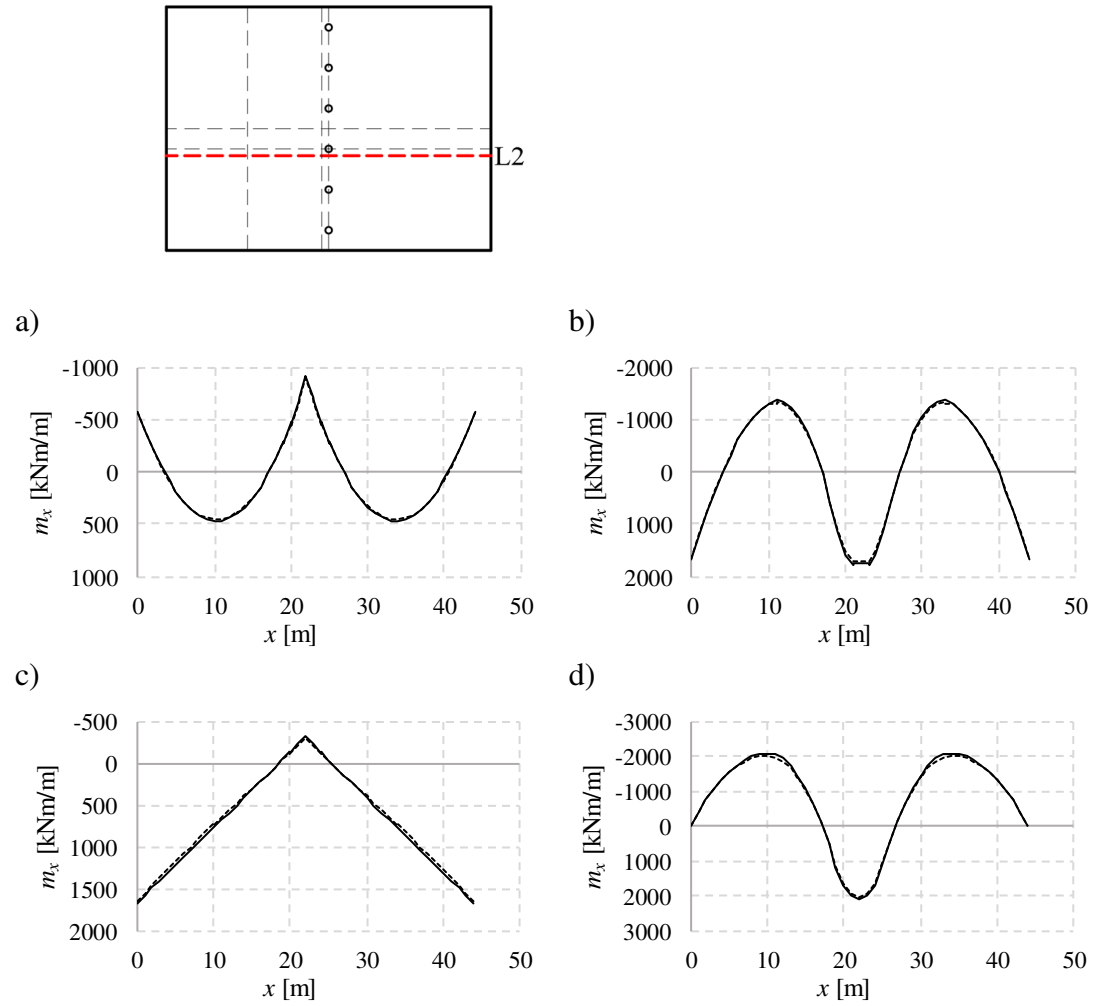

Figure H.5 Results along the section L2. a) Moment caused by the permanent load, b) resultant moment, c) restraint moment, d) primary moment

Table H.4 Comparison of the moments [kNm/m] in Figure H.5 at certain points. If no coordinate is specified, the given value is the peak value in that region. Deviation is the difference between the moments when the prestressing load is defined as either load or element.

	a	b	c	d
Tendon modeled as:	Support x=22	Support x=22	Support x=22	Support x=22
Load	-923	1763	-316	2079
Element	-897	1720	-299	2019
Deviation [%]	2.86	2.50	5.69	2.97
	Span	Span	Left support	Span
Load	471	-1371	1675	-2089
Element	457	-1321	1655	-2022
Deviation [%]	3.01	3.81	1.20	3.30

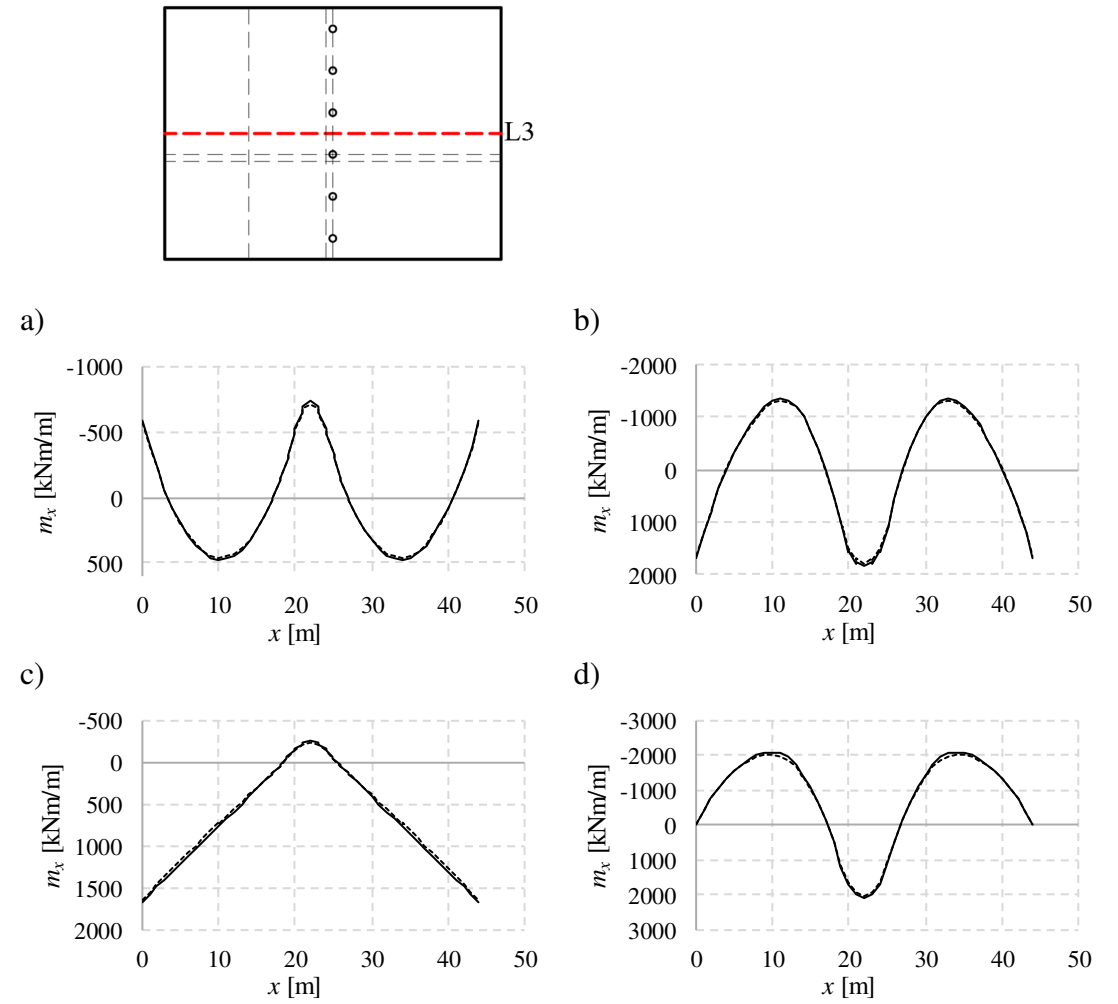

Figure H.6 Results along the section L3. a) Moment caused by the permanent load, b) resultant moment, c) restraint moment, d) primary moment

Table H.5 Comparison of the moments [kNm/m] in Figure H.6 at certain points. If no coordinate is specified, the given value is the peak value in that region. Deviation is the difference between the moments when the prestressing load is defined as either load or element.

	a	b	c	d
Tendon modeled as:	Support x=22	Support x=22	Support x=22	Support x=22
Load	-740	1833	-246	2079
Element	-716	1789	-230	2019
Deviation [%]	3.39	2.49	6.71	2.97
	Span	Span	Left support	Span
Load	470	-1371	1675	-2089
Element	456	-1321	1655	-2022
Deviation [%]	3.01	3.81	1.20	3.30

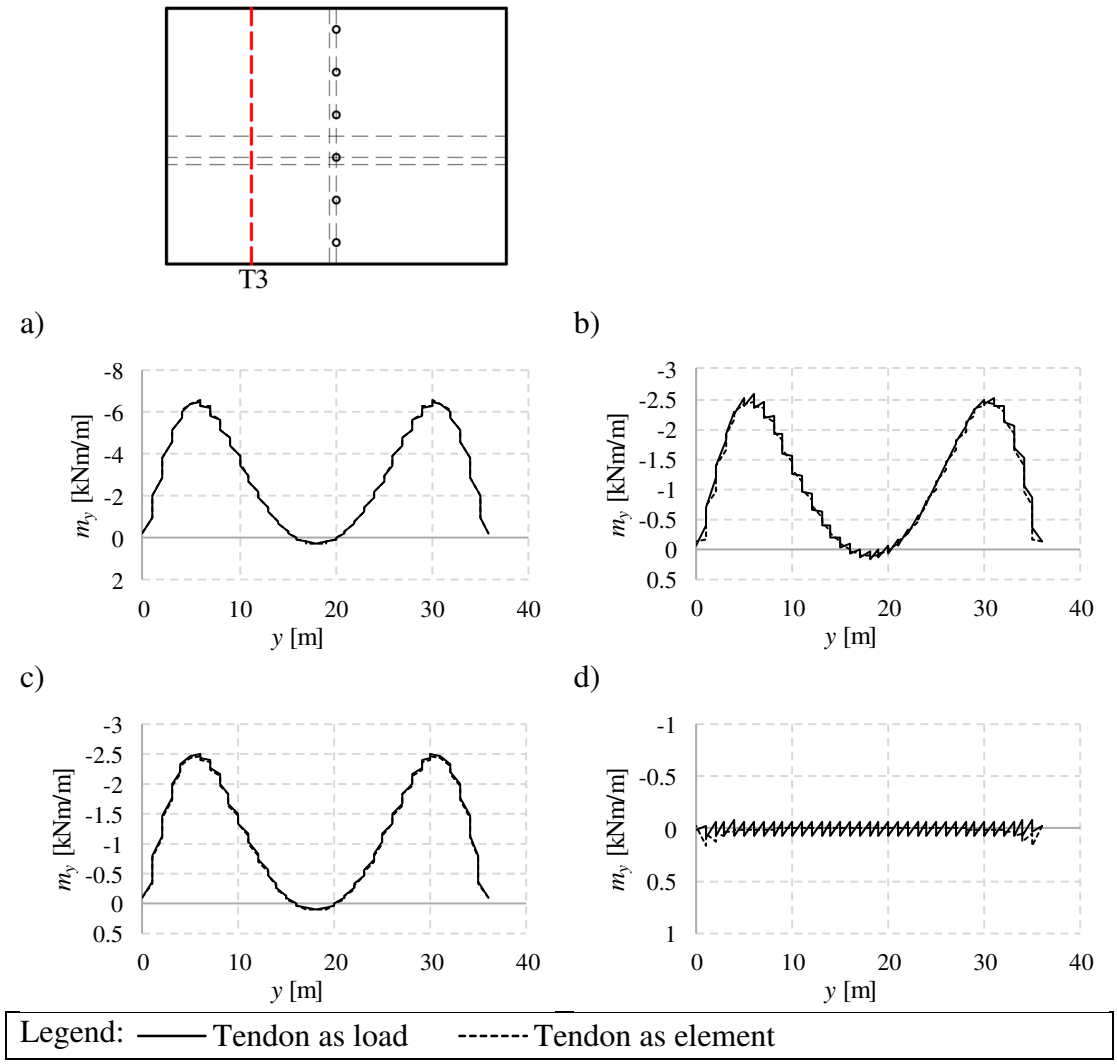

Figure H.7 Results along the section T3. a) Moment caused by the permanent load, b) resultant moment, c) restraint moment, d) primary moment

Table H.6 Comparison of the moments [kNm/m] in Figure H.7 at certain points. If no coordinate is specified, the given value is the peak value in that region. Deviation is the difference between the moments when the prestressing load is defined as either load or element.

	a	b	c	d
Tendon modeled as:	Mid y=18	Mid y=18	Mid y=18	Mid y=18
Load	0.3	0.2	0.1	0.1
Element	0.3	0.1	0.1	0.0
Deviation [%]	-6.90	52.72	-14.33	-1682.61

H.2.2 Shell

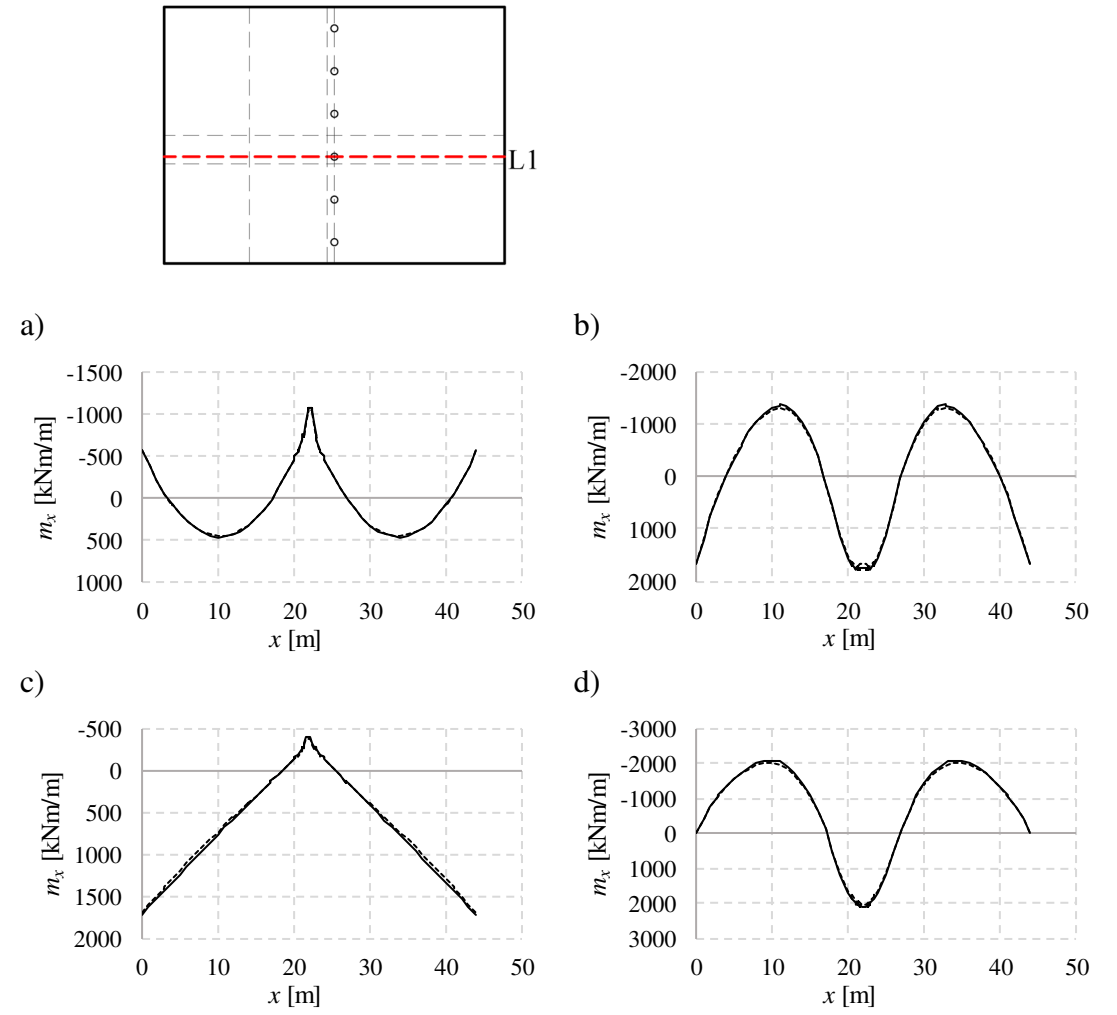

Figure H.8 Results along the section L1. a) Moment caused by the permanent load, b) resultant moment, c) restraint moment, d) primary moment

Table H.7 Comparison of the moments [kNm/m] in Figure H.8 at certain points. If no coordinate is specified, the given value is the peak value in that region. Deviation is the difference between the moments when the prestressing load is defined as either load or element.

	a	b	c	d
Tendon modeled as:	Support x=22	Support x=22	Support x=22	Support x=22
Load	-1063	1729	-394	2123
Element	-1039	1669	-377	2045
Deviation [%]	2.32	3.62	4.47	3.77
	Span	Span	Left support	Span
Load	468	-1357	1719	-2085
Element	455	-1317	1701	-2019
Deviation [%]	2.87	3.09	1.06	3.29

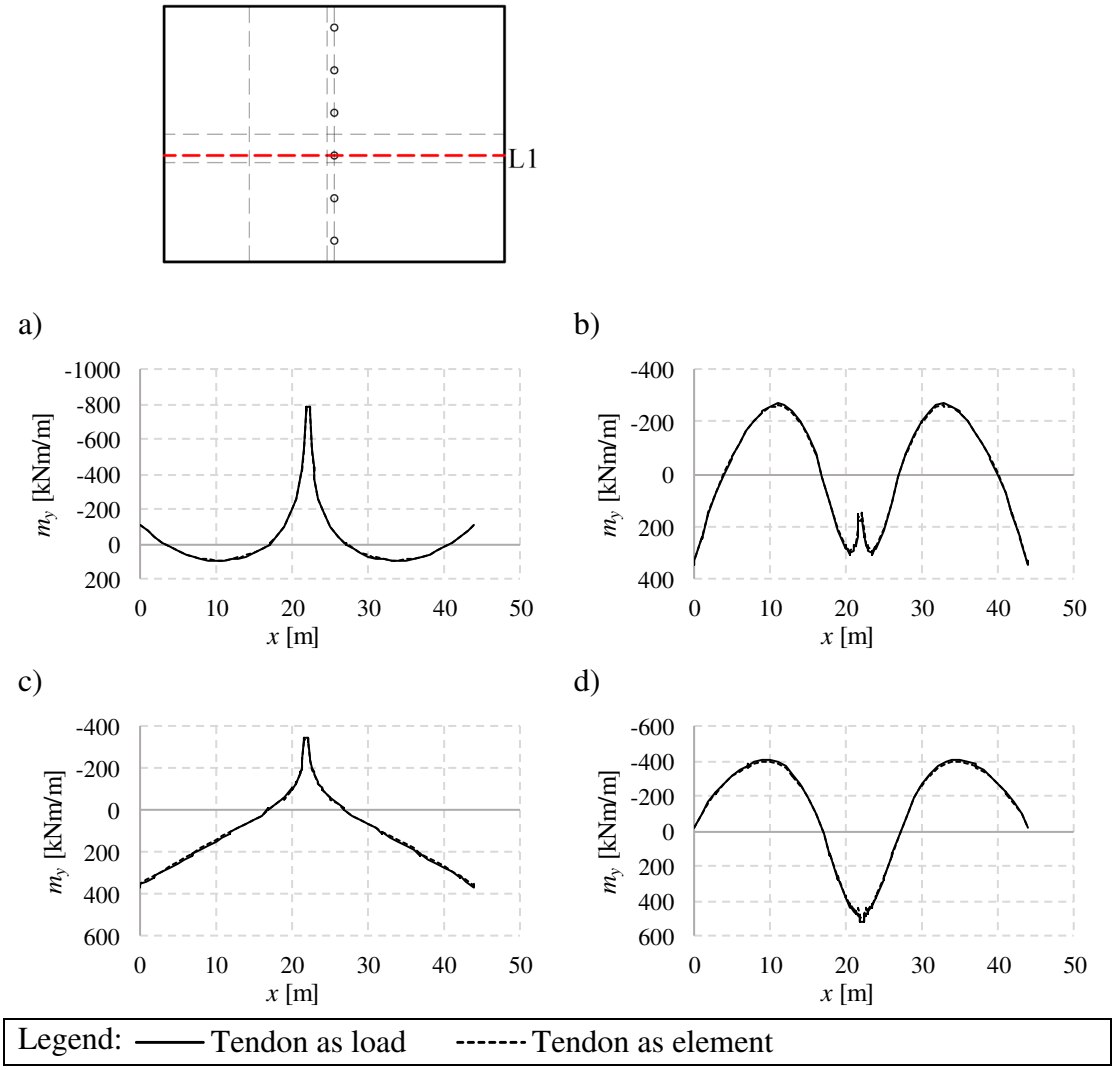

Figure H.9 Results along the section L1. a) Moment caused by the permanent load, b) resultant moment, c) restraint moment, d) primary moment

Table H.8 Comparison of the moments [kNm/m] in Figure H.9 at certain points. If no coordinate is specified, the given value is the peak value in that region. Deviation is the difference between the moments when the prestressing load is defined as either load or element.

	a	b	c	d
Tendon modeled as:	Support x=22	Support x=22	Support x=22	Support x=22
Load	-788	176	-344	520
Element	-783	159	-336	495
Deviation [%]	0.65	11.06	2.38	5.17
	Span	Span	Left support	Span
Load	93	-270	367	-410
Element	91	-261	363	-397
Deviation [%]	2.79	3.17	1.02	3.21

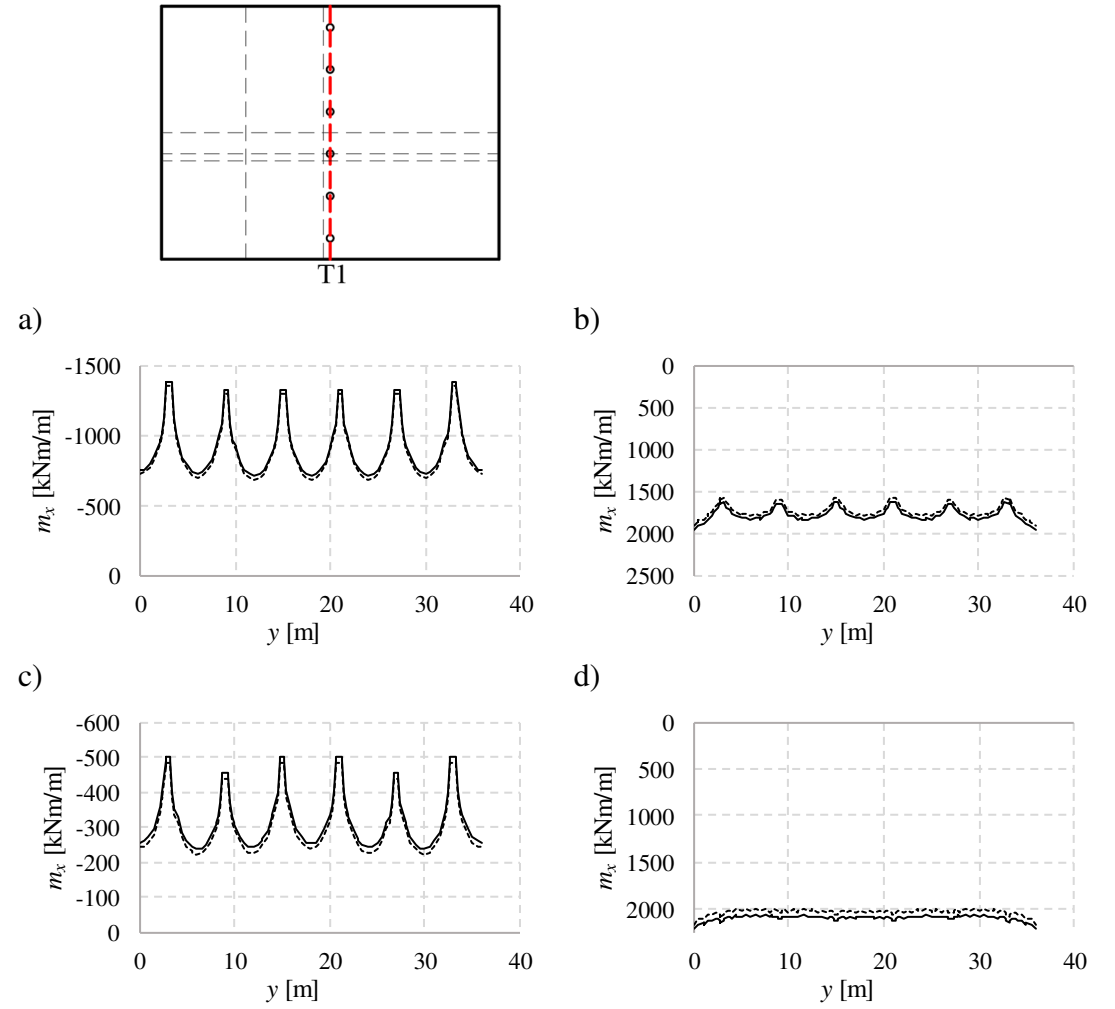

Figure H.10 Results along the section T1. a) Moment caused by the permanent load, b) resultant moment, c) restraint moment, d) primary moment

Table H.9 Comparison of the moments [kNm/m] in Figure H.10 at certain points. If no coordinate is specified, the given value is the peak value in that region. Deviation is the difference between the moments when the prestressing load is defined as either load or element.

	a	b	c	d
Tendon modeled as:	Support y=15	Support y=15	Support y=15	Support y=15
Load	-1326	1631	-500	2132
Element	-1302	1585	-482	2067
Deviation [%]	1.84	2.96	3.78	3.15
	Span y=18	Span y=18	Span y=18	Span y=18
Load	-709	1838	-253	2090
Element	-686	1797	-238	2035
Deviation [%]	3.32	2.25	6.03	2.70

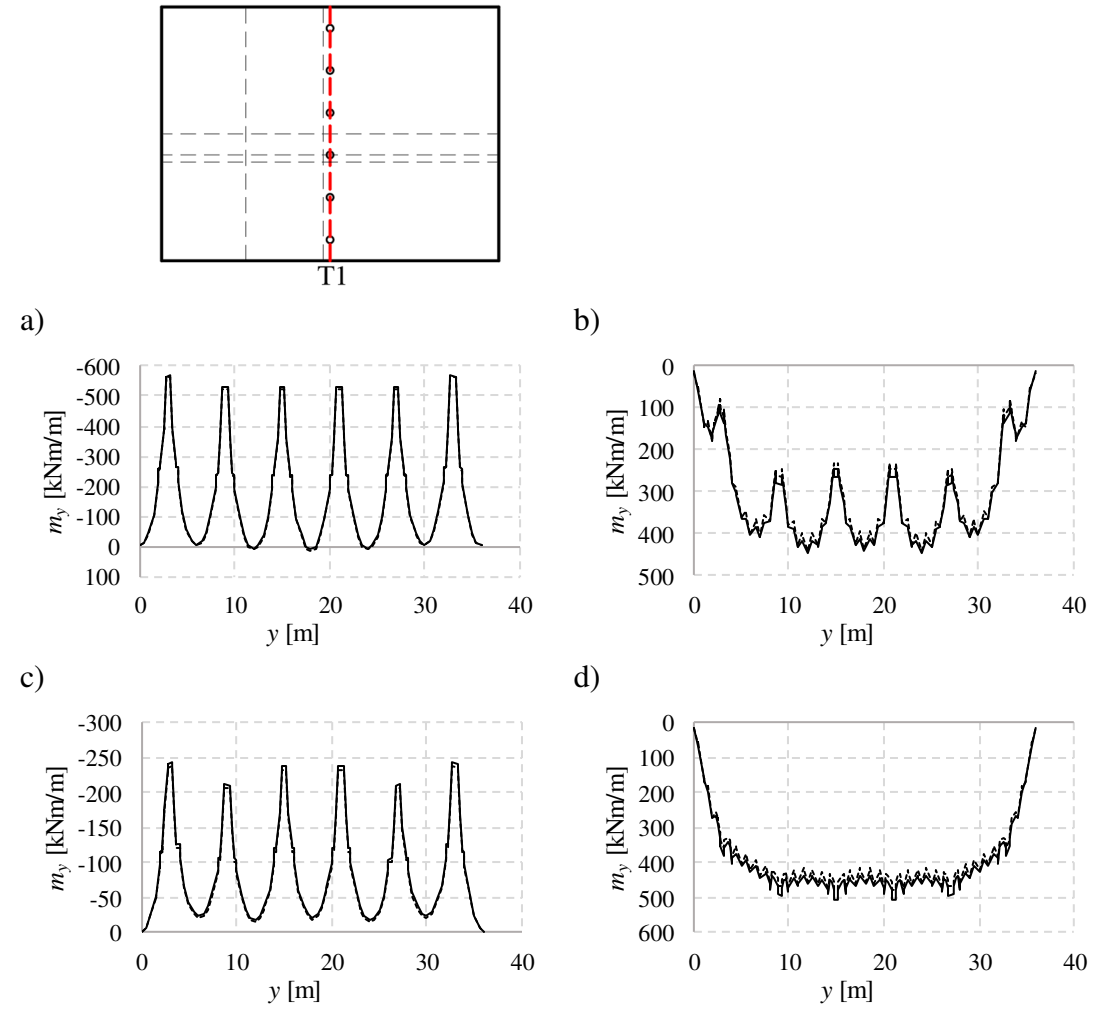

Figure H.11 Results along the section T1. a) Moment caused by the permanent load, b) resultant moment, c) restraint moment, d) primary moment

Table H.10 Comparison of the moments [kNm/m] in Figure H.11 at certain points. If no coordinate is specified, the given value is the peak value in that region. Deviation is the difference between the moments when the prestressing load is defined as either load or element.

	a	b	c	d
Tendon modeled as:	Support y=15	Support y=15	Support y=15	Support y=15
Load	-528	267	-238	505
Element	-523	248	-232	479
Deviation [%]	0.94	7.82	2.77	5.38
	Span y=18	Span y=18	Span y=18	Span y=18
Load	10	440	-21	461
Element	15	439	-17	456
Deviation [%]	-34.14	0.29	20.06	1.04

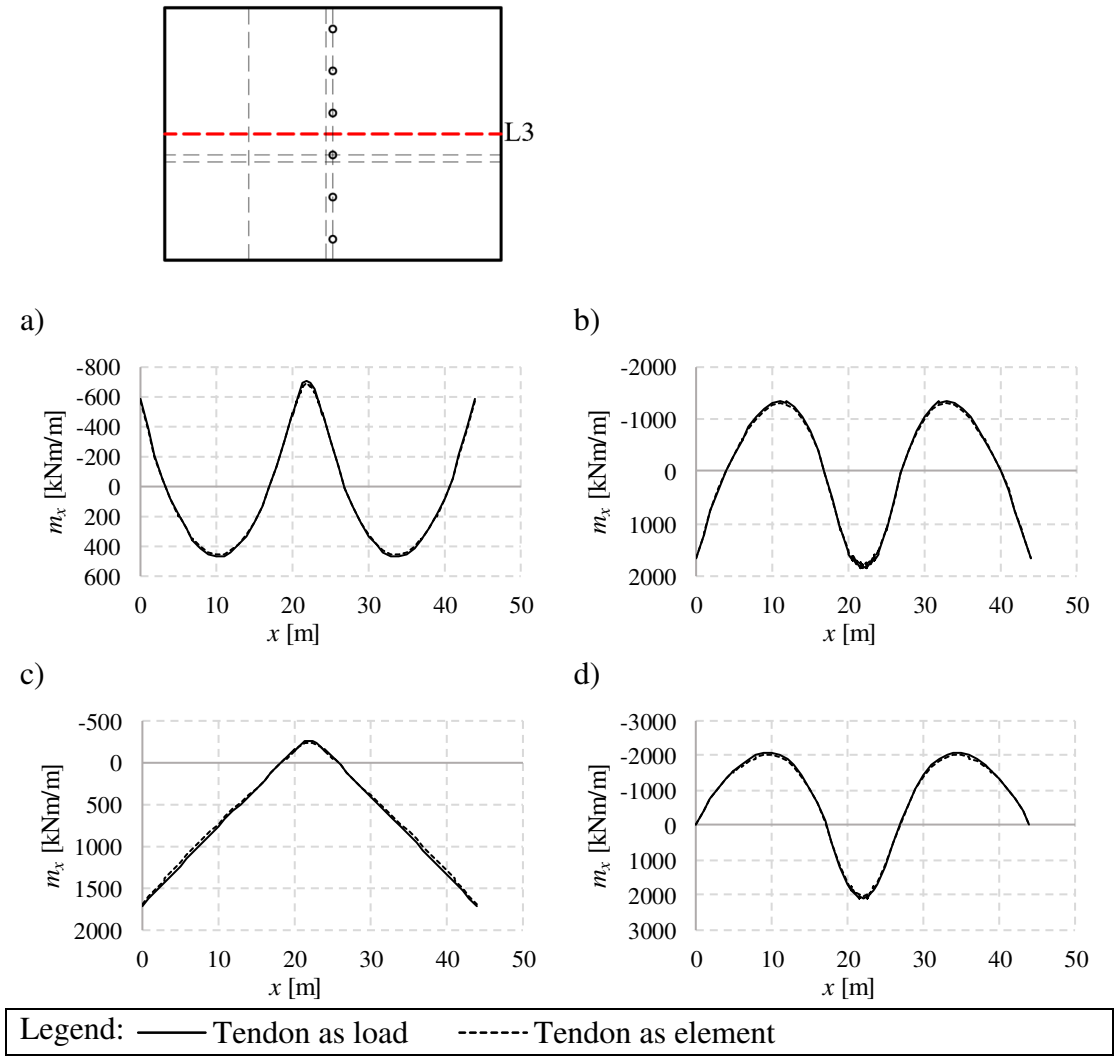

Figure H.12 Results along the section L3. a) Moment caused by the permanent load, b) resultant moment, c) restraint moment, d) primary moment

Table H.11 Comparison of the moments [kNm/m] in Figure H.12 at certain points. If no coordinate is specified, the given value is the peak value in that region. Deviation is the difference between the moments when the prestressing load is defined as either load or element.

	a	b	c	d
Tendon modeled as:	Support x=22	Support x=22	Support x=22	Support x=22
Load	-709	1838	-253	2090
Element	-686	1797	-238	2035
Deviation [%]	3.32	2.25	6.03	2.70
	Span	Span	Left support	Span
Load	468	-1357	1712	-2079
Element	455	-1316	1694	-2013
Deviation [%]	2.86	3.10	1.05	3.30

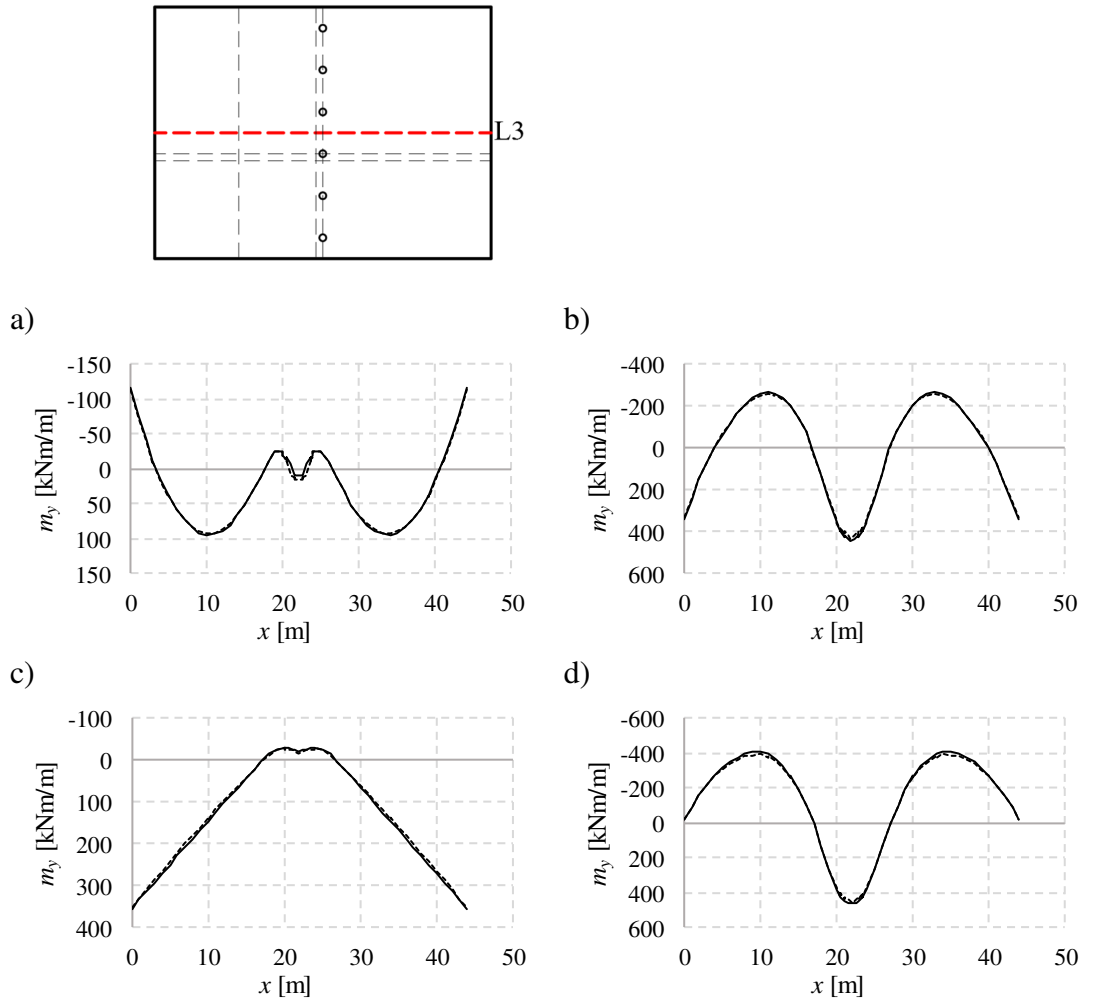

Figure H.13 Results along the section L3. a) Moment caused by the permanent load, b) resultant moment, c) restraint moment, d) primary moment

Table H.12 Comparison of the moments [kNm/m] in Figure H.13 at certain points. If no coordinate is specified, the given value is the peak value in that region. Deviation is the difference between the moments when the prestressing load is defined as either load or element.

	a	b	c	d
Tendon modeled as:	Support x=22	Support x=22	Support x=22	Support x=22
Load	10	440	-21	461
Element	15	439	-17	456
Deviation [%]	-34.14	0.29	20.06	1.04
	Span	Span	Left support	Span
Load	94	-270	355	-407
Element	92	-262	352	-394
Deviation [%]	2.77	3.19	1.03	3.22

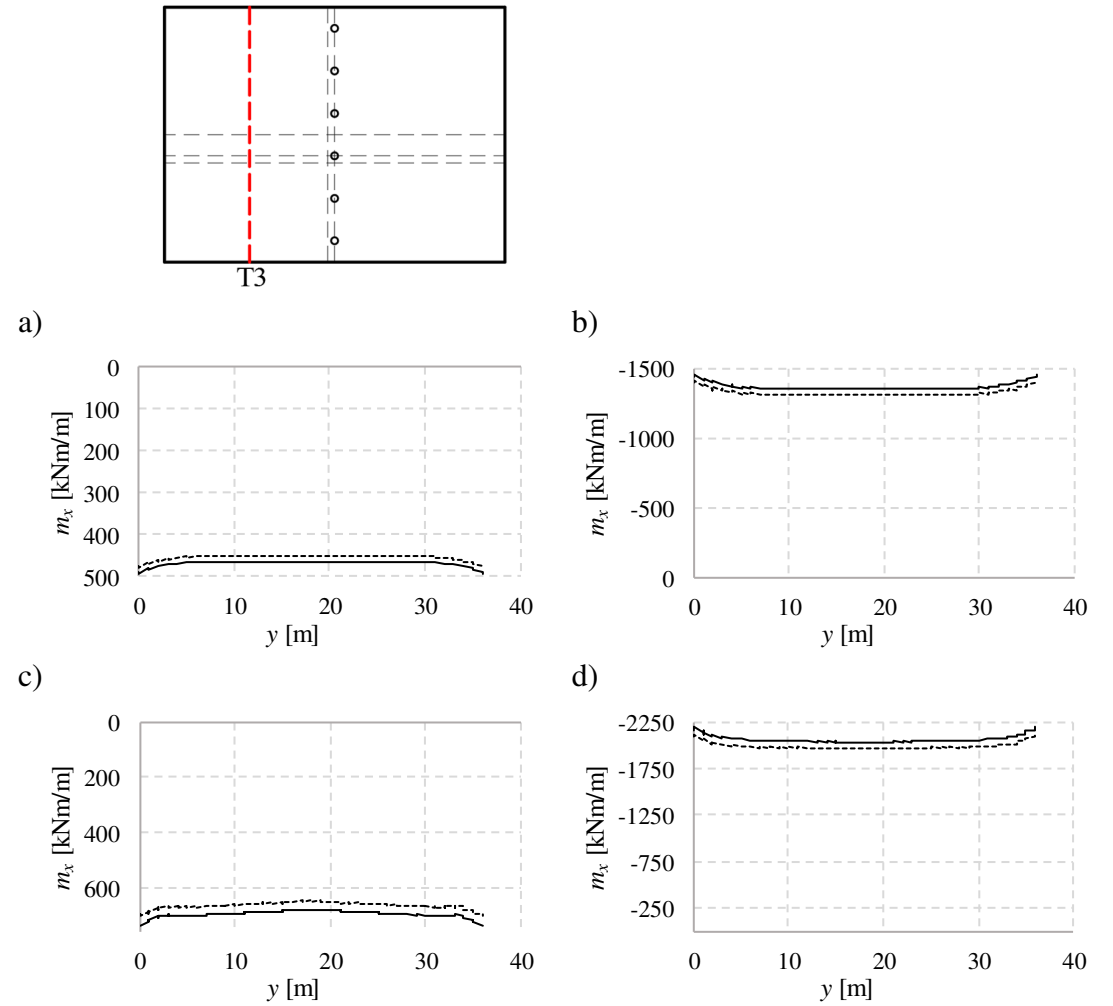

Figure H.14 Results along the section T3. a) Moment caused by the permanent load, b) resultant moment, c) restraint moment, d) primary moment

Table H.13 Comparison of the moments [kNm/m] in Figure H.14 at certain points. If no coordinate is specified, the given value is the peak value in that region. Deviation is the difference between the moments when the prestressing load is defined as either load or element.

	a	b	c	d
Tendon modeled as:	Mid y =18	Mid y =18	Mid y =18	Mid y =18
Load	463	-1357	683	-2041
Element	451	-1317	654	-1971
Deviation [%]	2.60	3.10	4.43	3.54

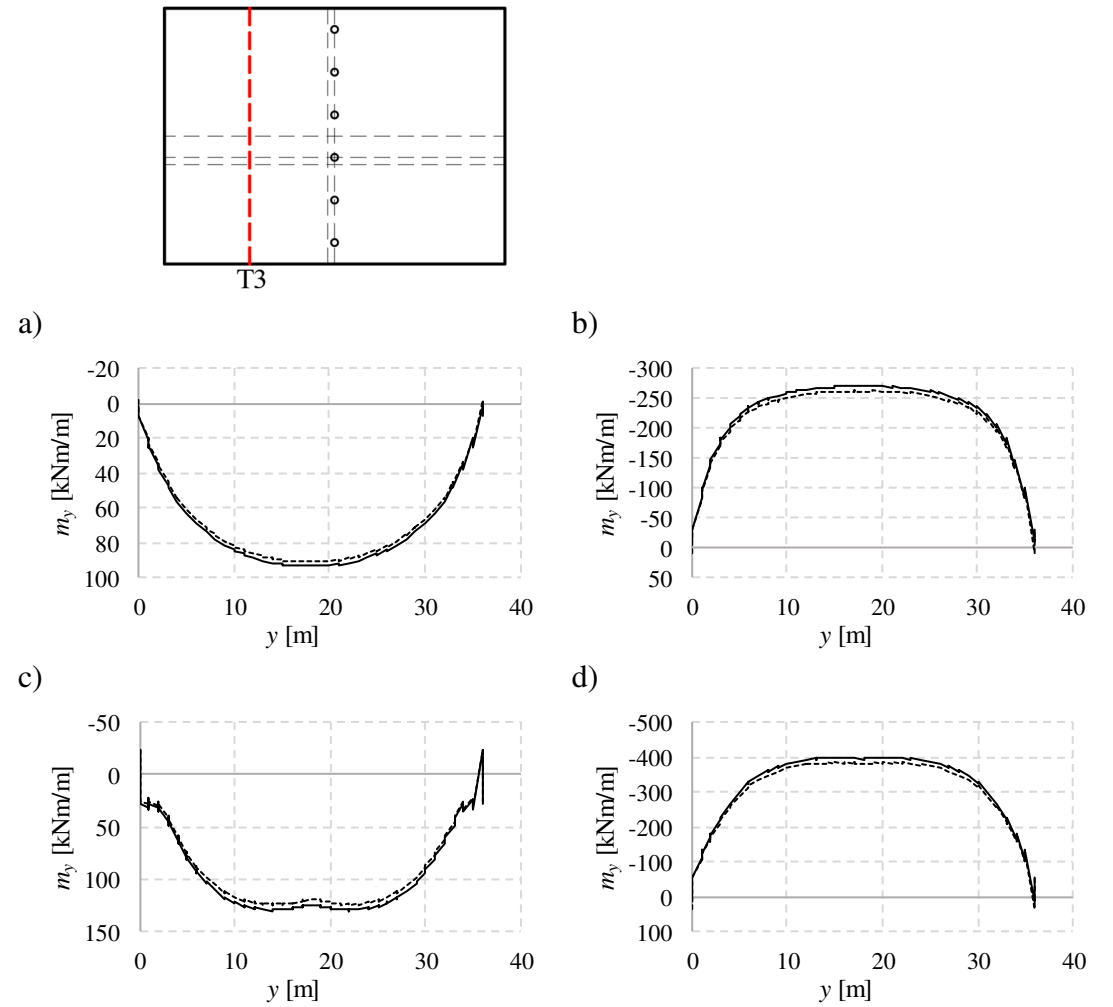

Figure H.15 Results along the section T3. a) Moment caused by the permanent load, b) resultant moment, c) restraint moment, d) primary moment

Table H.14 Comparison of the moments [kNm/m] in Figure H.15 at certain points. If no coordinate is specified, the given value is the peak value in that region. Deviation is the difference between the moments when the prestressing load is defined as either load or element.

	a	b	c	d
Tendon modeled as:	Mid y =18	Mid y =18	Mid y =18	Mid y =18
Load	93	-270	128	-398
Element	91	-262	119	-385
Deviation [%]	2.50	3.18	7.55	3.46

H.3 Comparison of 2D and 3D model

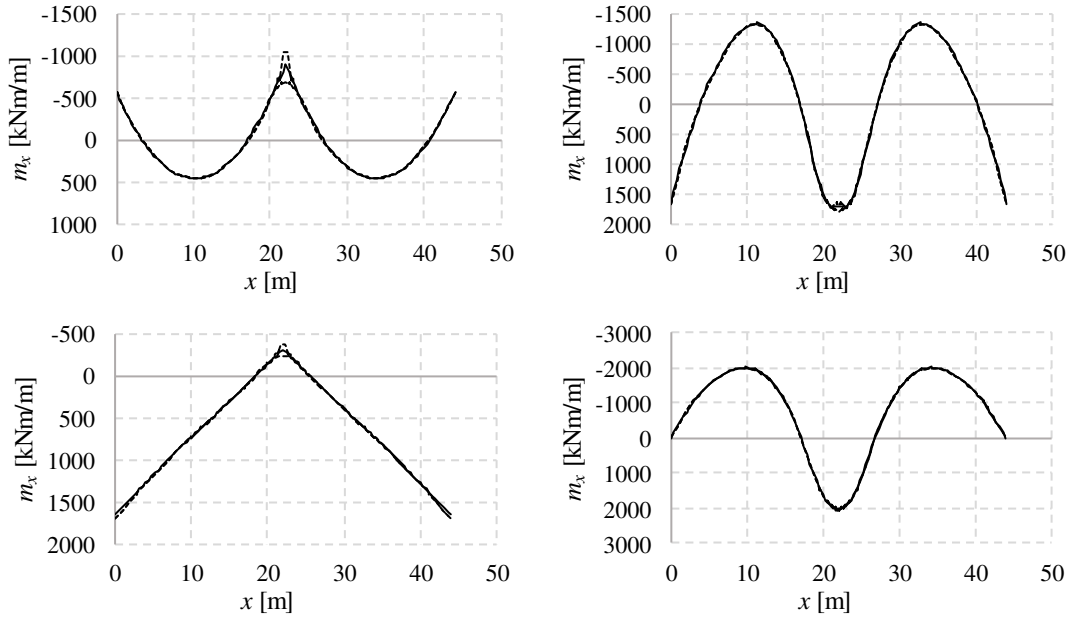

Figure H.16 Moment distributions in the longitudinal direction for the 2D model and a shell model in section L1 and L3. a) Moment distribution caused by the permanent load, b) resultant moment, c) restraint moment, d) primary moment

H.4 Comparison between shell and grillage models

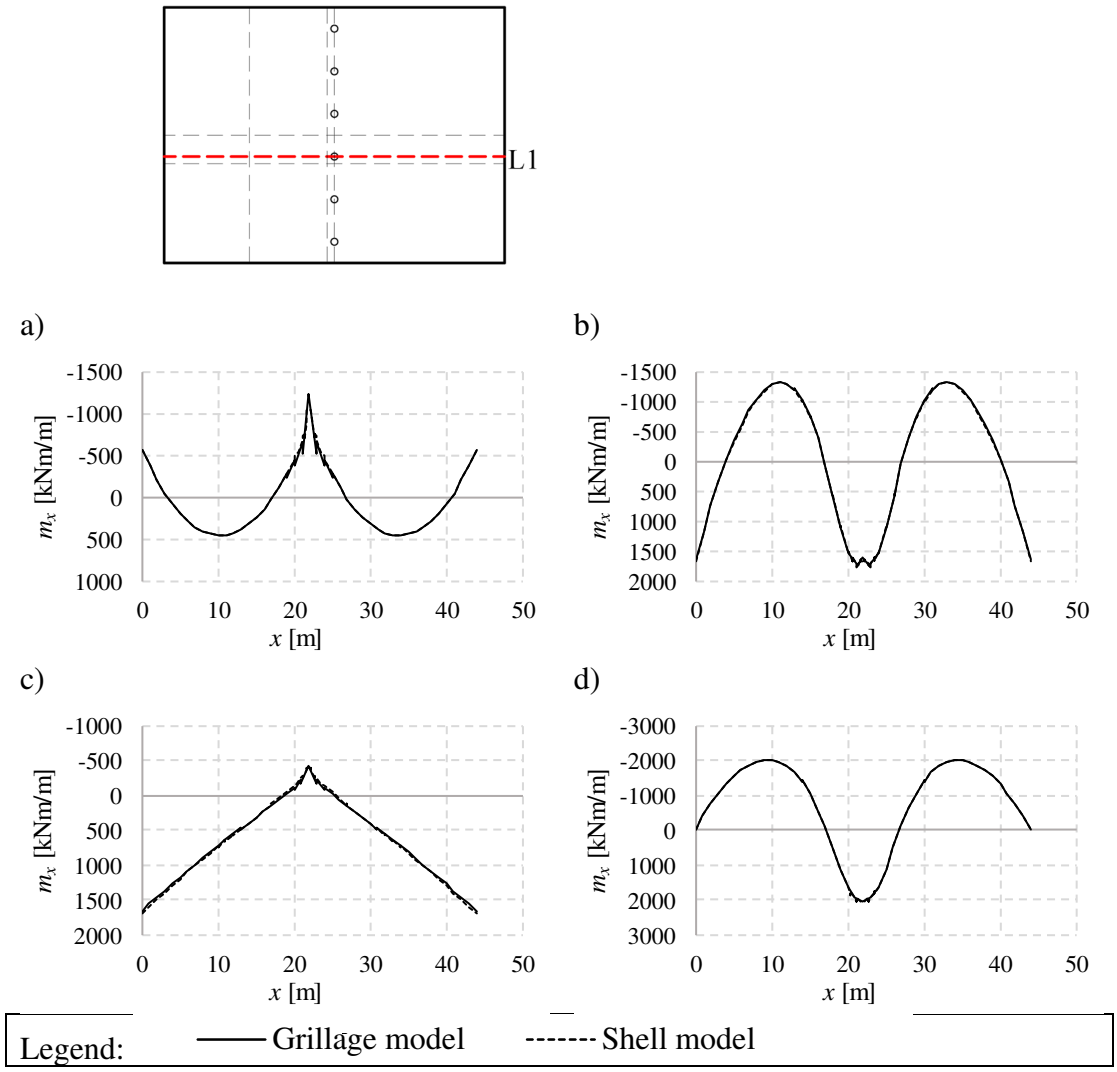

Figure H.17 Results along the section L1. a) Moment caused by the permanent load, b) resultant moment, c) restraint moment, d) primary moment

Table H.15 Comparison of the moments [kNm/m] in Figure H.17 at certain points. If no coordinate is specified, the given value is the peak value in that region. Deviation is the difference between the moment in the beam grillage model and shell model.

	a	b	c	d
Model	Support x=22	Support x=22	Support x=22	Support x=22
Grillage model	-1226	1596	-424	2019
Shell model	-1039	1669	-377	2045
Deviation [%]	18.03	-4.37	12.36	-1.29
	Span	Span	Left support	Span
Grillage model	457	-1321	1655	-2022
Shell model	455	-1317	1701	-2019
Deviation [%]	0.44	0.33	-2.70	0.15

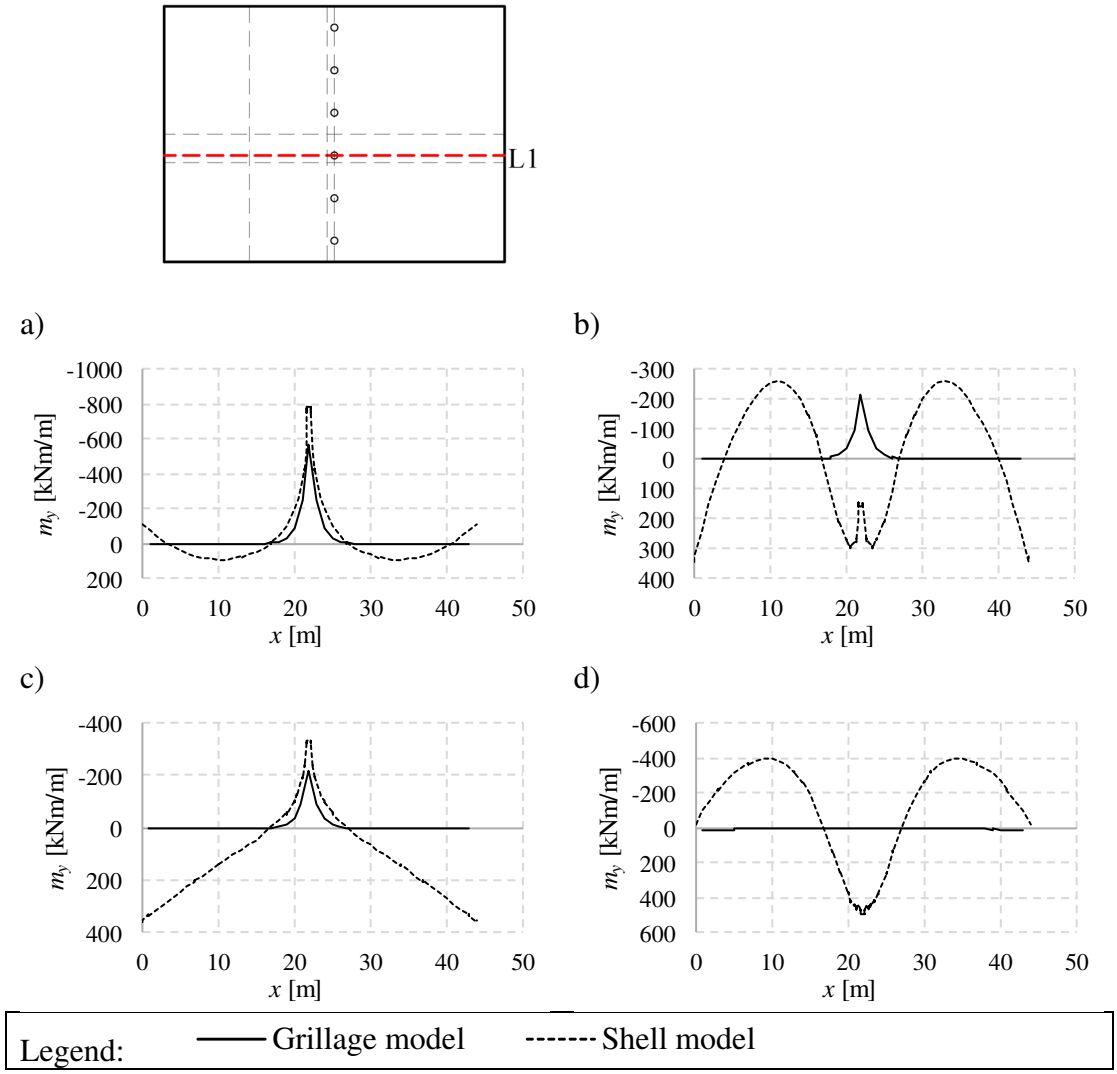

Figure H.18 Results along the section L1. a) Moment caused by the permanent load, b) resultant moment, c) restraint moment, d) primary moment

Table H.16 Comparison of the moments [kNm/m] in Figure H.18 at certain points. If no coordinate is specified, the given value is the peak value in that region. Deviation is the difference between the moment in the beam grillage model and shell model

	a	b	c	d
Model	Support x=22	Support x=22	Support x=22	Support x=22
Grillage model	-572	-217	-217	-
Shell model	-783	159	-336	495
Deviation [%]	-26.88	-236.45	-35.47	-
	Span	Span	Left support	Span
Grillage model	-	-	-	-
Shell model	91	-261	363	-397
Deviation [%]	-	-	-	-

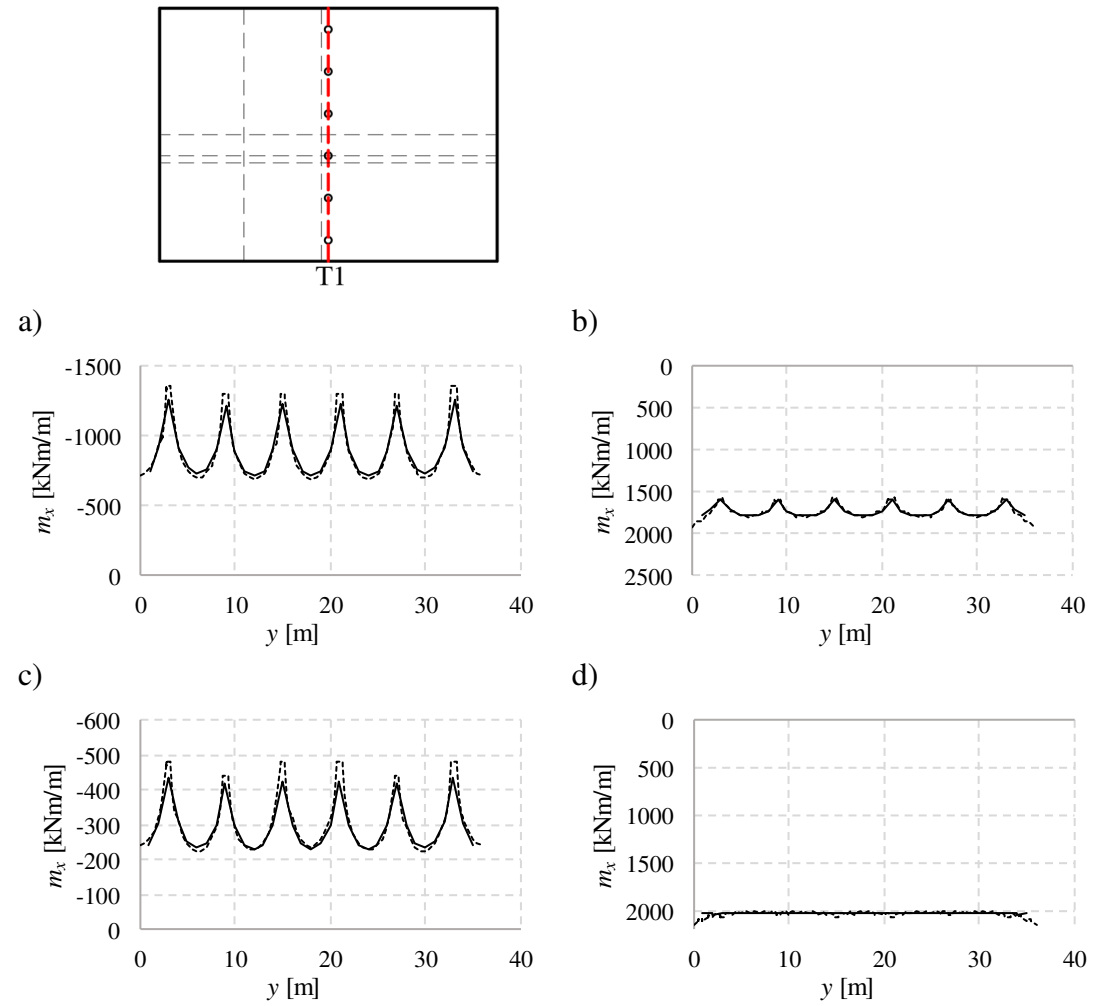

Figure H.19 Results along the section T1. a) Moment caused by the permanent load, b) resultant moment, c) restraint moment, d) primary moment

Table H.17 Comparison of the moments [kNm/m] in Figure H.19 at certain points. If no coordinate is specified, the given value is the peak value in that region. Deviation is the difference between the moment in the beam grillage model and shell model.

	a	b	c	d
Model	Support y=15	Support y=15	Support y=15	Support y=15
Grillage model	-1226	1596	-424	2019
Shell model	-1302	1585	-482	2067
Deviation [%]	-5.80	0.69	-12.18	-2.31
	Span y=18	Span y=18	Span y=18	Span y=18
Grillage model	-716	1789	-230	2019
Shell model	-686	1797	-238	2035
Deviation [%]	4.34	-0.46	-3.42	-0.81

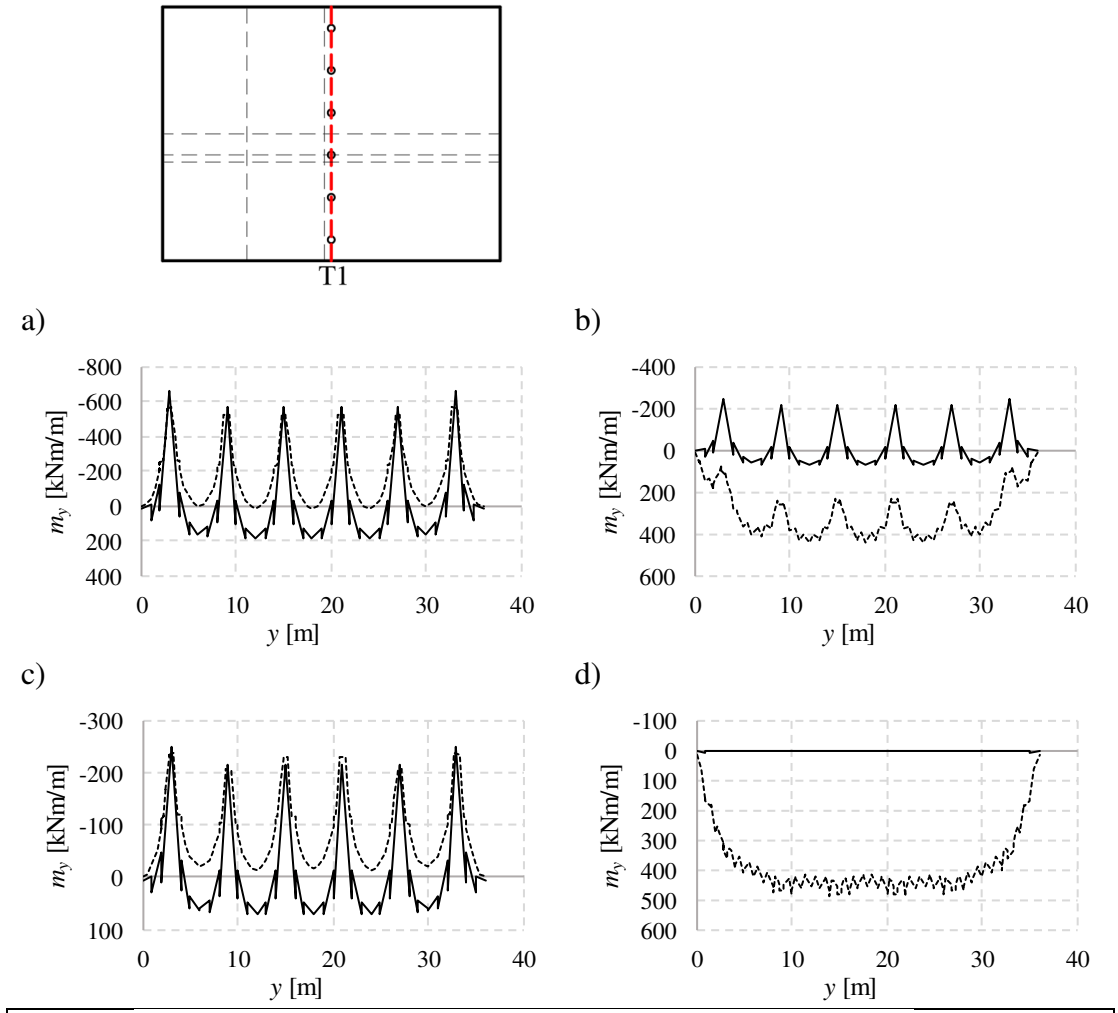

Figure H.20 Results along the section T1. a) Moment caused by the permanent load, b) resultant moment, c) restraint moment, d) primary moment

Table H.18 Comparison of the moments [kNm/m] in Figure H.20 at certain points. If no coordinate is specified, the given value is the peak value in that region. Deviation is the difference between the moment in the beam grillage model and shell model.

	a	b	c	d
Model	Support y=15	Support y=15	Support y=15	Support y=15
Grillage model	-572	-217	-217	0
Shell model	-523	248	-232	479
Deviation [%]	9.50	-	-6.50	-
	Span y=18	Span y=18	Span y=18	Span y=18
Grillage model	185	70	70	0
Shell model	15	439	-17	456
Deviation [%]	-	-	-	-

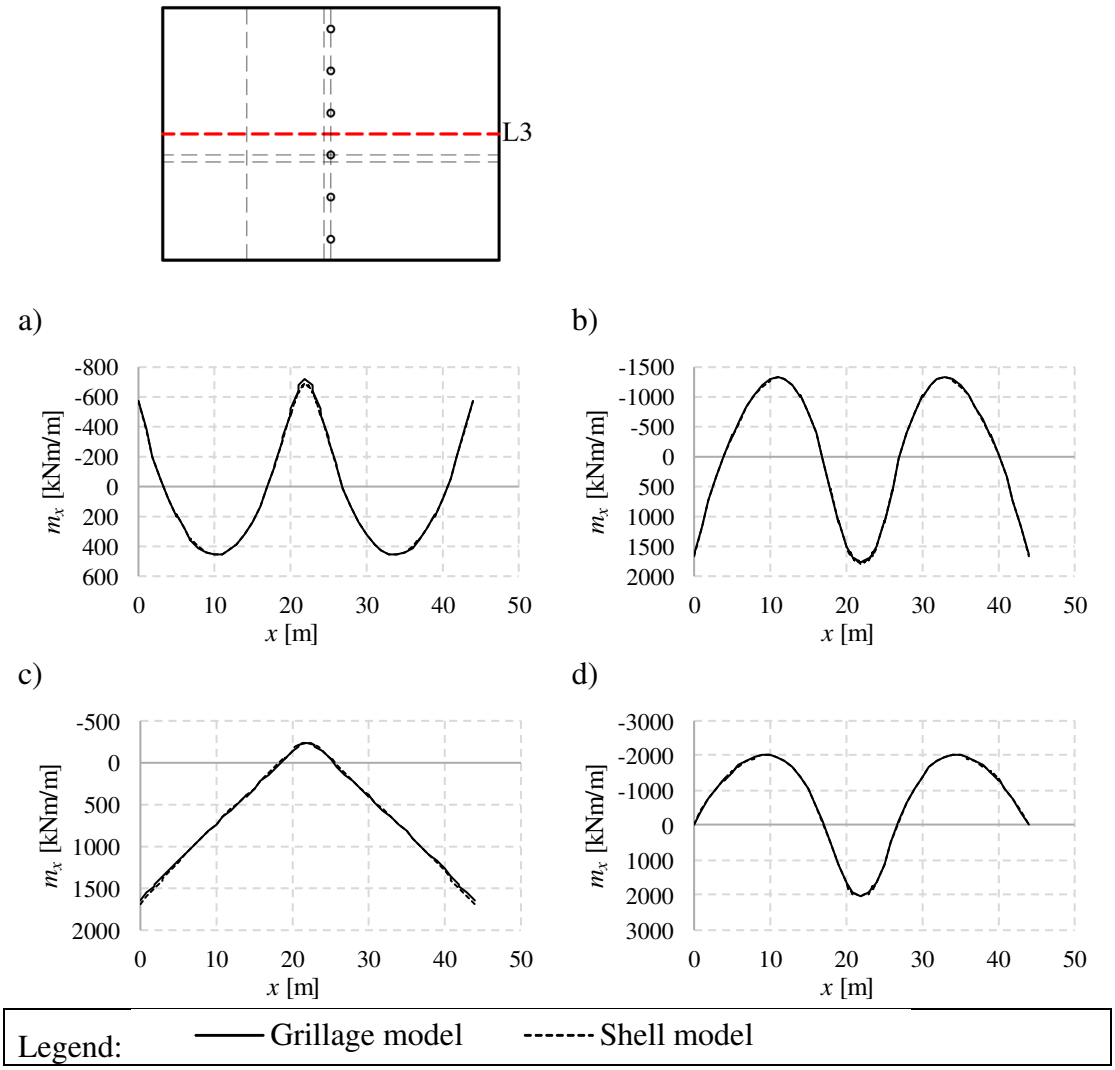

Figure H.21 Results along the section L3. a) Moment caused by the permanent load, b) resultant moment, c) restraint moment, d) primary moment

Table H.19 Comparison of the moments [kNm/m] in Figure H.21 at certain points. If no coordinate is specified, the given value is the peak value in that region. Deviation is the difference between the moment in the beam grillage model and shell model.

	a	b	c	d
Model	Support x=22	Support x=22	Support x=22	Support x=22
Grillage model	-716	1789	-230	2019
Shell model	-686	1797	-238	2035
Deviation [%]	4.34	-0.46	-3.42	-0.81
	Span	Span	Left support	Span
Grillage model	456	-1321	1655	-2022
Shell model	455	-1316	1694	-2013
Deviation [%]	0.41	0.35	-2.29	0.44

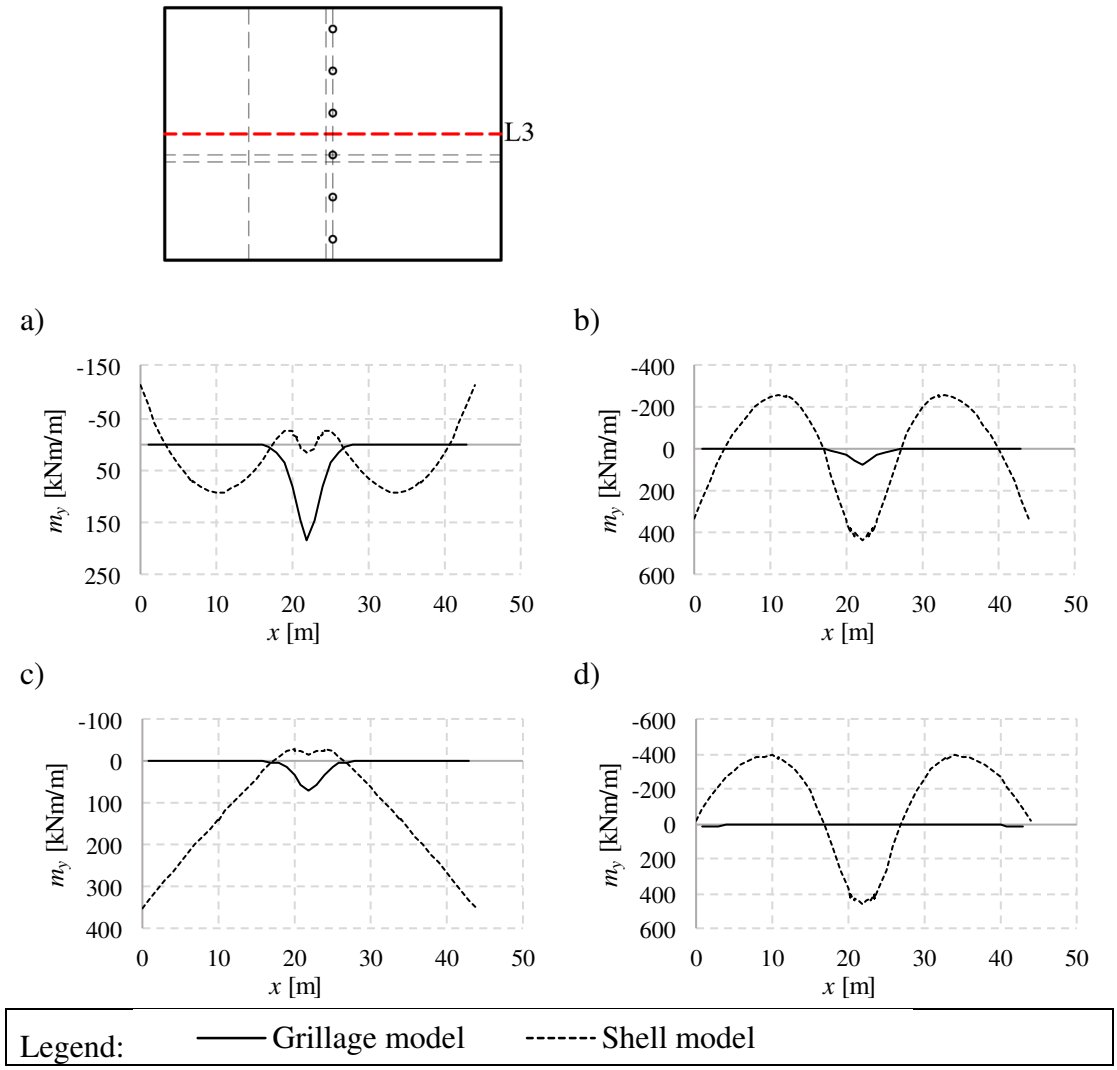

Figure H.22 Results along the section L3. a) Moment caused by the permanent load, b) resultant moment, c) restraint moment, d) primary moment

Table H.20 Comparison of the moments [kNm/m] in Figure H.22 at certain points. If no coordinate is specified, the given value is the peak value in that region. Deviation is the difference between the moment in the beam grillage model and shell model.

	a	b	c	d
Model	Support x=22	Support x=22	Support x=22	Support x=22
Grillage model	185	70	70	0
Shell model	15	439	-17	456
Deviation [%]	1152.78	-84.02	-507.04	-
	Span	Span	Left support	Span
Grillage model	-	-	-	0
Shell model	92	-262	352	-394
Deviation [%]	-	-	-	-

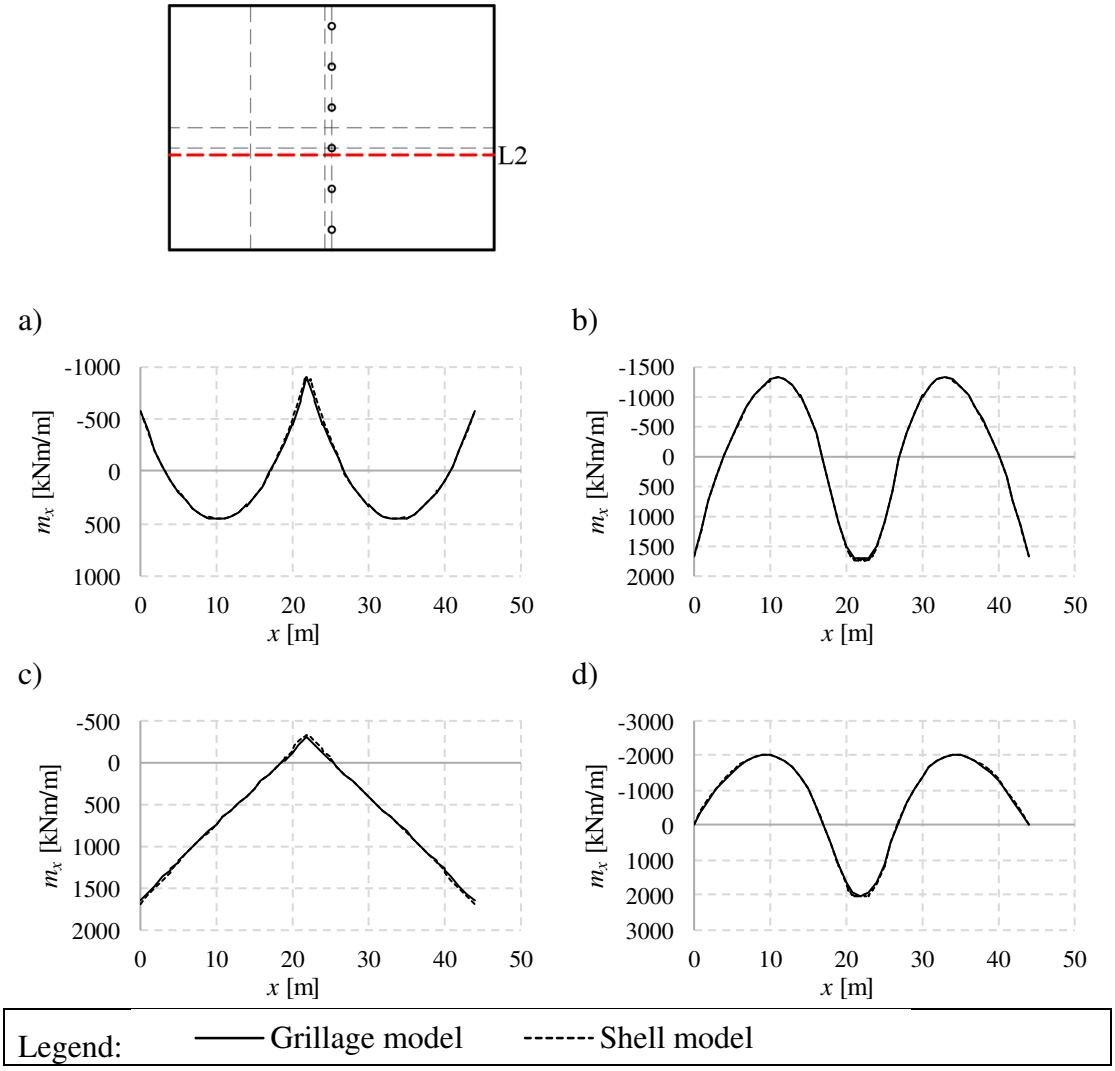

Figure H.23 Results along the section L2. a) Moment caused by the permanent load, b) resultant moment, c) restraint moment, d) primary moment

Table H.21 Comparison of the moments [kNm/m] in Figure H.23 at certain points. If no coordinate is specified, the given value is the peak value in that region. Deviation is the difference between the moment in the beam grillage model and shell model.

	a	b	c	d
Model	Support x=22	Support x=22	Support x=22	Support x=22
Grillage model	-897	1720	-299	2019
Shell model	-894	1728	-318	2046
Deviation [%]	0.35	-0.47	-5.86	-1.31
	Span	Span	Left support	Span
Grillage model	457	-1321	1655	-2022
Shell model	455	-1317	1704	-2020
Deviation [%]	0.49	0.33	-2.87	0.07

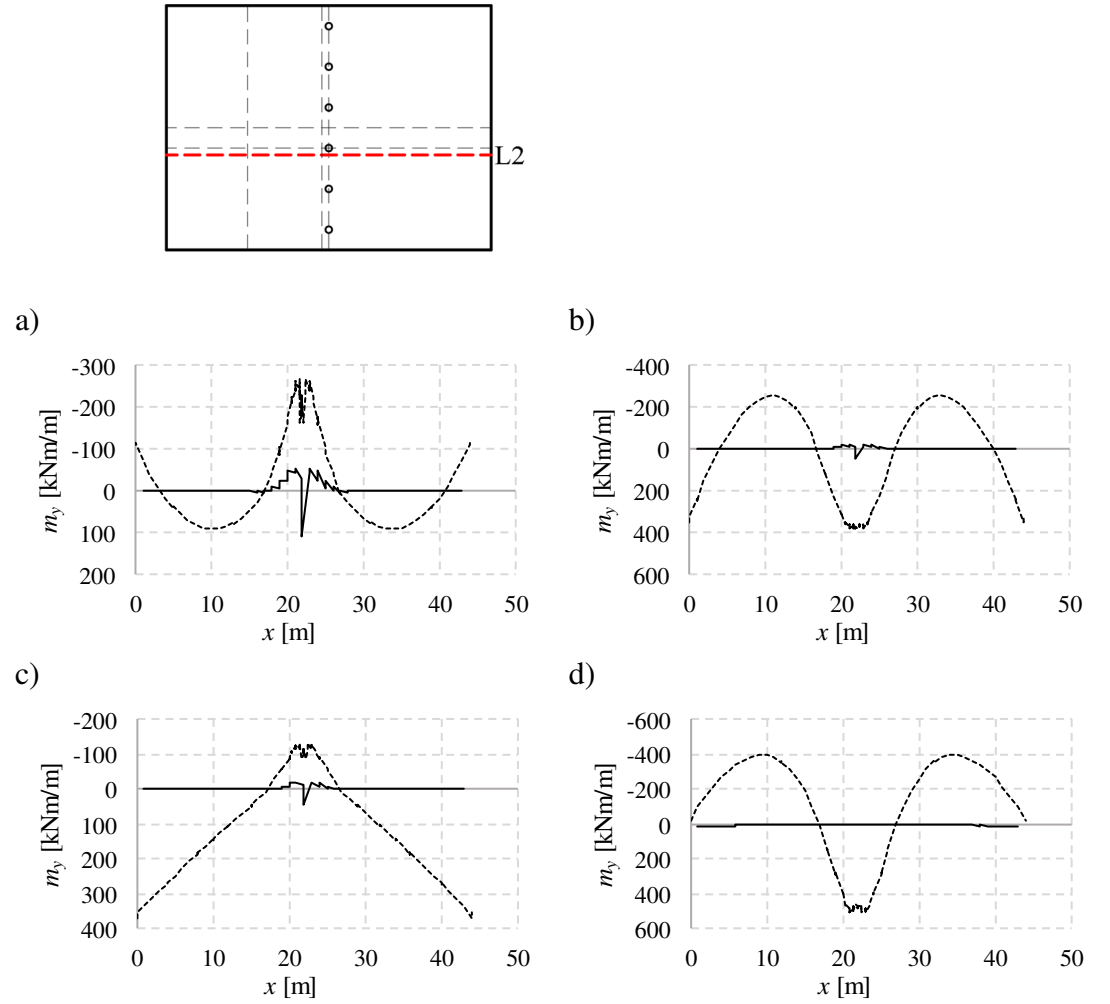

Figure H.24 Results along the section L2. a) Moment caused by the permanent load, b) resultant moment, c) restraint moment, d) primary moment

Table H.22 Comparison of the moments [kNm/m] in Figure H.24 at certain points. If no coordinate is specified, the given value is the peak value in that region. Deviation is the difference between the moment in the beam grillage model and shell model.

	a	b	c	d
Model	Support x=22	Support x=22	Support x=22	Support x=22
Grillage model	109	41	41	0
Shell model	-207	373	-106	478
Deviation [%]	-152.49	-88.95	-139.01	-
	Span	Span	Left support	Span
Grillage model	-	-	-	0
Shell model	90	-260	367	-397
Deviation [%]	-	-	-	-

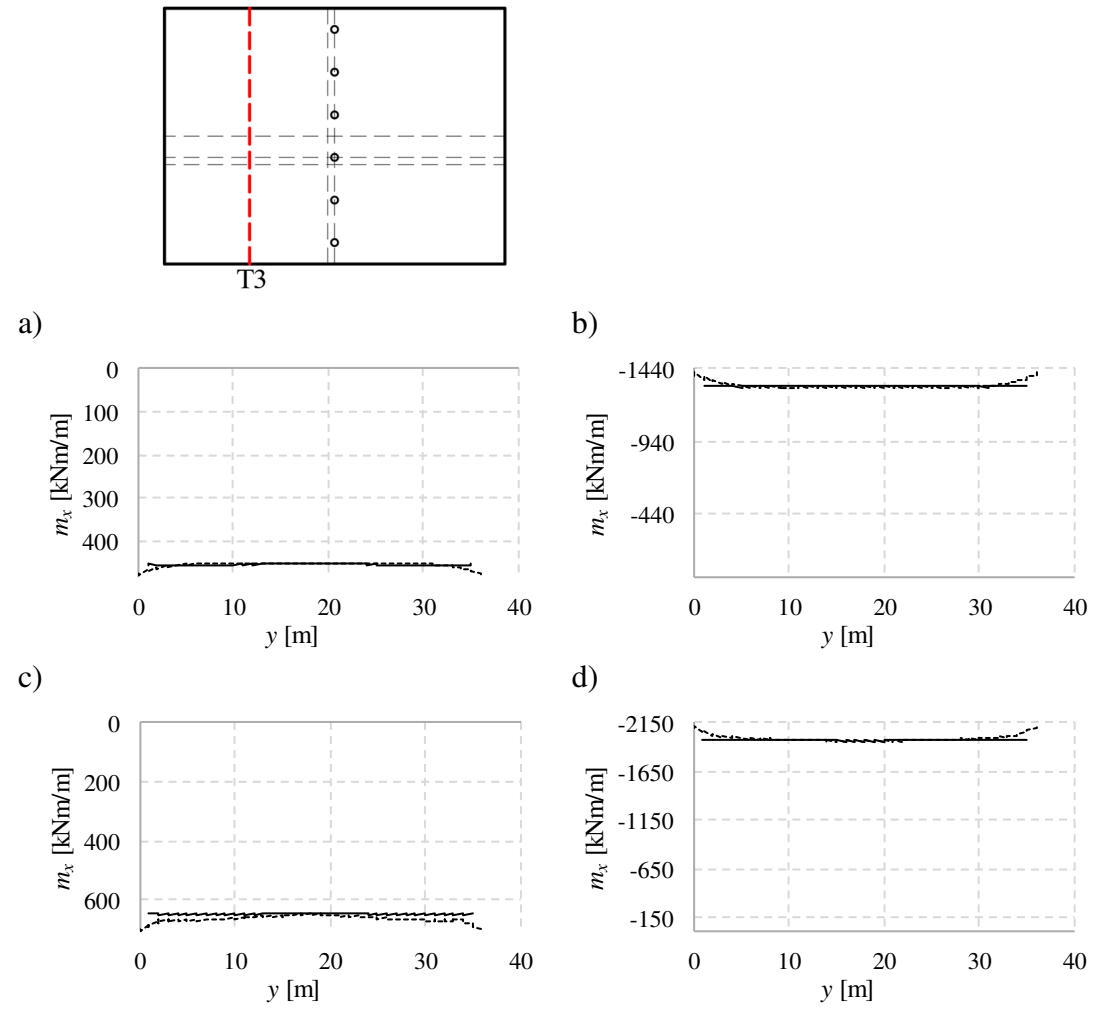

Figure H.25 Results along the section T3. a) Moment caused by the permanent load, b) resultant moment, c) restraint moment, d) primary moment

Table H.23 Comparison of the moments [kNm/m] in Figure H.25 at certain points. If no coordinate is specified, the given value is the peak value in that region. Deviation is the difference between the moment in the beam grillage model and shell model.

	a	b	c	d
Model	Mid y=18	Mid y=18	Mid y=18	Mid y=18
Grillage model	452	-1321	649	-1970
Shell model	451	-1317	654	-1971
Deviation [%]	0.18	0.33	-0.80	-0.05

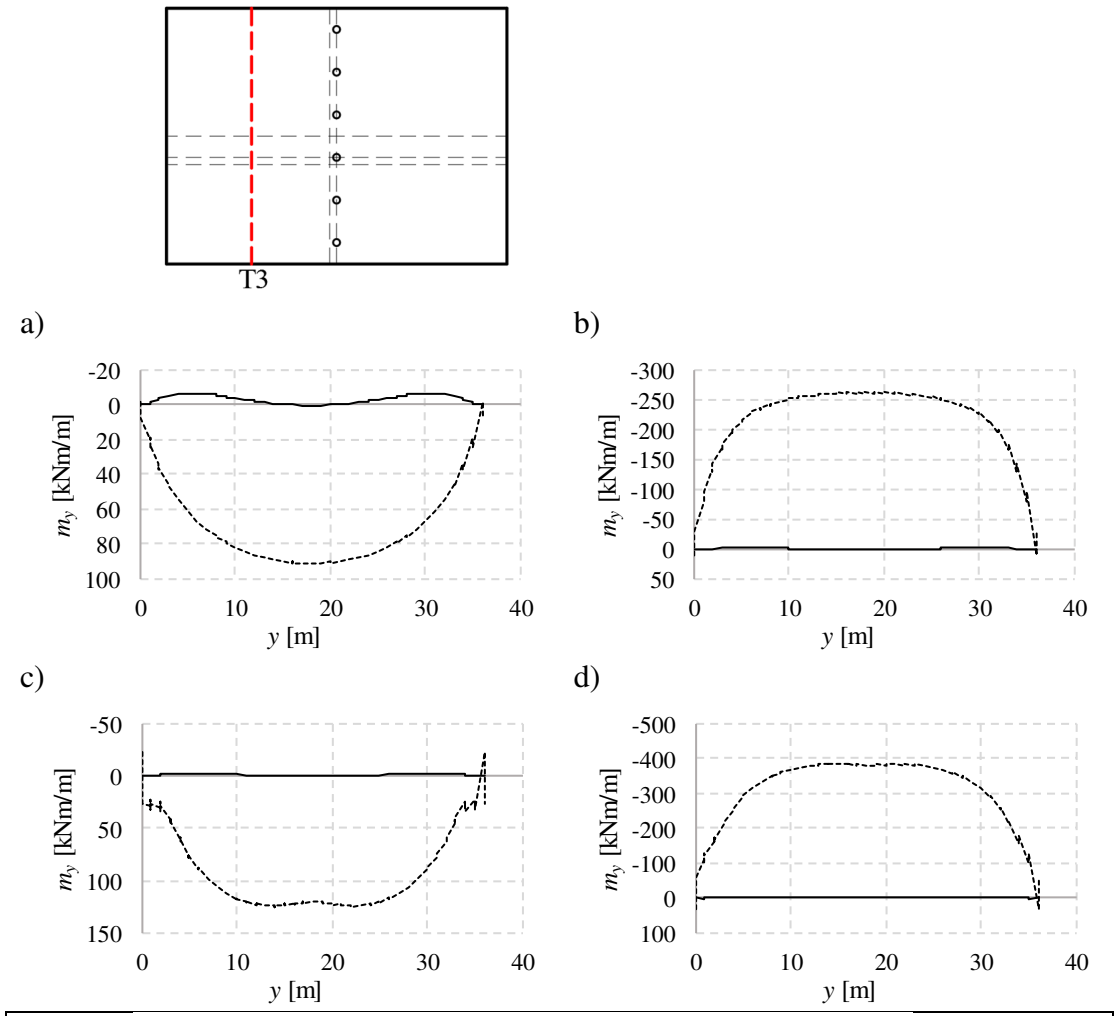

Figure H.26 Results along the section T3. a) Moment caused by the permanent load, b) resultant moment, c) restraint moment, d) primary moment

Table H.24 Comparison of the moments [kNm/m] in Figure H.26 at certain points. If no coordinate is specified, the given value is the peak value in that region. Deviation is the difference between the moment in the beam grillage model and shell model.

	a	b	c	d
Model	Mid y=18	Mid y=18	Mid y=18	Mid y=18
Grillage model	-	-	-	0
Shell model	91	-262	119	-385
Deviation [%]	-	-	-	-

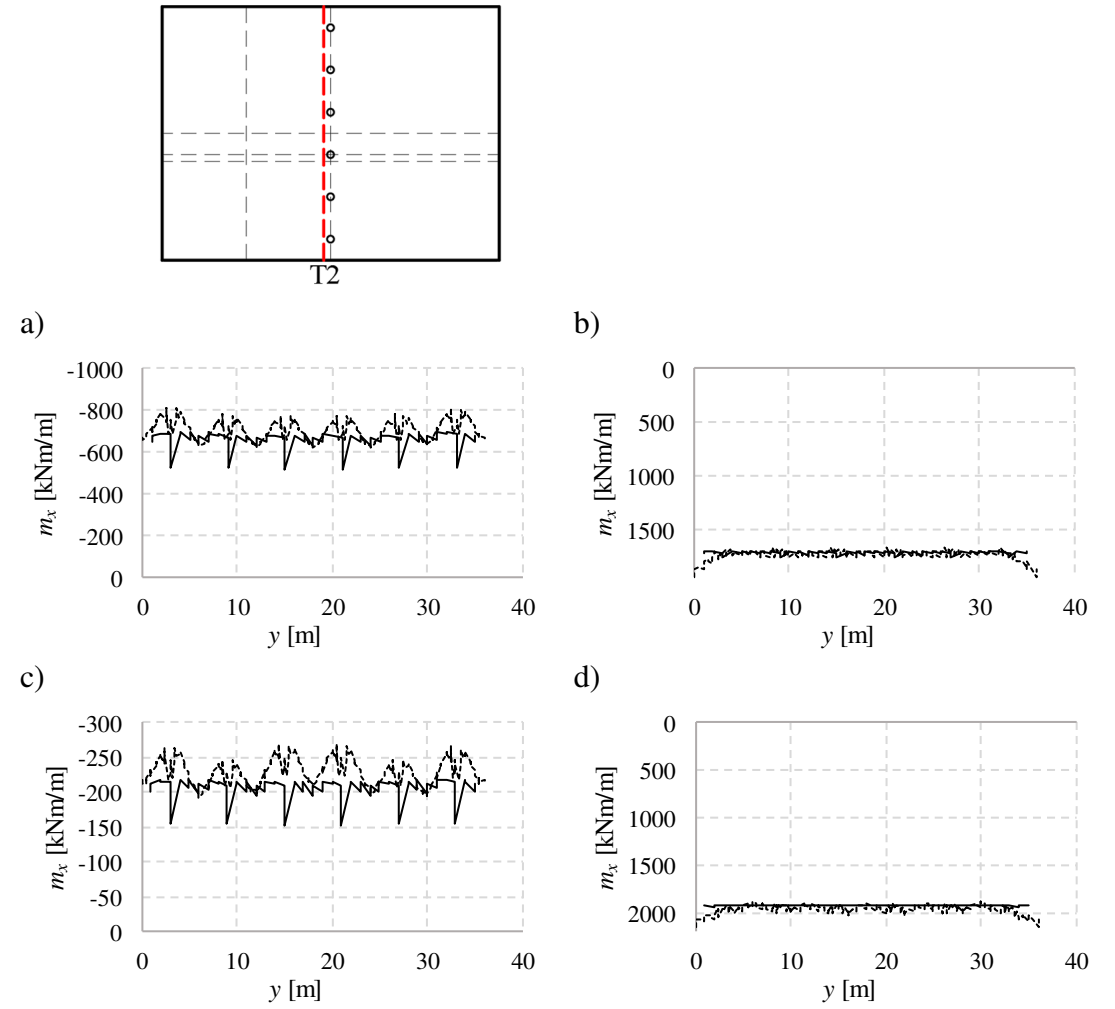

Figure H.27 Results along the section T2. a) Moment caused by the permanent load, b) resultant moment, c) restraint moment, d) primary moment

Table H.25 Comparison of the moments [kNm/m] in Figure H.27 at certain points. If no coordinate is specified, the given value is the peak value in that region. Deviation is the difference between the moment in the beam grillage model and shell model.

	a	b	c	d
Model	Support y=15	Mid y =18	Support y=15	Mid y =18
Grillage model	-595	1739	-153	1920
Shell model	-708	1708	-241	1949
Deviation [%]	-15.89	1.84	-36.55	-1.46
	Span y=18	Span y=18	Span y=18	Span y=18
Grillage model	-653	-	-203	-
Shell model	-627	-	-211	-
Deviation [%]	4.18	-	-3.98	-

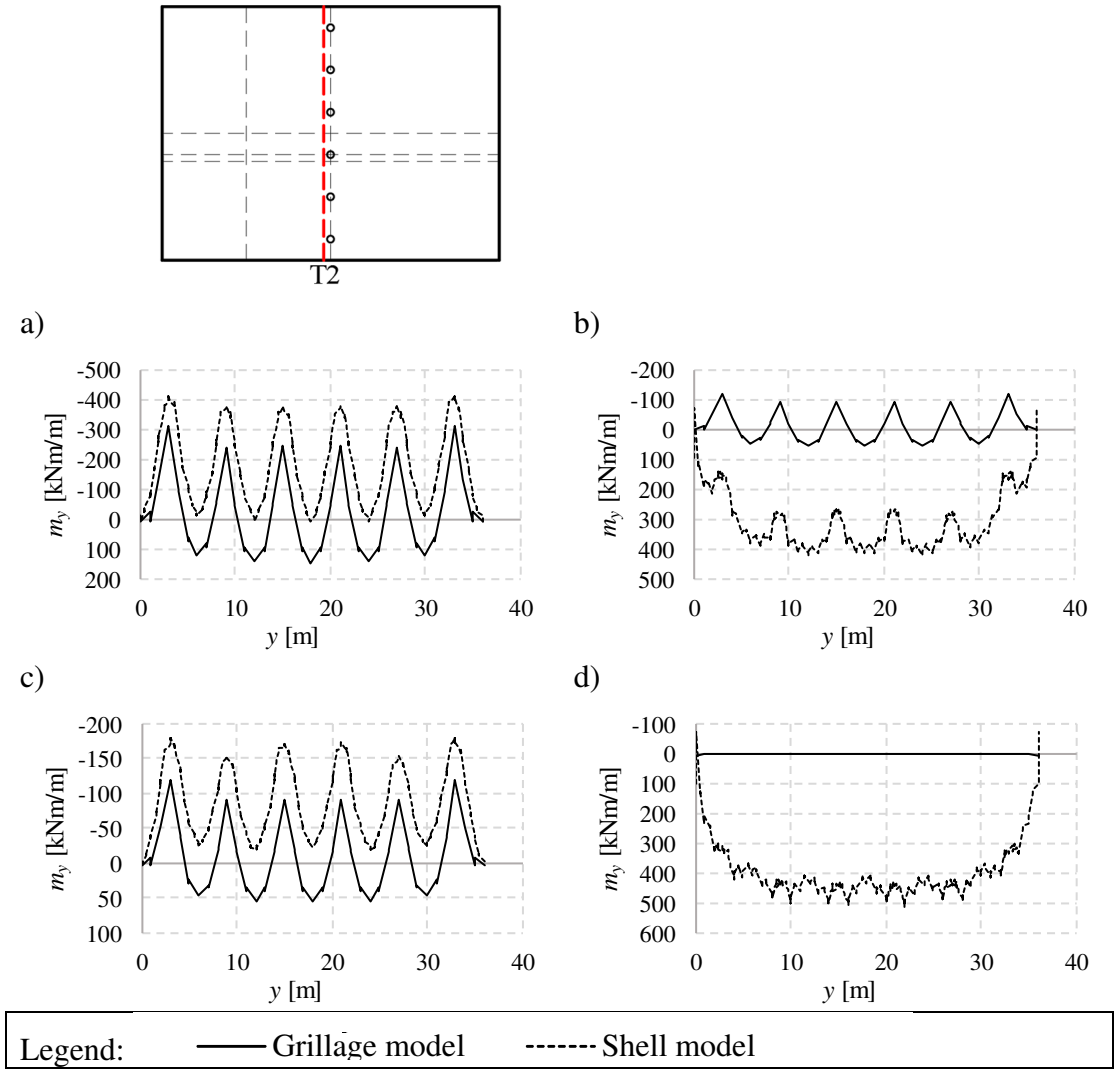

Figure H.28 Results along the section T2. a) Moment caused by the permanent load, b) resultant moment, c) restraint moment, d) primary moment

Table H.26 Comparison of the moments [kNm/m] in Figure H.28 at certain points. If no coordinate is specified, the given value is the peak value in that region. Deviation is the difference between the moment in the beam grillage model and shell model.

	a	b	c	d
Model	Support y=15	Support y=15	Support y=15	Support y=15
Grillage model	-243	-92	-92	0
Shell model	-374	274	-171	445
Deviation [%]	-	-	-	-
	Span y=18	Span y=18	Span y=18	Span y=18
Grillage model	145	55	55	0
Shell model	7	407	-23	430
Deviation [%]	-	-	-	-

H.5 Influence of transverse contraction

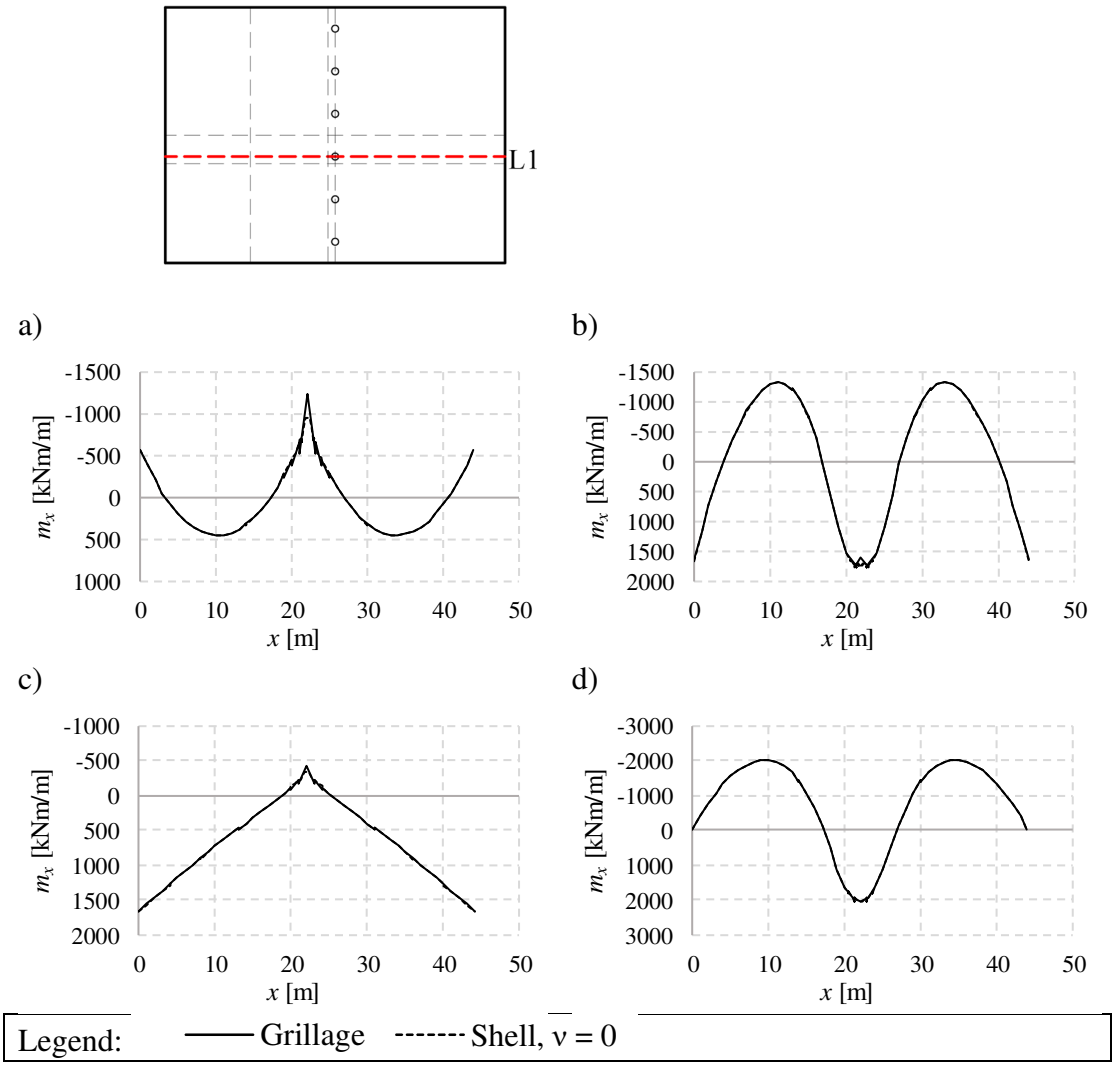

Figure H.29 Results along the section L1. a) Moment caused by the permanent load, b) resultant moment, c) restraint moment, d) primary moment

Table H.27 Comparison of the moments [kNm/m] in Figure H.29 at certain points. If no coordinate is specified, the given value is the peak value in that region. Deviation is the difference between the moment in the beam grillage model and shell model.

	a	b	c	d
Models	Support x=22	Support x=22	Support x=22	Support x=22
Grillage	-1226	1596	-424	2019
Shell, ν = 0	-950	1720	-335	2055
Deviation [%]	29.11	-7.24	26.45	-1.75
	Span	Span	Left support	Span
Grillage	457	-1321	1655	-2022
Shell, ν = 0	456	-1320	1680	-2022
Deviation [%]	0.23	0.04	-1.47	-0.02

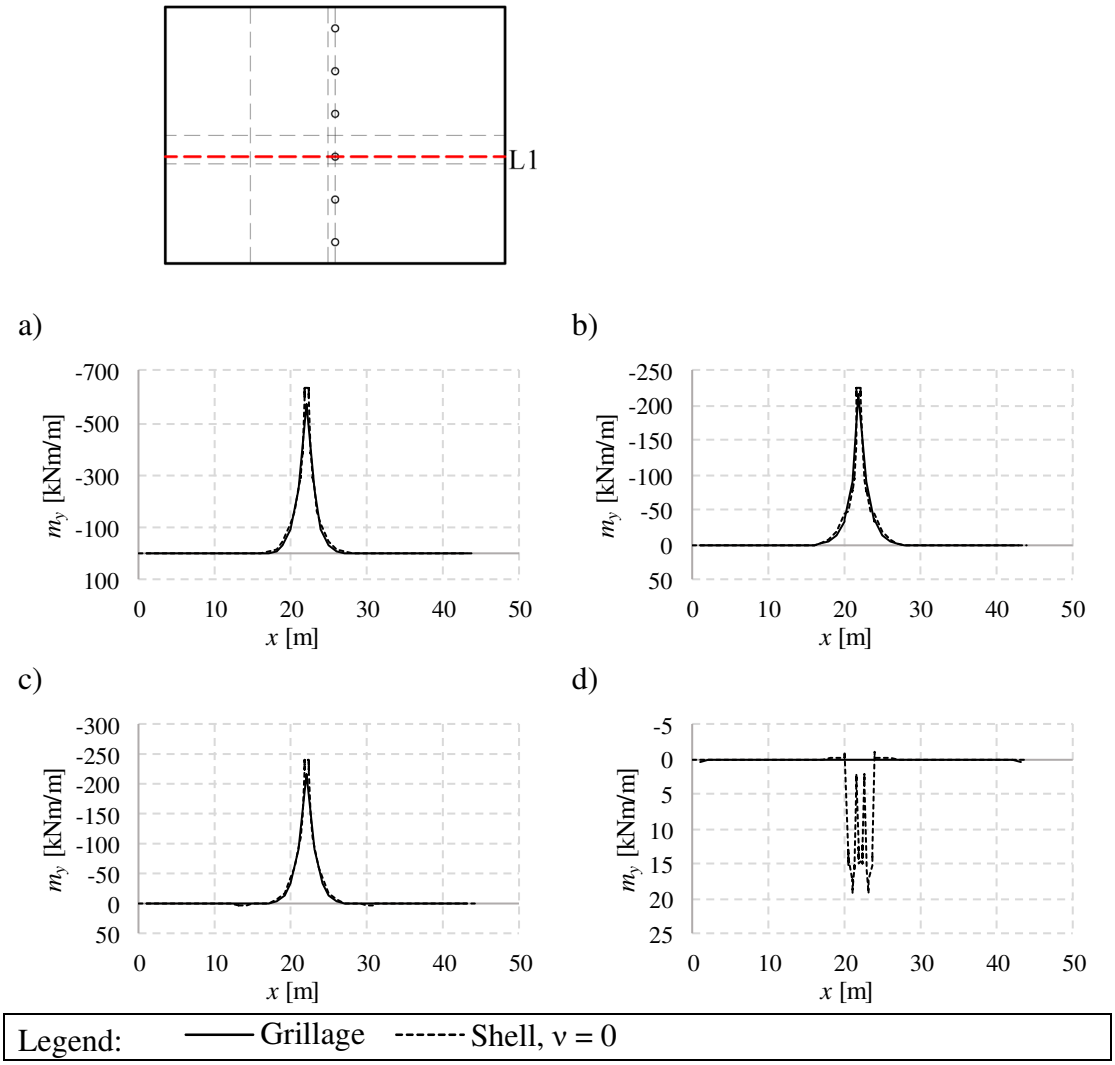

Figure H.30 Results along the section L1. a) Moment caused by the permanent load, b) resultant moment, c) restraint moment, d) primary moment

Table H.28 Comparison of the moments [kNm/m] in Figure H.30 at certain points. If no coordinate is specified, the given value is the peak value in that region. Deviation is the difference between the moment in the beam grillage model and shell model.

	a	b	c	d
Models	Support x=22	Support x=22	Support x=22	Support x=22
Grillage	-572	-217	-217	0
Shell, ν = 0	-631	-230	-245	15
Deviation [%]	-9.32	-5.82	-11.44	-
	Span	Span	Span	Span
Grillage	0	0	0	0
Shell, ν = 0	-	-	-	-
Deviation [%]	-	-	-	-

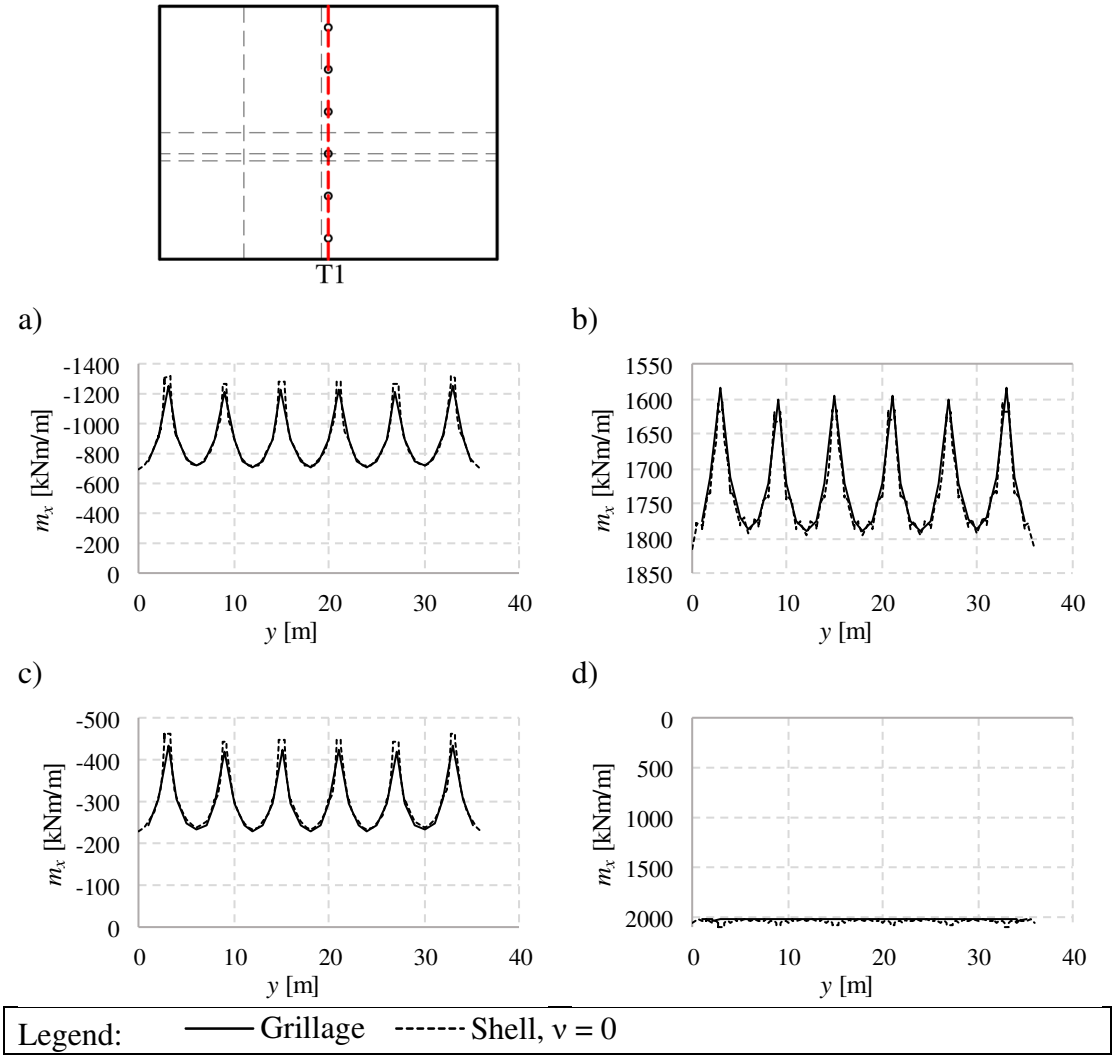

Figure H.31 Results along the section T1. a) Moment caused by the permanent load, b) resultant moment, c) restraint moment, d) primary moment

Table H.29 Comparison of the moments [kNm/m] in Figure H.31 at certain points. If no coordinate is specified, the given value is the peak value in that region. Deviation is the difference between the moment in the beam grillage model and shell model.

	a	b	c	d
Models	Support y=15	Support y=15	Support x=22	Support y=15
Grillage	-1226	1596	-424	2019
Shell, ν = 0	-1281	1617	-463	2080
Deviation [%]	-4.25	-1.33	-8.60	-2.95
	Span y=18	Span y=18	Span y=18	Span y=18
Grillage	-716	1789	-230	2019
Shell, ν = 0	-719	1785	-246	2031
Deviation [%]	-0.48	0.21	-6.38	-0.59

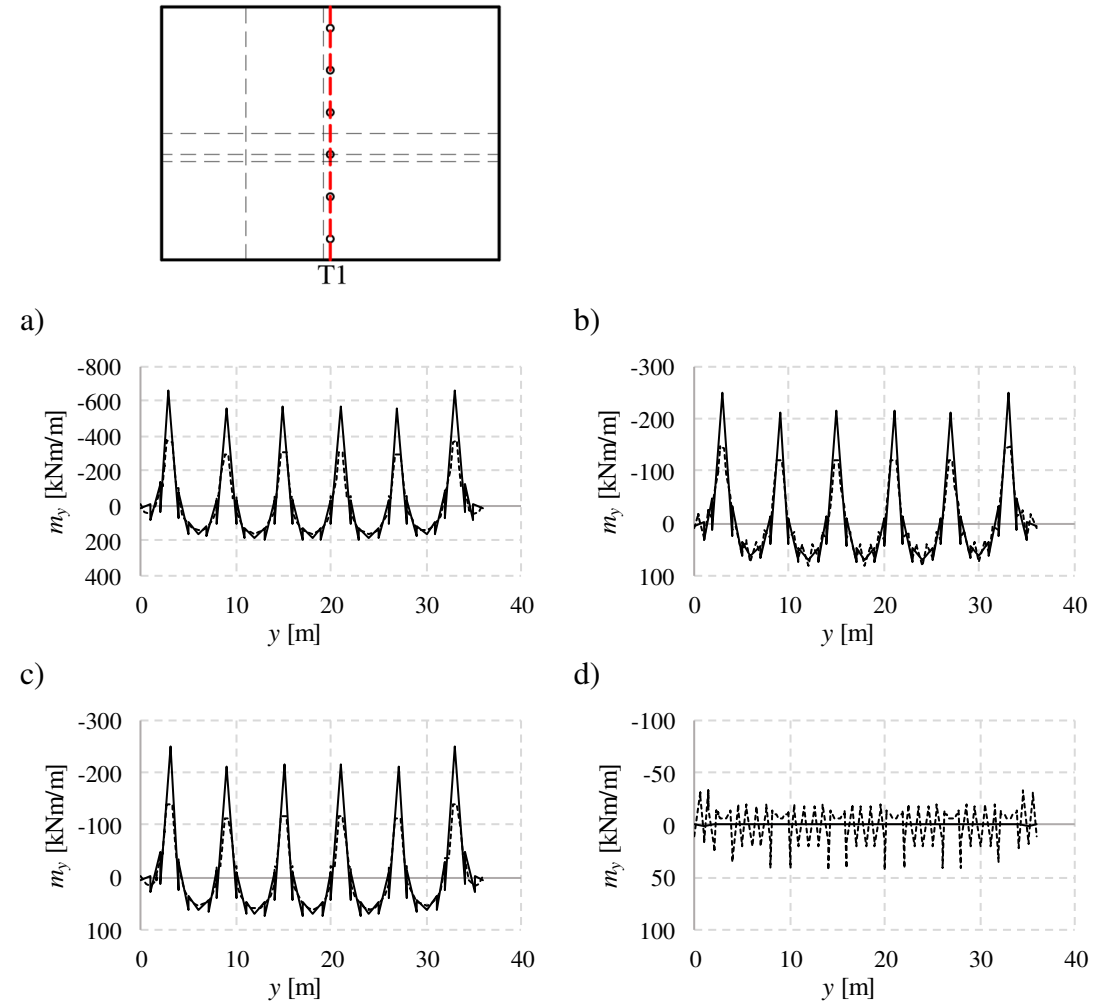

Figure H.32 Results along the section T1. a) Moment caused by the permanent load, b) resultant moment, c) restraint moment, d) primary moment

Table H.30 Comparison of the moments [kNm/m] in Figure H.32 at certain points. If no coordinate is specified, the given value is the peak value in that region. Deviation is the difference between the moment in the beam grillage model and shell model.

	a	b	c	d
Models	Support y=15	Support y=15	Support x=22	Support y=15
Grillage	-572	-217	-217	0
Shell, ν = 0	-303	-123	-117	-6
Deviation [%]	89.22	76.10	84.75	-
	Span y=18	Span y=18	Span y=18	Span y=18
Grillage	185	70	70	0
Shell, ν = 0	159	81	62	20
Deviation [%]	16.73	-13.79	14.01	-

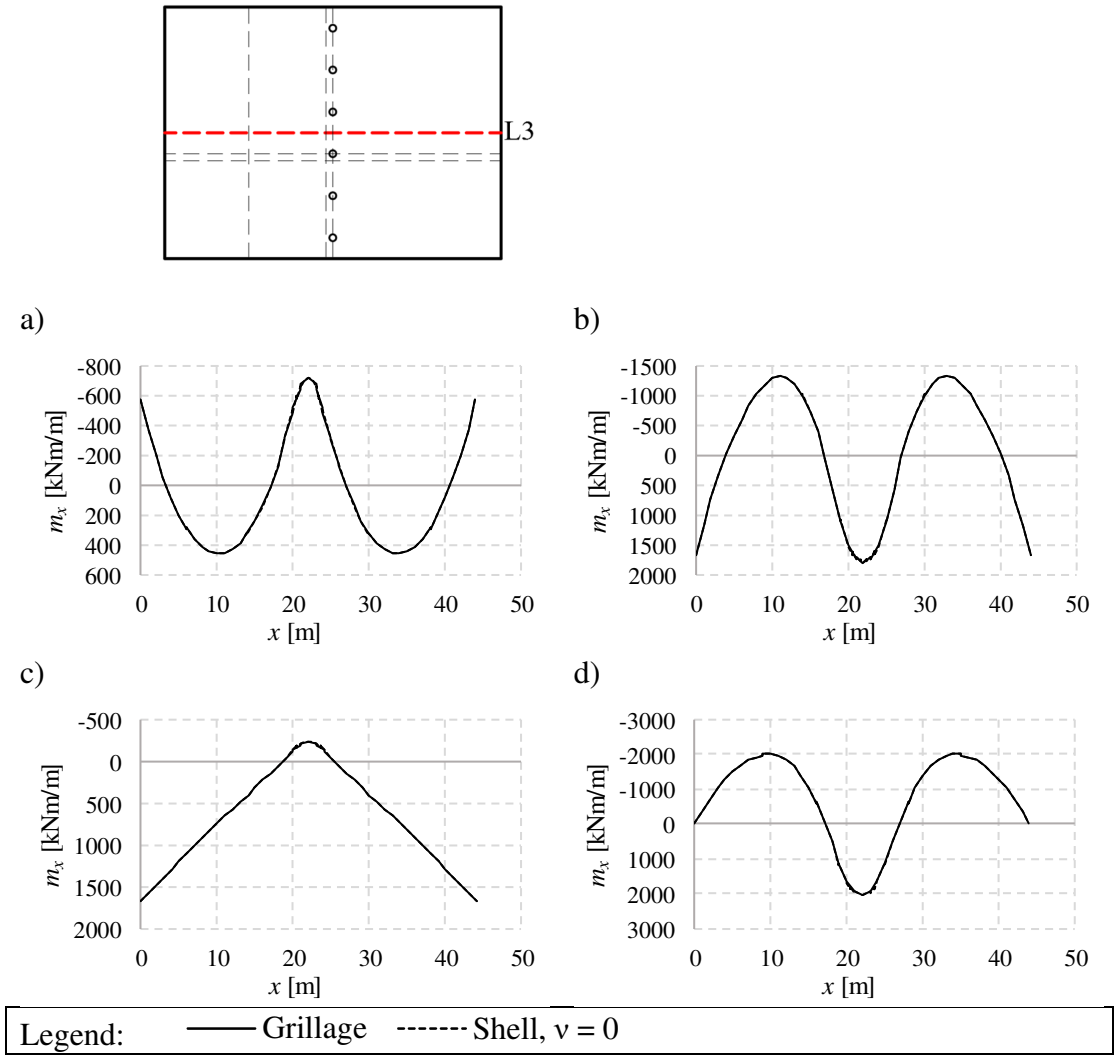

Figure H.33 Results along the section L3. a) Moment caused by the permanent load, b) resultant moment, c) restraint moment, d) primary moment

Table H.31 Comparison of the moments [kNm/m] in Figure H.33 at certain points. If no coordinate is specified, the given value is the peak value in that region. Deviation is the difference between the moment in the beam grillage model and shell model.

	a	b	c	d
Models	Support x=22	Support x=22	Support x=22	Support x=22
Grillage	-716	1789	-230	2019
Shell, ν = 0	-719	1785	-246	2031
Deviation [%]	-0.48	0.21	-6.38	-0.59
	Span	Span	Left support	Span
Grillage	456	-1321	1655	-2022
Shell, ν = 0	455	-1320	1680	-2022
Deviation [%]	0.31	0.06	-1.46	-0.01

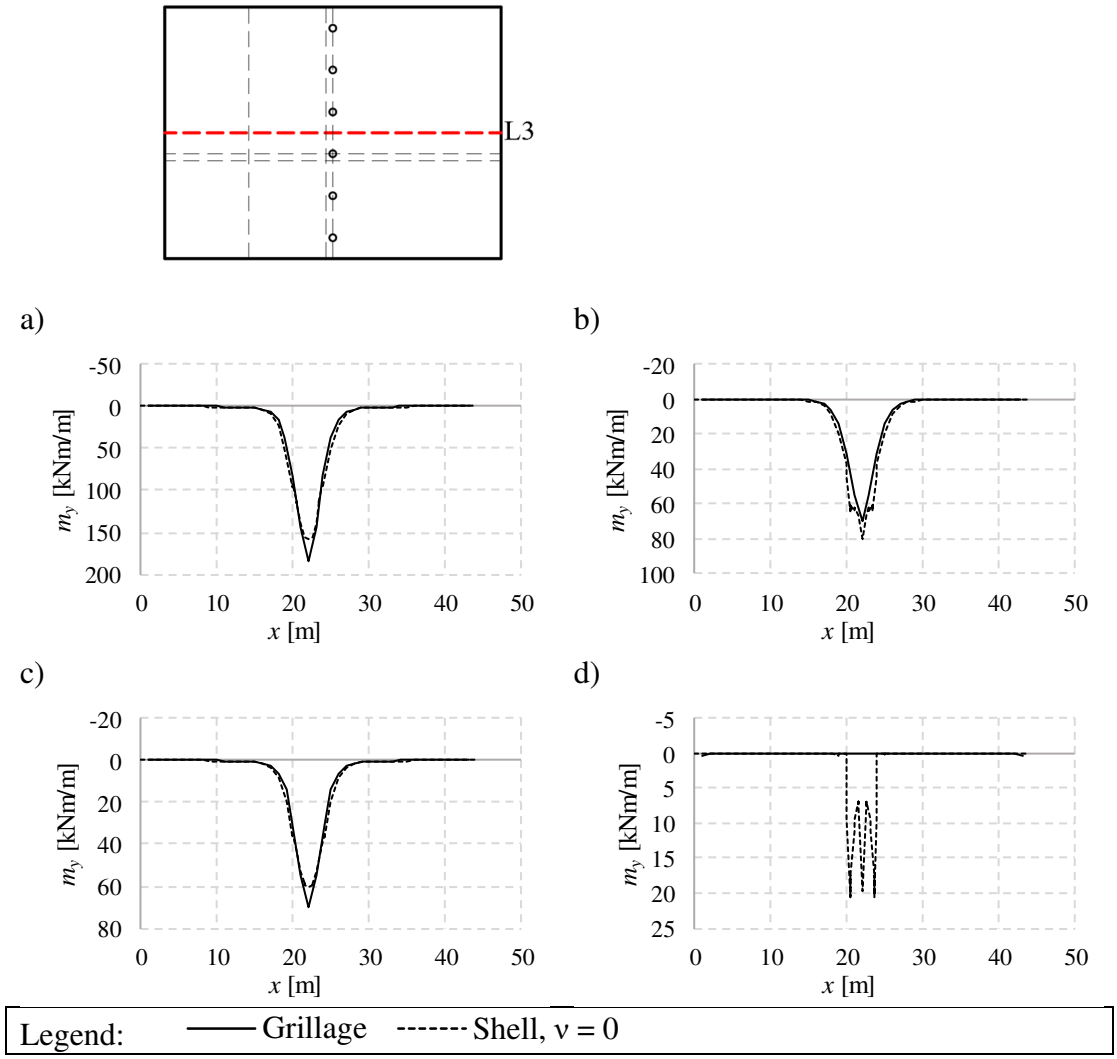

Figure H.34 Results along the section L3. a) Moment caused by the permanent load, b) resultant moment, c) restraint moment, d) primary moment

Table H.32 Comparison of the moments [kNm/m] in Figure H.34 at certain points. If no coordinate is specified, the given value is the peak value in that region. Deviation is the difference between the moment in the beam grillage model and shell model.

	a	b	c	d
Models	Support x=22	Support x=22	Support x=22	Support x=22
Grillage	185	70	70	0
Shell, ν = 0	159	81	62	20
Deviation [%]	16.73	-13.79	14.01	-
	Span	Span	Left support	Span
Grillage	0	0	0	0
Shell, ν = 0	-	-	-	-
Deviation [%]	-	-	-	-

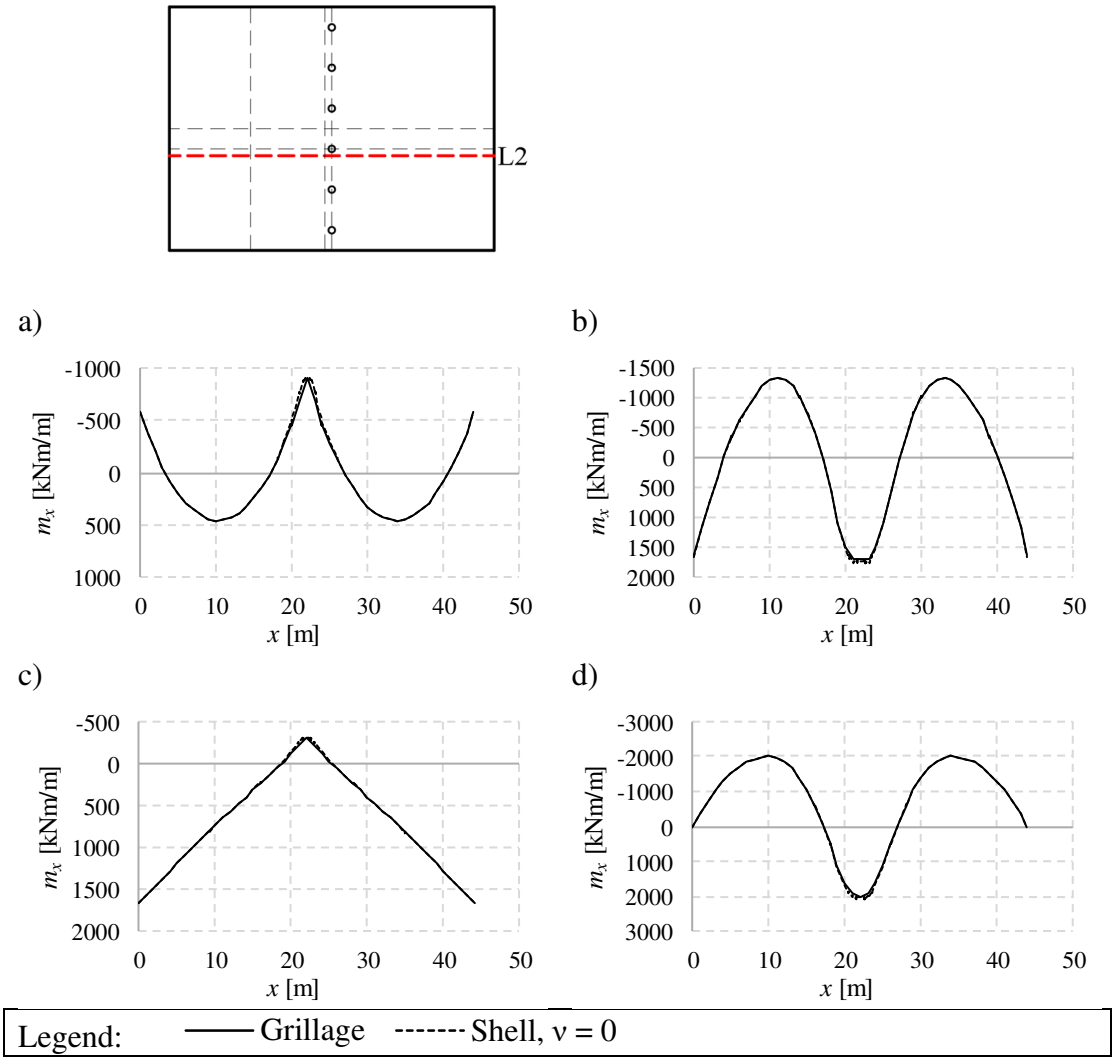

Figure H.35 Results along the section L2. a) Moment caused by the permanent load, b) resultant moment, c) restraint moment, d) primary moment

Table H.33 Comparison of the moments [kNm/m] in Figure H.35 at certain points. If no coordinate is specified, the given value is the peak value in that region. Deviation is the difference between the moment in the beam grillage model and shell model.

	a	b	c	d
Models	Support x=22	Support x=22	Support x=22	Support x=22
Grillage	-897	1720	-299	2019
Shell, ν = 0	-897	1730	-315	2044
Deviation [%]	0.00	-0.55	-5.05	-1.24
	Span	Span	Left support	Span
Grillage	457	-1321	1655	-2022
Shell, ν = 0	456	-1320	1680	-2022
Deviation [%]	0.21	0.03	-1.48	-0.02

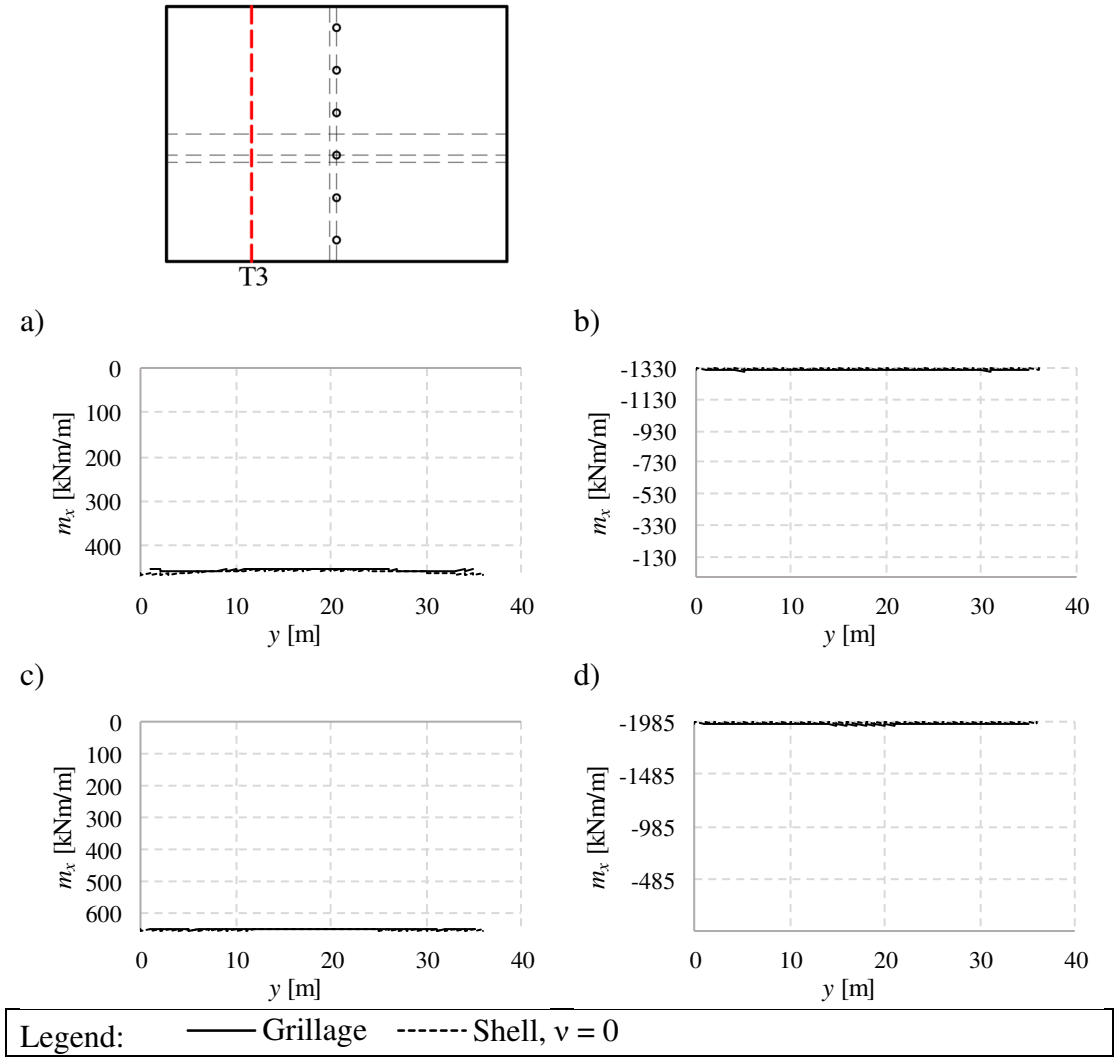

Figure H.36 Results along the section T3. a) Moment caused by the permanent load, b) resultant moment, c) restraint moment, d) primary moment

Table H.34 Comparison of the moments [kNm/m] in Figure H.36 at certain points. If no coordinate is specified, the given value is the peak value in that region. Deviation is the difference between the moment in the beam grillage model and shell model.

	a	b	c	d
Models	Mid y=18	Mid y=18	Mid y=18	Mid y=18
Grillage	452	-1321	649	-1970
Shell, ν = 0	453	-1320	656	-1977
Deviation [%]	-0.06	0.05	-1.12	-0.34

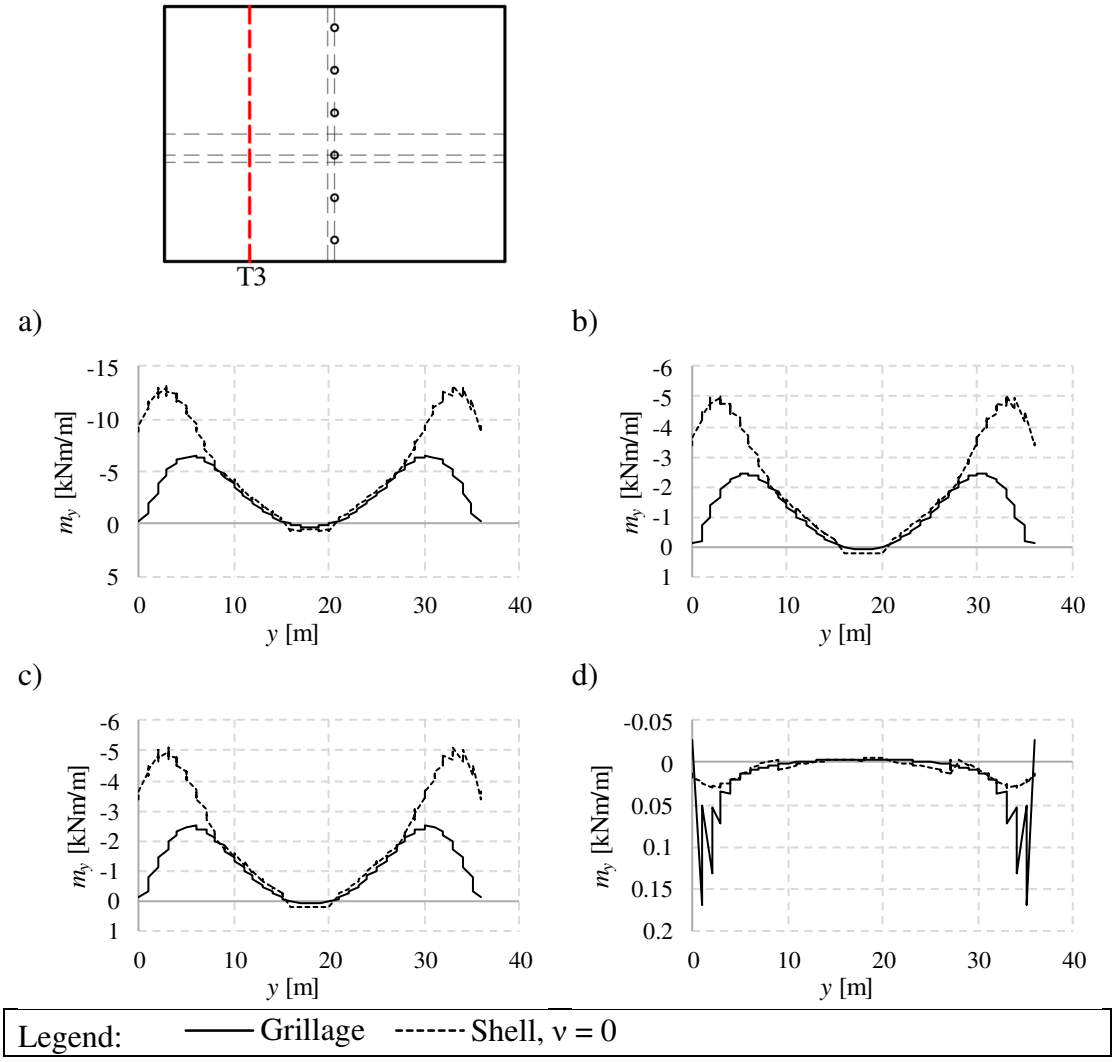

Figure H.37 Results along the section T3. a) Moment caused by the permanent load, b) resultant moment, c) restraint moment, d) primary moment

Table H.35 Comparison of the moments [kNm/m] in Figure H.37 at certain points. If no coordinate is specified, the given value is the peak value in that region. Deviation is the difference between the moment in the beam grillage model and shell model.

	a	b	c	d
Models	Mid y=18	Mid y=18	Mid y=18	Mid y=18
Grillage	0.00	0.00	0.1	0.00
Shell, ν = 0	0.00	0.00	0.6	-0.01
Deviation [%]	0.00	0.00	-	-

H.6 Influence of reduced stiffness in the transverse direction

H.6.1 Reduction with a factor of 0.5

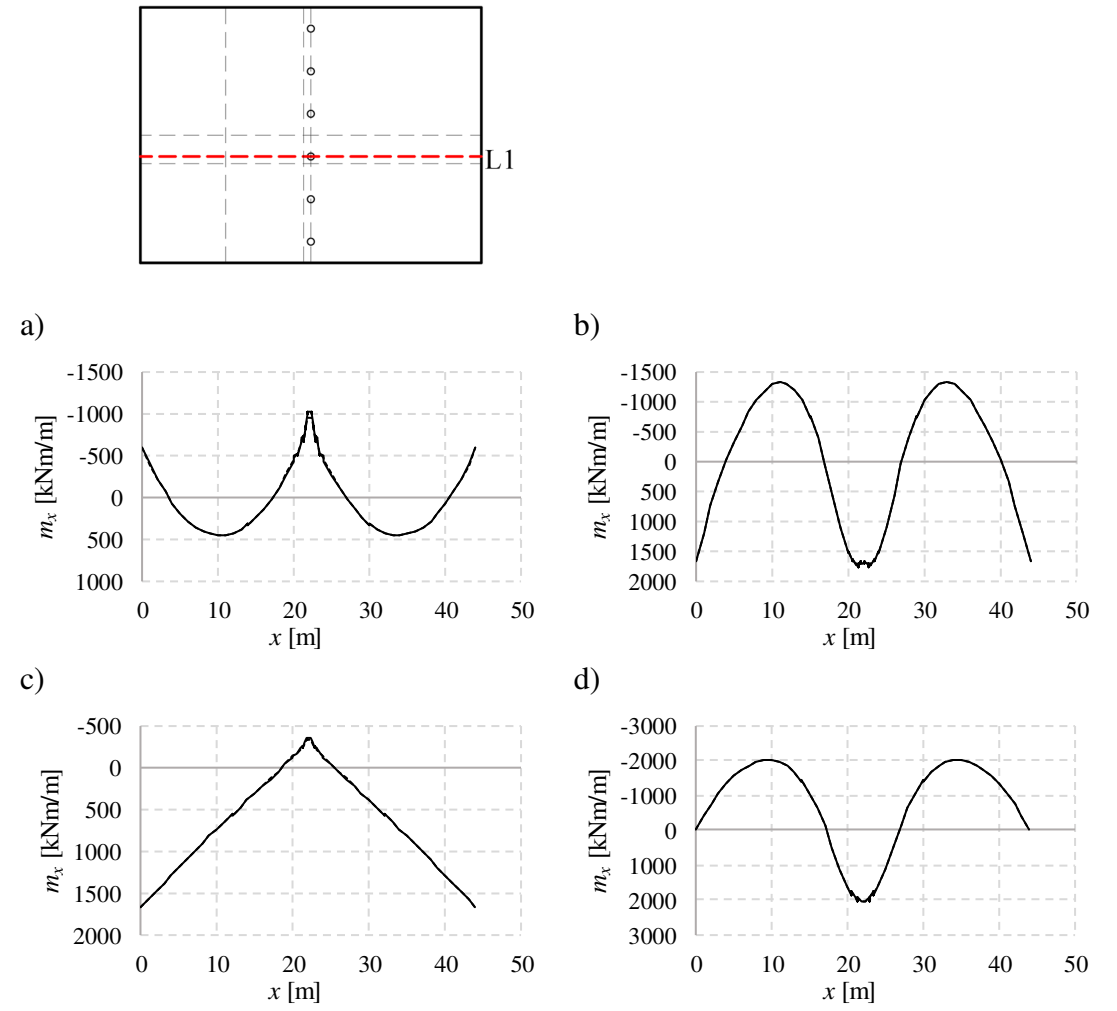

Figure H.38 Results along the section L1. a) Moment caused by the permanent load, b) resultant moment, c) restraint moment, d) primary moment

Table H.36 Comparison of the moments [kNm/m] in Figure H.38 at certain points. If no coordinate is specified, the given value is the peak value in that region. Deviation is the difference between the moments in the in the models with different stiffness.

	a	b	c	d
Stiffness	Support x=22	Support x=22	Support x=22	Support x=22
Reduced	-1004	1696	-356	2052
Regular	-950	1720	-335	2055
Deviation [%]	5.66	-1.37	6.26	-0.13
	Span	Span	Left support	Span
Reduced	455	-1320	1679	-2022
Regular	456	-1320	1680	-2022
Deviation [%]	-0.07	-0.01	-0.04	0.00

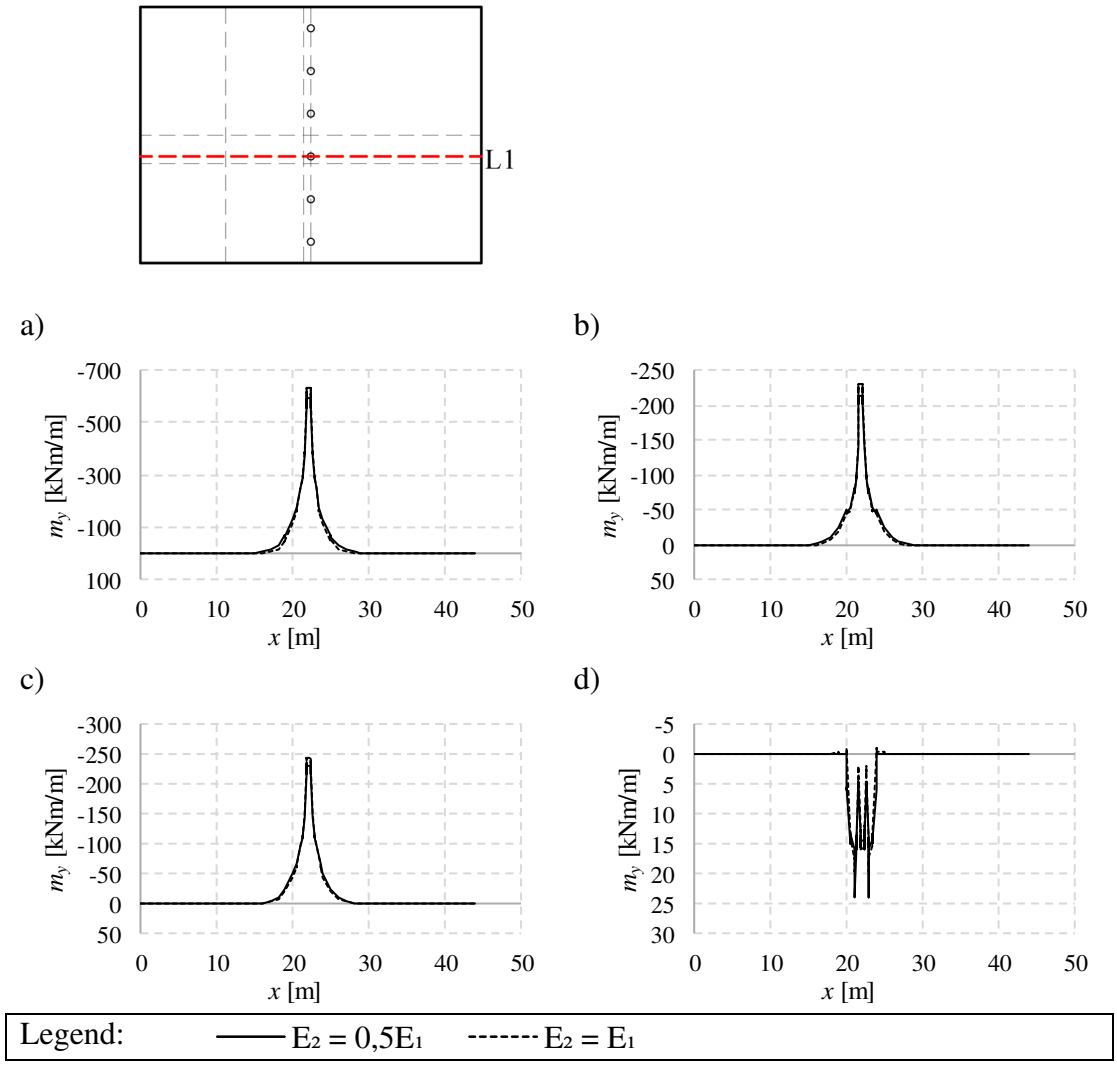

Figure H.39 Results along the section L1. a) Moment caused by the permanent load, b) resultant moment, c) restraint moment, d) primary moment

Table H.37 Comparison of the moments [kNm/m] in Figure H.39 at certain points. If no coordinate is specified, the given value is the peak value in that region. Deviation is the difference between the moments in the in the models with different stiffness.

	a	b	c	d
Stiffness	Support x=22	Support x=22	Support x=22	Support x=22
Reduced	-592	-214	-229	16
Regular	-631	-230	-245	15
Deviation [%]	-6.22	-7.16	-6.23	8.40

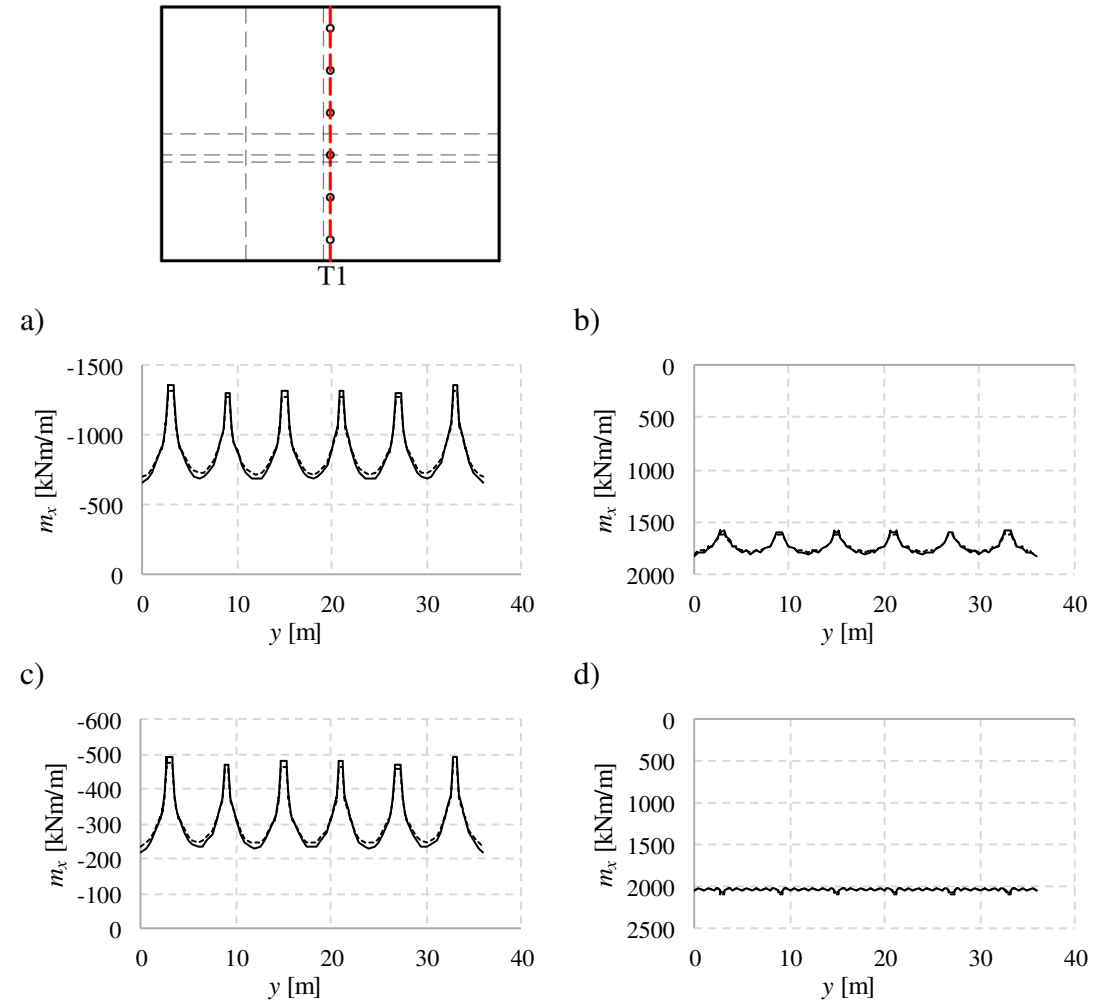

Figure H.40 Results along the section T1. a) Moment caused by the permanent load, b) resultant moment, c) restraint moment, d) primary moment

Table H.38 Comparison of the moments [kNm/m] in Figure H.40 at certain points. If no coordinate is specified, the given value is the peak value in that region. Deviation is the difference between the moments in the in the models with different stiffness.

	a	b	c	d
Stiffness	Supporty=15	Supporty=15	Supporty=15	Supporty=15
Reduced	-1323	1594	-480	2033
Regular	-1281	1617	-463	2031
Deviation [%]	3.30	-1.44	3.55	0.09
	Span y=18	Span y=18	Span y=18	Span y=18
Reduced	-686	1800	-233	-
Regular	-719	1785	-246	-
Deviation [%]	-4.59	0.82	-5.16	-

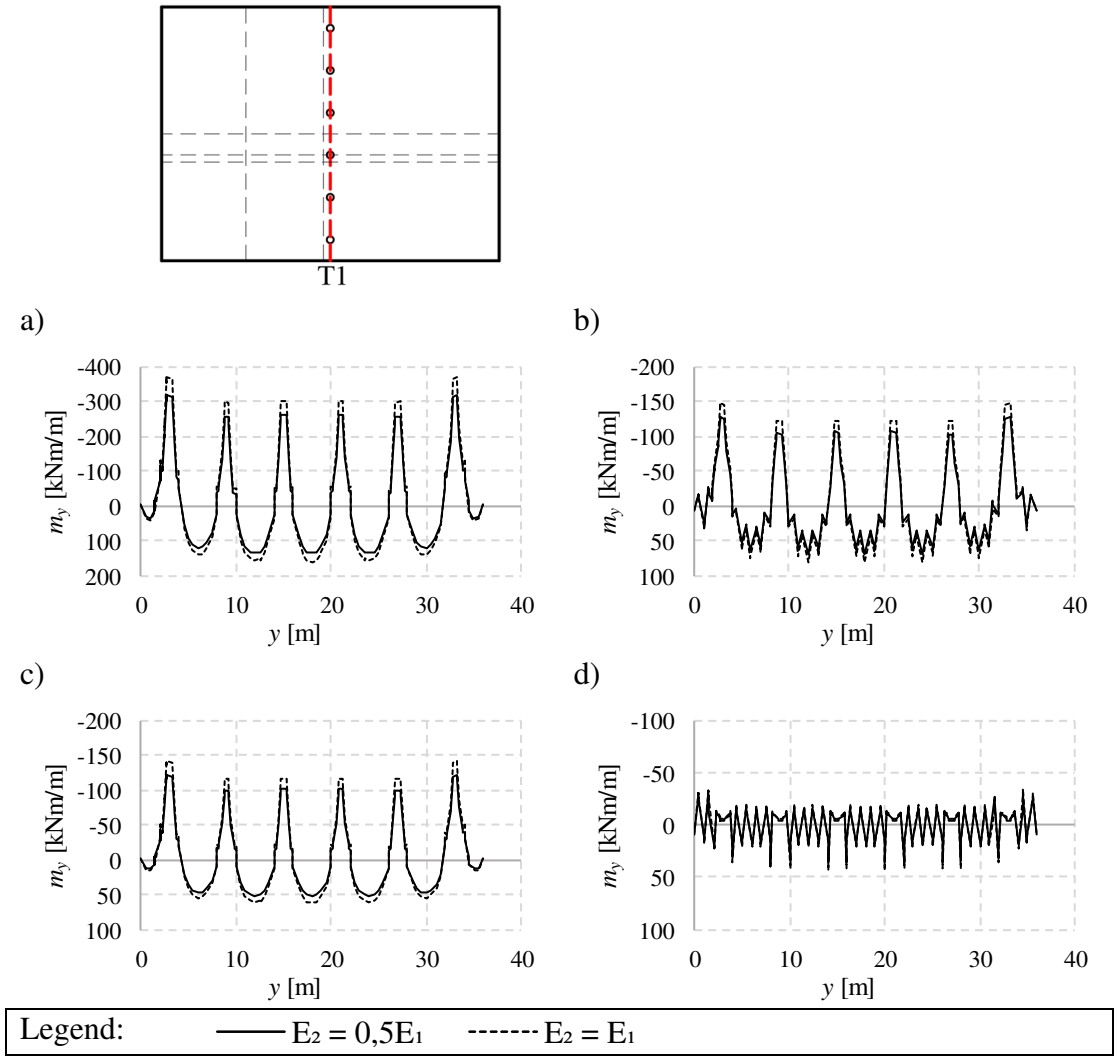

Figure H.41 Results along the section T1. a) Moment caused by the permanent load, b) resultant moment, c) restraint moment, d) primary moment

Table H.39 Comparison of the moments [kNm/m] in Figure H.41 at certain points. If no coordinate is specified, the given value is the peak value in that region. Deviation is the difference between the moments in the in the models with different stiffness.

	a	b	c	d
Stiffness	Supporty=15	Supporty=15	Supporty=15	Supporty=15
Reduced	-262	-106	-102	18
Regular	-303	-123	-117	20
Deviation [%]	-13.30	-13.64	-13.31	-9.07
	Span y=18	Span y=18	Span y=18	Span y=18
Reduced	135	70	52	-
Regular	159	81	62	-
Deviation [%]	-14.88	-13.49	-14.92	-

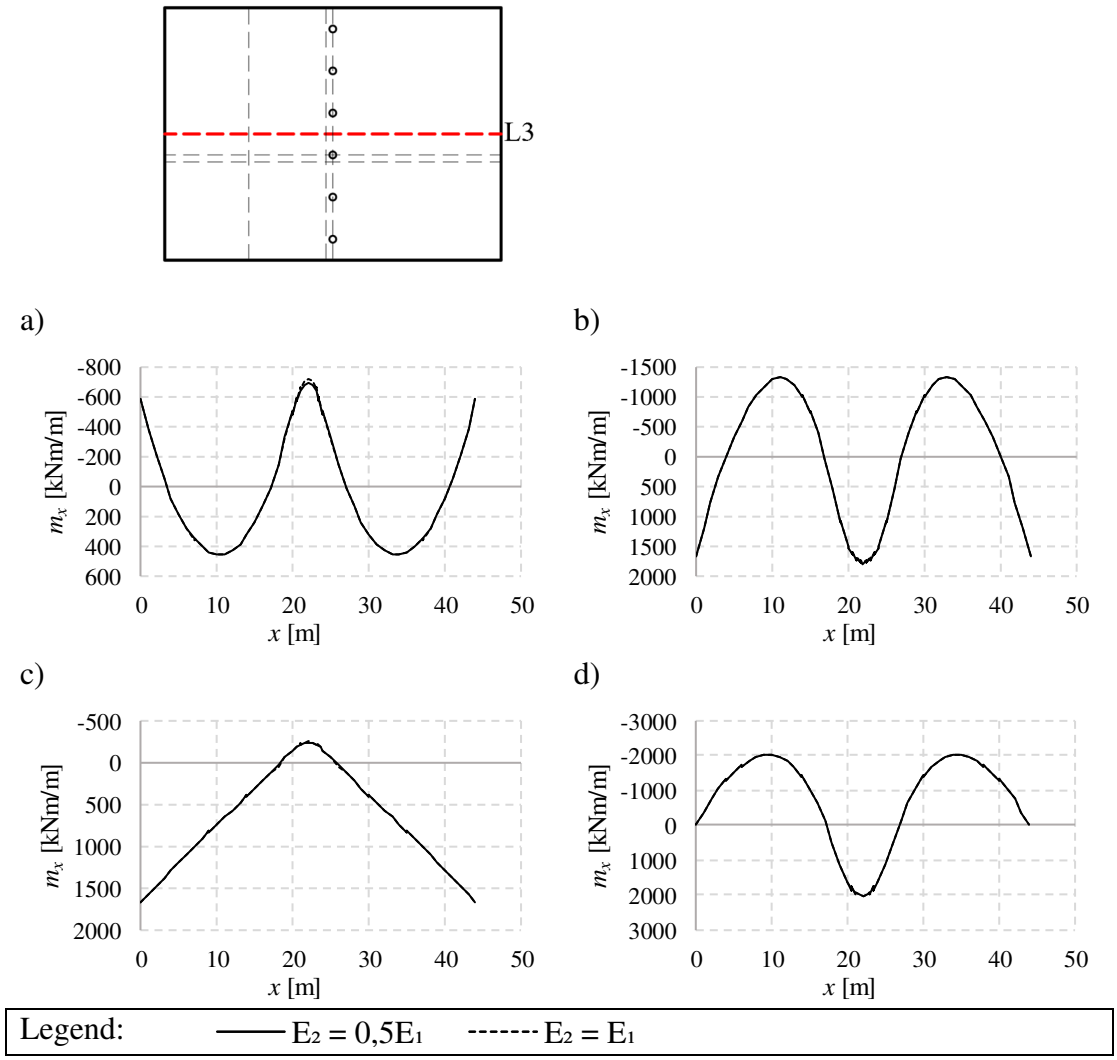

Figure H.42 Results along the section L3. a) Moment caused by the permanent load, b) resultant moment, c) restraint moment, d) primary moment

Table H.40 Comparison of the moments [kNm/m] in Figure H.42 at certain points. If no coordinate is specified, the given value is the peak value in that region. Deviation is the difference between the moments in the in the models with different stiffness.

	a	b	c	d
Stiffness	Support x=22	Support x=22	Support x=22	Support x=22
Reduced	-686	1800	-233	2033
Regular	-719	1785	-246	2031
Deviation [%]	-4.59	0.82	-5.16	0.09
	Span	Span	Left support	Span
Reduced	455	-1320	1679	-2022
Regular	455	-1320	1680	-2022
Deviation [%]	-0.05	-0.01	-0.04	0.00

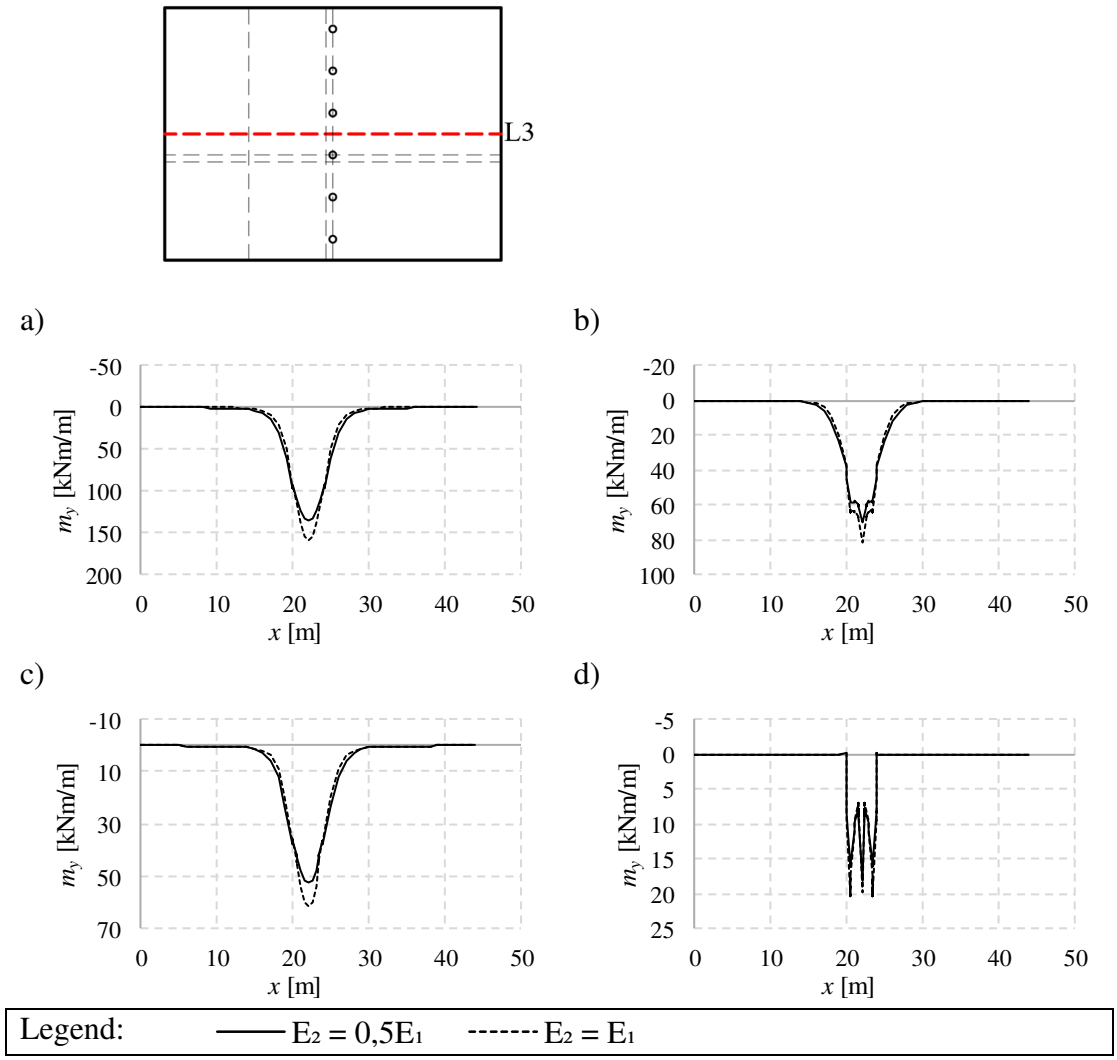

Figure H.43 Results along the section L3. a) Moment caused by the permanent load, b) resultant moment, c) restraint moment, d) primary moment

Table H.41 Comparison of the moments [kNm/m] in Figure H.43 at certain points. If no coordinate is specified, the given value is the peak value in that region. Deviation is the difference between the moments in the in the models with different stiffness.

	a	b	c	d
Stiffness	Support x=22	Support x=22	Support x=22	Support x=22
Reduced	135	70	52	18
Regular	159	81	62	20
Deviation [%]	-14.88	-13.49	-14.92	-9.07

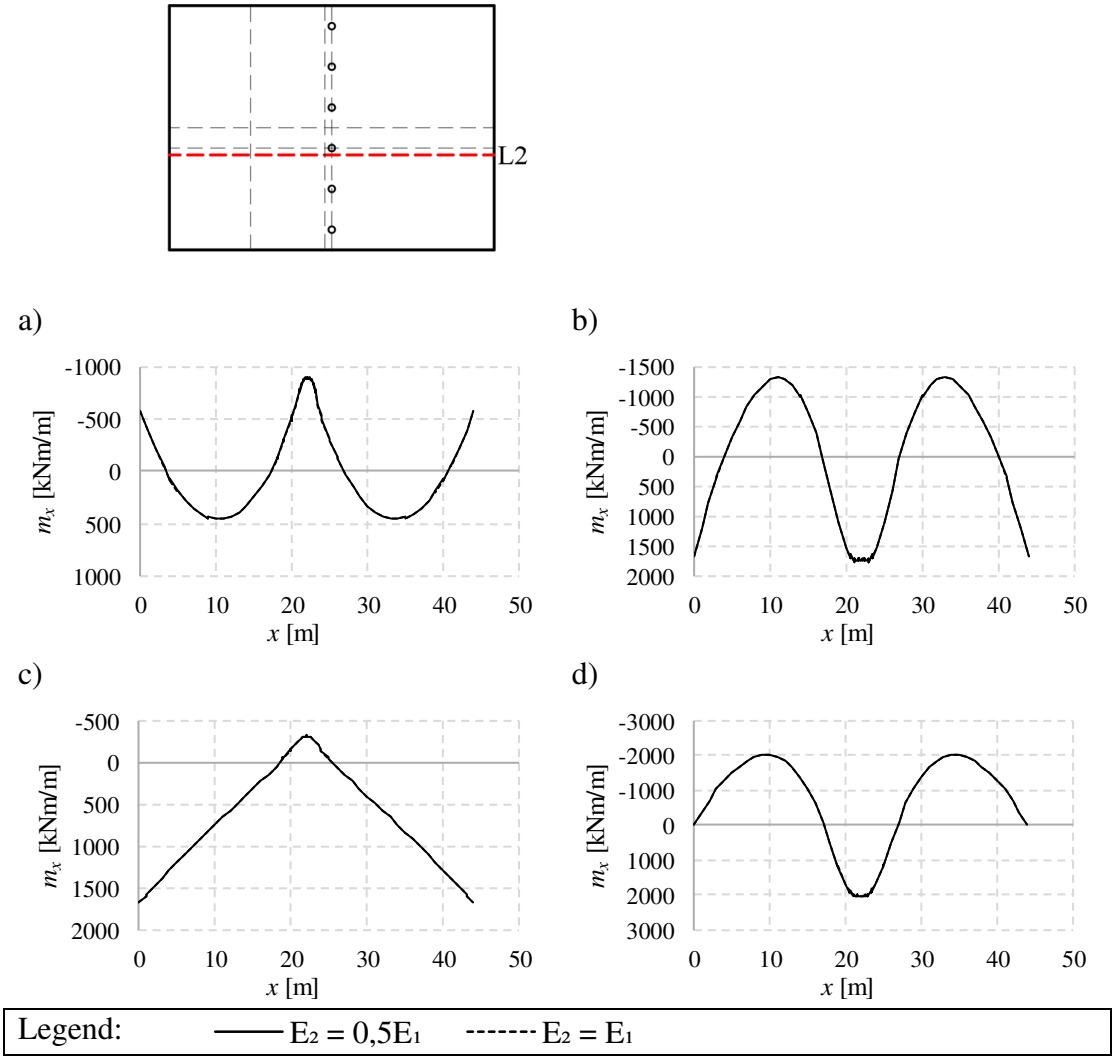

Figure H.44 Results along the section L2. a) Moment caused by the permanent load, b) resultant moment, c) restraint moment, d) primary moment

Table H.42 Comparison of the moments [kNm/m] in Figure H.44 at certain points. If no coordinate is specified, the given value is the peak value in that region. Deviation is the difference between the moments in the in the models with different stiffness.

	a	b	c	d
Stiffness	Support x=22	Support x=22	Support x=22	Support x=22
Reduced	-890	1732	-312	2044
Regular	-897	1730	-315	2044
Deviation [%]	-0.77	0.14	-0.81	-0.01
	Span	Span	Left support	Span
Reduced	455	-1320	1679	-2023
Regular	456	-1320	1680	-2022
Deviation [%]	-0.08	0.00	-0.04	0.01

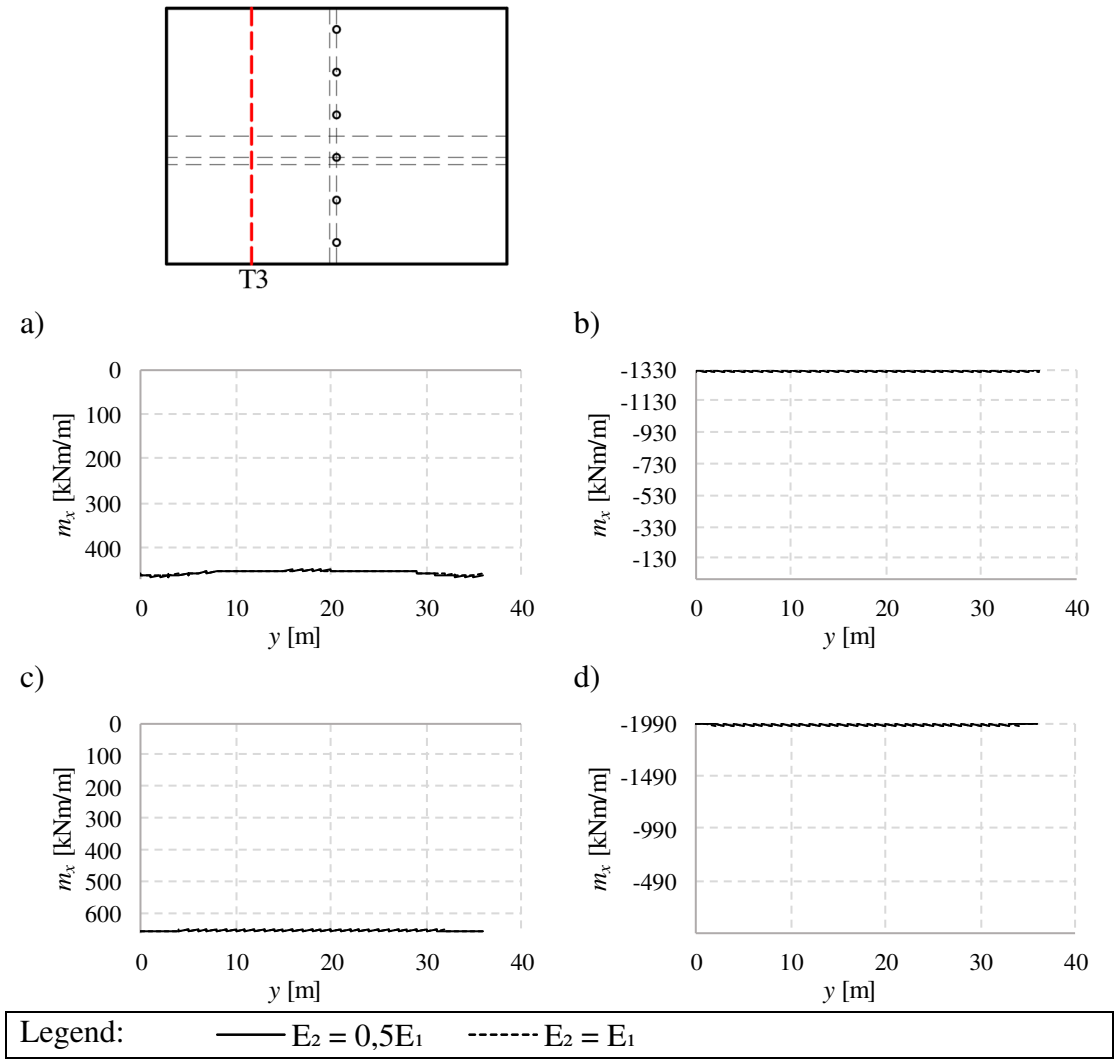

Figure H.45 Results along the section T3. a) Moment caused by the permanent load, b) resultant moment, c) restraint moment, d) primary moment

Table H.43 Comparison of the moments [kNm/m] in Figure H.45 at certain points. If no coordinate is specified, the given value is the peak value in that region. Deviation is the difference between the moments in the in the models with different stiffness.

	a	b	c	d
Stiffness	Mid y=18	Mid y=18	Mid y=18	Mid y=18
Reduced	452	-1320	657	-1977
Regular	453	-1320	656	-1977
Deviation [%]	-0.03	-0.01	0.02	0.00

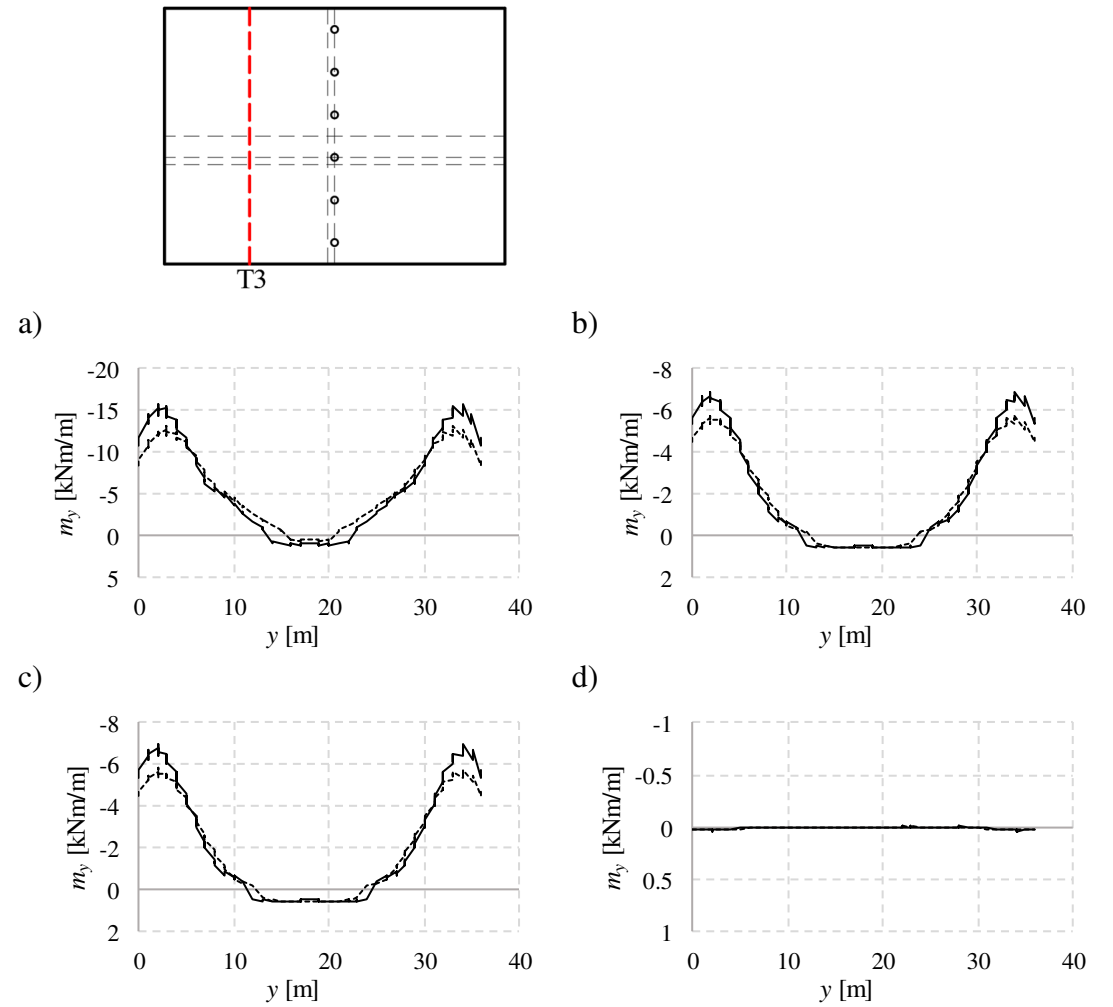

Figure H.46 Results along the section T3. a) Moment caused by the permanent load, b) resultant moment, c) restraint moment, d) primary moment

Table H.44 Comparison of the moments [kNm/m] in Figure H.46 at certain points. If no coordinate is specified, the given value is the peak value in that region. Deviation is the difference between the moments in the in the models with different stiffness.

	a	b	c	d
Stiffness	Mid y=18	Mid y=18	Mid y=18	Mid y=18
Reduced	1.0	0.5	0.5	0.0
Regular	0.5	0.6	0.6	0.0
Deviation [%]	-	-	-	-

H.6.2 Reduction with a factor of 0.1

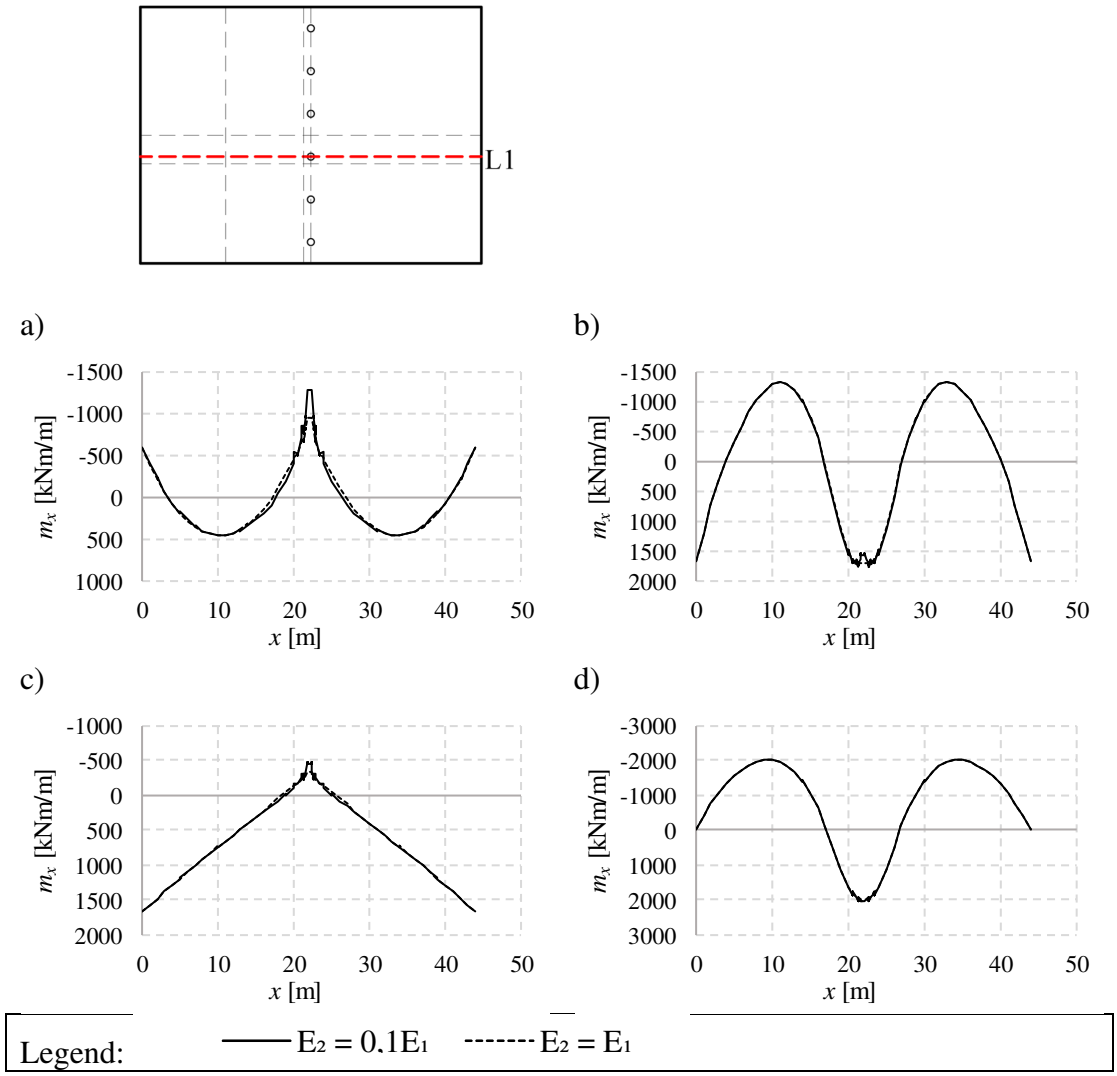

Figure H.47 Results along the section L1. a) Moment caused by the permanent load, b) resultant moment, c) restraint moment, d) primary moment

Table H.45 Comparison of the moments [kNm/m] in Figure H.47 at certain points. If no coordinate is specified, the given value is the peak value in that region. Deviation is the difference between the moments in the in the models with different stiffness.

	a	b	c	d
Stiffness	Support x=22	Support x=22	Support x=22	Support x=22
Reduced	-1272	1568	-460	2027
Regular	-950	1720	-335	2055
Deviation [%]	33.88	-8.86	37.26	-1.34
	Span	Span	Left support	Span
Reduced	456	-1319	1675	-2022
Regular	456	-1320	1680	-2022
Deviation [%]	0.03	-0.11	-0.28	-0.02

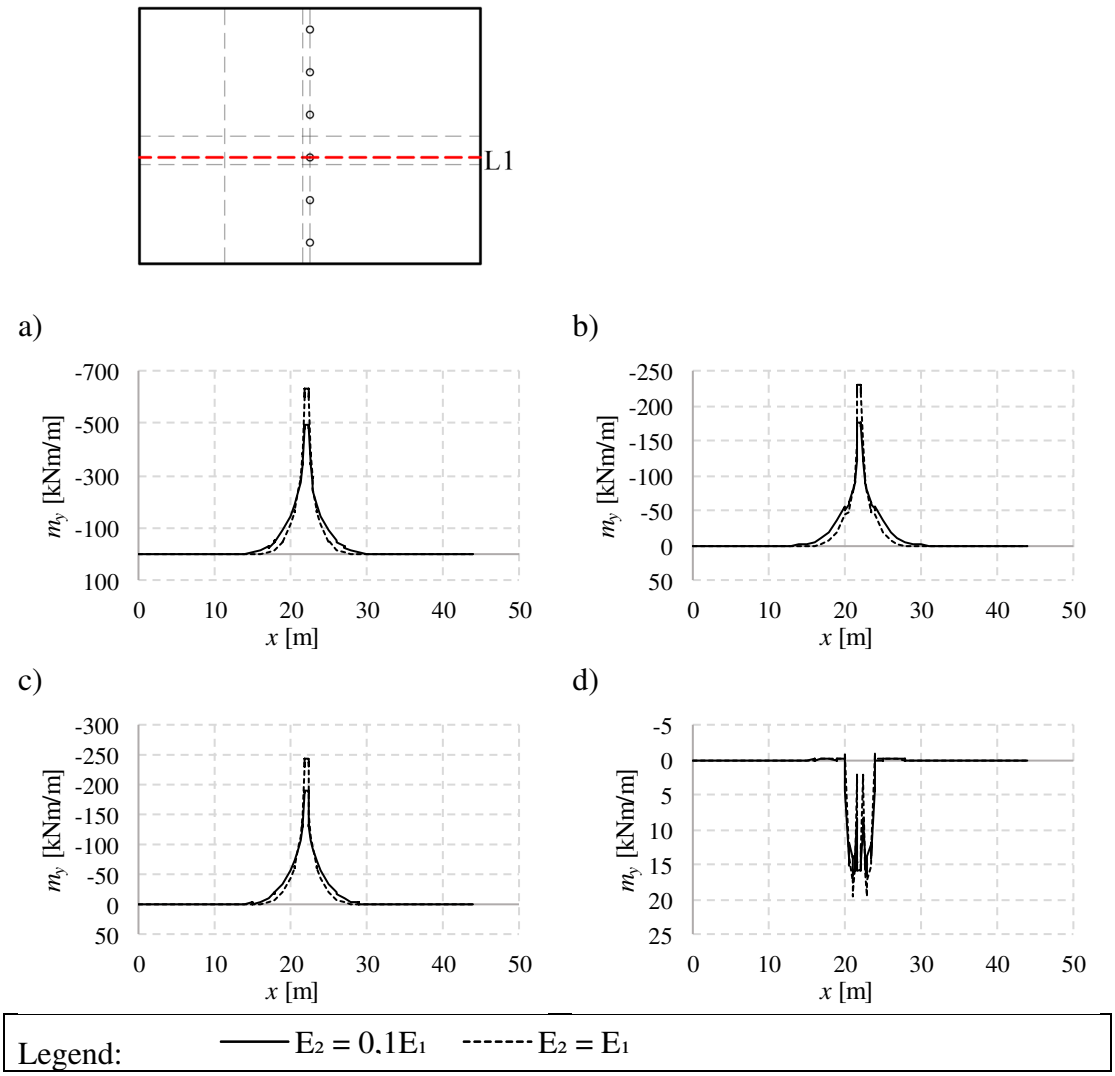

Figure H.48 Results along the section L1. a) Moment caused by the permanent load, b) resultant moment, c) restraint moment, d) primary moment

Table H.46 Comparison of the moments [kNm/m] in Figure H.48 at certain points. If no coordinate is specified, the given value is the peak value in that region. Deviation is the difference between the moments in the in the models with different stiffness.

	a	b	c	d
Stiffness	Support x=22	Support x=22	Support x=22	Support x=22
Reduced	-493	-175	-191	16
Regular	-631	-230	-245	15
Deviation [%]	-21.87	-23.88	-21.94	8.60

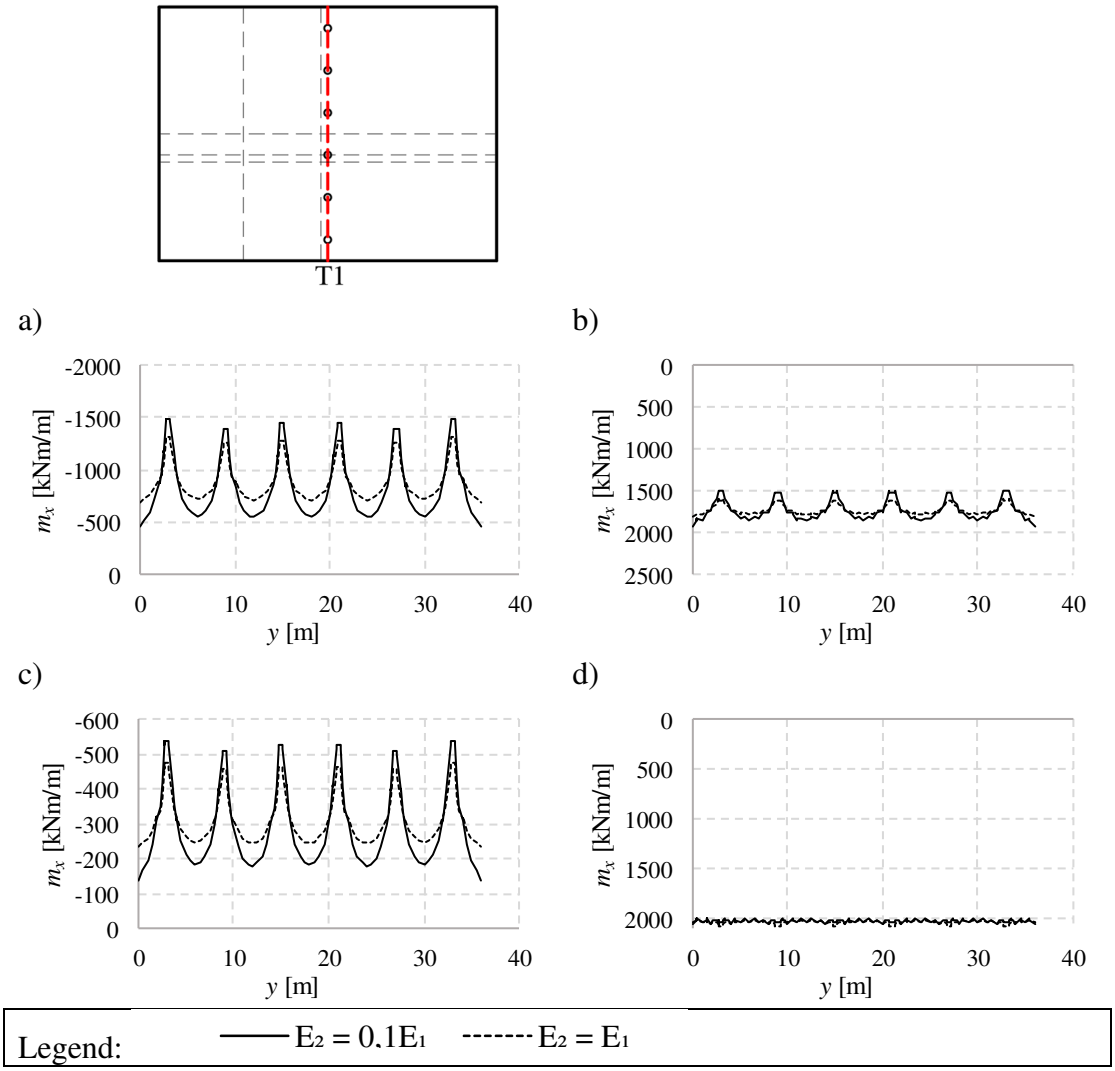

Figure H.49 Results along the section T1. a) Moment caused by the permanent load, b) resultant moment, c) restraint moment, d) primary moment

Table H.47 Comparison of the moments [kNm/m] in Figure H.49 at certain points. If no coordinate is specified, the given value is the peak value in that region. Deviation is the difference between the moments in the in the models with different stiffness.

	a	b	c	d
Stiffness	Support y=15	Support y=15	Support y=15	Support y=15
Reduced	-1445	1514	-527	2040
Regular	-1281	1617	-463	2031
Deviation [%]	12.82	-6.40	13.73	0.45
	Span y=18	Span y=18	Span y=18	-
Reduced	-557	1857	-183	-
Regular	-719	1785	-246	-
Deviation [%]	-22.58	4.03	-25.56	-

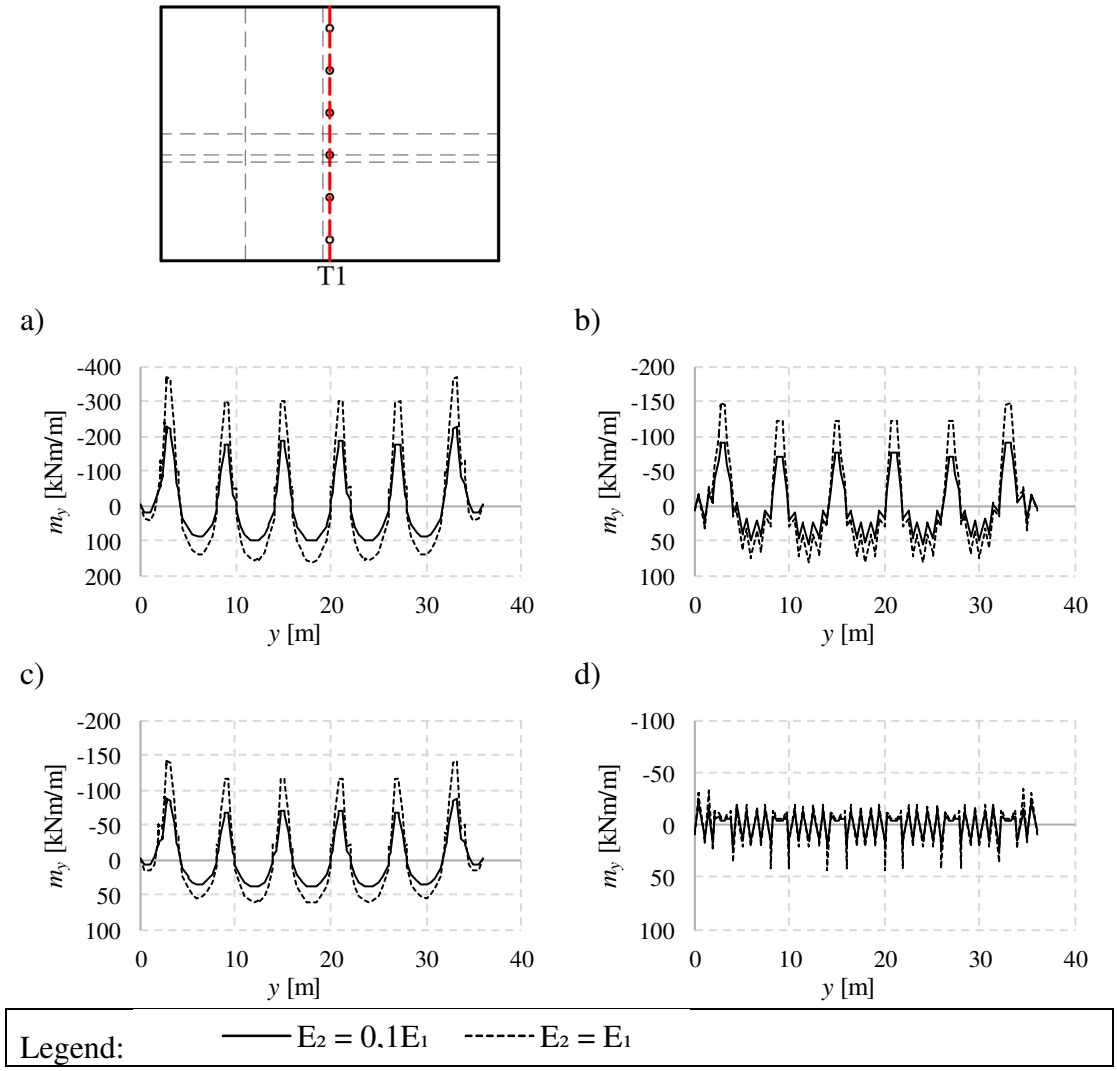

Figure H.50 Results along the section T1. a) Moment caused by the permanent load, b) resultant moment, c) restraint moment, d) primary moment

Table H.48 Comparison of the moments [kNm/m] in Figure H.50 at certain points. If no coordinate is specified, the given value is the peak value in that region. Deviation is the difference between the moments in the in the models with different stiffness.

	a	b	c	d
Stiffness	Support y=15	Support y=15	Support y=15	Support y=15
Reduced	-185	-75	-72	15
Regular	-303	-123	-117	20
Deviation [%]	-38.94	-38.78	-38.98	-26.31
	Span y=18	Span y=18	Span y=18	-
Reduced	100	53	39	-
Regular	159	81	62	-
Deviation [%]	-36.96	-34.44	-37.05	-

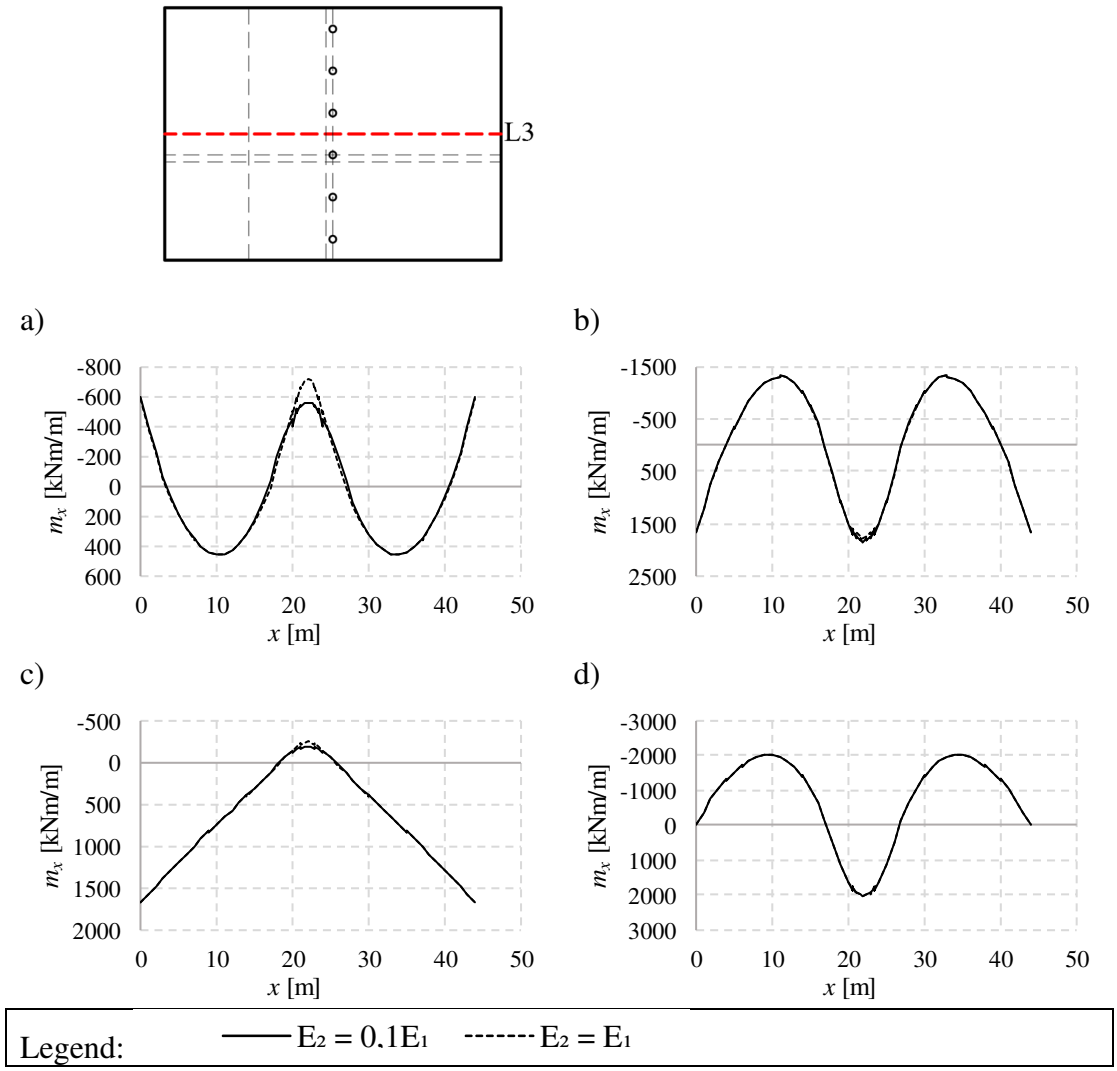

Figure H.51 Results along the section L3. a) Moment caused by the permanent load, b) resultant moment, c) restraint moment, d) primary moment

Table H.49 Comparison of the moments [kNm/m] in Figure H.51 at certain points. If no coordinate is specified, the given value is the peak value in that region. Deviation is the difference between the moments in the in the models with different stiffness.

	a	b	c	d
Stiffness	Support x=22	Support x=22	Support x=22	Support x=22
Reduced	-557	1857	-183	2040
Regular	-719	1785	-246	2031
Deviation [%]	-22.58	4.03	-25.56	0.45
	Span	Span	Left support	Span
Reduced	456	-1320	1675	-2022
Regular	455	-1320	1680	-2022
Deviation [%]	0.22	-0.05	-0.30	0.00

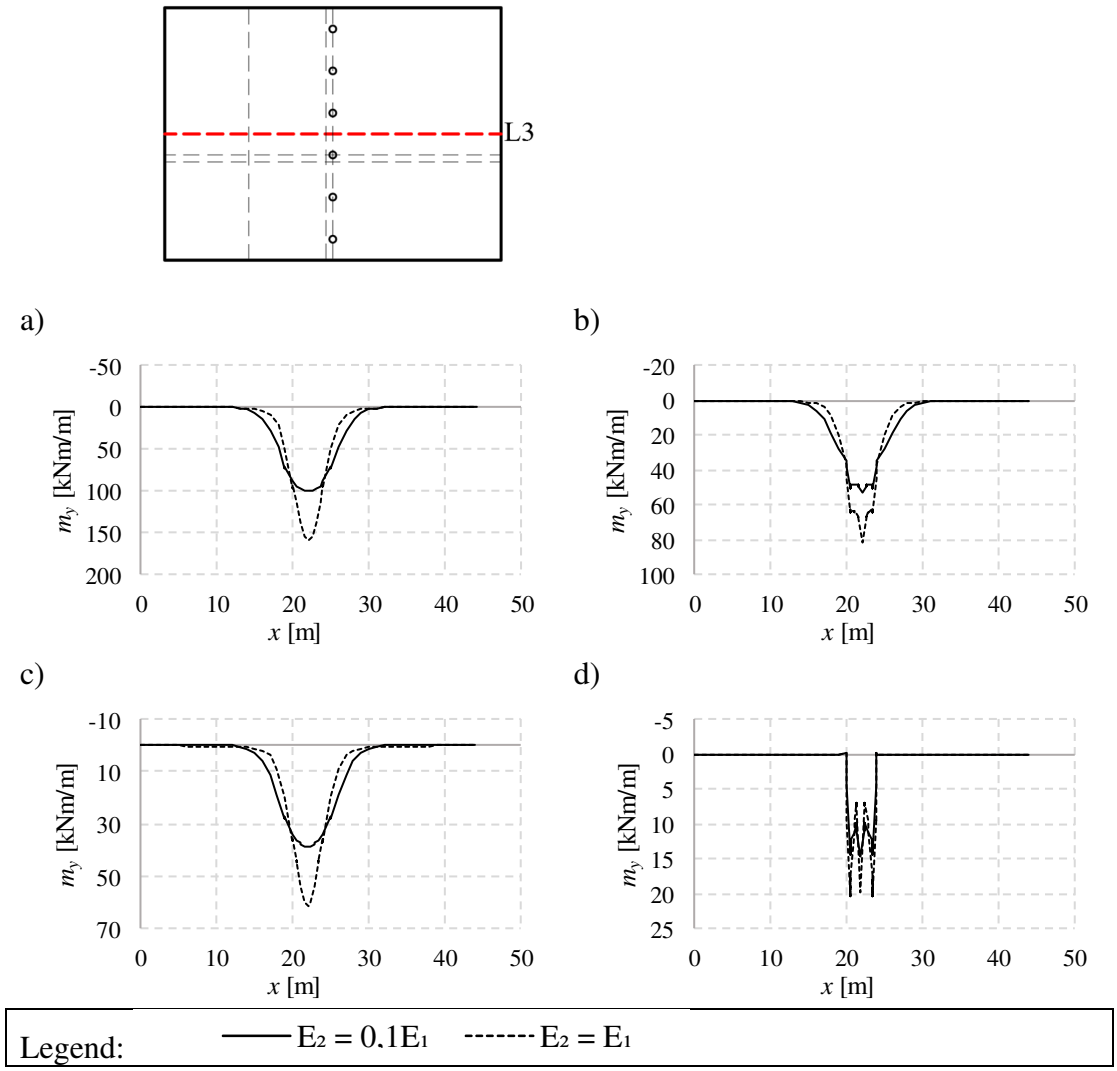

Figure H.52 Results along the section L3. a) Moment caused by the permanent load, b) resultant moment, c) restraint moment, d) primary moment

Table H.50 Comparison of the moments [kNm/m] in Figure H.52 at certain points. If no coordinate is specified, the given value is the peak value in that region. Deviation is the difference between the moments in the in the models with different stiffness.

	a	b	c	d
Stiffness	Support x=22	Support x=22	Support x=22	Support x=22
Reduced	100	53	39	15
Regular	159	81	62	20
Deviation [%]	-36.96	-34.44	-37.05	-26.31

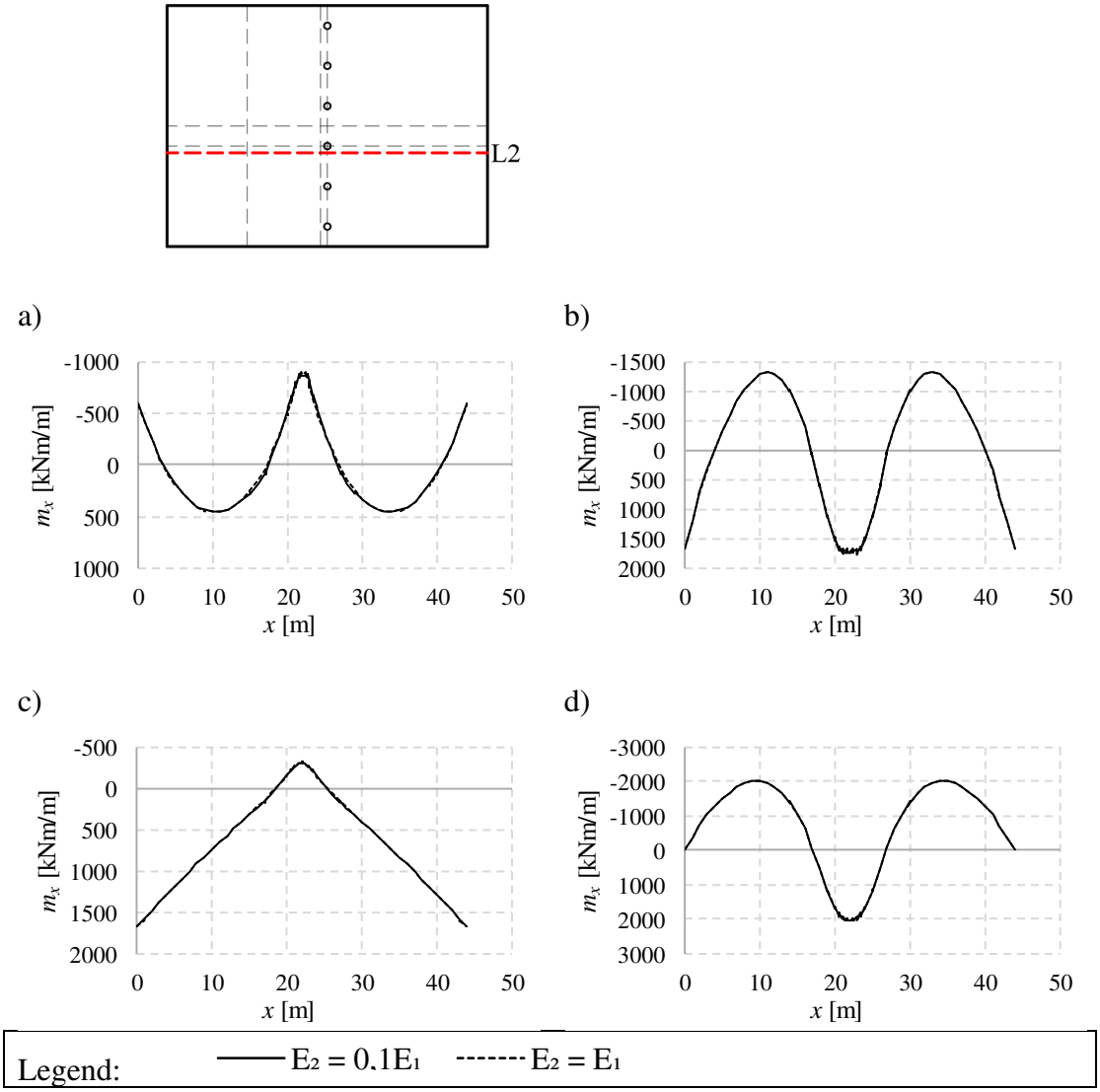

Figure H.53 Results along the section L2. a) Moment caused by the permanent load, b) resultant moment, c) restraint moment, d) primary moment

Table H.51 Comparison of the moments [kNm/m] in Figure H.53 at certain points. If no coordinate is specified, the given value is the peak value in that region. Deviation is the difference between the moments in the in the models with different stiffness.

	a	b	c	d
Stiffness	Support x=22	Support x=22	Support x=22	Support x=22
Reduced	-868	1744	-304	2047
Regular	-897	1730	-315	2044
Deviation [%]	-3.31	0.83	-3.58	0.15
	Span	Span	Left support	Span
Reduced	455	-1320	1675	-2022
Regular	456	-1320	1680	-2022
Deviation [%]	-0.18	-0.07	-0.28	-0.01

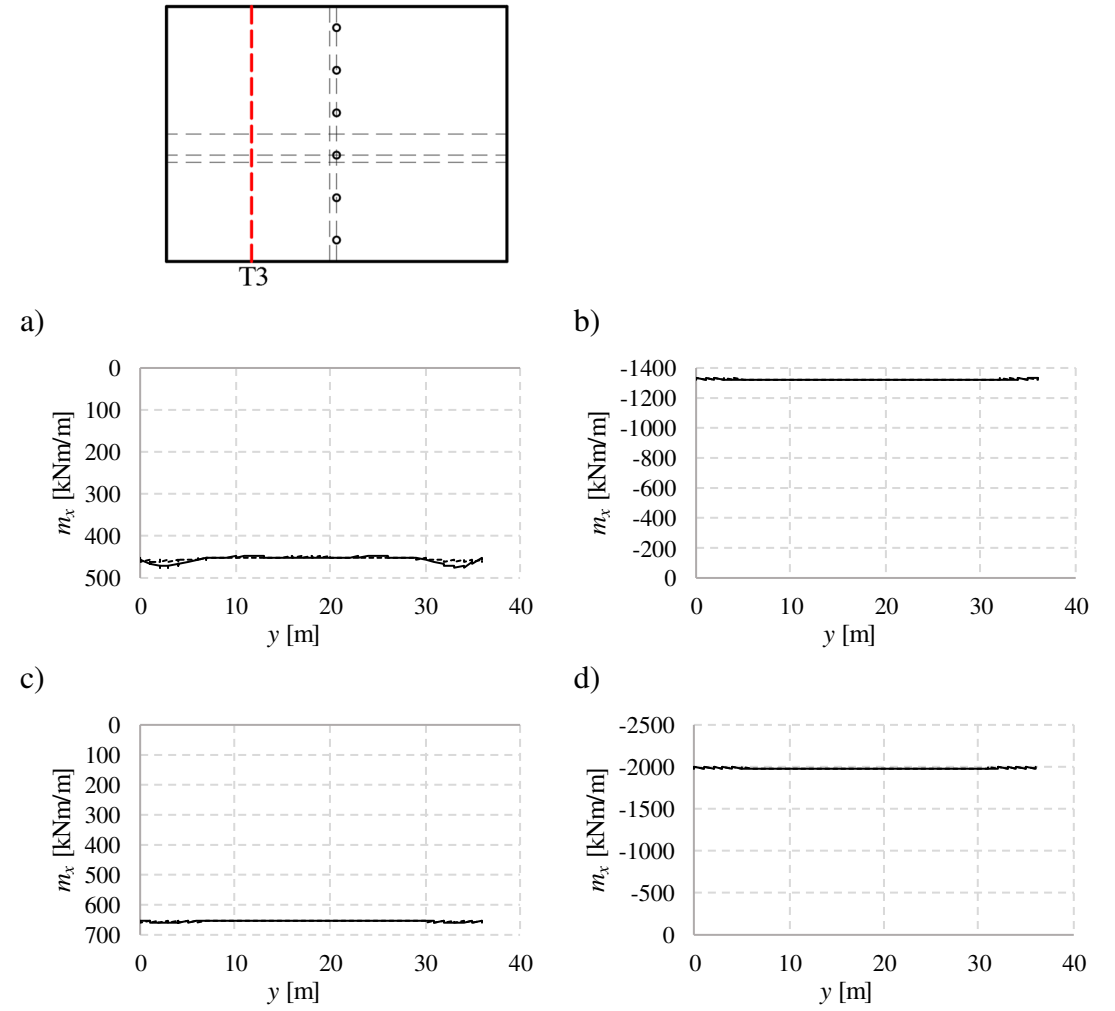

Figure H.54 Results along the section T3. a) Moment caused by the permanent load, b) resultant moment, c) restraint moment, d) primary moment

Table H.52 Comparison of the moments [kNm/m] in Figure H.54 at certain points. If no coordinate is specified, the given value is the peak value in that region. Deviation is the difference between the moments in the in the models with different stiffness.

	a	b	c	d
Stiffness	Mid y=18	Mid y=18	Mid y=18	Mid y=18
Reduced	455	-1320	658	-1977
Regular	453	-1320	656	-1977
Deviation [%]	0.52	-0.06	0.17	-0.01

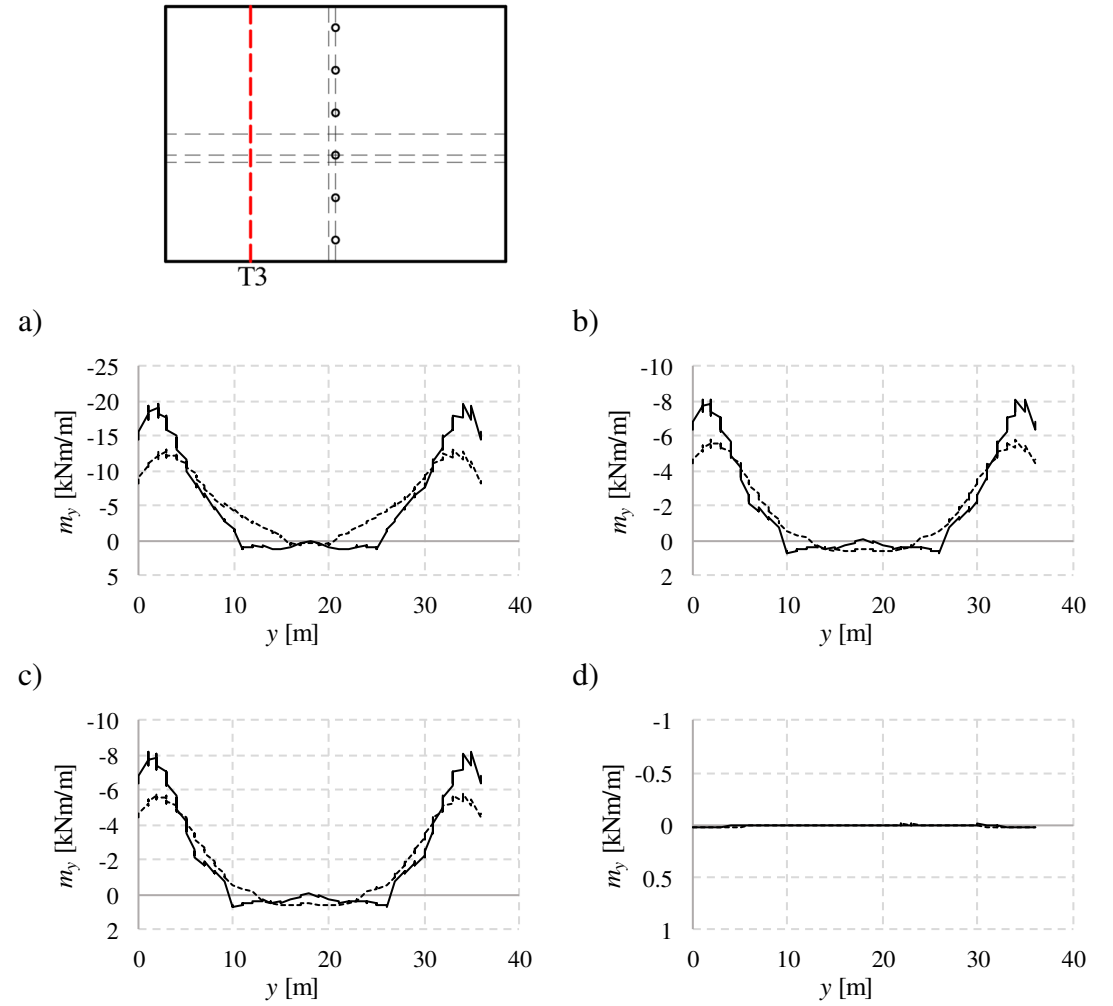

Figure H.55 Results along the section T3. a) Moment caused by the permanent load, b) resultant moment, c) restraint moment, d) primary moment

Table H.53 Comparison of the moments [kNm/m] in Figure H.55 at certain points. If no coordinate is specified, the given value is the peak value in that region. Deviation is the difference between the moments in the in the models with different stiffness.

	a	b	c	d
Stiffness	Mid y=18	Mid y=18	Mid y=18	Mid y=18
Reduced	0.9	-0.1	-0.1	0.0
Regular	0.5	0.6	0.6	0.0
Deviation [%]	-	-	-	-

H.6.3 Reduction using property modifiers

M22

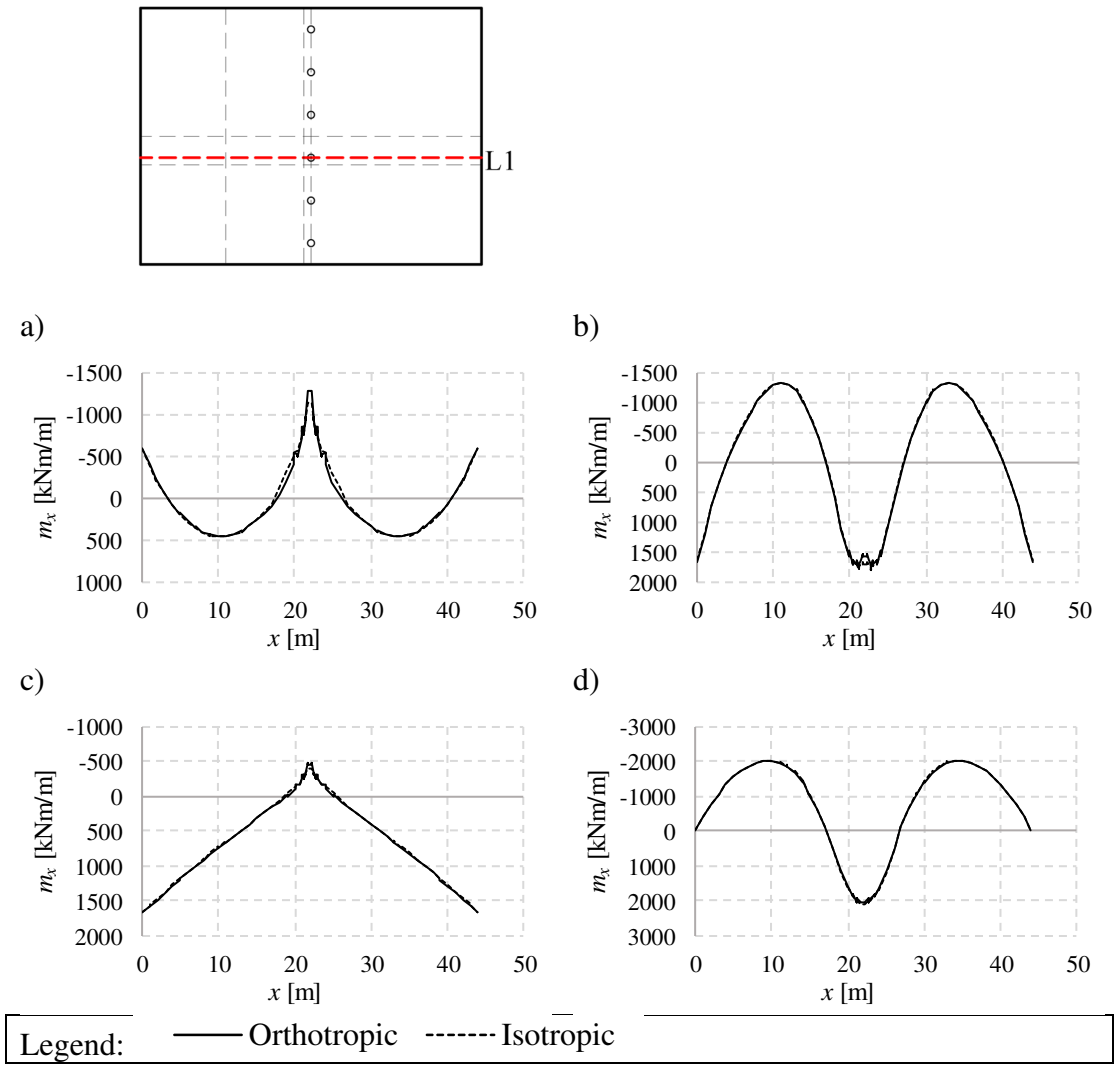

Figure H.56 Results along the section L1. a) Moment caused by the permanent load, b) resultant moment, c) restraint moment, d) primary moment

Table H.54 Comparison of the moments [kNm/m] in Figure H.56 at certain points. If no coordinate is specified, the given value is the peak value in that region. Deviation is the difference between the moment in the models using orthotropic or isotropic material.

	a	b	c	d
Material	Support x=22	Support x=22	Support x=22	Support x=22
Orthotropic	-1272	1568	-460	2027
Isotropic	-1129	1714	-391	2106
Deviation [%]	12.65	-8.55	17.43	-3.72
	Span	Span	Left support	Span
Orthotropic	456	-1319	1675	-2022
Isotropic	465	-1325	1658	-2025
Deviation [%]	-1.95	-0.44	1.03	-0.14

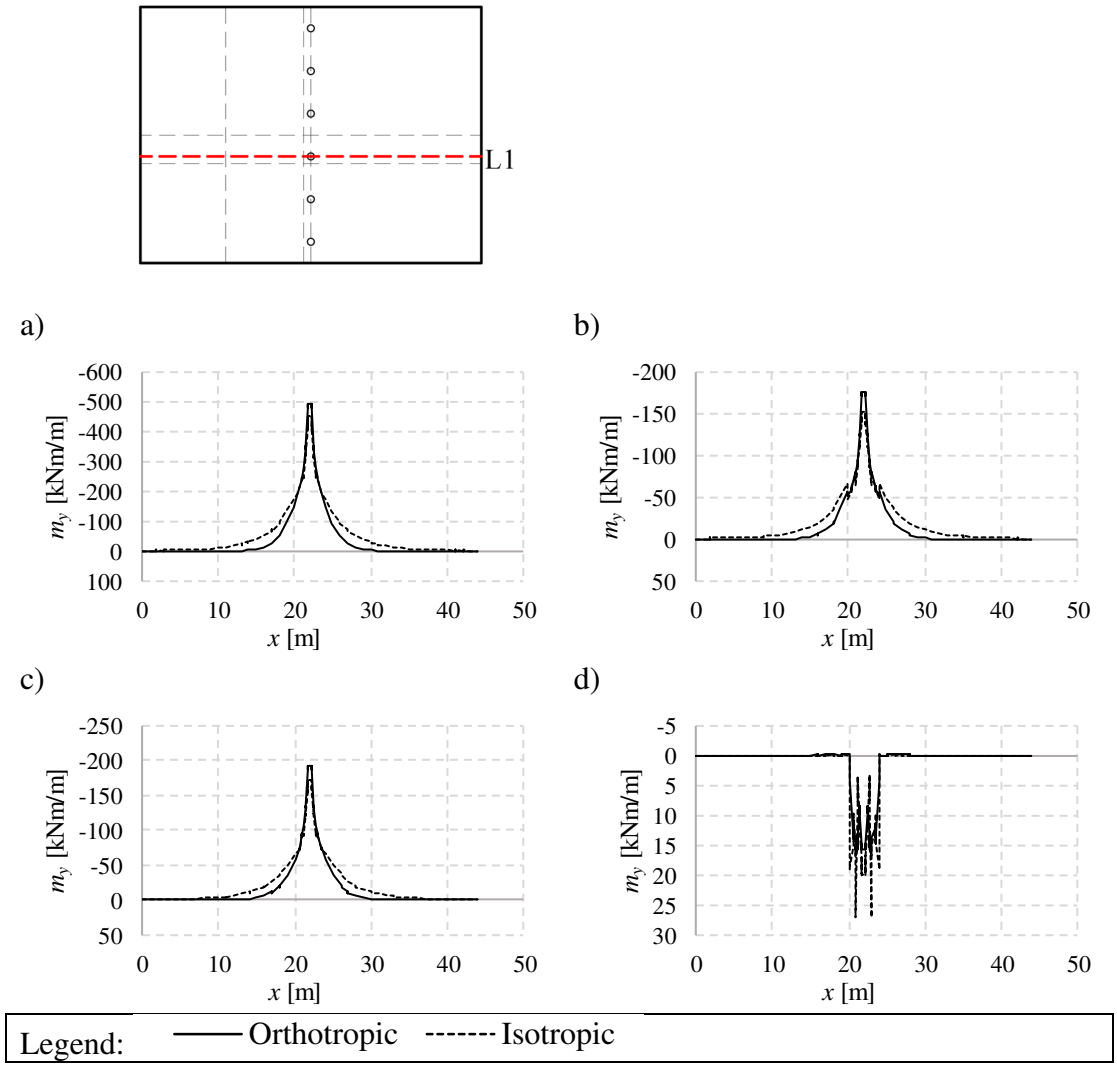

Figure H.57 Results along the section L1. a) Moment caused by the permanent load, b) resultant moment, c) restraint moment, d) primary moment

Table H.55 Comparison of the moments [kNm/m] in Figure H.57 at certain points. If no coordinate is specified, the given value is the peak value in that region. Deviation is the difference between the moment in the models using orthotropic or isotropic material.

	a	b	c	d
Material	Support x=22	Support x=22	Support x=22	Support x=22
Orthotropic	-493	-175	-191	16
Isotropic	-449	-151	-171	20
Deviation [%]	9.88	16.24	11.86	-21.07

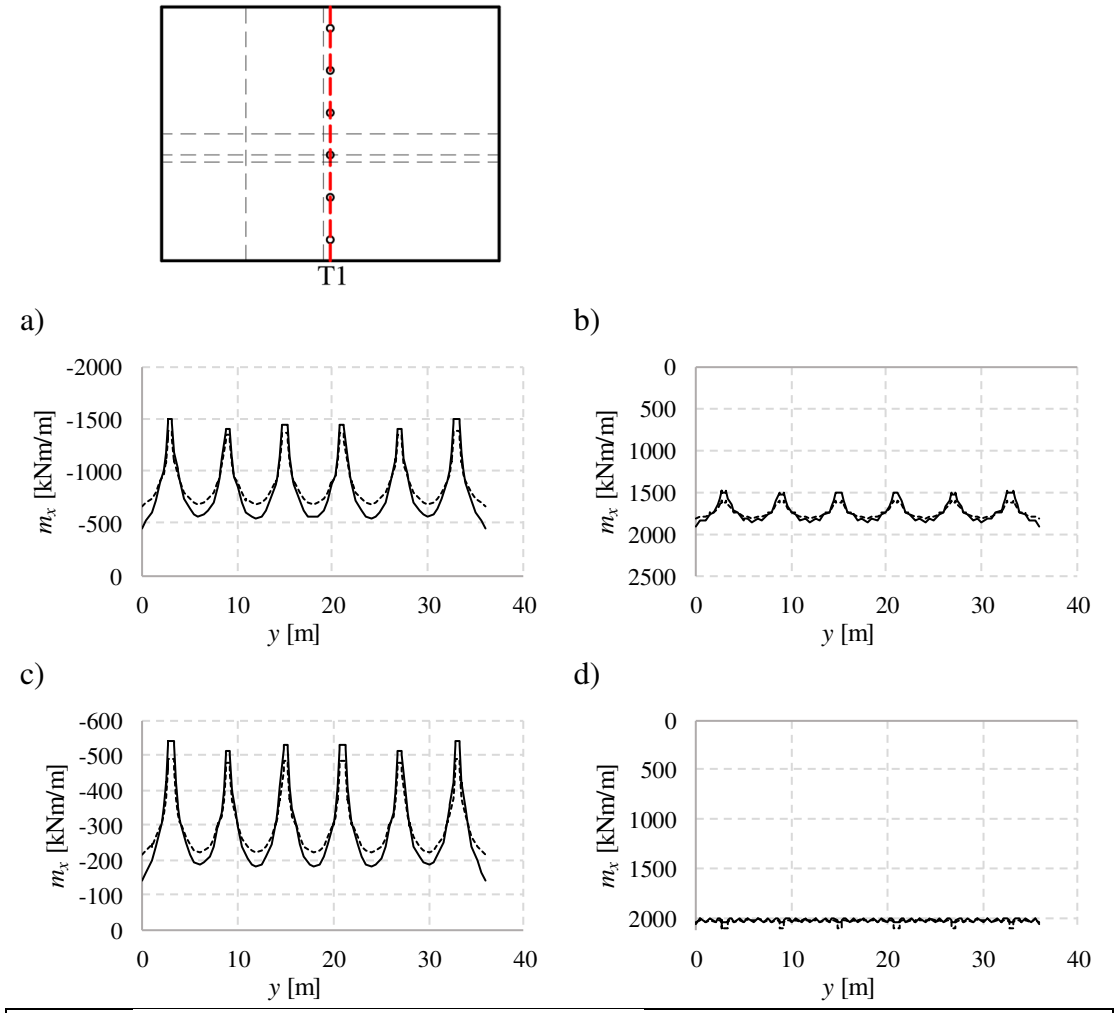

Figure H.58 Results along the section T1. a) Moment caused by the permanent load, b) resultant moment, c) restraint moment, d) primary moment

Table H.56 Comparison of the moments [kNm/m] in Figure H.58 at certain points. If no coordinate is specified, the given value is the peak value in that region. Deviation is the difference between the moment in the models using orthotropic or isotropic material.

	a	b	c	d
Material	Support y=15	Support y=15	Support y=15	Support y=15
Orthotropic	-1445	1514	-527	2040
Isotropic	-1368	1624	-483	2034
Deviation [%]	5.63	-6.82	9.20	0.29
	Span y=18	Span y=18	Span y=18	-
Orthotropic	-557	1857	-183	-
Isotropic	-682	1812	-222	-
Deviation [%]	-18.35	2.45	-17.44	-

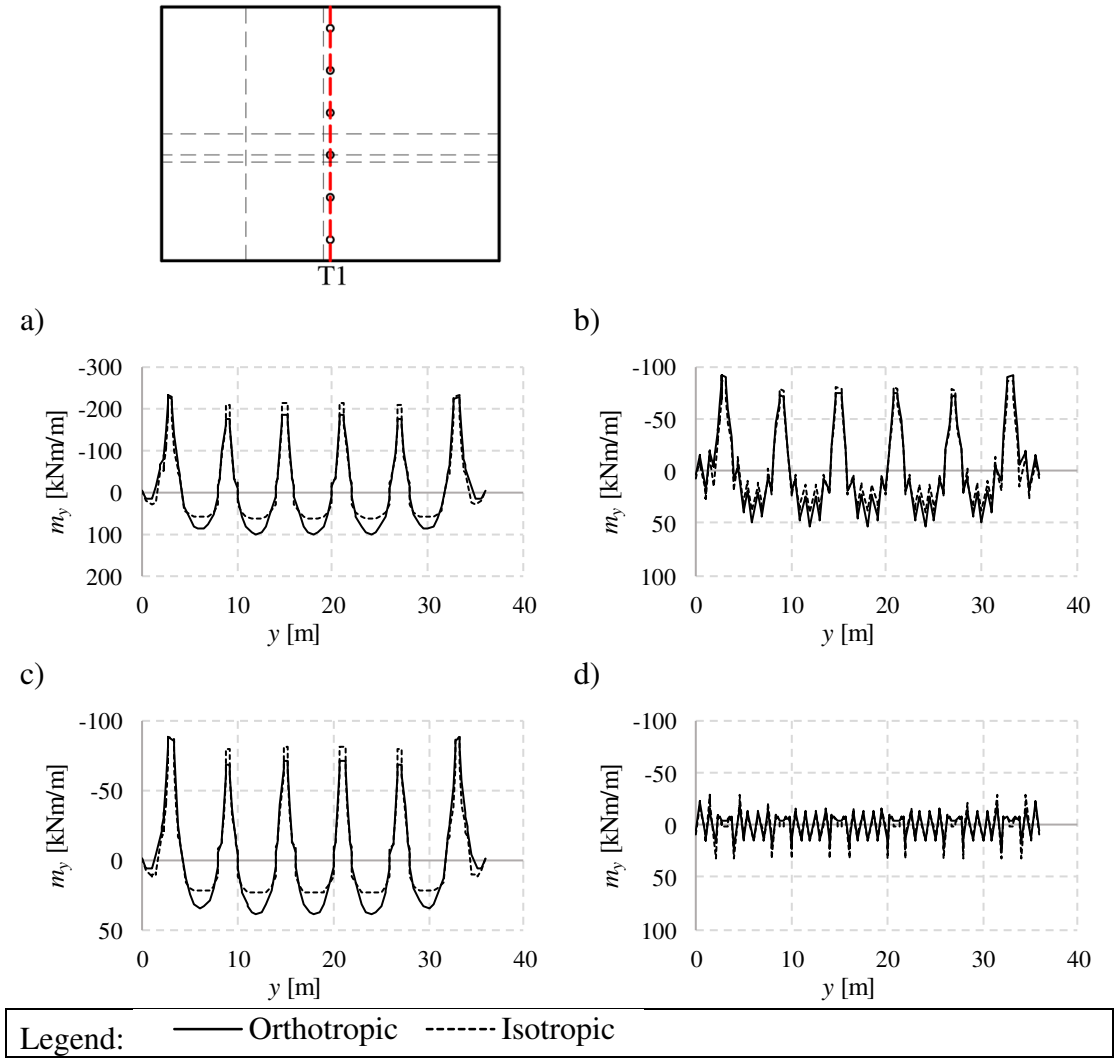

Figure H.59 Results along the section T1. a) Moment caused by the permanent load, b) resultant moment, c) restraint moment, d) primary moment

Table H.57 Comparison of the moments [kNm/m] in Figure H.59 at certain points. If no coordinate is specified, the given value is the peak value in that region. Deviation is the difference between the moment in the models using orthotropic or isotropic material.

	a	b	c	d
Material	Support y=15	Support y=15	Support y=15	Support y=15
Orthotropic	-185	-75	-72	15
Isotropic	-213	-79	-81	15
Deviation [%]	-13.13	-4.95	-11.55	-1.57
	Span y=18	Span y=18	Span y=18	-
Orthotropic	100	53	39	-
Isotropic	62	39	24	-
Deviation [%]	60.44	38.24	63.12	-

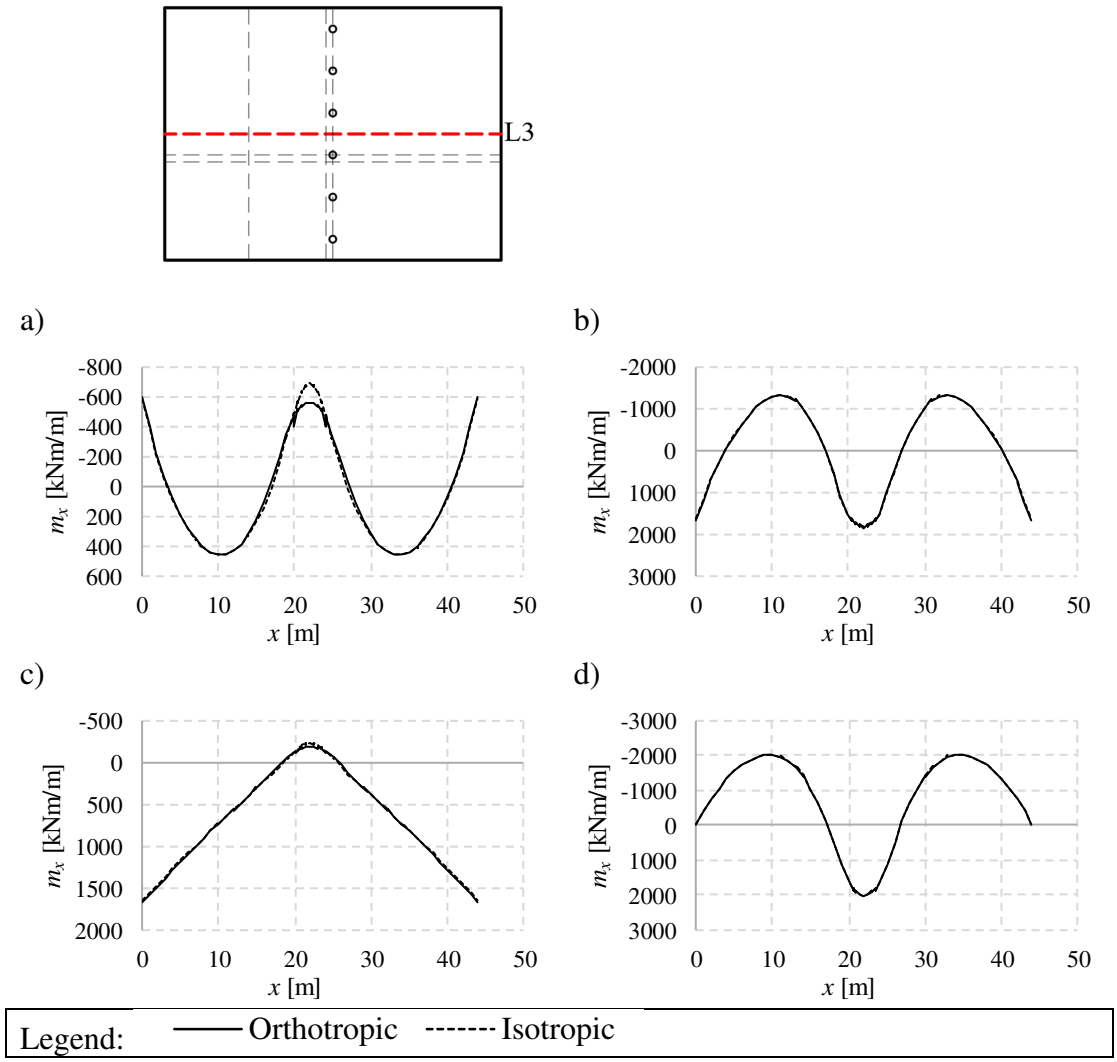

Figure H.60 Results along the section L3. a) Moment caused by the permanent load, b) resultant moment, c) restraint moment, d) primary moment

Table H.58 Comparison of the moments [kNm/m] in Figure H.60 at certain points. If no coordinate is specified, the given value is the peak value in that region. Deviation is the difference between the moment in the models using orthotropic or isotropic material.

	a	b	c	d
Material	Support x=22	Support x=22	Support x=22	Support x=22
Orthotropic	-557	1857	-183	2040
Isotropic	-682	1812	-222	2034
Deviation [%]	-18.35	2.45	-17.44	0.29
	Span	Span	Left support	Span
Orthotropic	456	-1320	1675	-2022
Isotropic	458	-1328	1657	-2025
Deviation [%]	-0.50	-0.61	1.10	-0.13

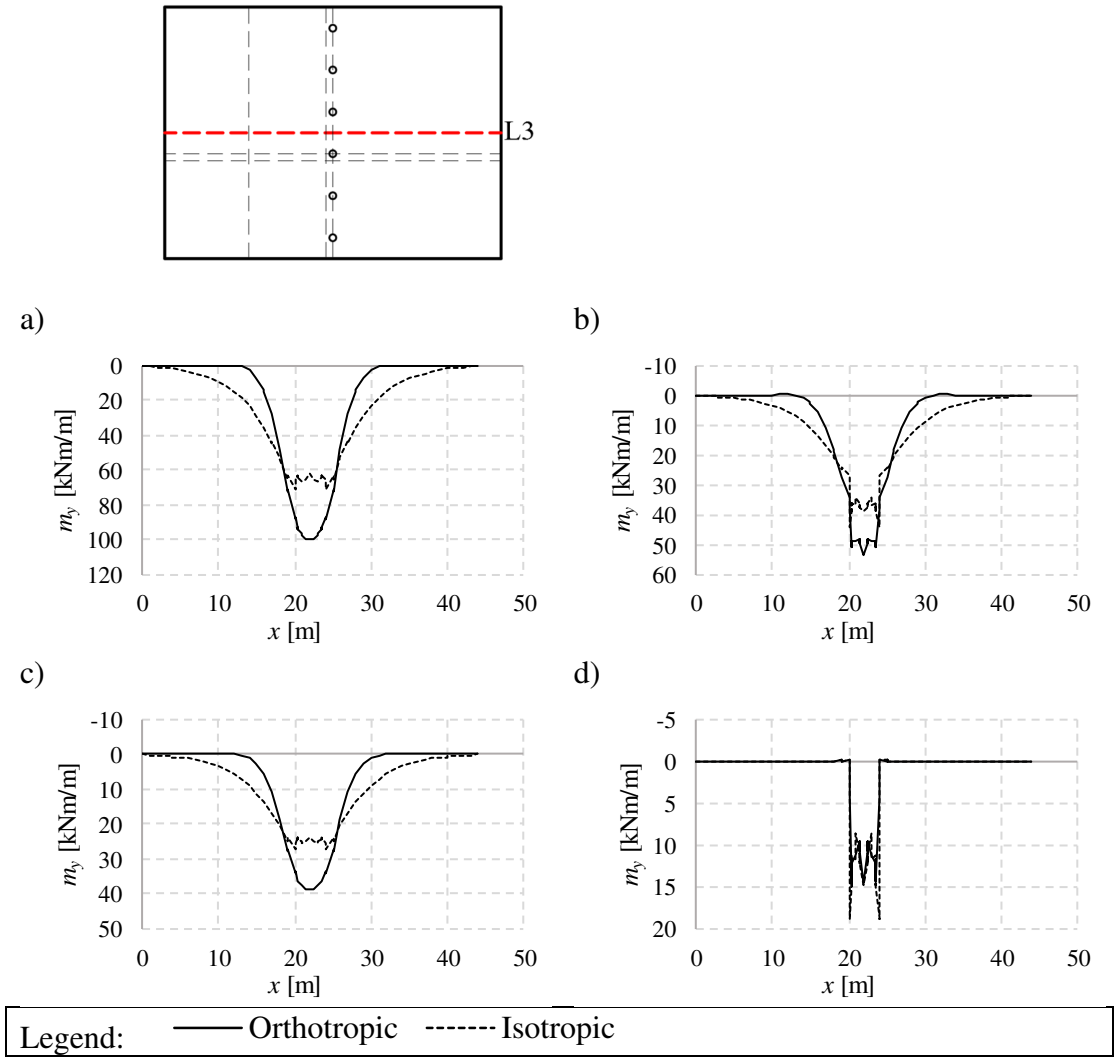

Figure H.61 Results along the section L3. a) Moment caused by the permanent load, b) resultant moment, c) restraint moment, d) primary moment

Table H.59 Comparison of the moments [kNm/m] in Figure H.61 at certain points. If no coordinate is specified, the given value is the peak value in that region. Deviation is the difference between the moment in the models using orthotropic or isotropic material.

	a	b	c	d
Material	Support x=22	Support x=22	Support x=22	Support x=22
Orthotropic	100	53	39	15
Isotropic	62	39	24	15
Deviation [%]	60.44	38.24	63.12	-1.57

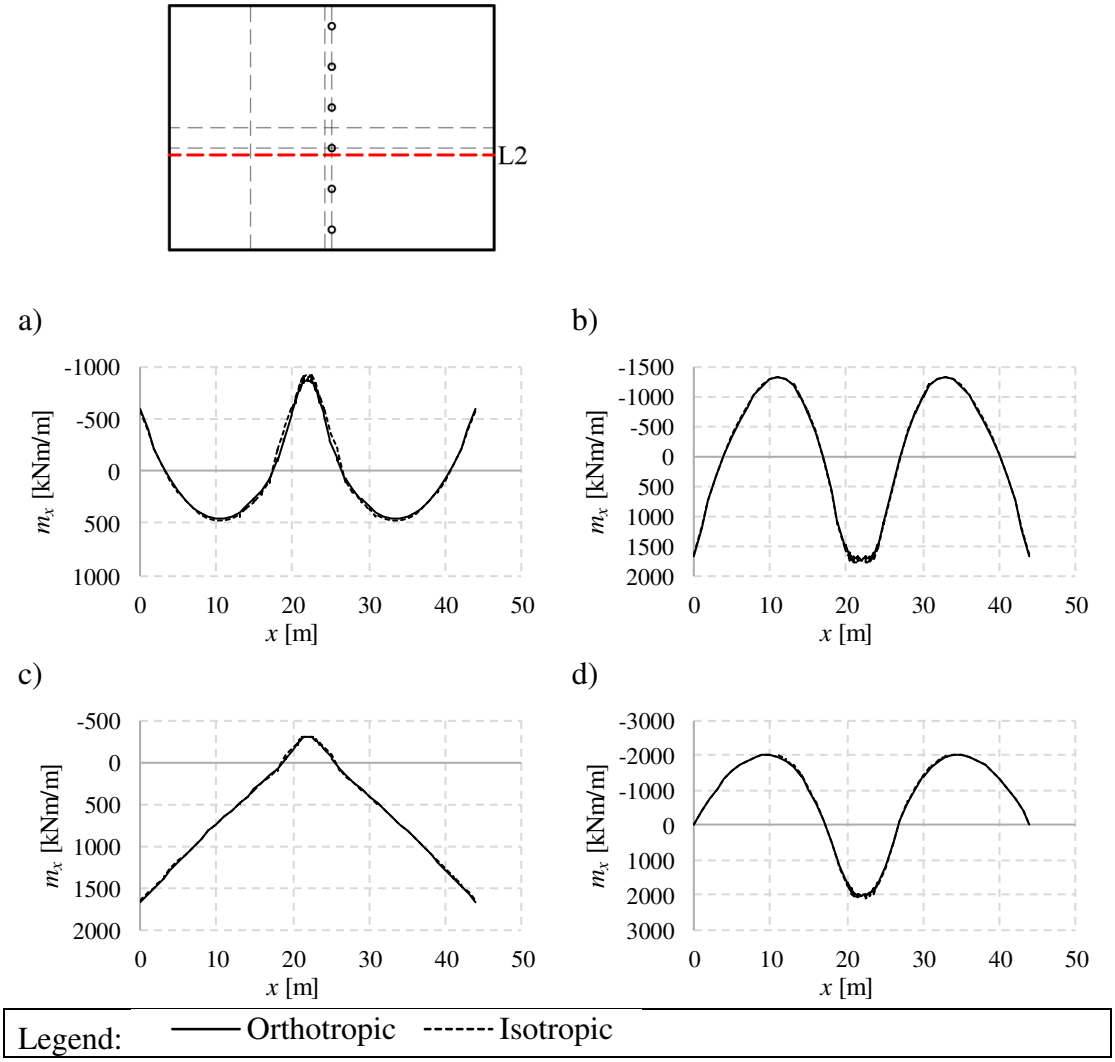

Figure H.62 Results along the section L2. a) Moment caused by the permanent load, b) resultant moment, c) restraint moment, d) primary moment

Table H.60 Comparison of the moments [kNm/m] in Figure H.62 at certain points. If no coordinate is specified, the given value is the peak value in that region. Deviation is the difference between the moment in the models using orthotropic or isotropic material.

	a	b	c	d
Material	Support x=22	Support x=22	Support x=22	Support x=22
Orthotropic	-868	1744	-304	2047
Isotropic	-899	1746	-304	2050
Deviation [%]	-3.45	-0.11	-0.20	-0.12
	Span	Span	Left support	Span
Orthotropic	455	-1320	1675	-2022
Isotropic	475	-1331	1658	-2032
Deviation [%]	-4.14	-0.83	1.05	-0.50

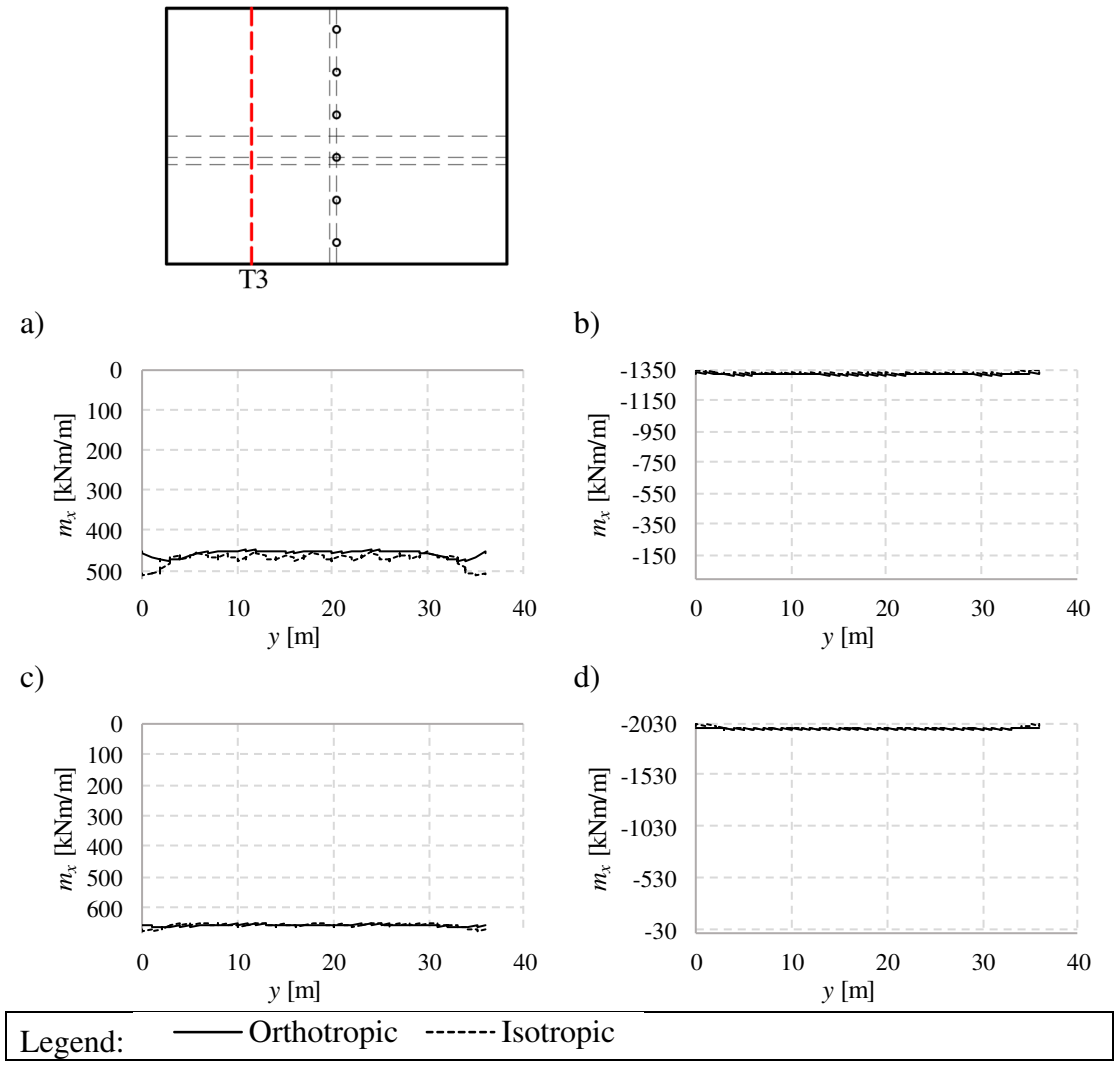

Figure H.63 Results along the section T3. a) Moment caused by the permanent load, b) resultant moment, c) restraint moment, d) primary moment

Table H.61 Comparison of the moments [kNm/m] in Figure H.63 at certain points. If no coordinate is specified, the given value is the peak value in that region. Deviation is the difference between the moment in the models using orthotropic or isotropic material.

	a	b	c	d
Material	Mid y=18	Mid y=18	Mid y=18	Mid y=18
Orthotropic	455	-1320	658	-1977
Isotropic	475	-1332	659	-1990
Deviation [%]	-4.18	-0.92	-0.28	-0.67

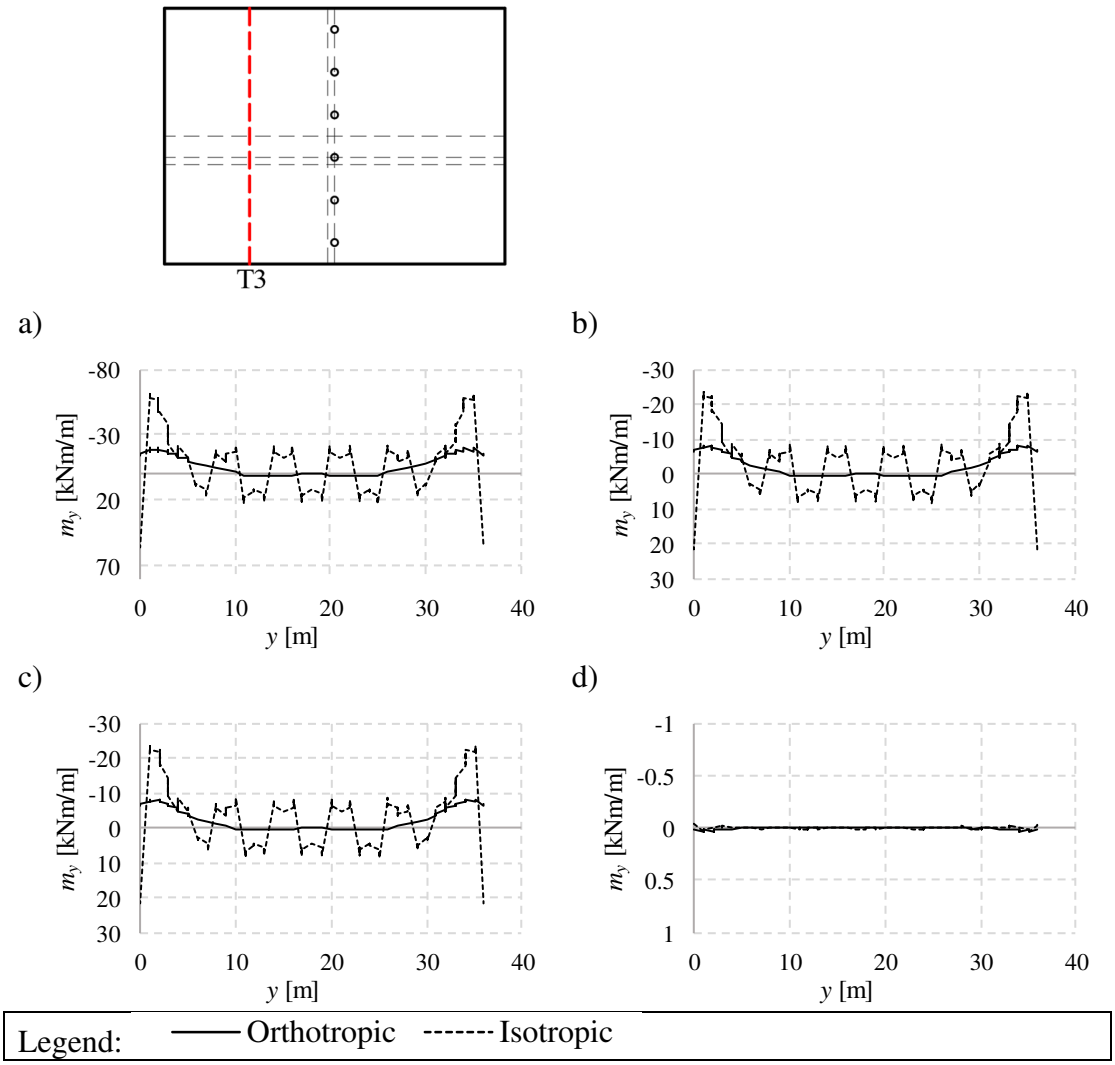

Figure H.64 Results along the section T3. a) Moment caused by the permanent load, b) resultant moment, c) restraint moment, d) primary moment

Table H.62 Comparison of the moments [kNm/m] in Figure H.64 at certain points. If no coordinate is specified, the given value is the peak value in that region. Deviation is the difference between the moment in the models using orthotropic or isotropic material.

	a	b	c	d
Material	Mid y=18	Mid y=18	Mid y=18	Mid y=18
Orthotropic	0.9	-0.1	-0.1	0.0
Isotropic	21.1	8.0	8.0	0.0
Deviation [%]	-	-	-	-

M22 and M12

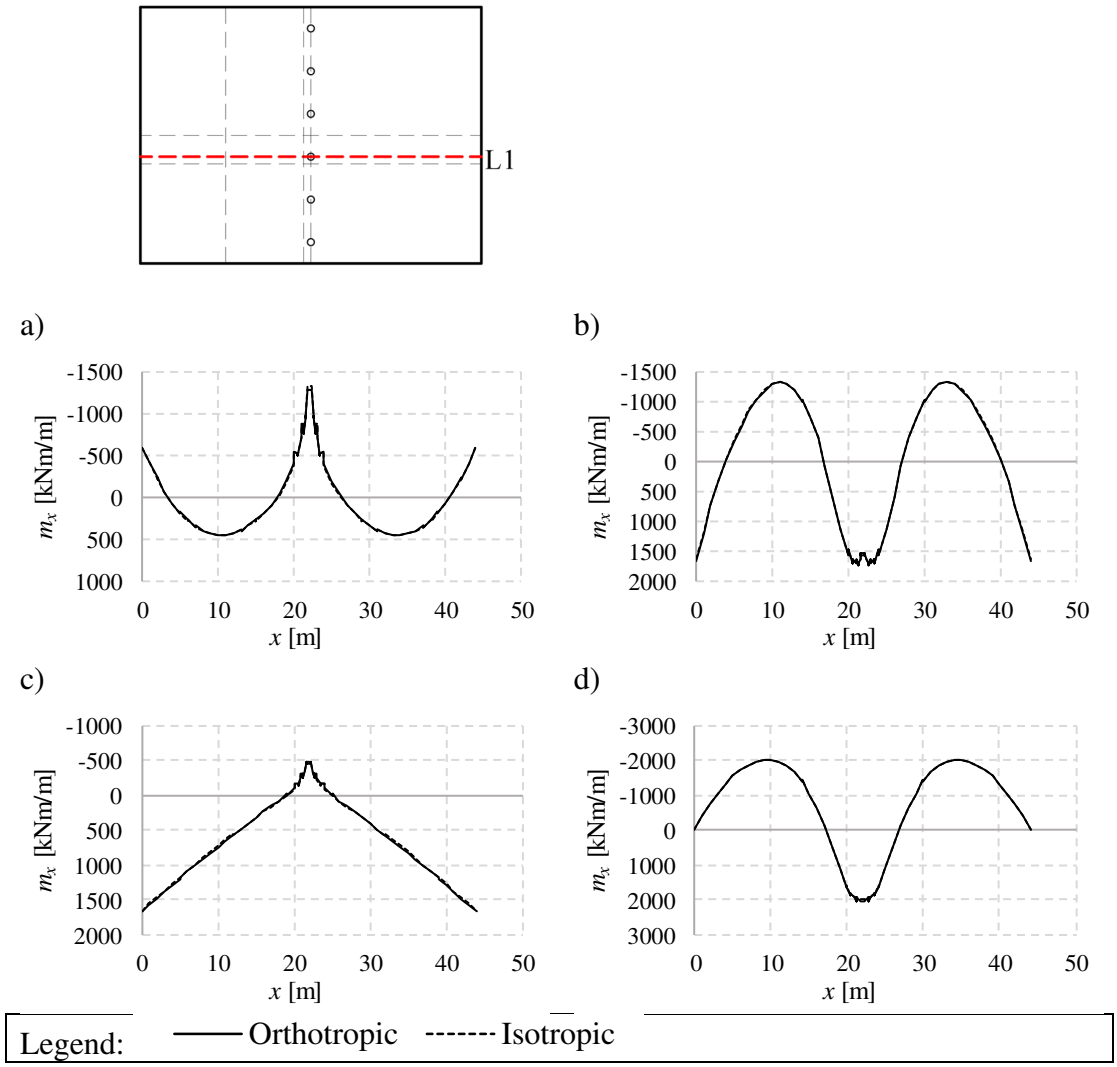

Figure H.65 Results along the section L1. a) Moment caused by the permanent load, b) resultant moment, c) restraint moment, d) primary moment

Table H.63 Comparison of the moments [kNm/m] in Figure H.65at certain points. If no coordinate is specified, the given value is the peak value in that region. Deviation is the difference between the moment in the models using orthotropic or isotropic material.

	a	b	c	d
Material	Support x=22	Support x=22	Support x=22	Support x=22
Orthotropic	-1272	1568	-460	2027
Isotropic	-1321	1544	-465	2009
Deviation [%]	-3.71	1.53	-1.03	0.94
	Span	Span	Left support	Span
Orthotropic	456	-1319	1675	-2022
Isotropic	456	-1325	1655	-2022
Deviation [%]	-0.11	-0.45	1.21	0.00

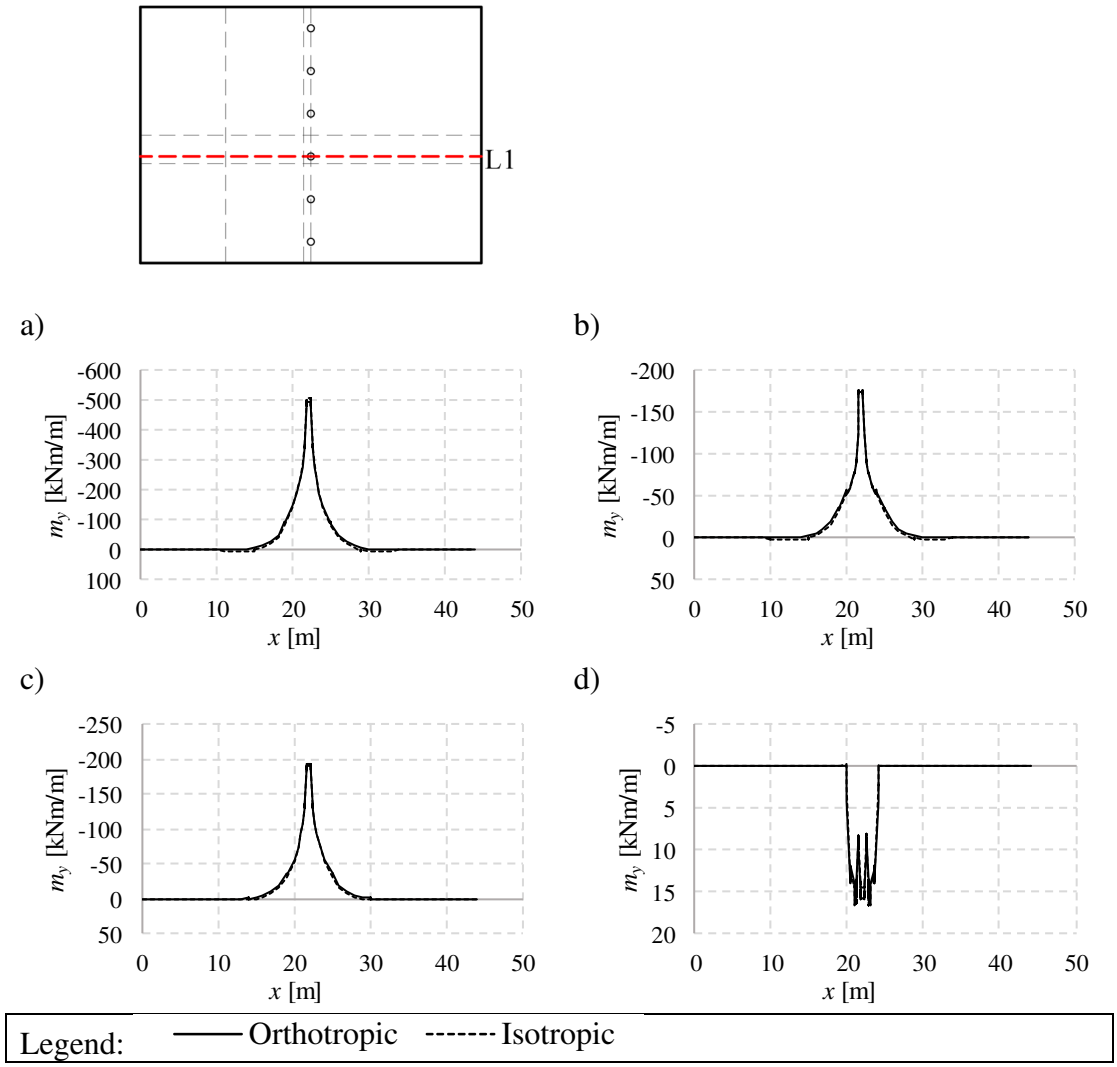

Figure H.66 Results along the section L1. a) Moment caused by the permanent load, b) resultant moment, c) restraint moment, d) primary moment

Table H.64 Comparison of the moments [kNm/m] in Figure H.66 at certain points. If no coordinate is specified, the given value is the peak value in that region. Deviation is the difference between the moment in the models using orthotropic or isotropic material.

	a	b	c	d
Material	Support x=22	Support x=22	Support x=22	Support x=22
Orthotropic	-493	-175	-191	16
Isotropic	-505	-177	-192	14
Deviation [%]	-2.26	-1.30	-0.51	9.27

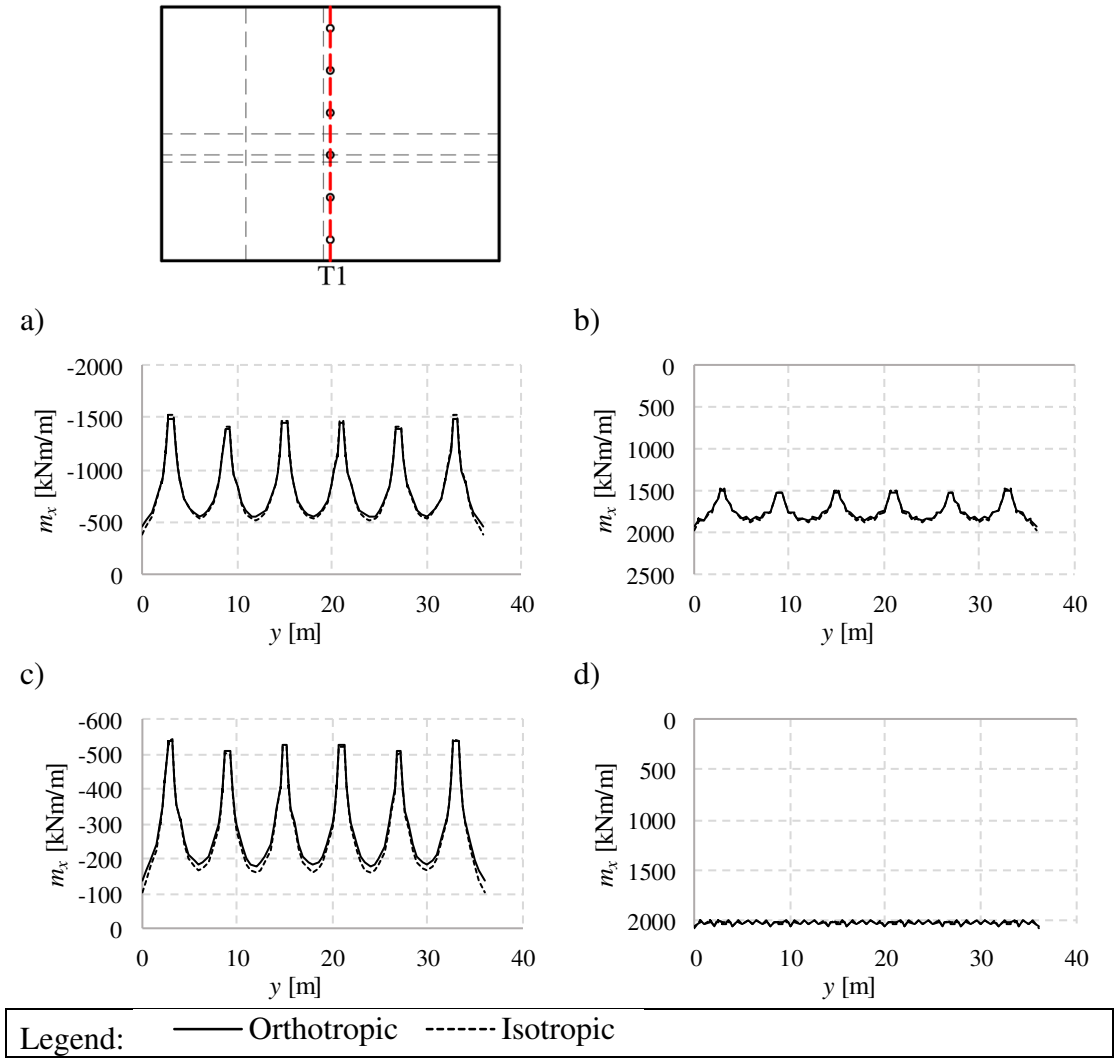

Figure H.67 Results along the section T1. a) Moment caused by the permanent load, b) resultant moment, c) restraint moment, d) primary moment

Table H.65 Comparison of the moments [kNm/m] in Figure H.67 at certain points. If no coordinate is specified, the given value is the peak value in that region. Deviation is the difference between the moment in the models using orthotropic or isotropic material.

	a	b	c	d
Material	Support y=15	Support y=15	Support y=15	Support y=15
Orthotropic	-1445	1514	-527	2040
Isotropic	-1464	1504	-519	2042
Deviation [%]	-1.32	0.63	1.48	-0.08
	Span y=18	Span y=18	Span y=18	-
Orthotropic	-557	1857	-183	-
Isotropic	-530	1878	-164	-
Deviation [%]	5.06	-1.11	11.67	-

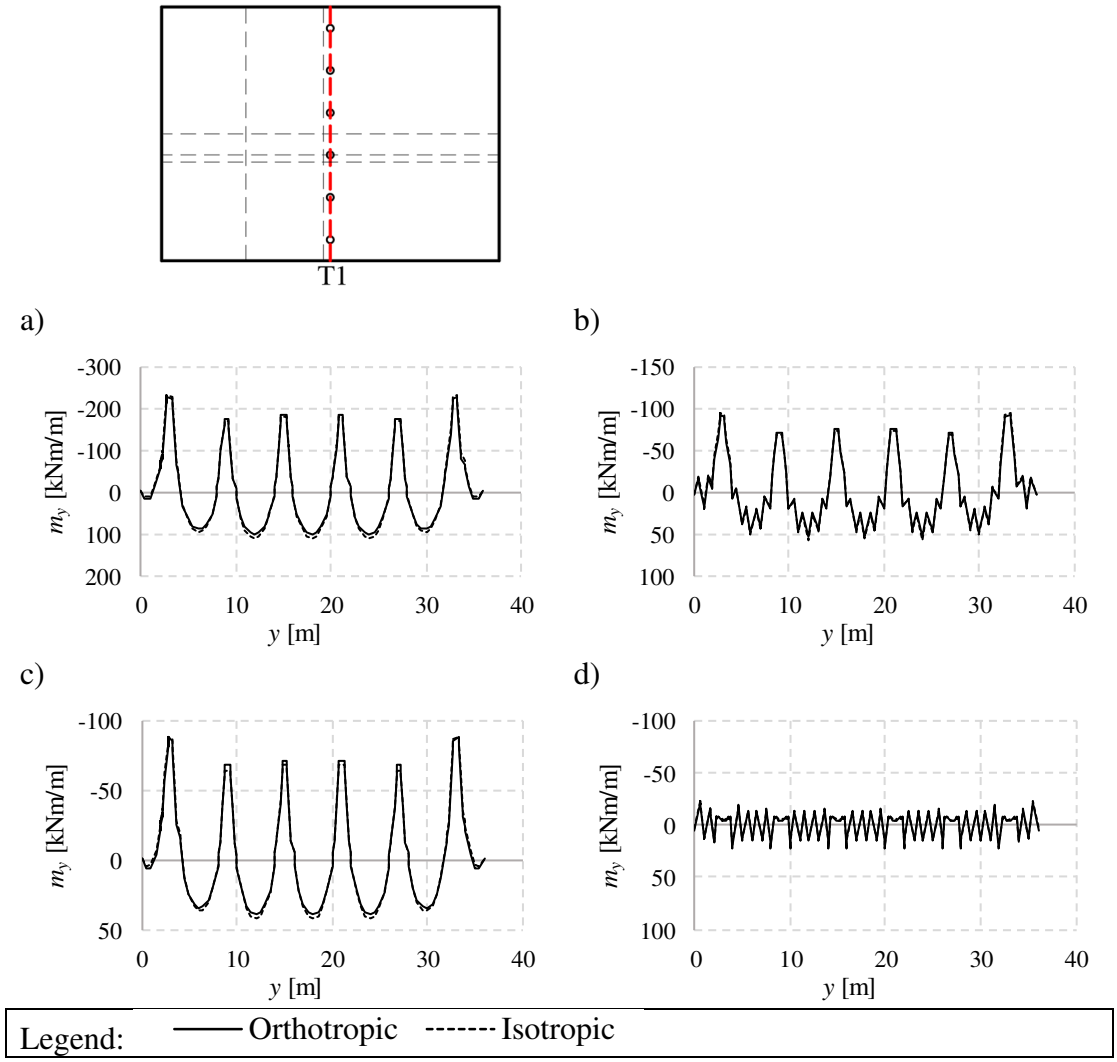

Figure H.68 Results along the section T1. a) Moment caused by the permanent load, b) resultant moment, c) restraint moment, d) primary moment

Table H.66 Comparison of the moments [kNm/m] in Figure H.68 at certain points. If no coordinate is specified, the given value is the peak value in that region. Deviation is the difference between the moment in the models using orthotropic or isotropic material.

	a	b	c	d
Material	Support y=15	Support y=15	Support y=15	Support y=15
Orthotropic	-185	-75	-72	15
Isotropic	-180	-73	-68	14
Deviation [%]	2.84	2.56	4.69	1.27
	Span y=18	Span y=18	Span y=18	Span y=18
Orthotropic	100	53	39	-
Isotropic	110	56	42	-
Deviation [%]	-8.72	-4.98	-7.14	-

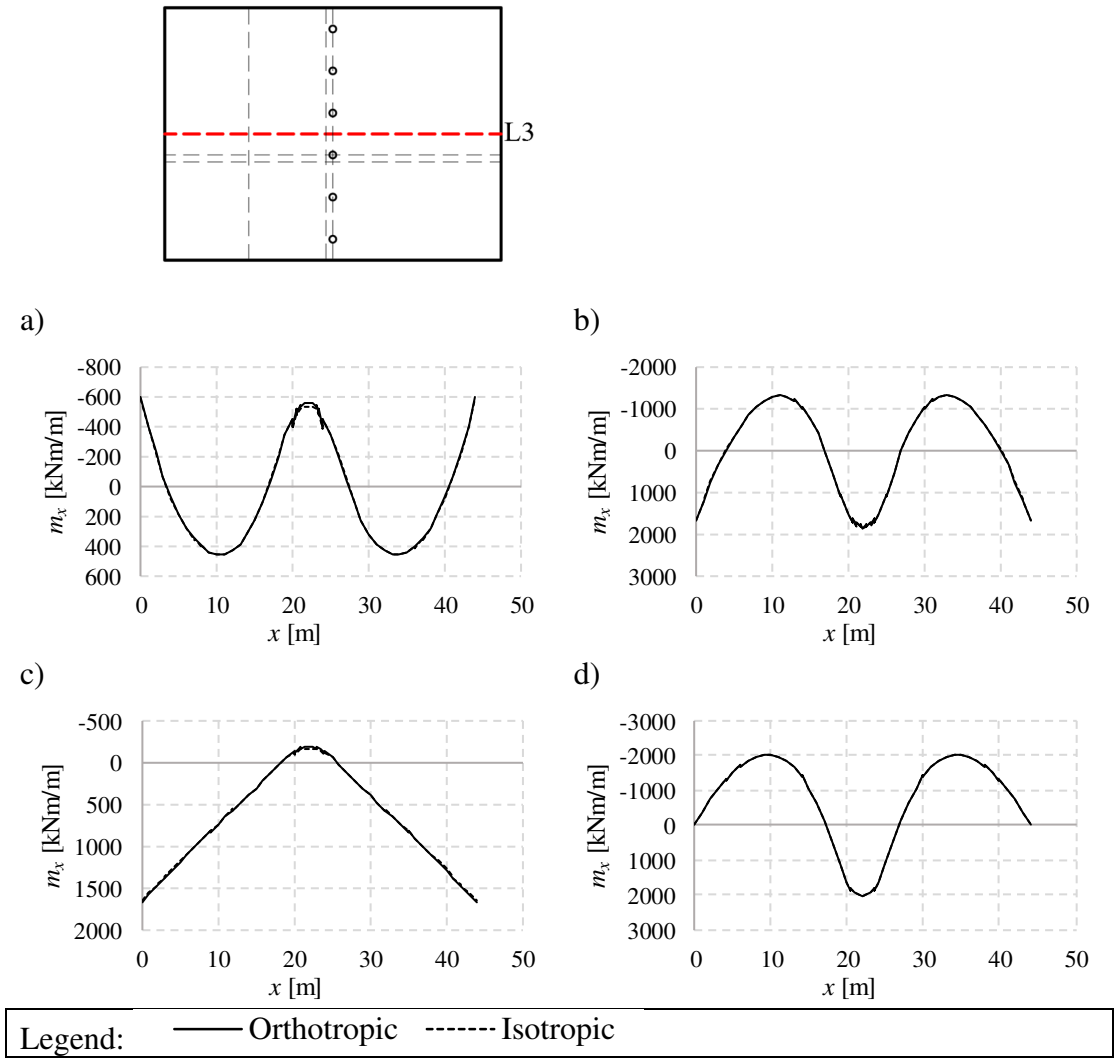

Figure H.69 Results along the section L3. a) Moment caused by the permanent load, b) resultant moment, c) restraint moment, d) primary moment

Table H.67 Comparison of the moments [kNm/m] in Figure H.69 at certain points. If no coordinate is specified, the given value is the peak value in that region. Deviation is the difference between the moment in the models using orthotropic or isotropic material.

	a	b	c	d
Material	Support x=22	Support x=22	Support x=22	Support x=22
Orthotropic	-557	1857	-183	2040
Isotropic	-530	1878	-164	2042
Deviation [%]	5.06	-1.11	11.67	-0.08
	Span	Span	Left support	Span
Orthotropic	456	-1320	1675	-2022
Isotropic	460	-1324	1654	-2022
Deviation [%]	-0.93	-0.31	1.23	0.00

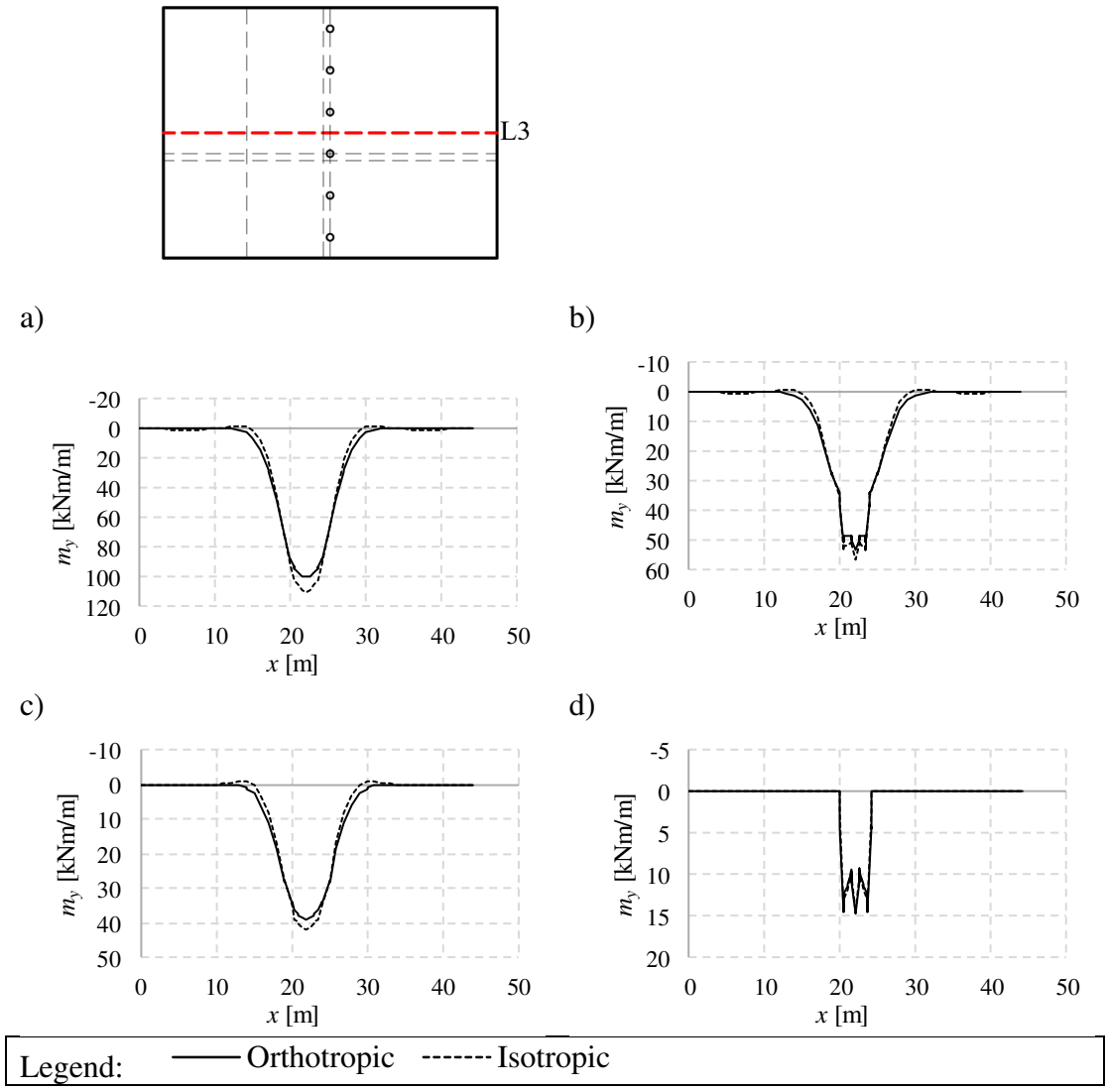

Figure H.70 Results along the section L3. a) Moment caused by the permanent load, b) resultant moment, c) restraint moment, d) primary moment

Table H.68 Comparison of the moments [kNm/m] in Figure H.70 at certain points. If no coordinate is specified, the given value is the peak value in that region. Deviation is the difference between the moment in the models using orthotropic or isotropic material.

	a	b	c	d
Material	Support x=22	Support x=22	Support x=22	Support x=22
Orthotropic	100	53	39	15
Isotropic	110	56	42	14
Deviation [%]	-8.72	-4.98	-7.14	1.27

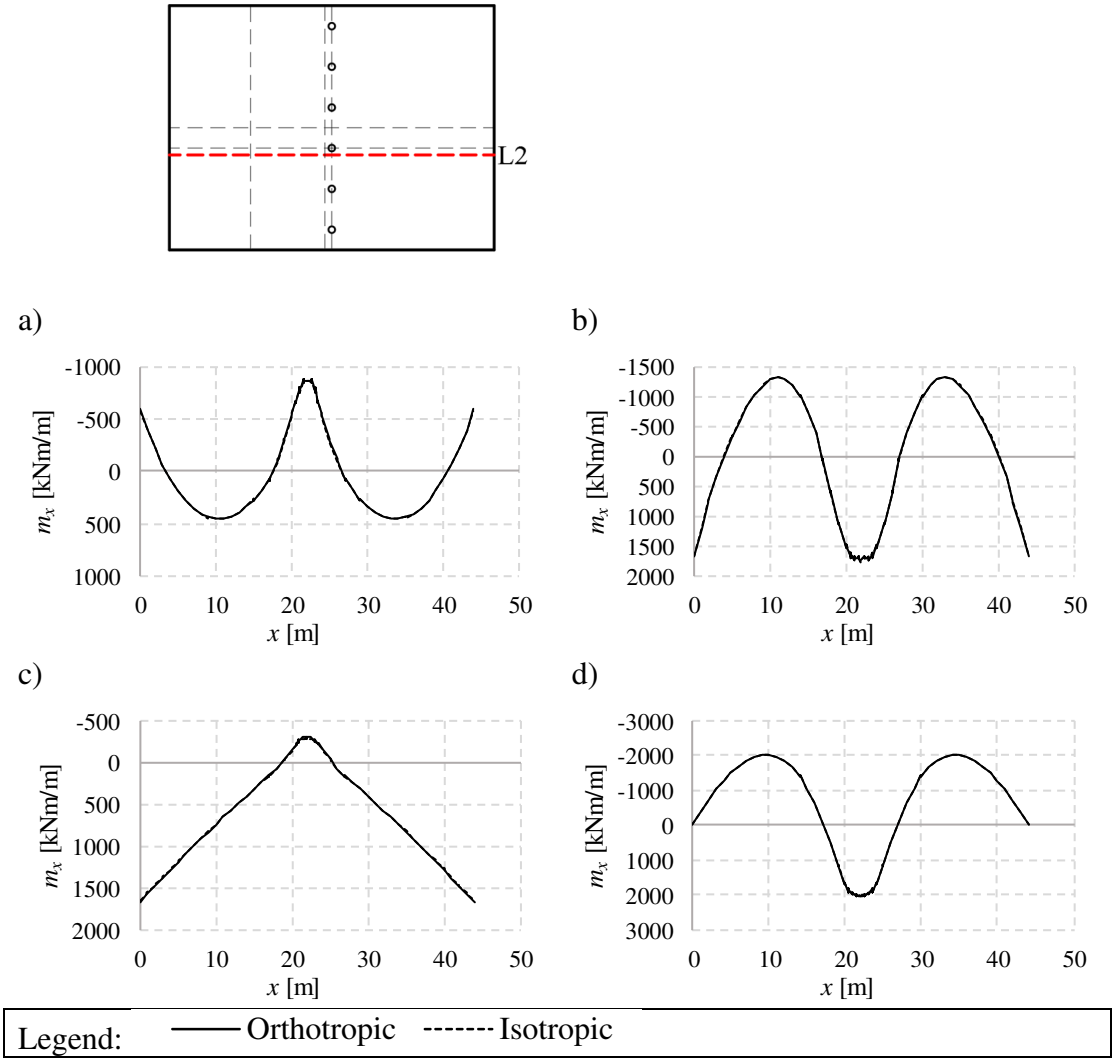

Figure H.71 Results along the section L2. a) Moment caused by the permanent load, b) resultant moment, c) restraint moment, d) primary moment

Table H.69 Comparison of the moments [kNm/m] in Figure H.71 at certain points. If no coordinate is specified, the given value is the peak value in that region. Deviation is the difference between the moment in the models using orthotropic or isotropic material.

	a	b	c	d
Material	Support x=22	Support x=22	Support x=22	Support x=22
Orthotropic	-868	1744	-304	2047
Isotropic	-866	1756	-292	2047
Deviation [%]	0.16	-0.67	4.01	0.00
	Span	Span	Left support	Span
Orthotropic	455	-1320	1675	-2022
Isotropic	456	-1325	1655	-2022
Deviation [%]	-0.25	-0.43	1.21	-0.01

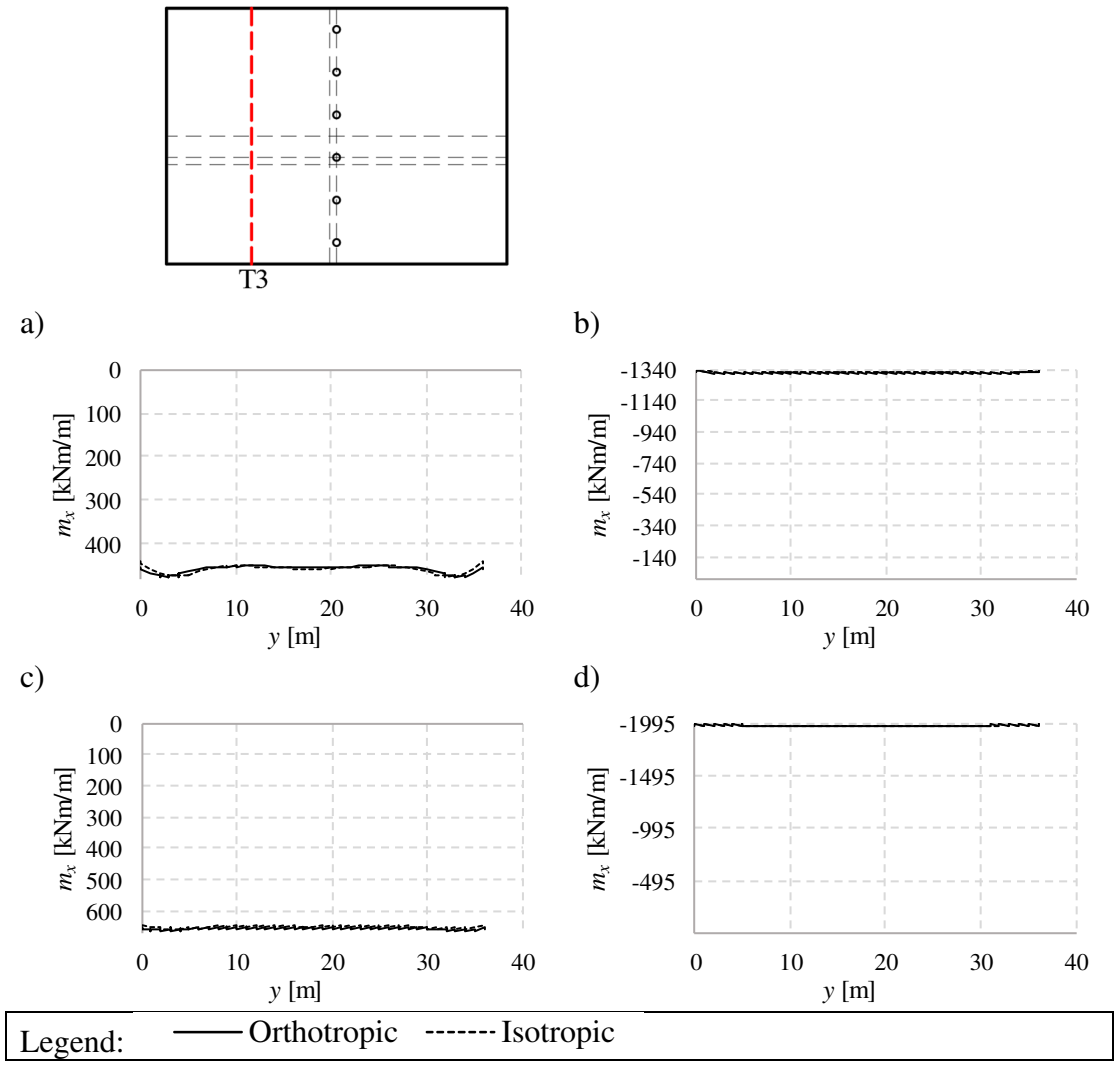

Figure H.72 Results along the section T3. a) Moment caused by the permanent load, b) resultant moment, c) restraint moment, d) primary moment

Table H.70 Comparison of the moments [kNm/m] in Figure H.72 at certain points. If no coordinate is specified, the given value is the peak value in that region. Deviation is the difference between the moment in the models using orthotropic or isotropic material.

	a	b	c	d
Material	Mid y=18	Mid y=18	Mid y=18	Mid y=18
Orthotropic	455	-1320	658	-1977
Isotropic	458	-1325	653	-1977
Deviation [%]	-0.70	-0.38	0.69	-0.02

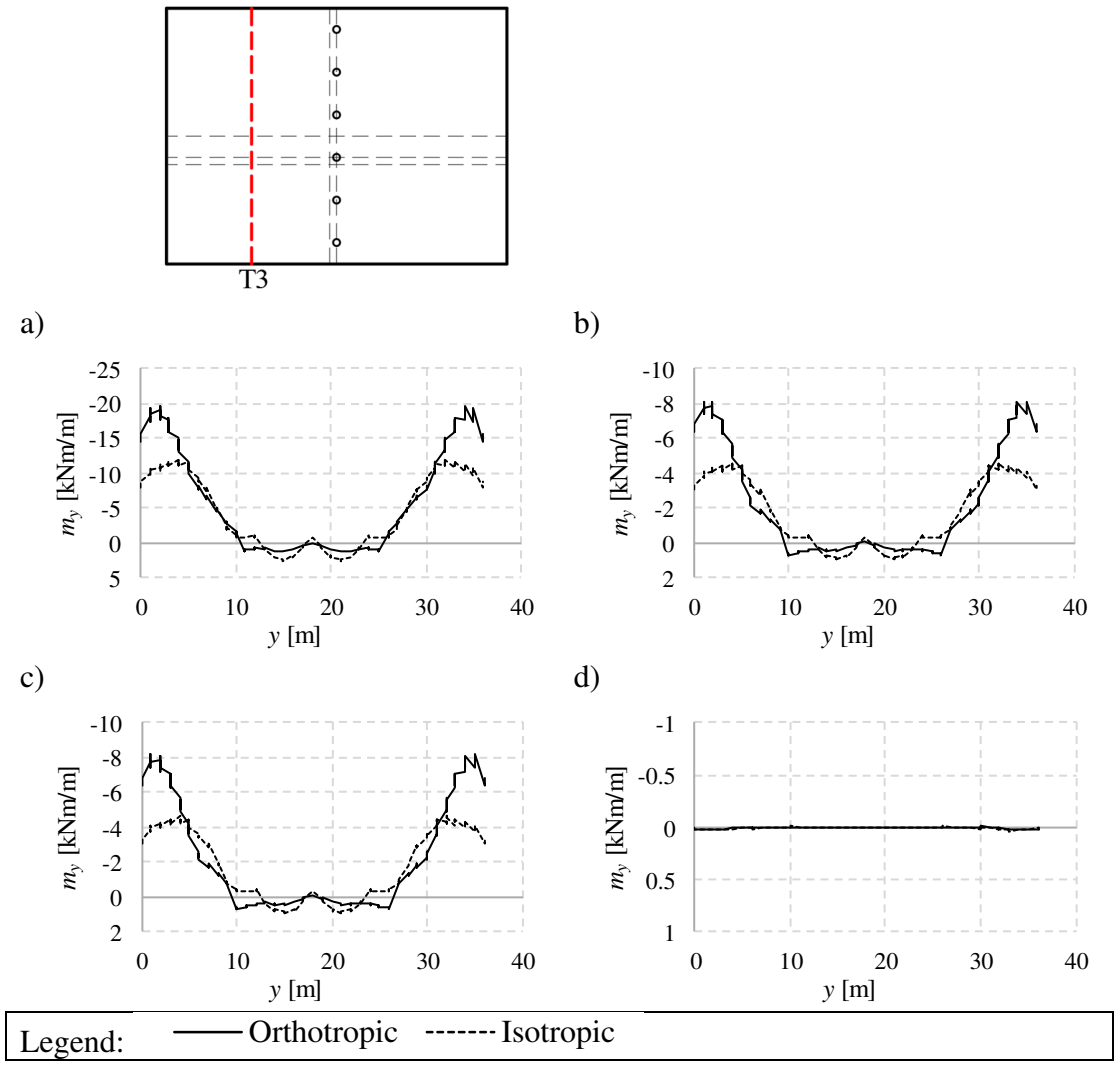

Figure H.73 Results along the section T3. a) Moment caused by the permanent load, b) resultant moment, c) restraint moment, d) primary moment

Table H.71 Comparison of the moments [kNm/m] in Figure H.73 at certain points. If no coordinate is specified, the given value is the peak value in that region. Deviation is the difference between the moment in the models using orthotropic or isotropic material.

	a	b	c	d
Material	Mid y=18	Mid y=18	Mid y=18	Mid y=18
Orthotropic	0.9	-0.1	-0.1	0.0
Isotropic	-0.8	-0.3	-0.3	0.0
Deviation [%]	-	-	-	-